The Contribution of Macrophages to Tumour Growth and Metastasis

Thesis presented for the degree of Doctor of Philosophy

October 2021

Valentina M T Bart

Contents

Summary

Triple negative breast cancer (TNBC) accounts for 10 to 20 percent of breast cancers diagnosed and with a poor response to therapeutic options is associated with high mortality. The immune cell infiltrate of breast cancers is dominated by tumour associated macrophages (TAMs), which have the potential to eliminate tumour cells, but have also been implicated in various processes supporting tumour growth. For the work summarised in this thesis, it was hypothesised that different types of TAMs exist in TNBC that could differently affect tumour outcome. Single cell sequencing of immune cells in the 4T1 mouse model of breast cancer allowed the identification of four different TAM subsets, some of which have not been described before. The work summarised in this thesis indicates that a global reduction of all TAM populations is not beneficial in reducing primary tumour growth, but does reduce metastatic burden in the lungs. While the effects of TAMs and regulatory T cells (Tregs) on each other could not be deciphered, the data do suggest that a combination of immune-targeting therapeutics affecting these two cell populations needs careful consideration, as a combined inhibition of both TAMs and Tregs resulted in the loss of all effects observed with either therapeutic on its own.

Acknowledgements

This thesis would not exist without the contributions of a number of people: first of all, I would like to thank my primary supervisors, Phil Taylor and Awen Gallimore for all the support, patience, guidance and time invested over the past few years.

Thanks also to Barbara Szomolay and Rob Andrews for computational support as well as to Natacha Ipseiz for all the initial lab training and Sarah Lauder for extensive guidance on animal work.

I am further grateful to past and current members of the Taylor and Gallimore groups for memorable Christmas parties, regular table football breaks, plant babysitting, and countless scientific and trivial discussions.

A big thank you as well to science and non-science friends who have been there through all the highs and lows.

Der meiste Dank aber gebührt meiner Familie die mich in allen Abenteuern unterstützt, mich in schweren Zeiten auffängt und in guten Zeiten meine Erfolge mehr feiert als ich selbst. Danke für alles – ihr seid Panama.

Es ist nicht das Ziel der Wissenschaft, der unendlichen Weisheit eine Tür zu öffnen, sondern eine Grenze zu setzen dem unendlichen Irrtum.

Bertolt Brecht

Abbreviations

ADP	Adenosindiphosphat
AGM	Aorta–gonad–mesonephros
APC	Antigen presenting cell
Arg1	Arginase 1
ATP	Adenosintriphosphat
BAC	Bacterial artificial chromosome
BMM	Bone marrow derived macrophage
CSF1	Colony stimulating factor 1/ Macrophage-colony stimulating factor
CSF1R	Colony stimulating factor 1 receptor
DC	Dendritic cell
DEREG	Depletion of regulatory T cell
DTR	Diphteria toxin receptor
DT	Diphteria toxin
EGR	Epidermal growth factor
EMP	Erythroid-myeloid progenitor
EMT	Endothelial to mesenchymal transition
FBS	Fetal bovine serum
FGF-2	Fibroblast growth factor
G-CSF	Granulocyte stimulating factor
GEM	Gel bead in emulsion
GFP	Green fluorescent protein
GM-CSF	Granulocyte-macrophage colony stimulating factor
HCC	Hepatocellular carcinoma

HER-2	Human epidermal growth factor receptor 2
HIF	Hypoxia inducible factor
HSC	Hematopoietic stem cell
IDO	Indolamine-2,3-dioxygenase
iNOS	Inducible nitric oxide synthase
i.p.	Intraperitoneal
IPA	Ingenuity pathway analysis
i.v.	Intravenous
LPS	lipopolysaccharide
Mϕ	Macrophage
Mϕp	Primitive macrophage
Mac1	Macrophage-1 antigen
MDSC	Myeloid derived suppressor cell
MET	Mesenchymal to endothelial transition
M-MDSC	Monocytic MDSC
MMP	Matrix metalloprotease
NO	Nitric oxide
Nrp1	Neuropilin-1
PBS	Phosphate-buffered saline
PBMC	Peripheral blood mononuclear cell
PDAC	Pancreatic ductal adenocarcinoma
PD-1	Programmed cell death 1
PD-L1	Programmed cell death 1 ligand 1
PHH3	Phosphohistone H3
PI	Propidium Iodide

PI3K	Phosphatidylinositol 3-kinase
PMN-MDSC	Polymorphonuclear MDSC
PRR	Pattern recognition receptor
pTreg	Peripheral regulatory T cell
s.c.	Subcutaneous
scRNA-Seq	Single cell RNA sequencing
TAM	Tumour associated macrophage
TCA	Tricarboxylic acid
TCR	T cell receptor
TIMP	Tissue inhibitor of MMP
TL	Thermolysin
TNBC	Triple negative breast cancer
TNF	Tumour necrosis factor
Treg	Regulatory T cell
t-SNE	t-distributed stochastic neighbour embedding
tTreg	Thymic regulatory T cell
UMAP	Uniform Manifold Approximation and Projection
UMI	Unique molecular identifier
VEGF	Vascular endothelial growth factor

Chapter 1: Introduction

Macrophages

Macrophages (Mϕ) are a type of innate immune cell defined by the ability to engulf and destroy microscopic particles (Gordon, 2007). In addition to acting as a first line of defence against pathogens, macrophages are also vital for the maintenance of homeostasis by clearing dead and apoptotic cells and producing bioactive molecules (Kim *et al.*, 2017).

Macrophage development

While initially macrophages were thought to be derived from blood monocytes, it has become clear that certain Mϕ populations can be detected even before hematopoietic stem cells are present in the embryo (Perdiguero and Geissmann, 2015). Although findings are largely based on murine data, it is now widely accepted that macrophages arise in three distinct but overlapping waves in embryogenesis (Figure 1.1). In rodents, erythroid-myeloid progenitors (EMPs) in the blood islands of the yolk sack generate primitive Mϕ (Mϕp) from 7.5 postcoital days (E 7.5) onwards. These cells develop without monocyte intermediates and are distributed throughout embryonic tissues. In most of those tissues they persist into adulthood retaining their ability to self-renew without monocyte influx (Yona *et al.*, 2013). EMPs also exit the yolk sack independently of blood circulation to the fetal liver giving rise to macrophages, monocytes, erythrocytes and granulocytes (Perdiguero and Geissmann, 2015). In contrast, the first definitive hematopoietic stem cells (HSCs) can be detected in the aorta–gonad–mesonephros (AGM) region surrounding the dorsal aorta around E10 and migrate to the yolk sack and fetal liver where they appear from E11. Those multipotent cells then colonise primary hematopoietic organs (bone marrow, spleen) via the blood circulation, localising to specialised stem cell niches and giving rise to leukocyte populations in a process termed adult hematopoiesis (Jagannathan-Bogdan and Zon, 2013).

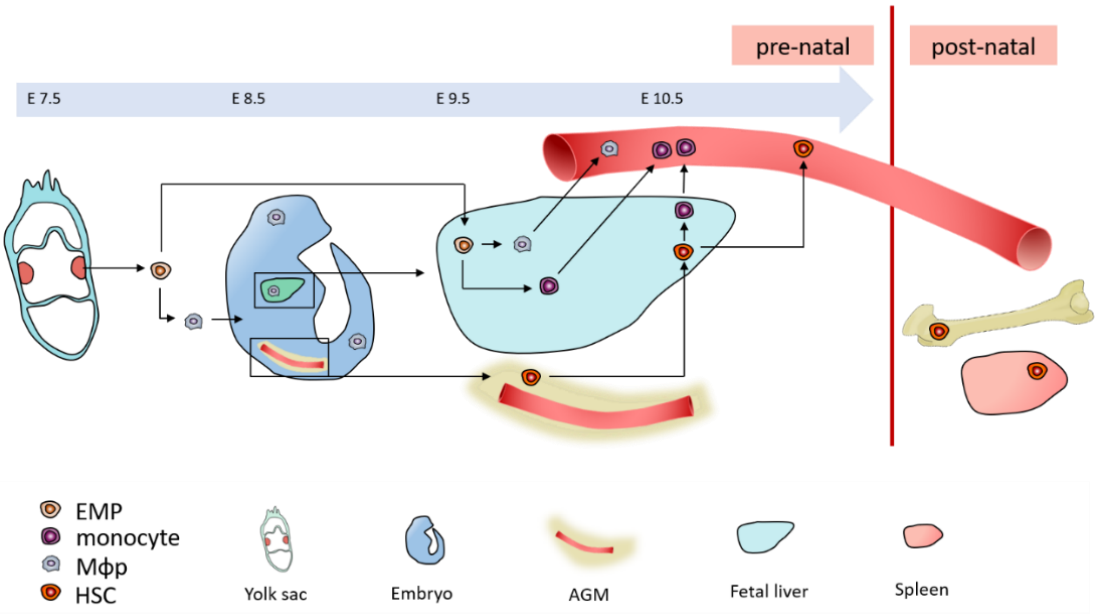

Figure 1.1: Murine macrophage development

In mice, EMPs (light orange) can be detected in the extraembryonic yolk sac blood islands from embryonic day 7.5 (E7.5) giving rise to Mϕp (blue) that seed to embryonic tissues around E8.5. EMPs migrate to the fetal liver around E9.5, expanding and differentiating into myeloid cells, including macrophages and monocytes (purple). HSCs (dark orange) are also detected in the fetal liver. They first appear in the AGM region around E10 and seed to the fetal liver by E11, generating, amongst other immune cells, monocytes that migrate into the blood and embryonic tissues to differentiate into monocyte derived macrophages, diluting the population of yolk sac-derived macrophages with few exceptions. HSCs derived from the fetal liver then colonise the spleen and bone marrow.

All macrophage populations require expression of the transcription factors Runx1 and PU.1 as illustrated by knockout models (Scott *et al.*, 1994; Okada *et al.*, 1998). In contrast to yolk sac derived cells, HSC derived macrophages further rely on c-Myb expression (Mucenski *et al.*, 1991; Buchrieser, James and Moore, 2017). This finding has allowed fate mapping experiments, revealing the co-existence of yolk sack derived and HSC-derived macrophages in most tissues (Yona *et al.*, 2013; Shaw *et al.*, 2018).

Tissue resident macrophages

Macrophages throughout all tissues of the body share phagocytotic and trophic functions. However, in different anatomical locations the specific properties of those cells can vary. This heterogeneity is caused by the individual tissue environment altering transcriptional profiles to enable macrophages' adaptation to tissue specific needs. This allows alveolar

macrophages in the lungs to clear inhaled particles and surfactant (Rider, Ikegami and Jobe, 1992) while brain resident microglia direct neural development via synaptic pruning (Hong, Dissing-Olesen and Stevens, 2016) and maintain neurotransmitter homeostasis (Newsholme, Gordon and Newsholme, 1987).

Generally, all macrophages express a variety of cell surface and cytosol based pattern recognition receptors (PRRs) that allow the recognition of different host and non-host derived ligands (Taylor *et al.*, 2005). This enables the detection of danger related signals to which macrophages can respond by the production of pro- but also anti-inflammatory mediators to initiate inflammation and restore homeostasis.

Macrophage dependence on CSF1

Macrophage-colony stimulating factor (Colony Stimulating Factor 1 (CSF1)) is a growth factor important in the development, motility and function of mononuclear phagocytes. CSF1 is synthesised by different stomal and epithelial cell types (Galy, Spits and Hamilton, 1993; Lidor *et al.*, 1993) as well as macrophages themselves. It can be expressed bound to the cell surface or in its predominant state secreted as a proteoglycan (Priece *et al.*, 1992; Chang *et al.*, 1998).

CSF1 binds the CSF1 receptor (CSF1R), a tyrosine kinase receptor expressed bymacrophages (Stanley *et al.*, 1983), monocytes and their precursors (Byrne, Guilbert and Stanley, 1981), as well as osteoclasts (Felix *et al.*, 1994), B cells (Baker *et al.*, 1993) and neurons (Wang, Berezovska and Fedoroff, 1999). CSF1R expression has also been found on smooth muscle cells (Inaba *et al.*, 1992) where CSF1 binding promotes DNA synthesis and growth (Herembert *et al.*, 1997).

In addition, IL-34 can also bind CSF1R, although it shares no sequence homology with CSF1 (Lin *et al.*, 2008). The two ligands elicit similar biological responses after receptor activation but differ in spatiotemporal expression, with CSF1 being systemically expressed and IL-34 expression restricted to the skin and central nervous system (Wei *et al.*, 2010).

The extracellular domain of CSF1R contains five Ig-like subunits, of which three are involved in ligand recognition while the other two stabilise the ligand-receptor complex (Mun, Park and Park-Min, 2020). The transmembrane domain links to the juxtamembrane domain and a kinase domain which is interrupted by a kinase insert (Stanley and Chitu, 2014).

Ligand binding initially leads to rapid dimerisation, kinase activation and auto-phosphorylation of its six tyrosine residues. This is followed by receptor ubiquitination and uptake of the CSF1/CSF1R complex for degradation (Pixley and Stanley, 2004). Tyrosine phosphorylation creates binding sites for downstream effectors and initiates signalling cascades associated with cytoskeletal remodelling and transcriptional and translational processes (Stanley and Chitu, 2014).

Role of CSF1 in macrophage development

CSF1 is essential in the differentiation of myeloid cells from hematopoietic stem cells by activating the transcription factor PU.1 (Mossadegh-Keller *et al.*, 2013). This importance is illustrated by mouse models: mice homozygous for the osteopetrosis spontaneous mutation (*Csf1*^{op}) are unable to produce all forms of biologically active CSF1 due to an inactivating mutation. Among other phenotypical manifestations they present with severe reductions in certain tissue macrophages as well as osteoclasts early in life (Wiktor-Jedrzejczak *et al.*, 1990). The macrophage populations affected included all investigated except for skin resident Langerhans cells and thymus resident macrophages (Cecchini *et al.*, 1994). Transgenic expression of the CSF1 precursor in these mice recovers CSF1 levels and fully restores tissue macrophage populations (Ryan *et al.*, 2001). Importantly, while transgenic expression of only the membrane bound isoform corrects gross defects, it is not sufficient to fully restore macrophage populations in all tissues illustrating the importance of secreted CSF1 (Dai *et al.*, 2004).

Also, even without interference, the levels of macrophages in *Csf1*$^{op/op}$ mice have been suggested to gradually recover with age (Begg *et al.*, 1993). This stands in contrast to Csf1r^{-}/Csf1r^{-} mice which fail to express CSF1R and show a more severe phenotype that does not improve with age. This discrepancy is due to CSF1R's ability to also interact with IL-34, which has shown to be increased in bones and spleens of aged *Csf1*$^{op/op}$ mice (Wei *et al.*, 2010; Nakamichi, Udagawa and Takahashi, 2013). Thus, it is likely that IL-34 compensates for lack of CSF1 expression, although no study has directly investigated the effects of IL-34 inhibition in *Csf1*$^{op/op}$ mice.

Early in macrophage differentiation CSF1 alone is not sufficient and synergy with other growth factors including IL-3 and stem cell factor is important to generate mononuclear phagocyte progenitor cells (Bartelmez *et al.*, 1989). After this initial step however, CSF1 on its own can drive monocyte and macrophage differentiation from those progenitors.

While CSF1 was initially identified for its ability to generate mature macrophage type cells from bone marrow precursors *in vitro* (Burgess and Metcalf, 1980) this growth factor also acts on mature macrophages (Whetton and Dexter, 1989) CSF1 has been found to be important for macrophage survival and proliferation (Stanley, Chen and Lin, 1978): CSF1R triggering results in activation of the PI3K/AKT pathway culminating in AKT phosphorylation and the induction of anti-apoptotic proteins Bcl-x_L and Bcl-2 as well as reduction of pro-apoptotic Bax, BAD and caspase-9 (Hunter *et al.*, 2009). Importantly, receptor ligation results in CSF1 uptake from the environment which might be important for the regulation of macrophage numbers, as low doses of CSF1 sufficient for macrophage survival (22 pM) (Boocock *et al.*, 1989) cannot induce macrophage proliferation *in vitro* (Tushinski *et al.*, 1982). Macrophages cultured in the presence of CSF1 concentrations only sufficient for survival differ in cell size, membrane ruffling and vacuole number from those cultured in conditions that permit proliferation (Tushinski *et al.*, 1982).

Throughout different tissues resident macrophages have been shown to self-renew as summarised by Röszer(2018). In contrast to macrophage survival, such proliferation is not regulated by PI3K/AKT signalling. The cell cycle is divided into four different stages: gap 1 (G1), synthesis (S), interphase (G2) and mitosis (M). During G1 the cell decides whether or not it will divide based on environmental signals. In order to initiate cell division macrophages require the presence of CSF1 throughout G1 to commit to the S phase of DNA synthesis. Once this commitment is made, CSF1 stimulation becomes negligible (Roussel, 1997).

Culturing CSF1 induced bone marrow derived macrophages (BMM) in the absence of CSF1 or at low CSF1 concentration results in the induction of a quiescent state characterised by reduced DNA and protein synthesis. Here, addition of CSF1 triggers entry into the S phase (Tushinski and Stanley, 1985). This transition is dependent on activation of the Ras/Raf/MEK/ERK (MAPK) pathway resulting in the transcription of immediate early response genes coding for c-Fos, c-Jun and MYC which trigger DNA and protein synthesis (Roussel, 1997). In line with this, blockade of CSF1 signalling via anti-CSF1 antibodies *in vivo* was shown to inhibit proliferation of resident macrophages in the peritoneal cavity in response to zymosan challenge (Davies *et al.*, 2013).

Role of CSF1 in macrophage activation

In addition to regulating cell survival and proliferation, CSF1 has been shown to induce certain macrophage functions such as cytotoxicity, phagocytosis, chemotaxis and cytokine release. Culture of primary human microglia in the presence of CSF1 resulted in proliferation evidenced by BrdU incorporation and KI67 expression. The cells, however, also displayed microglial process elongation and enhanced phagocytosis (Smith *et al.*, 2013). CSF1's effect on macrophage phenotype is also illustrated by tissue resident macrophages in liver, bone marrow and thymus of CSF1 deficient mice showing alterations in cytoskeletal reorganisation and cytoplasmic process formation that can be rescued by CSF1 injection (Naito *et al.*, 1991; Usuda *et al.*, 1994).

Membrane ruffling and spreading driven by actin polymerisation are the first events detected after CSF1R signalling (Boocock *et al.*, 1989). Such cytoskeletal changes are largely dependent on PI3K, as treatment of cells with a PI3K inhibitor was shown to abolish CSF1 induced actin polymerisation (Diakonova, Bokoch and Swanson, 2002). PI3K mediated activation of WAVE2 is important for full membrane ruffling and subsequent migration toward CSF1 (Kheir *et al.*, 2005). This step is likely dependent on the induction of Rho which regulates cell contraction, as well as Rac and Cdc42 which induce the development of lamellipodia and filopodia respectively (Allen *et al.*, 1998). Those flat extensions forming at the leading edge of motile cells are important for cell adhesion, motility and cellular navigation within the environment (Yamaguchi and Condeelis, 2007).

In addition, roles have been suggested for CSF1 in macrophage polarisation: CSF1 primes tissue resident but not circulating mononuclear phagocytes to produce IL-6 and TNFα in response to LPS challenge (Chapoval *et al.*, 1998). Ligation of the CSF1R further primes macrophage responses to lipopolysaccharide (LPS) by down-regulating various Toll-like receptors (but not TLR4) and increasing CD14 expression (Sweet *et al.*, 2002).

Macrophage M1/M2 paradigm

Traditionally, macrophages were often viewed as classically activated M1 or alternatively activated M2 type cells. Historically, classical activation was defined as the antigen dependent enhanced activity of macrophages upon secondary exposure to a pathogen associated with Th1 cytokines (Mackaness, 1962). The concept of alternative activation then developed from the finding that Th2 associated cytokines induce an activation state characterised by reduced production of proinflammatory mediators (Stein *et al.*, 1992).

Over the years this concept of two distinct activation types merged with the concept of M1/M2 polarisation: in response to LPS and IFNγ macrophages from Th1 mouse strains (e. g. C57BL/6) preferentially produce nitric oxide while Th2 strain (BALB/c) macrophages activate arginine metabolism (Mills *et al.*, 2000). This lead to the image of the M1 macrophage, which in response to LPS produces TNF-α, IL-1 and nitric oxide synthase and the M2 macrophage stimulated by IL-4 to produce arginase. Attribution of multiple other cytokines and surface markers to either one of the extremes over the years separated the macrophage population into opposing pro- and anti-inflammatory forces. In an attempt to further dissect macrophage activation states, different types of M2 macrophages have been introduced, namely M2a, M2b, M2c and M2d, which all are associated with a specific type of cytokine response to specific stimuli as reviewed by (Yao, Xu and Jin, 2019).

Importantly, the M1/M2 model it is mainly based on *in vitro* differentiation of blood monocytes into one of the above categories with a designed set of factors. However, it is not considered very relevant *in vivo* where macrophages exist across a wide spectrum and are observed to co-express markers associated with both activation types. Indeed, while the M1/M2 distinction is still widely used in the field, some researchers have also argued the case for abandoning the M1/M2 model (Murray *et al.*, 2014; Nahrendorf and Swirski, 2016).

Thus, in the remainder of this thesis such terminology will only be used when referring to experiments conducted by researchers that chose to apply these labels.

Cancer

Tumour development

Cancer is a major cause of morbidity and mortality worldwide. The term groups more than hundred different diseases resulting from dysregulated cellular behaviour caused by the accumulation of mutations. Such random alterations can be genetic or epigenetic in nature, affecting regulatory systems directing cellular proliferation and homeostasis. The resulting selective advantage allows clonal expansion of the altered cell which can acquire additional mutations. Eventually, this process will give rise to a transformed cell exhibiting the classic hallmarks of cancer: the ability to induce and sustain persistent proliferation, evade growth inhibition, resist programmed cell death, evade senescence, induce neovascularisation, invade local and distant tissues and organs, reprogram cellular energy metabolism and actively evade an immune response (Hanahan and Weinberg, 2011).

Immune surveillance

Logically, the immune system should act as a defence mechanism against transformed cells preventing tumour formation. The idea that the organism would be able to eliminate mutated cells was proposed by Paul Ehrlich (1909) and later developed into the concept of tumour immune surveillance (Burnet, 1970).

This hypothesis was supported by findings in mouse models: due to their essential role in antigen-receptor arrangement, homozygous deletion of Rag1 or Rag2 causes lymphodepletion and increased susceptibility to tumour development after injection with a chemical carcinogen (Shankaran *et al.*, 2001). Comparable effects on tumour formation were observed upon elimination of STAT1-dependent IFN-γ signalling (Kaplan *et al.*, 1998), together suggesting an essential role of both lymphocytes and IFN-γ in tumour suppression.

Key cells of tumour immunosurveillance are derived from both – the adaptive and the innate immune system. They most importantly include αβ and γδ $CD8^+$ T cells (Girardi *et al.*, 2003), as well as natural killer cells (Waldhauer and Steinle, 2008), resident macrophages (Iannello *et al.*, 2016) and dendritic cells (Vicari, Caux and Trinchieri, 2002).

While elimination is the preferred outcome of immune surveillance, it is not the only option (Shankaran *et al.*, 2001) as summarised in the concept of immunoediting: initially, transformed cells are recognised by immune cells, which can lead to a full elimination of malignant cells preventing morbidity. However, the selective pressure exerted by immune cells can also select for rapidly mutating cells escaping the immune response. This can drive the second phase of immunoediting where a dynamic state of equilibrium develops between malignant and immune cells. This phase can last for years and eventually culminates in the escape process: here, tumour cells that have acquired mutations enabling them to resist or even suppress the immune response proliferate and expand, with the immune system no longer able to control this growth, resulting in clinical disease (Dunn *et al.*, 2002).

Established tumours are heterogeneous tissues with reciprocal interactions between healthy and neoplastic cells regulating proliferation, metabolism and potential immune evasion (Bissell & Radisky, 2001). Malignant cells interact not only with the stromal compartment (i.e. healthy cells of surrounding tissue and blood and lymphatic vessels) but also with infiltrating immune cells.

While benign tumours remain confined to their original location and can be resected, the primary cause of cancer mortality is metastasis, the spread of malignant cells into surrounding and distant tissues (Steeg, 2006). This process is driven by the primary tumour's growing need for nutrients and oxygen. Tumour metastasis is a multistep process, simplified in Figure 1.2.

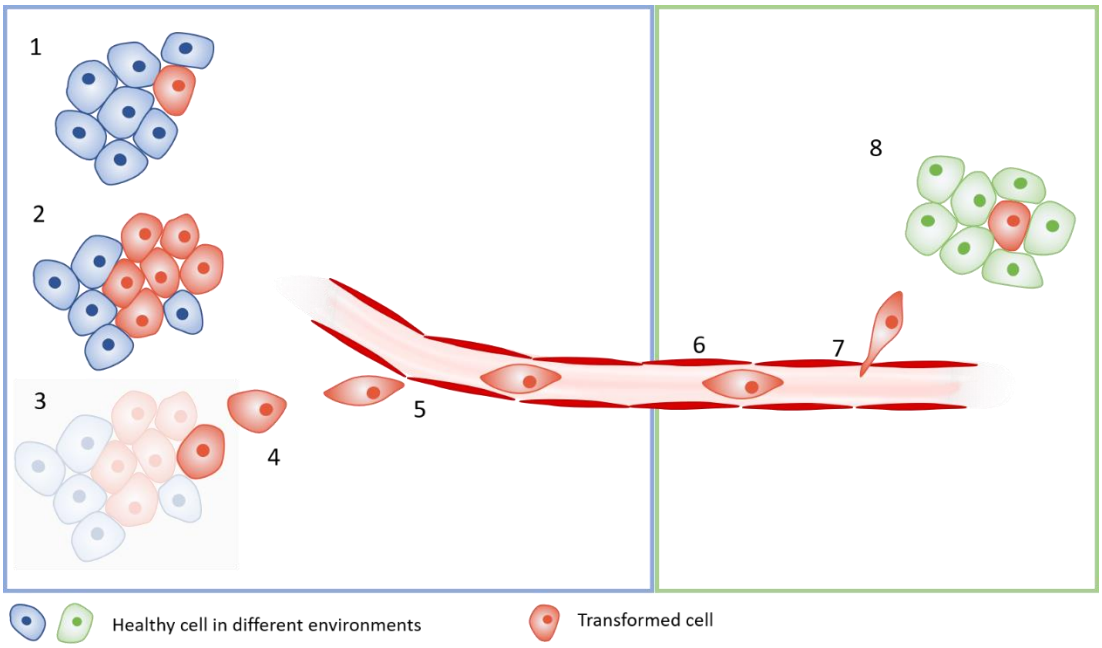

Figure 1.2: Summary of tumour metastasis

A healthy cell acquires sufficient mutations to become cancerous (1). If the immune system fails to eliminate the transformed cell this eventually results in the formation of a primary tumour as the cancerous cell multiplies (2). Single cells within the primary tumour gain an invasive phenotype (3) allowing them to infiltrate the local surrounding tissues (4) and enter circulation (5). Detached cancer cells will travel to a distant site (6) and extravasate to invade a new tissue microenvironment (7). Here they will need to evade the immune system and adapt to the new tissue microenvironment to proliferate and form metastases (8).

The first step of metastasis involves a physical detachment of one or more transformed cells from the primary tumour. This process requires cancerous cells to acquire the ability to migrate and invade, which can be aided by morphological and phenotypical conversions. One such conversion is epithelial to mesenchymal transition (EMT): in epithelial architecture, neighbouring cells form continuous cell layers and tight junctions. Individual cells are polarised and sessile. In contrast, mesenchymal cells show no or loose cell to cell

interactions with a lack of cytoskeletal and organelle component polarisation. They are motile and can be invasive (Savagner, 2015). Under physiological conditions EMT drives essential parts of embryonic development with several rounds of EMT and its reverse action mesenchymal to epithelial transition (MET) necessary for the arrangement of complex three dimensional organ structures (Thiery *et al.*, 2009).

Hypoxia, nutrient deprivation and inflammation in a cell's microenvironment result in the local release of basic fibroblast growth factor 2 which can activate specific transcription factors (e.g. SNAI1/2, TWIST1) which can initiate EMT (Strutz *et al.*, 2002; Lundgren, Nordenskjöld and Landberg, 2009). In a mouse model of 4T1 cancer, inhibition of TWIST1 resulted in a drastic reduction of lung metastasis along with less tumour cells detected in peripheral blood (Yang *et al.*, 2004). In contrast, genetic deletion of *Twist* or *Snai1* in a model of pancreatic ductal adenocarcinoma was not associated with any significant change in tumour metastasis (Zheng *et al.*, 2015).

It is unclear at present whether EMT is essential to enter circulation or whether tumour cells can exist on a spectrum between the two extremes: in a study investigating circulating CD45 negative cells in triple negative breast cancer (TNBC) patients a correlation was found between cells co-expressing both epithelial and mesenchymal markers and reduced overall survival (Bulfoni *et al.*, 2016). It is further unclear whether tumour cells' migration into and through vasculature is an active or passive mechanism: the possibility of chemotaxis of tumour cells in response to epidermal growth factor produced by macrophages has been suggested by *in vivo* experiments in mammary carcinomas (Wyckoff et al. 2004).

In any case, circulating tumour cells need to survive in the circulation: they can establish close interactions with platelets, with platelet depletion associated with reduced metastasis (Camerer *et al.*, 2004). Such interactions are thought to be important to protect tumour cells from immune cell recognition (Borsig *et al.*, 2001; Palumbo and Degen, 2007) and are crucial for tumour cell extravasation at the target organ (Weber *et al.*, 2016).

While these steps of metastasis are carried out by tumour cells themselves, it is thought that the site of metastasis needs to be prepared before tumour cell migration takes place: the seed and soil hypothesis was proposed by Paget (1889), comparing tumour cell dissemination to the distribution of plant seeds that need to fall on congenial soil in order to grow. This hypothesis suggests that a target organ for metastasis must offer specific conditions for tumour cells to be able to colonise and grow. Indeed, several molecular interactions between tumour and stromal cells have been identified that differ across

various target sites and govern organ specific metastasis. This includes chemokines such as CXCL12 and CCL21 which are highly expressed in lungs and lymph nodes, directing homing of $CXCR4^+$ and $CCR7^+$ cancer cells respectively (Müller *et al.*, 2001), was well as CXCL5 attracting $CXCR2^+$ cancer cells to the bones (Romero-Moreno *et al.*, 2019). There is increasing evidence that immune cell subsets also play a role in various steps along the metastatic process (see: TAMs' role in metastasis).

Breast cancer

Breast cancer is a heterogeneous condition with four different molecular subtypes: luminal A, luminal B, human epidermal growth factor receptor 2 (HER-2) overexpression and TNBC. Luminal breast cancers test positive for hormone receptors (oestrogen receptor and/or progesterone receptor) while HER-2 dependent cancer is hormone receptor negative but HER-2 positive (Gao and Swain, 2018). These types of cancer caused by hormones and growth factors account for approximately 75% of diagnosed mammary carcinomas (Zelnak and O'Regan, 2015). The rest is made up of different types of TNBCs which test negative for hormone receptors and do not overexpress HER-2 protein. TNBCs do not respond to treatment with hormonal therapy or HER-2 inhibitors used for the treatment of the other subclasses. Due to the lack of efficient therapeutics and the difficulties in identifying molecular drivers of those conditions, TNBCs are associated with high risk of recurrence, metastasis and overall poor survival (Mersin *et al.*, 2008; Lin *et al.*, 2012).

Role of CSF1 in TNBC

Different types of TNBCs have been attributed to defects in various signalling pathways (Ossovskaya *et al.*, 2011). While TNBCs do not express HER-2 and thus are not driven by human epidermal growth factor, other growth factors might be involved in TNBC carcinogenesis. High levels of CSF1 expression have been detected in a variety of human malignancies and are often associated with increased metastasis and poor prognosis (Behnes *et al.*, 2014; Espinosa *et al.*, 2014; Baghdadi *et al.*, 2018). This is especially true in terms of breast cancer: under homeostatic conditions CSF1 and CSF1R are only expressed in breast tissue during puberty, pregnancy and lactation as CSF1 plays an important role in mammary tissue development. While healthy mammary tissue outside of these conditions does not express CSF1, CSF1 expression is detected in 17-25% of human breast cancers (Beck *et al.*, 2009) and especially common in TNBC (Ding *et al.*, 2016). *In vitro* analysis of the human TNBC cell lines MDA-MB-231 and HCC1937 showed high expression of CSF1 and macrophage recruitment compared to the non TNBC cell line MCF-7 (Lu *et al.*, 2019). The

increased production of CSF1 has been suggested to be due to upregulation of Kindlin-2, an important regulator of integrin function (Plow *et al.*, 2016). Kindlin-2 levels were significantly higher in TNBC breast cancer cell lines and mammary tissue of patients with TNBC compared to other molecular subtypes (Sossey-Alaoui *et al.*, 2017; Azorin *et al.*, 2018). Kindlin-2 expression was associated with poor prognosis and high infiltration with tumour associated macrophages and Kindlin-2-deficient tumour cells showed reduced TGF-β signalling resulting in lower expression and release of CSF1 (Sossey-Alaoui *et al.*, 2017). Since TGF-β augments CSF1 mediated macrophage proliferation (Celada and Maki, 1992), a reduction would be associated with reduced macrophage numbers.

Tumour associated macrophages

Macrophages infiltrating cancerous tissues are known as tumour associated macrophages (TAM) and depending on the type of cancer can constitute up to 50% of total tumour mass (Kelly et al., 1988).

TAM origin

Considering the multiple origins of tissue resident macrophages, it seems likely that the same concept of diverse ontology also applies to TAMs. Indeed, this has been confirmed in some types of tumours: crossing a mouse model where circulating monocytes express green fluorescent protein (GFP), while cells developing independently of HSC express a tomato reporter protein to a genetically engineered glioma model, it has been shown that both- tissue resident microglia and recruited monocytes contribute to the glioma TAM population (Bowman *et al.*, 2016). These findings have been confirmed in a different glioma model where distinct fluorescent reporters were expressed under the control of the monocyte specific *Cx3cr1* and the embryonic macrophage specific *Ccr2* promoter (Chen *et al.*, 2017), demonstrating that the glioma TAM population was made up of both – infiltrating monocytes (about 85%) and resident microglia (about 15%). Similar results were also suggested for the TAM compartment in pancreatic (Zhu *et al.*, 2017) and lung cancer (Loyher *et al.*, 2018).

Monocyte recruitment

While tissue resident macrophages are already present at the site of tumour development, monocyte derived macrophages need to be recruited from the circulation. This process relies on chemokines and their respective receptors: chemokines are soluble proteins involved in cell migration and activation. They and their receptors are expressed by various

cell types orchestrating immune cell trafficking under physiological (Takeda, Sasaki and Miyasaka, 2017) and pathological (Charo and Ransohoff, 2006) conditions.

Human monocytes are classified based on their surface expression of CD14 and CD16 into classical (CD14 high, $CD16^-$), intermediate (CD14 high, $CD16^+$) and non-classical (CD14 low, $CD16^+$) subtypes. Classical types give rise to intermediate ones which then develop into non-classical monocytes. In mice, monocytes are classified based on Ly6C expression, where $Ly6C^+$ cells are the equivalent to human classical, and Ly6C low the equivalent of non-classical cell types (Kawamura and Ohteki, 2018). The $Ly6C^+$ subpopulation is characterised by expression of chemokine receptor CCR2, while $Ly6C^-$ monocytes express higher levels of CX3CR1 (Geissmann *et al.*, 2010). These monocyte populations are attracted to specific tissues in response to the chemokines CCL2 and CX3CL1 respectively. While those chemokines are produced constitutively, plasma levels of CCL2 and CX3CL1 are significantly elevated in response to ischemia (Cochain *et al.*, 2010).

In the tumour context, ischemia is a result of rapid cellular proliferation with insufficient neovascularisation and thus limited oxygen supply (Gatenby and Gillies, 2004). Indeed, areas of hypoxia and anoxia have been detected in most forms of human tumours and highly hypoxic tumours are associated with shorter survival (Hockel and Vaupel, 2001). Co-staining markers of hypoxia (pimonidazole) with those identifying macrophages (F4/80) has shown that macrophages tend to accumulate in tumour regions of low oxygen availability and necrosis. This infiltration is caused by an increase in CCL2, CCL5 and other soluble factors such as CSF1 and vascular endothelial growth factor (VEGF) (Murdoch, 2004) as well as eotaxin and oncostatin M (Tripathi *et al.*, 2014). Initially, these molecules are produced by tumour and stromal cells in response to the hypoxic environment. However, as monocytes infiltrate the tissue and develop into macrophages, their own production of the aforementioned factors could amplify the positive feedback loop.

The individual contribution of TAMs derived from different progenitors is not well understood and likely differs depending on the tissue: in a mouse model of pancreatic ductal adenocarcinoma (PDAC) reduction of circulating monocytes did not affect tumour progression, while depletion of pancreatic tissue resident macrophages significantly reduced tumour burden (Zhu *et al.*, 2017). It has also been proposed that TAMs derived from tissue resident cells support tumour growth, while monocyte derived TAMs are involved in spreading of tumour cells (Loyher *et al.*, 2018). However, regardless of origin, once macrophages are present in the tumour they are influenced by their

microenvironment and the differentiation between tissue resident and monocyte derived cells is very difficult.

While additional studies are needed to confirm TAMs' mixed ontogeny in different tumour tissues, current research suggests that both – tissue resident and monocyte derived macrophage populations contribute to the pool of TAMs, which might be reflected in the different pro- and anti-tumour properties that have been assigned to TAMs in different contexts.

TAM Phenotype

TAMs were long thought to comprise an M2-like phenotype. However, just as regular macrophages, TAMs are highly heterogenous with overlapping features influenced by a variety of factors such as location in the tumour microenvironment and stage and type of cancer: Helm and colleagues (2014) isolated TAMs from freshly resected human PDAC tissue and compared them to monocyte derived *in vitro* polarised M1- and M2-macrophages:M2-macrophages were marked by a high expression of CD163 and IL-10 and low expression of IL-1β and TNF-α compared to M1-macrophages. PDAC-derived TAMs exhibited elevated expression of IL-10 and only slightly lower expression of CD163 compared to M2 macrophages. However, they also strongly expressed IL-1β and TNF-α similar to the *in vitro* polarised M1-macrophages. Also, TAMs were characterised by enhanced expression of various other pro- and anti-inflammatory cytokines such as IL-6 and TGF-β1. Importantly, these data are derived from flow cytometry experiments and subpopulations were not considered, so that the identified TAMs and could represent a mixed population of M1 and M2 type cells. Further, it is unclear how M1 and M2 type macrophages were derived *in vitro*.

Utilising different tumour models Bowman and colleagues (Bowman *et al.*, 2016) found significant differences in the transcriptomes of both – yolk sac and monocyte derived TAMs compared to blood monocytes and microglia. Both TAM populations showed an upregulation of cell-cycle related genes, extracellular matrix components, growth factors as well as chemokines and cytokines. The group also found transcriptional differences between the bone marrow and yolk sac derived TAM populations. Similar results were obtained in human breast cancer, where three distinct TAM subtypes were identified differing in their cell surface expression of CSFR1, CCR2, CD68, CD163 and Siglec1 (Cassetta *et al.*, 2019). While the origin of these cells is unclear, the data suggest TAM heterogeneity

independent of cell ontogeny, indicating the presence of TAM subpopulations that could play differential roles in tumour progression and resistance to therapy.

TAMs' role in primary tumour progression

Macrophages act as a first line of defence against pathogens. Their activation through danger and pathogen associated molecular patterns and their ability to phagocytose suggest that macrophages could potentially eliminate neoplastic cells. Indeed, macrophages have been shown to exhibit cytotoxicity against tumour cells *in vitro* (Bucana *et al.*, 1976). However, this does not always seem to hold true in the tumour microenvironment. While TAM infiltration has been reported to have anti-tumour effects in some cases of colon cancer (Forssell *et al.*, 2007; Sconocchia *et al.*, 2011) most studies report a correlation between TAM accumulation and worse prognosis (Jian-sheng Wang *et al.*, 2016; Qiu *et al.*, 2018).

The location of TAMs within the tumour may affect their properties: It has been reported that TAMs expressing high levels of MHCII locate in normoxic regions and display anti-tumourogenic properties, while TAMs expressing low MHCII accumulate in hypoxic areas and support tumour growth and angiogenesis (Kiavash Movahedi *et al.*, 2010). In line with this, the entry of macrophages into such hypoxic areas has been proposed to be regulated by hypoxia induced Sema3A produced by cancer cells binding to Neuropilin-1 (Nrp1) expressed by macrophages. This signalling cascade culminates in the activation of vascular endothelial growth factor (VEGF) receptor1 (VEGFR1) on TAMs' surface and migration towards areas of VEGF release. As TAMs enter hypoxic regions Nrp1 is downregulated and the cells are retained within these areas by stop signals mediated by PlexinA1/PlexinA4. A loss of Nrp1 has been shown to keep TAMs in normoxic regions of the tumour, reducing angiogenesis and inhibiting tumour growth and metastasis (Casazza *et al.*, 2013).

While incompletely understood, exposure to the hypoxic environment seems to reprogram TAMs into a tumour-supportive phenotype that finds expression in their contribution to angiogenesis, immune suppression, metastasis and potentially the resistance to anti-tumour therapeutics.

TAMs' role in Angiogenesis

Angiogenesis is the formation of new blood vessels from pre-existing vasculature (Folkman, 1984). Without this process the primary tumour is restricted in growth to a size of one to three mm^3. During this avascular stage the tumour's metabolic needs are met by diffusion.

Many such dormant lesions have been discovered in patients who died from causes other than cancer (Black and Welch, 1993). To increase in size, the development of a tumour vasculature is essential to support the increased metabolic demand of the growing cell mass. Initially, tumour cells were thought to be the main drivers of angiogenesis (Kandel *et al.*, 1991). Indeed, a link has been shown between a mutation in the p53 tumour suppressor gene and increased blood vessel development. This is due to the loss of p53 mediated regulation of thrombospondin 1 which acts as an inhibitor of angiogenesis (Dameron *et al.*, 1994).

Increasing evidence also points towards a pivotal role of TAMs in angiogenesis: this is reflected by enhanced microvessel density in human tumours with high TAM infiltration (Leek *et al.*, 1996a; Valković *et al.*, 2002). In line with this, in a transgenic mouse model of mammary cancer an increase in vessel density was associated with transition to malignancy (E. Y. Lin *et al.*, 2006). In this model, macrophages infiltrated the tumour lesions prior to the formation of a tumour vessel network and macrophage depletion was associated with a significant delay in tumour progression.

In healthy adults, angiogenesis is restricted to specific tissues, such as the female reproductive system (Fraser and Lunn, 2000), as well as specific conditions, such as those present during wound healing (Li, Zhang and Kirsner, 2003). However, disruption of homeostasis through increased cellular metabolism or functional impairment of existing blood vessels can elicit extensive neovascularisation in other contexts. This is due to hypoxia or hypoglycaemia in the local microenvironment which trigger the release of angiogenic factors. While such factors can be produced by tumour and stromal cells, macrophages are also known to release significant levels of different molecules with pro-angiogenic properties including growth factors such as VEGF, TNF-α, granulocyte-macrophage colony stimulating factor (GM-CSF) and fibroblast growth factor-2.

VEGF-A is one of the most commonly detected pro-angiogenic factors in growing tumours: its transcription is controlled by hypoxia inducible factor (HIF) a heterodimer made up of HIF1α and HIF1β (Wang *et al.*, 1995). While HIF1α is transcribed equally during hypoxia and normoxia, its mRNA is rapidly degraded under physiological conditions. It is, however, stabilised by hypoxia and dimerises with HIF1β allowing the complex to interact with a hypoxia responsive element in the VEGF-A promoter region (Maxwell *et al.*, 1999). In line with this, VEGF mRNA was found to be highest in necrotic areas of human glioblastomas (Shweiki *et al.*, 1992). VEGF directly affects endothelial cells by inducing them to form

capillary-like structures, and indirectly provides anti-apoptotic signals maintaining immature blood vessels (Alon *et al.*, 1995). TAMs significantly contribute to the pool of VEGF-A present in the tumour: in the example of CSF1 depleted PyMT tumours where vascularity and tumour growth was reduced by the lack of TAM infiltration, restoring just VEGF-A expression promoted tumour growth to match wild type controls (Lin *et al.*, 2007).

Macrophages also produce a variety of angiogenesis-modulating enzymes including inducible nitric oxide synthase (iNOS), COX-2 (Klimp *et al.*, 2001) and several matrix metalloproteases (MMPs) that can indirectly affect vascularisation. MMPs are a family of enzymes which upon activation cleave a variety of protein substrates (Stamenkovic, 2003). In a model of cervical cancer, tumour incidence and volume as well as intra-tumoral blood vessel density were reduced in *Mmp9*$^{-/-}$ mice compared to controls (Giraudo, Inoue and Hanahan, 2004).

TAMs' role in metastasis

The exact role of TAMs in metastasis, as indeed primary tumour formation, is controversial with many open questions waiting to be resolved.

Role in local tissue invasion

One crucial step discussed earlier is the contribution of TAMs to tumour neo-angiogenesis as new blood vessels are needed for tumour cells to spread to metastatic niches. MMPs are involved in tissue remodelling and invasion: co-culture of peripheral blood derived human macrophages with the human carcinoma line A549 increased macrophage expression of MMP-1. Additionally, when A549 cells had been pre-exposed to cigarette smoke, co-culture reduced macrophage levels of tissue inhibitor of MMP (TIMP) mRNA. Since MMP-1 is not expressed by mice, transgenic mice with macrophage-specific expression of MMP-1 (Mac-MP-1) under the control of the scavenger receptor promoter-enhancer A and lung-specific expression (lung-MMP-1) under the haptoglobin promoter (D'Armiento *et al.*, 1992) were used for *in vivo* studies: in both, Mac-MMP-1 and lung-MMP-1 mice a decrease in collagen deposition was observed in primary tumours with effects being amplified by exposure to cigarette smoke (Morishita *et al.*, 2018). Thus, it has been suggested that TAM produced MMP-1 could promote lung metastasis in smokers.

Further, MMP-9 has been shown to be upregulated in a transgenic mouse model of epithelial cancer and homozygous disruption of MMP-9 decreased tumour incidence. MMP-9 was not produced by tumour cells but stromal and infiltrating immune cells and

restoring MMP-9 expression only in bone marrow derived cells was sufficient to restore tumour incidence to that of wild type controls (Coussens *et al.*, 2000). In a different study, co-culture with B16-F10-M3 murine melanoma cells was enough to increase macrophage MMP-9 mRNA. Melanoma cells exposed to the co-culture media were more invasive through matrigel, with effects being reversed by anti-MMP-9 antibodies (Marconi *et al.*, 2008).

While data do suggest a role of MMPs in local extracellular matrix remodelling facilitating tumour cell migration, MMP production is not restricted to macrophages, with tumour and stromal cells also able to contribute to the MMP pool.

Role in EMT

As mentioned earlier, EMT might be an important step in tumour cell dissemination. *In vitro* experiments suggest a role for TAMs in cancer cell EMT: co-culture of pancreatic cancer cell lines with the mouse macrophage RAW 264.7 cell line pre-exposed to IL-4 resulted in an increased expression of mesenchymal and decreased expression of epithelial markers by cancer cells (Liu *et al.*, 2013). Similar results were found after co-culture of RAW264.7 activated by LPS and a human hepatocellular carcinoma cell line (C.-Y. Lin *et al.*, 2006). Investigating hepatocellular carcinoma (HCC) tissue samples, a correlation was found between TAMs' preferential location and EMT high areas (Fu *et al.*, 2015). In the same study co-culturing macrophages with HCC cells increased HCC cell expression of SNAI and N-Cadherin while downregulating E-Cadherin expression, promoting EMT. This process has been suggested to depend on TAMs' production of inflammatory cytokines including TNF-α and IL-1β (Kawata *et al.*, 2012).

While these data do imply a potential involvement of TAMs in the EMT process of tumour cells and TAMs are known to be able to produce growth factors and cytokines which have been linked to EMT initiation (Jing *et al.*, 2011), direct *in vivo* evidence for the contribution of TAMs to EMT is still lacking.

Role in tumour cell intravasation

Using intravital imaging in the mammary specific MMTV-PyMT mouse model of breast cancer, it has been found that gradients of either epidermal growth factor (EGF) or CSF1 mobilised both – macrophages which only expressed CSF1R and tumour cells only expressing EGF receptor but no other cells. Macrophages produced EGF and tumour cells were shown to release CSF1. In CSF1 deficient mice where primary tumour growth was

unaffected, a substantial reduction in cells collected from tumours by use of both types of gradients was found, suggesting that the migratory capacity of tumour cells in response to EGF depends on the presence of macrophages (Wyckoff *et al.*, 2004). Also, macrophage production of EGF is enhanced by CSF1 and CSF1 production of tumour cells is enhanced by EGF. This results in a paracrine loop between tumour cells and macrophages where macrophages create an EGF gradient inducing asymmetrical activation of tumour cells and the formation of elongated protrusions enabling migration towards blood vessels (Goswami *et al.*, 2005).

Role in tumour cell survival in the circulation

Tumour cells in circulation are likely to interact with peripheral monocytes: co-culturing peripheral blood mononuclear cells (PBMCs) with circulating tumour cell lines derived from advanced stage small cell lung cancer patient blood samples or with media conditioned by such tumour cells *in vitro* was shown to cause monocytes in PBMC cultures to differentiate into macrophages expressing CD163 and CD68. Those macrophages were shown to express high levels of markers associated with worse prognosis (Hamilton *et al.*, 2016) including osteopontin (Li *et al.*, 2015) and CCL2 (Ueno *et al.*, 2000). The tumour conditioned macrophages also produced IL-8 which has been associated with EMT (Li *et al.*, 2012) and MMP-9 enabling tissue invasion. It is possible that macrophages conditioned by tumour cells could aid their survival in the periphery by providing stimulation needed to maintain a mesenchymal phenotype and invade distant tissues.

While the goal of a macrophage would be to phagocytose and eliminate tumour cells, it has been demonstrated that the uptake of apoptotic epithelial tumour cells by macrophages induced macrophage expression of epithelial and stem cell markers *in vitro*. The data suggested that these phenotypical changes were associated with horizontal transfer of DNA from the apoptotic cancer cells, which also allowed macrophages to proliferate. Internalised DNA was detected in the nucleus of the phagocytosing cell, although it was not investigated why the phagocytosed material was not destroyed and could enter the nucleus (Holmgren *et al.*, 1999).Indeed, a subset of macrophages expressing tumour markers was found in the peripheral blood of patients with breast and colorectal cancer. While these cells carried tumour specific DNA in their nucleus and possessed tumorigenic ability, including increased proliferation even in serum-free media and expression of stem cell and epithelial genes, they retained cell surface markers associated with macrophages. This could allow them to evade immune recognition in the periphery, facilitating tumour

spread (Zhang *et al.*, 2017). It is unclear whether these macrophages could also present tumour derived genetic material to adaptive cell types.

Role in tumour cell extravasation

After migrating tumour cells have reached the capillaries of target tissues they need to once again cross the blood vessel wall. *Ex-vivo* imaging of physiologically intact lung structures allowed the visualisation of interactions between intravenously (i.v.) injected Met-1 tumour cells with macrophages in the blood vessels. After macrophage depletion with liposomal clodronate the migration process was delayed and extravasation rates were reduced (Qian *et al.*, 2009a).

Role in pre-metastatic niche preparation

The seed and soil hypothesis suggests that the pre-metastatic niche needs to be prepared for tumour cells to settle and establish metastatic colonies. Bone marrow derived $VEGFR1^+$ precursor cells have been shown to accumulate at such sites before tumour cells can be detected (Kaplan *et al.*, 2005). In mouse models of melanoma and lung cancer the primary tumours have been shown to induce MMP-9 expression in lung endothelial cells and macrophages dependent on VEGFR1 expression. Genetic disruption of MMP-9 resulted in reduced tumour cell accumulation in the lungs. MMP-9 expression was also significantly increased in normal lung endothelial cells of patients with primary tumours in distant organs compared to tumour free controls (Hiratsuka *et al.*, 2002). In line with this, immature myeloid cells defined as $CD11b^+$, $Gr\text{-}1^+$ were detected in lungs of mice with mammary adenocarcinomas prior to metastasis. These cells produced high amounts of proinflammatory cytokines as well as MMP-9 which were associated with disorganisation of capillary vascular structure (Yan *et al.*, 2010). Such myeloid cells expressing Macrophage-1 antigen (Mac 1) (CD11b/CD18 complex) were shown to be recruited into premetastatic niches by the expression of the chemoattractants S100A8 and S100A9 induced by primary tumours. *In vitro* experiments showed that this was at least partially dependent on TNF-α, TGF-β and VEGF-A produced by tumour cells. Blocking of S100A8 and S100A9 significantly reduced the numbers of tumour cells in the lungs even after tumour cells were detected in the circulation (Hiratsuka *et al.*, 2006).

TAMs' role in immune suppression

In addition to their pro-angiogenic and metastatic effects, TAMs also actively suppress immune responses within the primary tumour. Effector T cells recognising tumour antigen

via their T cell receptors (TCR) are able to destroy tumour cells through cytotoxicity and induction of apoptosis via death receptors, while releasing immunogenic cytokines and chemokines to promote an anti-tumour environment. TAMs are able to interfere with T cell activation in a variety of ways:

Depletion of metabolites

TAMs can express indolamine-2,3-dioxygenase (IDO), an inducible catabolic enzyme catalysing the rate limiting step in L-tryptophan degradation. IDO overexpression has been reported in various types of human cancer where it was associated with unfavourable clinical outcome (Inaba *et al.*, 2010; Laimer *et al.*, 2011; Hascitha *et al.*, 2016). T cells are very sensitive to tryptophan depletion which causes cell cycle arrest through different pathways (Munn *et al.*, 2005; Metz *et al.*, 2012). Further, increased IDO activity results in the accumulation of tryptophan catabolites, some of which have been shown to induce T cell apoptosis (Terness *et al.*, 2002).

Activation of effector T cells is associated with a metabolic shift from oxidative phosphorylation to glycolysis (Fox, Hammerman and Thompson, 2005). Glycolysis in activated T cells is largely controlled by the amino acid L-arginine which is a precursor for many metabolites (Geiger *et al.*, 2016). Two main enzymes consuming L-arginine have been reported to be involved in suppressive mechanisms of myeloid cells: iNOS and arginase (Arg1). Both of these enzymes have been shown to be upregulated in a HIF-1α dependent manner in macrophages (Doedens *et al.*, 2010). T cell stimulation *in vitro* in the absence of L-arginine results in a loss of the TCR ζ-chain and reduced proliferation (Taheri *et al.*, 2001; Rodriguez *et al.*, 2002).

Production of anti-inflammatory mediators

iNOS converts L-arginine to L-citrulline enabling the production of nitric oxide (NO) (Geller and Billiar, 1998). While at high levels (>200nM) NO possesses anti-tumour properties, lower levels have been associated with tumour promoting roles *in vitro* (Ridnour *et al.*, 2008).

TAMs are also known to produce anti-inflammatory cytokines: macrophage released IL-10 impairs effector T cells indirectly by reducing dendritic cell and macrophage production of IL-12 which is needed for optimal $CD8^+$ T cell activation (Sica *et al.*, 2000; Ruffell *et al.*, 2014). Further, TAMs and immature myeloid cells in the tumour microenvironment can

produce TGF-β which can suppress cytotoxic $CD8^+$ T cells (Terabe *et al.*, 2003; Ye *et al.*, 2012; Cai *et al.*, 2019).

Direct interaction with cell surface receptors

TAMs can also suppress effector T cells directly via binding to T cell inhibitory and apoptotic receptors: macrophages and immature myeloid cells in the tumour microenvironment have been shown to express programmed cell death 1 ligand 1 (PD-L1) induced by Hif-1α (Noman *et al.*, 2014). Binding of PD-L1 to its ligand PD-1 expressed on T cells upon activation impairs T cell effector function by providing inhibitory signals (Simon and Labarriere, 2017). In human ovarian carcinoma a fraction of TAMs was also shown to express B7-H4 which binds inhibitory CTLA-4 expressed on T cells and prevents proliferation, cytokine production and cytotoxicity of tumour associated antigen specific T cells *in vitro* and *in vivo* (Sica *et al.*, 2003; Kryczek *et al.*, 2006).

TAMs' effect on regulatory T cells

TAMs are thought to promote regulatory T cell (Treg) infiltration into the tumour microenvironment: TAMs secrete cytokines including CCL22 (Curiel *et al.*, 2004) and CCL18 (Chen *et al.*, 2011) which recruit Tregs into tumour tissues. In a mouse model of colorectal cancer macrophage depletion was associated with decreased levels of CCL20, inhibition of Treg infiltration and reduced tumour growth (Liu *et al.*, 2011). Further, macrophages have been observed to induce Tregs *in vitro:* supernatants of monocyte derived macrophages generated with a combination of IL-4, IL-10 and TGF-β were shown to upregulate FOXP3 and CTLA-4 in naïve human $CD4^+$ T cells along with enhanced immunosuppressive activity compared to control T cells. Treg generation was critically dependent on TGF-β (Schmidt *et al.*, 2016). The same has been observed in resident macrophages isolated from murine adipose tissue which were able to induce Tregs under steady state conditions *in vitro*. *In vivo* depletion of these macrophages in epididymal white adipose tissue significantly reduced resident Treg numbers while injection of adipose tissue macrophages significantly increased Treg proportion and number (Onodera *et al.*, 2015).

TAMs' interference with therapeutic intervention

Along with surgical resection, chemo- and radiotherapy are standard procedures for cancer treatment. The primary goal of established therapeutic regimes is to achieve maximal tumour destruction by inducing tumour cell death and blocking uncontrolled cellular

proliferation (Zitvogel *et al.*, 2008). Various depletion models have uncovered a role of TAMs in tumour resistance to therapeutic intervention.

Role in tumour cell resistance to chemotherapy

Chemotherapeutic agents act on all rapidly dividing cells. While they are widely used and beneficial in the treatment of some patients, the overall response rate especially to chemotherapy on its own is low in many cases (Kuo *et al.*, 2010; Wilson, 2013). TAMs have been shown to interfere with tumour cell apoptosis in response to such therapeutic interventions: TAM-released IL-10 acts on dendritic cells limiting their ability to produce IL-12 in response to standard of care chemotherapy. Depletion of TAMs or removal of IL-10 resulted in enhanced $CD8^+$ T cell responses and increased therapy efficacy (Ruffell *et al.*, 2014). An *in vitro* model of breast cancer further suggested that IL-10 released by TAMs enhanced bcl-2 gene expression and STAT3 signalling in tumour cells (Yang *et al.*, 2015). The anti-apoptotic bcl-2 protects cells from apoptotic stimuli (Tsujimoto, 1998) while STAT3 activation in tumour cells is associated with expression of immune suppressive factors and resistance to cell death (Catlett-Falcone *et al.*, 1999). In addition to IL-10, IL-6 has also been shown to upregulate the tumour cell STAT3 pathway and was associated with resistance to chemotherapy in colorectal cancer (Yin *et al.*, 2017).

NO produced via iNOS by TAMs has also been shown to contribute to tumour cell resistance to cisplatin chemotherapy by protecting tumour cells from apoptosis (Perrotta *et al.*, 2018). TAMs have further been reported to produce MFG-E8 (Jinushi *et al.*, 2011), cytidine deaminase (Amit and Gil, 2013) and cathepsin (Shree *et al.*, 2011) which have been implicated in contributing to tumour cell resistance to apoptosis induced by different anti-tumour agents. In line with this, high TAM infiltration has been associated with poor response to chemotherapy with a variety agents (Pei *et al.*, 2014; Xuan *et al.*, 2014; Sugimura *et al.*, 2015).

Role in tumour cell resistance to radiotherapy

In contrast to the systemic effects of chemotherapy, radiotherapy is applied locally and effectively destroys tumour cells reached by the radiation beams via the production of reactive oxygen and nitrogen species. During an acute phase of tissue damage in response to radiation, inflammatory cells are recruited to the target site (Travis, 1980). Importantly, animal models have shown that especially macrophage infiltration is elevated after local irradiation, which has been associated with increased metastasis compared to non-treated

controls (Timaner *et al.*, 2015). In line with this, a positive correlation between TAM infiltration and reduction of local tissue response to radiotherapy was identified in murine sarcomas and carcinomas (Milas *et al.*, 1987). Irradiation of human monocyte derived macrophages with cumulative doses comparable to cancer treatment upregulated pro-inflammatory CD80, CD86 and HLA-DR while downregulating anti-inflammatory CD163 and IL-10 molecules. Irradiated macrophages also retained their ability to drive cancer cell invasion and cancer cell induced angiogenesis *in vitro* (Teresa Pinto *et al.*, 2016). Depletion of macrophages with either anti-CSF1 antibody or a kinase inhibitor targeting CSF1R has been shown to impair tumour regrowth after radiotherapy associated with increased tumour infiltration with $CD8^+$ T cells in a mouse model of mammary cancer (Shiao *et al.*, 2015). Further, in a model of prostate cancer as well as patient samples, CSF1 was shown to be increased in tumours after radiation and using an CSF1 inhibitor in combination with radiotherapy reduced tumour growth better than radiation alone (Xu *et al.*, 2013).

Targeting macrophages in the tumour microenvironment

Macrophages in the tumour microenvironment can directly be inhibited with various methods. Only two therapeutic options relevant for this thesis will be discussed here.

Interfering with CSF1R signalling

In different murine tumours monocyte recruitment into the tumour and maturation into MHCII low TAMs depends on CSF1R signalling. Blockade via anti–CSF1R antibodies results in reduced TAM infiltration and preferential differentiation of monocytes into MHCII high macrophages (Van Overmeire *et al.*, 2016). CSF1 signalling can also be inhibited via the use of small molecule kinase inhibitors: GW2580 is cell permeable and selectively acts on the major kinase domain of CSF1R inhibiting downstream signalling cascades (Figure 1.3).

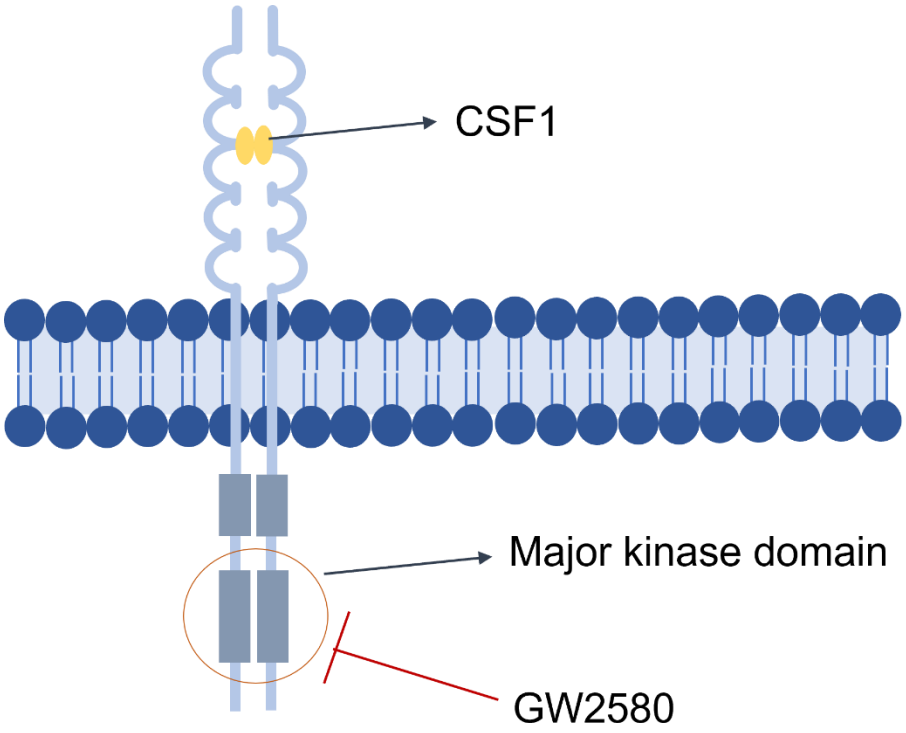

Figure 1.3: Action of GW2580 on CSF1R signalling

Ligation of CSF1 to the CSF1 binding region of CSF1R induces receptor dimerisation, kinase activation and phosphorylation of receptor tyrosine residues which then act as binding sites for downstream adaptor proteins. The small kinase inhibitor GW2580 which is specific for CSF1R penetrates the cell membrane and competitively blocks the ATP binding site of the major kinase domain preventing its activation and function that is needed to induce all other downstream effector pathways.

Graph adapted from Hamilton et al., 2008

GW2580 has a high specificity for CSF1R and when tested against 442 different kinases only inhibited CSF1R and the neurotrophic tyrosine kinase receptor expressed in the central nervous system (Davis *et al.*, 2011). Use of the small molecule inhibitor GW2580 in a model of mammary tumour driven by erbB2/Neu oncogene expression was associated with a decrease in F4/80 high, MHCII moderate TAMs but not F4/80 low, MHCII high ones although the impact of this selective depletion on tumour growth was not investigated (Tymoszuk *et al.*, 2014). In contrast, GW2580 has also been reported to cause a significant reduction in MHCII high TAMs in PDAC, while MHCII low TAMs seemed unaffected (Mitchem *et al.*, 2013). In this study MHCII high TAMs dominated the tumour microenvironment suppressing T cell responses and a reduction was associated with reduced metastases, better responses to chemotherapy and increased T cell activation. A different inhibitor of the same kinase, JNJ-40346527, has been shown to result in increased

growth of the primary tumour in the 4T1 model (Kumar *et al.*, 2017). The group described a decrease in TAMs but increase in $CD11b^+$, Ly6C low, $Ly6G^+$ cells which they classified as a type of myeloid derived suppressor cell. These cells might actually be neutrophils, as neutrophils are also capable of suppressing other immune cells (Negorev *et al.*, 2018).

Inducing macrophage apoptosis via clodronate liposomes

In contrast to blocking macrophage recruitment and function, depletion of macrophages can be achieved via the use of clodronate liposomes (clodrosomes). Liposomes are small (50-1000 nm) spherical vesicles consisting of one or more phospholipid bilayers enclosing an aqueous centre. They are automatically formed by the dispersion of phospholipids into water (Rooijen and Sanders, 1994). Clodronate is a strongly hydrophilic molecule that can be dissolved in aqueous solution when encapsulated during liposome formation. For macrophage depletion clodronate containing liposomes are injected *in vivo* to be taken up by phagocytes. Once internalised, the phagosome will fuse with a lysosome resulting in degradation of the phospholipid bilayer by phospholipases and release of clodronate into the cytosol. Here, clodronate is metabolised to AppCCl2p which interferes with energy metabolism in the macrophage and will eventually cause cell death by apoptosis (Van Rooijen, Sanders and Van Den Berg, 1996) as illustrated in Figure 1.4 (Lehenkari *et al.*, 2002). While apoptosis can cause local inflammation, this could either be beneficial in a tumour microenvironment as in an acute state this could result in increased activation of adaptive immune cells. Long term clodronate administration, on the other hand, could cause chronic inflammation and drive tumour progression independently of macrophage content, although this has not been reported in the literature.

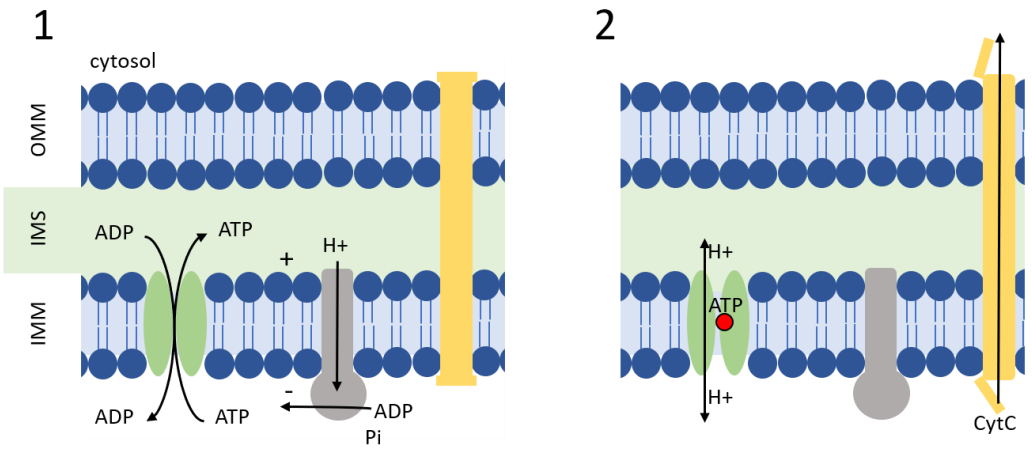

IMM = Inner mitochondrial membrane, IMS = Intermembranous space, OMM = Outer mitochondrial membrane, ATP● = $AppCCl_2p$, CytC = Cytochrome C

Figure 1.4: Clodronate mediated induction of apoptosis

1) The mitochondria is responsible for the generation of adenosinetriphosphate (ATP) from adenosindiphosphate (ADP) via the tricarboxylic acid (TCA) cycle: high energy protons are generated and delivered into the intermembranous space along the electron transport chain. This creates an electrochemical proton gradient providing energy for the ATP synthase (grey) to convert ADP into ATP. ATP is transported into the cytosol by the ATP/ADP translocase (green) which simultaneously transfers one molecule of cytosolic ADP into the mitochondria.

2) AppCCl2p present in the cytosol can cross the outer mitochondrial membrane and bind the ATP binding site on the ATP/ADP translocase blocking its function. This eventually results in hyperpolarisation and opening of permeability transition pores (yellow) depleting electrochemical and proton gradients and releasing mitochondrial proapoptotic factors such as cytochrome C into the cytosol.

Graph adapted from Lehenkari et al., 2002

The free drug on its own does not cross cell membranes and can thus neither escape the macrophage nor affect other cells once released by the dying macrophage. The molecule also has a short half life in circulation being cleared within minutes by the renal system (Fleisch, 1989).

Different routes of administration have been tested to not only induce systemic macrophage depletion but also target specific tissue resident subsets to study their function *in vivo:* intravenous (i.v.) injections deplete macrophages in liver, spleen and bone marrow (Van Rooijen *et al.*, 1990). Subcutaneous (s.c.) administration mainly affects macrophages in draining lymph nodes (Delemarre *et al.*, 1990), intraperitoneal (i.p.) injection rapidly depletes peritoneal macrophages and after passage through draining

lymph nodes can, depending on the volume injected, affect macrophages in liver and spleen (Biewenga *et al.*, 1995). Intranasal administration depletes alveolar macrophages (Thepen, Van Rooijen and Kraal, 1989), intraventricular injection depletes perivascular and meningeal macrophages in the central nervous system (Polfliet *et al.*, 2001) and intra-articular injection selectively depletes phagocytes lining synovial membranes (Van Lent *et al.*, 1993; Barrera *et al.*, 2000). Clodrosomes can also be injected locally in most tissues, however, the ability to spread from the site of injection through the whole tissue does vary between tissue structures.

In the context of cancer, administration of liposomal clodronate in different murine models has been associated with TAM depletion and inhibition of primary tumour growth (Zeisberger *et al.*, 2006; Piaggio *et al.*, 2016; Bader *et al.*, 2018). Interestingly, clodrosome administration in dogs with soft tissue sarcoma achieved reduced TAM infiltration in less than half of the subjects, possibly due the use of significantly lower doses compared to murine models (Guth *et al.*, 2013).

Myeloid derived suppressor cells

Myeloid derived suppressor cells (MDSCs) are a heterogenous population of immature myeloid cells that have been identified in pathological conditions, including cancer, infection and traumatic stress (Atochina *et al.*, 2001; Kusmartsev and Gabrilovich, 2002; Makarenkova *et al.*, 2006). These cells are sub-divided into a granulocytic (polymorphonuclear (PMN), $CD11b^{+}LY6G^{+}LY6C^{low}$) and a monocytic ((M), $CD11b^{+}LY6G^{-}LY6C$) subset, morphologically resembling neutrophils and monocytes respectively (Bronte *et al.*, 2016). The extent to which the different subsets are induced differs between tumours (Youn *et al.*, 2008).

Importantly, while immature myeloid cells are a normal intermediated step in myelopoiesis, these cells usually differentiate in to mature DCs, macrophages, monocytes or granulocytes. Acute inflammatory conditions drive emergency myelopoiesis with immature cells differentiating mostly into neutrophils and monocytes (Gabrilovich, 2017). In contrast, it is thought that during chronic inflammation cell maturation is prevented, resulting in this expansion of MDSCs. Several factors such as VEGF, GM-CSR, CSF1, IL6 and IL10 produced by tumour cells have been implicated in increasing immature myeloid cell release (Kusmartsev and Gabrilovich, 2002).

MDSCs are defined by their ability to suppress T cell responses and thus have to be characterised *in vitro* by functional assays. The two subsets differ in that PMN-MDSCs

express high levels of reactive oxygen species and low levels of nitric oxide, with the reverse phenotype observed in M-MDSCs (Youn *et al.*, 2008). Both types have been suggested to suppress T cells via arginine, IDO, tryptophan starvation and potentially the upregulation of PD-L1 as summarised by Fleming *et al.*, (2018).

It is controversial whether cells that morphologically and phenotypically appear like neutrophils and monocytes need to be classified as MDSCs (Bronte *et al.*, 2016). Indeed in the absence of functional assays it is difficult to distinguish tumour associated neutrophils and PMN-MDSCs. Thus, for the remainder of this thesis $CD11b^{+}LY6G^{-}LY6C^{+}$ cells will be referred to as monocytes, and $CD11b^{+}LY6G^{+}LY6C^{low}$ cells as neutrophils, with the note that these populations may also include MDSCs.

Regulatory T cells

TAMs are not the only immune cells that can affect tumour outcomes: Tregs are a subpopulation of T cells classified by the expression of FOXP3, CD4 and CD25 that contributes to the maintenance of immune homeostasis and prevents autoimmunity by regulating immune responses (Sakaguchi *et al.*, 1995).

Importantly, conventional T cells ($FOXP3^{-}$) can also produce anti-inflammatory cytokines such as IL-10 and TGFβ (Dennis *et al.*, 2015). Studies have shown that chronic inflammation and $CD4^{+}$ T cell activation in the presence of IL-10 creates $CD4^{+}$ $FOXP3^{-}$ Tr1 cells that produce high levels of IL-10 and low levels of IL-2 and suppress $CD4^{+}$ T cell activation in response to antigen (Groux *et al.*, 1997). Such cells have been described in different types of cancer (Bergmann *et al.*, 2008; Scurr *et al.*, 2014; Pedroza-Gonzalez *et al.*, 2015), although their individual contribution to the suppressive environment is not clear. While in some studies the suppressive ability of these cells is described as higher than that of $FOXP3^{+}$ Tregs (Scurr *et al.*, 2014), in other cases it been suggested that Tr1 cells could be beneficial, based on IL-10s immunostimulatory role: in a mouse model of glioma Tr1 cells have been shown to mediate tumour rejection by increasing natural killer cell and cytotoxic T cell responses against tumour cells (Segal, Glass and Shevach, 2002).

Treg development

There are two types of Tregs mainly defined by the location of their development. Thymic or natural Tregs (tTregs) develop in the thymus: all T lymphocytes are derived from bone marrow precursors and undergo important developmental steps in the thymus. Somatic DNA arrangement gives rise to random T cell receptors (TCRs) which govern the fate of the cell expressing them: in a first phase of positive selection T cells need to be able to recognise self in the context of MHC expression. T cells unable to bind MHC expressed by thymic epithelial cells die due to neglect, while those reactive to self MHC can proceed to the second step. This next stage termed negative selection is now antigen dependent: antigen presenting cells (APCs) express self peptide complexed with MHC molecules. T cells harbouring TCRs strongly responding to such self peptide-MHC complexes undergo clonal deletion, as they are autoreactive and would cause autoimmunity if released into the periphery. Only T cells receiving appropriate low to intermediate signals through their TCRs are positively selected and allowed to mature (Starr, Jameson and Hogquist, 2003). In this setting it has been shown that T cells that recognise self peptide-MHC complexes with an intermediate affinity i.e. stronger than conventional T cells but not strong enough to induce negative selection, will later develop into tTregs (Moran *et al.*, 2011). Such cells make up 5-10% of peripheral $CD4^+$ T cells. They are essential, as despite negative selection the healthy immune system still contains a small population of auto-reactive T cells due to a lack of expression of some tissue-specific genes in the thymus. In line with this, tTreg elimination in naïve mice results in spontaneous development of autoimmune conditions (Shih *et al.*, 2004; Kim, Rasmussen and Rudensky, 2007).

The exact origin of peripheral Tregs (pTregs) is less well understood, at least partly due to problems in distinguishing pTregs from tTregs in mixed cell populations. It is however known that naïve $CD4^+$ $FOXP3^-$ T cells can be transformed into pTregs upon exposure to TGF-β and IL-2 *in vitro* (Chen *et al.*, 2003) as well as in response to prolonged small doses of antigen *in vivo* (Apostolou and Von Boehmer, 2004). pTreg generation is thought to mostly rely on antigen presentation by APCs in an anti-inflammatory setting: dendritic cells (DCs) can be highly tolerogenic and in an anti-inflammatory setting generate pTregs to prevent immune activation against ligands that can not be expressed in thymus during tTreg induction. Thus, DC depletion results in lower levels of pTregs as well as enhanced effector T cell responses (Darrasse-Jèze *et al.*, 2009). Alternatively, pTreg development has been observed in situations of chronic inflammation in several murine models, possibly to

prevent an overreactive immune response, as removal of Treg in herpes simplex virus infection was shown to be associated with accelerated fatal disease progression (Lund *et al.*, 2008).

Given that the pTreg population stems from conventional $CD4^+$ T cells, the TCRs of pTregs are specific for non-self antigen, in contrast to those of highly self antigen reactive tTregs created in the thymus. The differentiation of regulatory cells in the periphery is thought to be the main cause of tolerance to non-pathogenic antigen including environmental substances as well as antigen from commensal organisms that can not be presented by thymus resident cells.

Treg phenotype

tTregs were originally defined as $CD4^+$, $CD25^+$ T cells. During development in the thymus stimulation through a TCR with high affinity for an MHC-peptide complex induces expression of CD25, the α-chain of the interleukin 2 (IL-2) receptor (Jordan *et al.*, 2001). CD25 is crucial for tTreg maturation in the thymus (Burchill *et al.*, 2008) as well as for Treg function and maintenance in the periphery: neutralisation of IL-2 reduces tTreg numbers and causes autoimmune conditions in genetically susceptible murine models (Setoguchi *et al.*, 2005). The data on the importance of CD25 and IL-2 in pTregs are less conclusive, but IL-2 is thought to be essential for pTreg generation from conventional T cells *in vitro* (Davidson *et al.*, 2007). Tregs also constitutively express CTLA-4 (Takahashi *et al.*, 2000) and LAG3 (Huang *et al.*, 2004).

While all these markers are often used to identify Tregs in experimental settings this has to be done with caution as many of them are also upregulated on conventional T cells upon activation. While no cell surface marker unique to Tregs exists, in mice FOXP3 is exclusively expressed in tTregs and certain suppressive pTreg populations. Indeed, FOXP3 is required for the generation of tTregs and its deficiency has been shown to result in a loss of this suppressive population driving lethal lymphoproliferative autoimmunity (Fontenot, Gavin and Rudensky, 2017).

While this is also true in humans, human activated T cells can express FOXP3, (Wang *et al.*, 2007), if only transiently (Allan *et al.*, 2007), without possessing regulatory functions. This suggests that FOXP3 expression on its own is not sufficient to induce a Treg phenotype in humans.

Treg suppressive mechanisms

Regardless of origin, all Tregs induce immune suppression via four main mechanisms: manipulation of APCs, production of anti-inflammatory cytokines, competition for growth factors and cytotoxicity (Sojka, Huang and Fowell, 2008; Magnani *et al.*, 2011).

Manipulation of antigen presenting cells

Effector T cell stimulation through ligation of the TCR to a peptide-MHC complex on its own does not provide enough signal strength to induce T cell activation. Anergy, a state in which naïve T cells fail to respond and become refractory to re-stimulation can only be prevented by simultaneous ligation of the TCR and at least one co-stimulatory receptor expressed on the T cell surface. In contrast, ligation of a co-inhibitory receptor with the TCR negatively regulates T cell activation. Integration of signals through positive and negative co-receptors ultimately decides the fate of the T cell (Takase and Saito, 1995). The ligands for such receptors are expressed by APCs. Tregs regulate effector T cell activation at least partly via their effect on APCs: Tregs express CTLA-4, binding its cognate ligands CD80 and CD86 on APCs with higher affinity than CD28 expressed by effector T cells. This allows Tregs to outcompete effector T cells for the ligand needed to provide co-stimulatory signals. Further, CTLA-4 ligation to its receptors on the DC surface has been shown to downregulate DC CD80/86 expression and CTLA-4 blockade could reduce DC suppression of effector T cells (Oderup *et al.*, 2006). CTLA-4 dependent Treg/DC interaction has also been shown to induce the production of IDO from certain subsets of DCs (Fallarino *et al.*, 2003) which potently suppresses effector T cells *in vivo* and *in vitro* (Mellor and Munn, 2004).

Cytokine production

The primary cytokines released by Tregs are the anti-inflammatory IL-10, TGF-β and IL-35. Treg produced IL-10 specifically has been shown to have important regulatory roles in models of allergic diseases (Francis, Till and Durham, 2003; Nouri-Aria *et al.*, 2004), due to its ability to inhibit mast cell (Arock *et al.*, 1996) and eosinophil activation (Takanaski *et al.*, 1994).

TGF-βs exist in three isoforms in mammals, with TGF-β1 being the predominant one in the immune system (Govinden and Bhoola, 2003). Tregs especially have been shown to produce high levels of TGF-β1, both in membrane bound and secreted form. T cell specific ablation of TGF-β1 is associated with fatal early-onset, multiorgan autoimmunity in mice (Marie, Liggitt and Rudensky, 2006). Also, although TGF-β was not necessary for Treg

suppression of effector T cell proliferation *in vitro*, TGF-β1 released by Tregs was essential to prevent colitis in several murine studies (Nakamura *et al.*, 2004).

The heterodimeric IL-35 has been identified as an essential suppressive cytokine released by Tregs. While mice with Tregs deficient in either chain did not present with overt autoimmunity, they showed significantly reduced suppression of effector T cells compared to wild type counterparts *in vitro* and *in vivo* (Collison *et al.*, 2007). In contrast to mice, human Tregs have been found to lack constitutive expression of IL-35 (Bardel *et al.*, 2008). Expression of the cytokine could, however, be induced upon activation with anti-CD3 and -CD28 antibodies and blocking IL-35 but not IL-10 or TGF-β reduced contact independent suppressive abilities *in vitro* (Chaturvedi *et al.*, 2011).

The relative importance of these cytokines varies across different models suggesting that the mode of suppression by Tregs is context dependent. For example, Treg production of IL-10 is rare in the spleen but abundant in the intestinal lamina propria, supporting a role for IL-10 in mucosal immunity (Uhlig *et al.*, 2006).

Competition for growth factors

While at least tTregs critically rely on IL-2 for survival, they can not produce it on their own and depend on IL-2 secreting effector cells. A high expression of CD25 allows them to outcompete effector T cells. The resulting lack of IL-2 in the environment has been shown to cause cytokine deprivation–induced apoptosis of effector cells *in vitro* (Pandiyan *et al.*, 2007). This method of suppression did rely on close proximity between Tregs and cytokine producing effector T cells but likely not direct cell to cell contact. In addition, Tregs reduce effector T cell production of IL-2 (Thornton and Shevach, 1998) in a contact dependent manner, while also downregulating cell surface CD25 expressed by effector cells (Annunziato *et al.*, 2002).

Cytotoxicity

Cytotoxicity describes the active killing of a target cell. One major pathway of inducing cell death is via the perforin/granzyme pathway in a cell contact dependent mechanism: the cytotoxic cell forms an immunological synapse with its target cell allowing secretory granules to fuse with the presynaptic membrane to release perforin and granzymes into the synaptic cleft. Pores in the postsynaptic membrane are formed by perforin enabling target cell entry of granzymes (Voskoboinik, Whisstock and Trapani, 2015). As there are a plethora of different granzymes, the pathway by which cell death is triggered will vary

across the different types (Bots and Medema, 2006). Human tTregs have been shown to predominately express granzyme A after stimulation *in vitro,* while *in vitro* induced pTregs preferentially upregulate granzyme B expression. The ability of both those Treg types to lyse allogeneic tumour cell lines was shown to be dependent on perforin but independent of MHC/TCR complex engagement, although the mechanism behind TCR independent recognition is unclear (Szymczak-Workman, Workman and Vignali, 2009). Both types were further shown to preferentially lyse activated effector T cells over naïve cells (Grossman, Verbsky, Barchet, *et al.*, 2004; Grossman, Verbsky, Tollefsen, *et al.*, 2004).

The combination of all these mechanisms is vital to prevent the activation of auto-reactive lymphocytes resulting in autoimmunity and to maintain tissue homeostasis in a healthy environment. In the context of cancer however, the suppressive action of infiltrating Tregs can be detrimental.

Tregs in the tumour microenvironment

Since the discovery of Tregs, increased numbers of tumour infiltrating Tregs have been documented in many solid cancers including breast (Bates, 2006), ovarian (Sato *et al.*, 2005) and gastrointestinal (Sasada *et al.*, 2003) malignancies. While some groups have reported an association of high Treg infiltration with improved prognosis (Correale *et al.*, 2010), it is likely that this is due to an increase in all tumour residing T cell populations as the most important parameter affecting disease outcome is the ratio between Tregs and effector T cells: a high $CD8^+$:Treg ratio was found to be associated with improved prognosis, both on its own and with chemotherapy in different types of human cancer (Sato *et al.*, 2005; Baras *et al.*, 2016; Takada *et al.*, 2018). Murine models support the idea of Tregs being detrimental: Treg depletion by administration of anti-CD25 monoclonal antibodies increased anti-tumour immune responses and tumour eradication by activation of tumour specific and non-specific T cells (Shimizu, Yamazaki and Sakaguchi, 1999). Further, adoptive transfer of tumour specific $CD8^+$ T cells on their own induced tumour elimination, while the simultaneous transfer of Tregs hindered this process (Antony *et al.*, 2005).

Tumour Treg phenotype and function

Tregs in the tumour microenvironment employ the same suppression strategies as in healthy tissues. Secreted TGF-β and IL-10 can support tumour progression by inhibiting expansion, cytokine release and cytotoxicity by effector T cells while also re-programming DCs into tolerogenic states (Yona *et al.*, 2013). Tregs were also shown to upregulate

granzyme B expression in mice challenged which melanoma, leukaemia and lymphoma cell lines, which prevented clearance of tumour cells by acting on natural killer cells and/or $CD8^+$ T cells (Cao *et al.*, 2007).

Further, $FOXP3^+$ T cells have been reported to establish long lasting interactions with DCs in tumour draining lymph nodes. These cell to cell contacts were tumour antigen dependent and induced DC death via perforin secretion. Such a reduction in APCs would limit effector T cell activation and reduce anti-tumour immune responses (Boissonnas *et al.*, 2010).

While tumour associated Tregs retain their usual suppressive functions, they also display phenotypic differences associated with transcriptional changes compared to both, circulating Tregs and Tregs infiltrating healthy tissue: single cell analysis of Tregs present in colorectal or non small cell lung cancers revealed elevated levels of genes associated with high suppressive function, including CTLA-4, OX40 and GITR, but also upregulation of genes not normally expressed in the Treg population including PD-L1. The group further identified a gene signature shared between Tregs in not only colorectal and lung cancer but also breast and gastric carcinomas (De Simone *et al.*, 2016).

In contrast, another study investigating transcription patterns of human breast cancer found resident Tregs displaying gene expression patterns similar to those of Tregs infiltrating normal breast tissue rather than activated peripheral blood Tregs. However, the group also found an upregulation in different cytokine and chemokine receptor genes including *Ccr8*, the expression of which was low in normal breast tissue and blood Tregs (Plitas *et al.*, 2016). *Ccr8* was also part of the identified tumour Treg signature and expressed across various cancer types (De Simone *et al.*, 2016).

Treg specific action on TAMs

While studies of Treg immune regulation mostly focus on their suppression of effector T cells, Tregs are able to interact with APCs and could manipulate TAM populations inducing an immune tolerant state. Co-culture of human monocyte derived macrophages with Tregs resulted in reduced production of several proinflammatory cytokines compared to culturing the same cells with effector T cells. Even after Treg removal from cultures, myeloid cells showed downregulation of CD80/86, human leukocyte antigen II and CD40 as well as reduced abilities to produce TNF-α and IL-6 upon stimulation with LPS (Taams *et al.*, 2005). *In vivo*, in a model of bacterially induced intestinal inflammation in $RAG2^{-/-}$ mice T cell independent inflammation driven by innate immune activation was inhibited by co-transfer of Tregs (Maloy *et al.*, 2003). Similarly, reconstitution of Tregs expressing high

levels of FOXP3 into SCID mice in a model of chronic renal disease resulted in significant reduction of renal injury associated with a drop in kidney macrophage numbers (Mahajan *et al.*, 2006).

Treg homing into the tumour

During homeostatic conditions Tregs are generally found within lymphoid tissues (Wei, Kryczek and Zou, 2006). Trafficking into target organs depends on the expression of chemokine and cytokine receptors that bind ligands produced within the tissue and drive chemotaxis. Tregs can express a variety of such trafficking and homing receptors that allow them to infiltrate specific non-lymphoid tissues. As it has been shown that in ovarian cancer tumour draining lymph nodes contain fewer Tregs compared to non-tumour draining lymphoid organs, it seems likely that Tregs traffic from those lymph nodes into cancer tissue (Curiel *et al.*, 2004). This recruitment is likely driven by different chemokine and receptor pairs: CCR8 binds to the chemokine CCL18 highly expressed across chronically inflamed tissues in humans (Pivarcsi *et al.*, 2004; de Nadaï *et al.*, 2006) where it is produced by myeloid cells including macrophages (Hieshima *et al.*, 1997). In human breast cancer TAMs have been shown to produce high levels of CCL18 which was associated with poor prognosis (Chen *et al.*, 2011). While the group identified PITPNM3 expressed on breast cancer cells as a receptor for CCL18 that was involved in the regulation of metastasis, CCL18 also acts as a chemoattractant for Tregs as the use of an anti-CCR8 blocking antibody significantly reduced $CCR8^+$ Tregs in a colorectal cancer model enhancing anti-tumour immunity (Villarreal *et al.*, 2018). CCR8 also binds to CCL1, which is upregulated in many tumours (Kuehnemuth *et al.*, 2018). Importantly, CCL1 not only activates Tregs but is also important in their *de novo* conversion and suppressive function (Hoelzinger *et al.*, 2010). Another chemokine abundantly expressed in the tumour microenvironment is CCL22 produced by both macrophages and tumour cells themselves, attracting CCR4 expressing Tregs (Curiel *et al.*, 2004).

Targeting Tregs in anti-tumour therapy

Treg depletion with an anti-CD25 immunotoxin caused tumour regression and increased anti-tumour immunity associated with $CD8^+$ T cell infiltration in different mouse models (Onda, Kobayashi and Pastan, 2019). The same effect was observed in different types of tumours with the use of anti-CD25 monoclonal antibodies (Jones *et al.*, 2002; Arce Vargas *et al.*, 2017), a nanodrug system (Gao *et al.*, 2019) or via a TCR mimic antibody binding a FOXP3-derived target bound to MHC (Dao *et al.*, 2019). In contrast, in a model of

pancreatic cancer Treg depletion was associated with enhanced tumour growth and myeloid cell recruitment caused by reprogramming of fibroblasts into inflammatory subtypes (Zhang *et al.*, 2020). While there are many ways to target Tregs in the tumour microenvironment, only two options relevant for this thesis will be discussed here.

PI3Kδ inhibition

One strategy is the use of the phosphatidylinositol 3-kinase (PI3K) δ inhibitor PI-3065 (Figure 1.5).PI3Ks are enzymes that generate intracellular lipid mediators regulating various functions governing cellular growth and survival. Mammals have eight PI3K isoforms which are divided into three different families. The most studied class I_A isoforms (PI3Kα, β, γ, δ) are heterodimers of the catalytic p110 subunit (p110α, p110β, p110γ, and p110δ) with a regulatory p85 subunit (Vanhaesebroeck *et al.*, 2010). In mammalian cells class I PI3Ks are expressed ubiquitously across different cell types, with p110δ and p110γ subunits especially enriched in leukocytes (Kok, Geering and Vanhaesebroeck, 2009). The different subunits are activated by engagement of different cell surface receptors: class 1_A (p110α, p110β, or p110δ) signalling is activated by tyrosine kinase activity including cytokine receptors and the TCR, while class 1_B (p110γ) subunits are primarily engaged after ligation of G protein-coupled receptors including chemokine receptors (Han, Patterson and Levings, 2012). Under physiological conditions binding of p110 to the regulatory subunit prevents PI3K activation. Ligation of the corresponding transmembrane receptor results in autophosphorylation of tyrosine residues in the cytoplasmic receptor region and ultimately PI3K recruitment to the receptor. Upon activation, the catalytic p110 subunit phosphorylates phosphatidylinositol-4,5-bisphosphate creating phosphatidylinositol-4,5-triphahosphate which acts as a secondary messenger recruiting proteins to the plasma membrane via their PH domains. The primary downstream mediator of PI3K activated signalling is AKT which has important roles in the regulation of various cellular events by the phosphorylation of different intracellular substrates (Xu *et al.*, 2012).

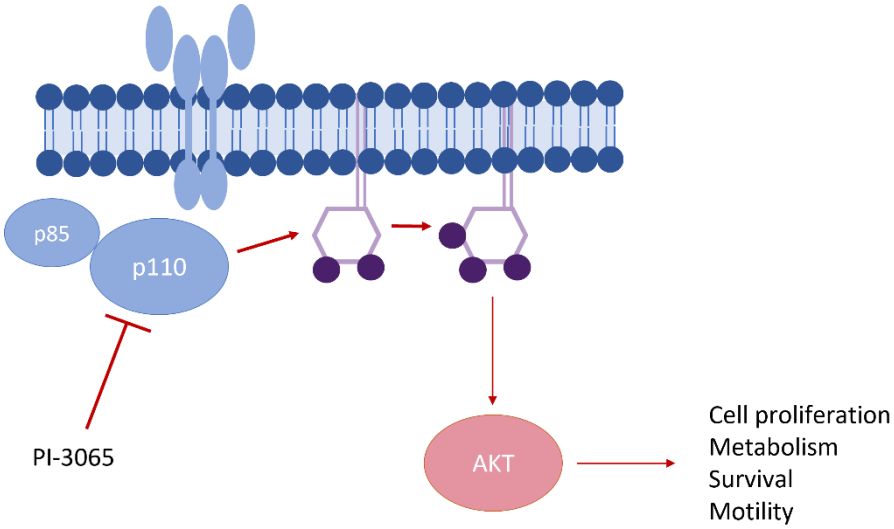

Figure 1.5: PI-3065 inhibition of T cell PI3Kδ signalling

Class 1_A PI3Ks consist of a regulatory (p85) and a catalytic subunit (p110). They act downstream of receptor tyrosine kinases and integrate signals derived from T cell receptors as well as receptors involved in co-stimulation and cytokine signalling. Ligand binding results in release of the catalytic subunit allowing the phosphorylation of phosphatidylinositol-4,5-bisphosphate (PI(3,4,5)P2) to PI(4,5)P3. The PH domains of PIP3 act as a binding site for AKT enabling its phosphorylation, activation and action on downstream substates affecting cell cycle, survival and metabolism.

PI-3065 is a small molecule inhibitor selectively inhibiting the class I p110δ which is highly expressed in leukocytes, preventing PIP2 phosphorylation and downstream signalling.

Graph adapted from Shi et al., 2019

In T cells, the PI3K-AKT axis is important for development (Juntilla *et al.*, 2007) and function, with different relative importance of the various subunits in different T cell subsets (Martin *et al.*, 2008; Thomas *et al.*, 2008). Tregs are more dependent on PI3K-AKT mediated signalling compared to conventional $CD4^+$ and $CD8^+$ T cells as PI3Kδ inhibitors significantly reduce activation and proliferation of Tregs but not conventional T cells *in vitro*. This is because Tregs predominately rely on p110δ, while in conventional T cells p110α and p110β can compensate for a loss of p110δ (Ahmad *et al.*, 2017). p110δ has also been shown to be important for TCR mediated immune suppression in Tregs. Tregs from

p110D910A/D910A mice do, however, retain some suppressive capacity as they do not develop lethal autoimmunity (Patton *et al.*, 2006).

Use of depletion of regulatory T cell (DEREG) mice

Another method of depleting the Treg population is the use of DEREG mice. The DEREG model was developed through bacterial artificial chromosome (BAC) transgenesis, inserting big genome fragments containing not only the target gene but also potential modulators and regulators into the genome. Here, the inserted BAC included the *foxp3* locus as well as a diphteria toxin receptor (DTR)-eGFP fusion protein inserted into the first *foxp3* exon to track gene expression (Lahl and Sparwasser, 2011). In the resulting transgenic mice only cells with endogenous FOXP3 expression produce the DTR and administration of diphteria toxin (DT) blocks intracellular protein synthesis resulting in target cell apoptosis (Pappenheimer *et al.*, 1982).

Tumour model used in this thesis

The 4T1 model is a murine mammary carcinoma isolated from a spontaneous tumour in BALB/cfC3H mice (Dexter *et al.*, 1978). The primary tumour grows progressively, culminating in lethal disease even after its surgical resection, by metastasising into organs also commonly affected by human breast cancer metastasis (lungs, bone, liver, brain) (Danna *et al.*, 2004). Thus, it provides an excellent model to study human metastatic breast cancer. As in every other malignancy, the 4T1 tumour microenvironment is complex and plastic, shaped by reciprocal interactions between malignant cells, stroma and immune cells. The immune cell infiltration of the primary tumour is dominated by myeloid cells, with $CD11b^+$ cells constituting up to 86% of the total $CD45^+$ content (DuPre´, Redelman and Hunter, 2007). This recruitment of myeloid cells is likely to be driven by tumour cell derived chemokines and cytokines: 4T1 cells are known to produce GM-CSF, with neutralising anti-GM-CSF antibodies reducing primary tumour growth at injection sites and preventing macrophage production of CCL2 (Yoshimura *et al.*, 2016). This reflects human BRCA1-IRIS-overexpressing TNBC where tumour cell production of high amounts of GM-CSF was shown to recruit macrophages (Sami *et al.*, 2020). While GM-CSF plays a role in macrophage attraction, GM-CSF deficient mice did not present with altered 4T1 primary tumour growth, cytokine production or immune cell infiltration (Yoshimura *et al.*, 2019), likely reflecting the fact that the 4T1 line comprises a mixture of cell types and tumour promoting mechanisms

are redundant (Wagenblast *et al.*, 2015). Heterogeneity within a tumour cell line has also been reported for the MDA-MB-231 (Norton, Popel and Pandey, 2015) and MCF7 breast cancer lines (Khan *et al.*, 2017) and has been attributed to asymmetric cell division.

4T1 cells also produce high amounts of granulocyte colony stimulating factor (G-CSF), the blockade of which reduced lung metastasis (duPre' and Hunter, 2007). G-CSF was found to be highly expressed in human TNBC, associated with poor overall survival (Hollmén *et al.*, 2016). Importantly, G-CSF acts as a growth factor for neutrophils, with G-CSF or $Ly6G^+$ $Ly6C^+$ cell neutralisation associated with reduced metastasis, pointing towards a role of neutrophils in tumour progression (Kowanetz *et al.*, 2010).

Further*, ex vivo* co-culture of peritoneal macrophages extracted from healthy mice together with 4T1 cells from primary tumours was shown to result in increased IL-6 production by both cell types, enhanced macrophage production of NO but decreased macrophage production of TNF-α compared with macrophages cultured alone (Beury *et al.*, 2014).

In addition to TAMs, elevated Treg numbers have been documented in 4T1 tumour bearing mice, and have been associated with suppressed antitumour immune responses (Liu *et al.*, 2009). Treg depletion resulted in increased immune responses in the primary tumour limiting metastasis. However, if metastases were already established, Treg depletion alone did not limit metastatic progression (Hughes *et al.*, 2020), indicating that therapeutics targeting Tregs alone will not be able to treat breast cancer associated lung metastasis. Thus, given TAMs' role in tumour metastasis, it is possible that a combination of Treg depletion and macrophage targeting therapeutics could be beneficial in controlling both, primary tumour growth and metastasis.

Hypothesis and Aims

The hypothesis of this thesis states that the primary tumour contains a heterogenous population of macrophages that differ in their function and effect on tumour growth and metastasis. I hypothesised that some of these macrophage populations would support tumour growth, while others would be protective. Furthermore, selective manipulation of TAMs, especially in combination with Treg inhibition, would be beneficial in the control of primary tumours and metastasis.

The aims of the experiments summarised in this thesis were to:

1: Optimise tumour processing for single cell sequencing.

2: Identify the distinct subsets of tumour infiltrating macrophages using single cell sequencing and investigate their function.

3: Manipulate immune cell subsets *in vivo* to achieve primary tumour regression and/or reduction of metastasis.

Chapter 2: Materials and methods

Mice

Female BALB/c were obtained from Charles River, DEREG mice (Lahl *et al.*, 2007) were bred inhouse. All animals were housed in filter-top cages in specific pathogen-free condition. All procedures were carried out in line with the Animals Scientific Procedures Act 1986 in accordance with UK Home Office regulations.

Tumour induction and tissue culture

4T1 is a verified cell line what was purchased from the American Type Culture Collection and tested for mycoplasma. Cells were cultured in full medium (RPMI-1640 (Sigma-Aldrich)) containing L-glutamine (Thermofisher) at 0.3 g/L, 10 % (v/v) fetal bovine serum (FBS) (Thermofisher), 0.2 U/µL Penicillin and 100 µg/ml Streptavidin (Thermofisher). Tumour cells were split 1/10 up to three times a week and were grown for 3 to 6 passages before being injected. To harvest cells, flasks were washed with warm phosphate-buffered saline (PBS), the wash was discarded, trypsin-EDTA (0.05 %), phenol red (Thermofisher) was added and left to incubate until cells detached. Full medium was added to inactivate trypsin, cells were centrifuged at 350 x g for 5 minutes, washed two times with PBS, stained with trypan blue (Thermofisher) and counted on a haemocytometer. On the day of injection, 1 x 10^5 cells resuspended in 100 µl PBS were injected subcutaneously (s.c.) around the mammary fat pad of the right or left lower quadrant using an insulin needle. Tumour growth was assessed by measuring two-dimensional size with electronic callipers: perpendicular measurements were used to calculate the mean diameter of the tumour. Mice were culled before tumours reached a diameter of 17 mm in either direction or at a maximum of 28 days after injection.

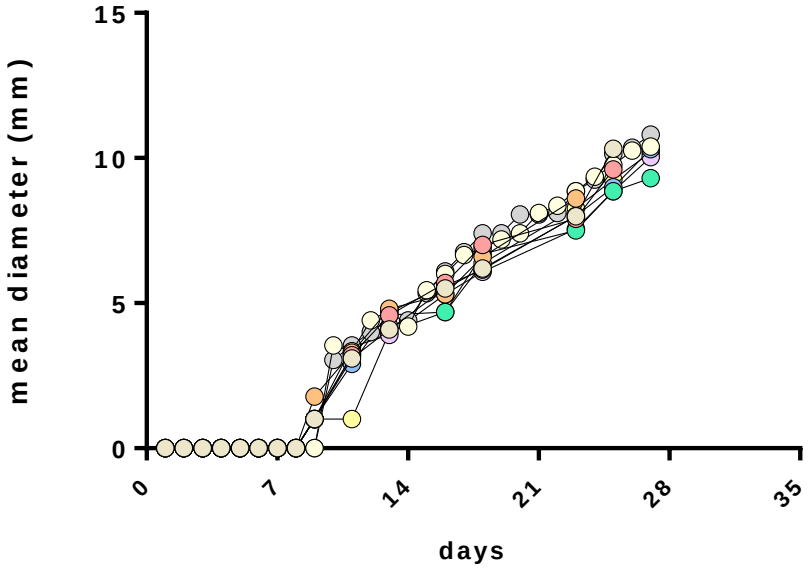

Figure 2.1: Typical growth curve of 4T1 tumours

Tumours were measured at least every other day and mean diameter was calculated by adding the height and length of a tumour and dividing by 2. Each colour represents a different mouse. N = 9, Data pooled from 2 different experiments; Curve is representative of typical growth observed in 4T1 tumours.

Enzymatic digestion of primary tumours and metastatic target organs

If lungs were taken to be analysed, transcardial perfusion with PBS was performed to remove blood and circulating leukocytes.

Tumours, lungs and spleens were excised, minced with scissors in 1 ml medium of choice containing a mixture of the following enzymes as indicated:

-Collagenase type IV (Sigma-Aldrich, C5138) (2 mg/ml)
-DNase I (Sigma-Aldrich, 11284932001) (0.03 mg/ml)
-Hyaluronidase (Sigma-Aldrich, H3506) (1.5 mg/ml)
-Liberase TL (Sigma-Aldrich, 05401020001) (0.015 mg/ml)

Samples were either directly incubated for 30 minutes at 37 °C shaking or placed in the gentleMACS™ dissociator (Miltenyi) using C-tubes with an organ specific program prior incubation.

After incubation, 15 µL of 0.5 mM of EDTA were added to each lung, spleen and tumour sample to stop enzymatic digestion and cells were passed through 40 µm strainers and centrifuged for 5 minutes at 350 x g and 4°C.

For lung and spleen samples, red blood cells were lysed with ACK lysis buffer (150 mM NH_4Cl, 10 mM $KHCO_3$, 0.1mM NA_2EDTA, pH 7.2) and samples were again passed through a 40 µm strainer. All samples were washed twice in PBS before being resuspended in MACS buffer (500ml PBS + 4 % (v/v) FBS + 1 mM EDTA).

Whole femurs were excised and flushed with PBS to collect bone marrow and resident cells.

Sample staining for flow cytometry

Cells were counted by haemocytometer or Muse Cell Analyser (Merck) and 1 x 10^6 cells per stain were plated in a 96 well V bottom plate. To assess viability LIVE/DEAD Fixable stains (Thermofisher) were reconstituted according to the manufacturer's protocol and 0.1 µl of dissolved dye in 100 µl of PBS was added per 1 x 10^6 cells. Samples were incubated for 15 minutes in the fridge before being washed 3 times with PBS.

If no intracellular antibody staining was required, cells were fixed in 50 µl of PBS, 2 % (w/v) PFA for 15 minutes, washed 1 x with PBS and resuspended in MACS buffer containing 10 % rat serum and 4 µg/ml rat anti-mouse FcyRII/III 2.4G2 antibody (home-made) for 15 minutes on ice before being stained for 30 minutes in the fridge.

If intracellular antibody staining was required, the FOXP3 Transcription Factor Staining Buffer Set (eBioscience) was used as follows: buffers and solutions were prepared according to the manufacturer's protocol. 50 µl of Fixation/Permeabilization Buffer were added to each well for 30 minutes at room temperature and the samples were protected from light. Samples were centrifuged at 350 x g for 5 minutes, supernatants were discarded and cells were washed 1 x with 100 µl of 1X Permeabilization Buffer. Cell pellets were resuspended in 50 µl of 1X Permeabilization Buffer with 10 % (v/v) rat serum and 4 µg/ml of rat anti-mouse FcyRII/III 2.4G2 antibody (home-made) for 15 minutes on ice before being stained 30 min in the fridge.

Following antibodies and dyes were used for flow cytometry:

Reagent	Supplier	Cat. no	Isotype	Clone	Concentration used
FITC – CD3e Monoclonal Antibody	Invitrogen	HM3401	Syrian hamster / IgG	500A2	0.25 µg/ml
FITC – rat anti-mouse CD86	Serotech	MCA1587F	Rat IgG2a	PO3	1.25 µg/ml
FITC – C1qa	Cambridge Bioscience	HM1096F	Mouse IgG2b	JL-1	0.25 µg/ml
FITC – rat anti-mouse I-A/I-E	BD Biosciences	553623	Rat IgG2a, κ	2G9	1.25 µg/ml
FITC – anti-mouse I-Ak (Aαk)	BioLegend	110006	Mouse (BALB/c) IgG2b, κ	11-5.2	1.25 µg/ml
Alexa Fluor® 488 – anti-mouse F4/80	BioLegend	123120	Rat IgG2a, κ	BM8	1.25 µg/ml
PE – anti-mouse CD45	Biolegend	103106	Rat IgG2b, κ	30-F11	1.25 µg/ml
PE – Rat anti-mouse Siglec-F	BD Biosciences	562068	OU/M IgG2a, κ	E50-2440	0.33 µg/ml (lung) 0.5 µg/ml (all other)
PE – anti mouse CD3	BioLegend	100205	Rat IgG2b, κ	17A2	0.33 µg/ml
PE – rat anti mouse CD19	BD Pharmingen	557399	Lewis IgG2a, κ	1D3	0.33 µg/ml
PE – anti-mouse CD335 (NKp46)	Biolegend	137601	Rat IgG2a, κ	29A1.4	1.66 µg/ml
PE – Rat anti-mouse TER-119/Erythroid Cells	BD Pharmingen	553673	IgG2b, κ	TER-119	0.5 µg/ml
PE – Nur77	Invitrogen	12-5965-82	Mouse IgG1, κ	12.14	0.5 µg/ml
PE – anti-mouse CD274	BioLegend	155403	Rat IgG2a, λ	MIH7	0.5 µg/ml
PE – Rat anti-mouse CD62L	BD Biosciences	553151	Rat IgG2a, κ	MEL-14	0.5 µg/ml

PE – hamster anti-mouse CD11c	BD Biosciences	557401	Armenian Hamster IgG1, λ2	HL3	0.5 µg/ml
Propidium Iodide Stain	Immuno-chemistry Technologies	638			
PerCP – anti-mouse CD11c	BioLegend	117326	Armenian Hamster IgG	N418	0.5 µg/ml
PerCP – anti-mouse Ly-6G	BioLegend	127654	Rat IgG2a, κ	1A8	0.25 µg/ml
PerCP-Cy™5.5 – hamster anti-mouse CD3e	BD Pharmingen	551163	Armenian Hamster IgG_1, κ	145-2C11	0.5 µg/ml
PE/Cy7 – FOXP3	Invitrogen	25-5773-82	Rat IgG2a, κ	FJK-16s	0.5 µg/ml
PE/Cy7 – anti-mouse CD64 (FcγRI)	BioLegend	139313	Mouse IgG1, κ	X54-5/7.1	0.5 µg/ml
PE/Cy7 – anti-mouse CD3ε	BioLegend	152314	Syrian Hamster IgG	500A2	0.5 µg/ml
APC – anti-mouse CD4	BioLegend	100412	Rat IgG2b, κ	GK1.5	0.5 µg/ml
APC – anti-mouse CD19	BioLegend	152409	Rat IgG2a, κ	1D3/CD19	0.66 µg/ml
APC – CD209b (SIGN-R1) Monoclonal Antibody	eBioscience	17-2093-80	Armenian hamster / IgG	eBio22D1 (22D1)	0.5 µg/ml
APC – iNOS Monoclonal Antibody	eBioscience	17-5920-82	Rat IgG2a, κ	CXNFT	0.5 µg/ml
APC – rat anti mouse F4/80	BioRAD	MCA497	IgG2b	Cl:A3-1	0.33 µg/ml
APC – anti-Siglec-E	BioLegend	677106	Rat IgG2a, κ	M1304A01	0.5 µg/ml
Alexa Fluor® 700 – anti-mouse/human CD11b	BioLegend	101222	Rat IgG2b, κ	M1/70	1.25 µg/ml

Alexa Fluor® 700 – CD206	BioLegend	141734	Rat IgG2b, κ	M1/70	1.25 µg/ml
eFluor 450 – CD8a Monoclonal	eBioscience™	48-0081-80	Rat IgG2a, κ	C068C2	1.25 µg/ml
eFlour 450 – FceR1 alpha Monoclonal	Thermofisher	48-5898-80	Rat / IgG2a, kappa	53-6.7	0.5 µg/ml
Brilliant Violet 421™ – anti-mouse/human CD11b	BioLegend	101235	Armenian hamster / IgG	MAR-1	0.5 µg/ml
Brilliant Violet 421™ – anti-mouse CD24	BioLegend	101825	Rat IgG2b, κ	M1/70	0.5 µg/ml
Brilliant Violet 421™ – anti-mouse CD14	BioLegend	123329	Rat IgG2b, κ	M1/69	0.25 µg/ml
Pacific Blue™ – anti-mouse Siglec H	BioLegend	129609	Rat IgG2a, κ	Sa14-2	0.5 µg/ml
Brilliant Violet – 510™ anti-mouse CD45	BioLegend	103137	Rat IgG1, κ	551	1.25 µg/ml
Brilliant Violet 605™ – anti-mouse CD11c	BioLegend	117333	Rat IgG2b, κ	30-F11	0.5 µg/ml
Brilliant Violet 605™ – anti-mouse F4/80 Antibody	BioLegend	123133	Armenian Hamster IgG	N418	0.5 µg/ml
Brilliant Violet 605™ – anti-mouse CD4 Antibody	BioLegend	100451	Rat IgG2a, κ	BM8	0.25 µg/ml
Brilliant Violet 605 - I-A/I-E Rat anti-Mouse	BD Biosciences	743872	Rat IgG2b, κ	2G9	0.5 µg/ml
Brilliant Violet 605™ – Streptavidin	Biolegend	405229	Rat IgG2b, κ	M5/11 4.15.2	0.5 µg/ml
Brilliant Violet 711™ – anti-mouse Ly-6C	BioLegend	128037	Rat IgG2c, κ	HK1.4	0.25 µg/ml

Biotin – C1q	Cambridge Bioscience	HM1096 BT	Rat IgG2c, κ	HK1.4	0.33 µg/ml
Biotin – 7/4	Home made	-	Mouse IgG2b	JL-1	0.25 µg/ml
LIVE/DEAD Fixable Aqua stain	Thermofisher	L34957			
LIVE/DEAD Fixable Near-IR stain	Thermofisher	L10119			

Flow cytometry

Flow cytometric data acquisition was performed using an Attune flow cytometer (Thermofisher) and analysis was performed using FlowJo analysis software (TreeStar Inc).

Dead cell removal

3 x 10^6 cells were mixed with 100 µL of dead cell removal beads (Miltenyi, 130-090-101) and passed through an MS column according to the manufacturer's protocol. The efflux was collected as the live cell fraction and the column was removed from the magnet and rinsed with binding buffer to collect the dead cell portion.

Cells were stained with Propidium Iodide (PI) or LIVE/DEAD Fixable Near-IR (Thermofisher, L10119) in PBS. PI labels dead cells by inserting between DNA bases, increasing in fluorescence 20-30 fold upon binding. It does not penetrate viable cells, and thus cannot stain unpermeabilised healthy cells.

Cell sorting

Single cell suspensions were stained with a Fixable Near IR viability dye , CD45, CD11c and CD11b and run through a flow cytometric cell sorter (BD FACSAria™ III) (see Figure 2.2 for the gating strategy).

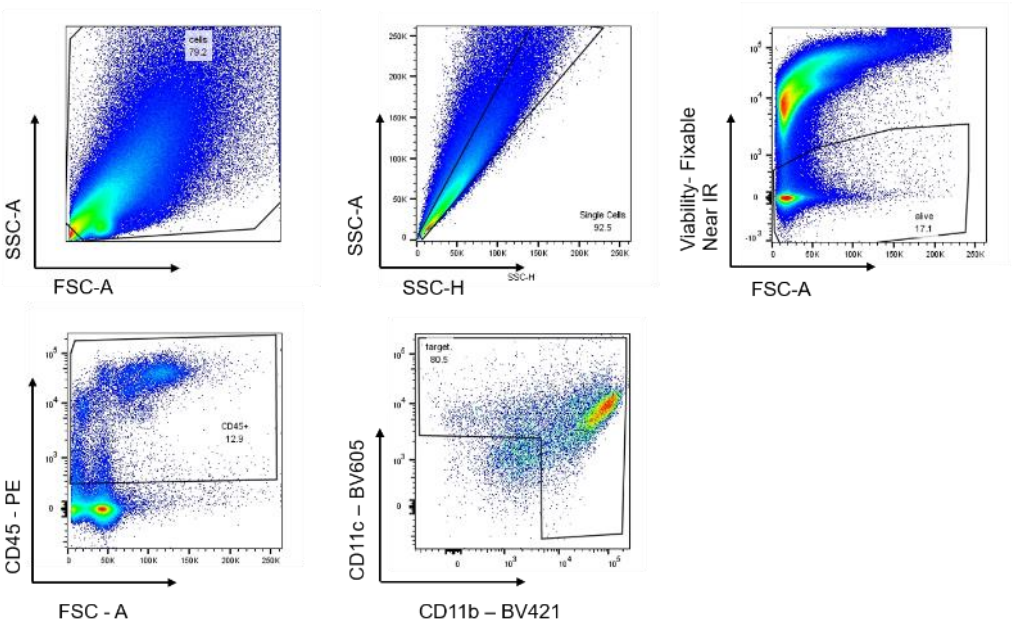

Figure 2.2: Gating strategy for cell sorting

The gating strategy involves sequential removal of debris, doublets and dead cells from the total tumour sample before selecting for $CD45^+$ cells and from this population gating on all $CD11b^+$ and/or $CD11c^+$ cells.

Sorted samples were either run on the ImageStream®X Mark II Imaging Flow Cytometer (Merk) or stained with Fixable Aqua and run on the Attune flow cytometer. Image stream data were analysed with IDEAS software (Merk).

Single cell sequencing

Flow cytometry sorted single cell suspensions were re-suspended in 0.04% BSA (w/v, 400 µg/ml) in magnesium and calcium free PBS, washed three times (350 x g for 5 min) and counted three times on the muse cell counter based on individual draws from the sample.

The 10x Genomics Chromium Genome Reagent Kit (v2 Chemistry) was used in all further steps. The cells were prepared at a concentration of 1,000 cells/µL and two samples of 10,000 cells (10 µL) each were loaded onto the chip of a Chromium Controller (10xGenomics) to wells containing 66.2 µL of master mix. Other wells were loaded with Single Cell 3' Gel Beads and partitioning oil before running the chromium controller and incubating the created gel beads in emulsion (GEMs) according to the manufacturer's protocol.

Sequencing libraries were constructed by a dedicated research assistant (R. Raybould). Post GEM-RT clean up, cDNA amplification reaction and post cDNA amplification reaction clean up were performed and 1 µL of the sample was run neat on the Agilent Bioanalyzer High Sensitivity chip to determine cDNA yield.

Sample libraries were pooled and sequenced together by Wales Gene Park using paired-end sequencing and single indexing. Post sequencing data processing was performed using cell ranger pipelines for t-distributed stochastic neighbour embedding (t-SNE) clustering as recommended by 10x Genomics and Seurat package in R for uniform manifold approximation and projection (UMAP) clustering (Freytag *et al.*, 2018).

UMAP clustering

The UMAP clustering algorithm relies on a series of parameters that significantly impact the outcome. These include k.param, prune.SNN and data resolution.

k.param determines the number of neighbours and balances the local vs global structure of clustering: K-means clustering aims to cluster data by comparing individual data points to a defined number of nearest neighbours (k). The algorithm starts with a random selection of cluster centres, assigning data points to the closest cluster before recalculating centre points for new cluster definitions until no more changes occur. The k value defines the number of neighbours included in the analysis; it is not based on a pre-defined statistical method and is data dependent, with currently no algorithm available to automatically detect the minimal k for a particular dataset. Generally, a low value of k forces the algorithm to focus on very local structure increasing noise, while large values potentially distort cluster boundaries (Mcinnes 2020).

Once the k number is defined, the nearest neighbours of each cell are identified. If two points are not within each others list of nearest neighbours, the similarity between the points equals 0, otherwise the similarity equals the number of shared neighbours. The

Jaccard index is a measurement of shared neighbours and is used for pruning, to remove edges between clusters. Prune.SNN defines the cutoff Jaccard index, where any value less than this parameter will be removed from the graph. A prune.SNN parameter of 0 equals no pruning and 1 equals pruning everything.

Data resolution is a parameter defining cluster numbers, where a value above 1.0 obtains a larger, and a value below a smaller number of clusters. Again, no default value exists for this parameter, and clusters identified with the algorithm need to be biologically validated.

Gene expression heatmaps

Significant log2 fold differences in gene expression between macrophage populations, between macrophage populations and other cell types, and between all cell type clusters were used to create heatmaps with R software.

Immunohistochemistry

Target organs and tumours were excised and frozen in optimum cutting temperature compound. Acetone-fixed 7 µm cryostat sections of tumours, lungs and spleen were blocked with PBS, 10 % (v/v) rat serum for 30 minutes before being stained with antibodies and Hoechst (1 µg/ml).

Images were taken with a LSM800 confocal laser scanning microscope (Zeiss) and the Axioscan Z1 slide scanner (Zeiss).

The following antibodies were used for histology:

Reagent	Supplier	Cat. no	Isotype	Clone	Concentration used
Alexa Fluor® 488 – anti-mouse Ly-6G	BioLegend	127625	Rat IgG2a, κ	1A8	5 µg/ml
Alexa Fluor® 488 – rat IgG2a, κ Isotype Ctrl	BioLegend	400525	Rat IgG2a, κ	RTK2758	5 µg/ml
FITC – anti-mouse CD64 (FcγRI)	BioLegend	139315	Mouse IgG1, κ	X54-5/7.1	5 µg/ml
FITC – mouse IgG1, κ Isotype Ctrl	BioLegend	400107	Mouse IgG1, κ	MOPC-21	5 µg/ml
FITC – C1qa	Cambridge Bioscience	HM1096F	Mouse IgG2b	JL-1	1 µg/ml
FITC – mouse IgG2b, κ Isotype Ctrl	BioLegend	400309	Mouse IgG2b, κ	MPC-11	1 µg/ml
Alexa Fluor® 488 – anti-mouse/human CD11b	BioLegend	101219	Rat IgG2b, κ	M1/70	5 µg/ml
Alexa Fluor® 488 – rat IgG2b, κ Isotype Ctrl	BioLegend	400625	Rat IgG2b, κ	RTK4530	5 µg/ml
PE – anti-mouse CD45	BioLegend	103105	Rat IgG2b, κ	30-F11	2 µg/ml
PE – Rat IgG2b, κ Isotype Ctrl	BioLegend	400607	Rat IgG2b, κ	RTK4530	2 µg/ml
PE – anti-mouse CD274 (B7-H1, PD-L1)	BioLegend	155403	Rat IgG2a, λ	MIH7	2 µg/ml
PE – rat IgG2a, λ Isotype Ctrl	BioLegend	402303	Rat IgG2a, λ	G013C12	2 µg/ml
PE – anti-mouse Ly-6G	BioLegend	127607	Rat IgG2a, κ	1A8	2 µg/ml
PE – anti-mouse CD206 (MMR)	BioLegend	141705	Rat IgG2a, κ	C068C2	2 µg/ml

PE – rat IgG2a, κ Isotype	BD Biosciences	554689	Rat IgG2a, κ	R35-95	2 µg/ml
Alexa Fluor 555 – Goat anti-Rabbit IgG (H+L) Cross-Adsorbed Secondary Antibody	Invitrogen	A-21428	Goat / IgG		5 µg/ml
APC – rat anti-mouse F4/80	BioRAD	MCA497	IgG2b	Cl:A3-1	0.66 µg/ml
APC – rat IgG2b Negative Control	BioRAD	MCA6006APC	IgG2b		0.66 µg/ml
Alexa Fluor® 647 – anti-mouse Ly-6C	BioLegend	128009	Rat IgG2c, κ	HK1.4	2 µg/ml
APC – rat IgG2c, κ Isotype Ctrl	BioLegend	400713	Rat IgG2c, κ	RTK4174	2 µg/ml
Alexa Fluor® 647 – anti-mouse CD14	BioLegend	123327	Rat IgG2a, κ	Sa14-2	2 µg/ml
Alexa Fluor® 647 – Donkey Anti-Goat IgG H&L	abcam	ab150131	Donkey polyclonal		10 µg/ml
unconjugated – Anti-NUR77 polyclonal antibody ChiP grade	Abcam	ab13851	Rabbit polyclonal		10 µg/ml
unconjugated – rabbit IgG, polyclonal Isotype Control	Abcam	ab37415	Rabbit polyclonal		10 µg/ml
unconjugated – mouse Siglec-E	R&D Systems	AF5806	Polyclonal Goat IgG		2 µg/ml
Unconjugated – goat IgG Isotype Control	Thermofisher	02-6202	Goat IgG Isotype Control		2 µg/ml
Unconjugated – Anti-HIF-1 alpha	Abcam	ab179483	Rabbit monoclonal		0.85 ug/ml

Spatial analysis immune cells in histological tumour sections

Whole tumour sections were analysed with ImageJ software. An ellipse was fitted to every tumour sample. Length and width of the ellipse were measured and an ellipse of half the length and width was created in the tumour centre to represent the central region, while everything outside was termed tumour periphery (see chapter 4, figure 4.15). The percentage area of staining covered in the two different regions was determined using a combination of markers to identify different cell types (see chapter 4, table 4.2).

Images were split into the different channels recorded and converted to 8bit, before a threshold was applied to the staining in every channel recorded and the picture was converted to binary. The threshold was used to create a selection that could then be applied to the whole tumour section stained with Hoechst and the percentage area of the selection covering tumour centre and periphery was measured.

Clonogenic assay

To quantify 4T1 metastasis, lungs were digested as described above. Cells were resuspended in medium (IMDM, Sigma) containing 60 µM 6-thioguanine (Sigma) and plated in 10 cm tissue culture plates. Plates were left to incubate for 14 days at 37°C and 5% CO_2. After 14 days any remaining media was removed and cells were fixed with methanol for 5 minutes. Plates were washed with sterile water and 6-thioguanine-resistant colonies were stained with 0.01 % (w/v) methylene blue. Colonies were counted manually, with each colony representing one initial metastatic cell. When lungs contained metastatic nodules resulting in densely packed assay plates, plates were divided into quarters with one quarter counted and multiplied by 4. Examples of positive and negative assay plates are shown in chapter 5, figure 5.9.

Immune cell manipulation

Anti-CCL2 antibody

200 µg ultra-LEAF™ Purified anti-mouse/rat/human CCL2 Antibody or Ultra-LEAF™ Purified Armenian Hamster IgG Isotype Ctrl Antibody (both BioLegend) were injected i.p. either prior to 4T1 inoculation (day -2 and day -1) or once tumour were palpable (day 7) and every 4 days until harvest.

Clodronate liposomes *in vivo*

Clodronate and empty (control) liposomes (Liposoma, CP-005-005) were used at different doses (25, 50, 100 and 150 µl/mouse). Mice were injected with 4T1 tumour cells as described earlier. For dose response experiments, liposomes were injected i.p. on day 7 after 4T1 inoculation, tissues were collected on day 14 post inoculation. For depletion experiments liposomes were injected IP on day -3 prior to 4T1 inoculation with injections repeated every 5 days until tissues were collected on day 21 post 4T1 inoculation.

CSF1R inhibition *in vitro*

Bone marrow was collected from 8-10 week old mice and resuspended in full medium (RPMI). Cells were left over night before supernatant was collected, cells were counted and plated as follows: 200,000 cells in 12 well plates in 1 ml full medium. Medium was replaced and 20 ng/ml CSF1 was added every two days until cells adopted a macrophage like phenotype.

For experimental purposes, cells were exposed to 20 ng/ml CSF1 and GW2580 (LC Laboratories) prepared in DMSO at a concentration of 0.6 uM, 6 uM and 60 uM for 24 hours. Cells were harvested and analysed by flow cytometry.

Phosphohistone H3 (PHH3) staining was used to determine cell proliferation: during mitosis the serine 10 of histone H3 is phosphorylated, which can be detected by antibody staining.

CSF1R inhibition *in vivo*

GW2580 (LC Laboratories) was prepared in 0.5% hydroxypropylmethylcellulose, 0.1% Tween 80 in water as described (Conway *et al.*, 2005). For study of cell proliferation in zymosan induced peritonitis mice received oral gavage with 160 mg/kg GW2580 in vehicle on day -1. On day 0 mice received a single i.p. injection of 10 µg zymosan in 100 µl PBS (~2 x

10^6) particles together with a second dose of GW2580. GW2580 gavage was continued on day 1 and peritoneal lavages were collected on day 2, 48 hours after zymosan injection.

For tumour experiments mice were treated daily via oral gavage with GW2580 (160 mg/kg) or vehicle (0.5% hydroxypropylmethylcellulose, 0.1% Tween 80) starting 24 hours before tumour cell injection.

PI3Kδ inhibition *in vivo*

PI-3065 was provided by Genentech and prepared in 0.5% methylcellulose, 0.2 % Tween 80 in distilled water. Mice were treated via oral gavage (75 mg/kg) or vehicle (0.5% methylcellulose, 0.2% Tween 80) once daily, starting 10 hours before injection of tumour cells.

Treg depletion *in vivo*

DEREG mice were injected with 4T1 tumour cells as described earlier. Tumours were allowed to grow to reach a pre-defined mean diameter (6 mm) before diphtheria toxin (DT) was injected i.p. every other day at a concentration of 15 µg/kg. Tumours were harvested after 28 days at latest. Control mice were either DEREG$^-$ littermate controls injected with DT or BALB/c mice injected i.p. with PBS.

Combination of Treg depletion and CSF1R inhibition *in vivo*

GW2580 (LC Laboratories) was prepared as described earlier. DEREG mice were treated via oral gavage (160 mg/kg) or vehicle once daily, starting 24 hours after tumour cell injection. Tumours were allowed to grow to reach a mean diameter of 6 mm before DT was injected i.p. every other day at a concentration of 15 µg/kg. Tumours were harvested after 28 days at latest.

Chapter 3: Optimisation of tissue dissociation

Rationale

To be able to perform effective single cell RNA sequencing (scRNA-Seq) a high viability of target cells is required. This is notoriously difficult to attain in the context of tumour dissociation. Thus, the primary aim of the work described in this chapter was to define methods for achieving highly viable single cell suspensions from the primary tumour and relevant organs.

Specific Aims

Optimise cell preparation for single cell sequencing by:

1) Improving the enzymatic digestion of different project related tissues to achieve best possible cell recovery and viability.

2) Developing a gating strategy for cell sorting.

3) Optimising cell sorting output and single cell sequencing data acquisition.

Introduction

A substantial area of biological research is focused on the development of strategies employing the immune system in the fight against cancer. Most immunotherapies concentrate on the adaptive branch of the immune system, such as adoptive T cell therapy and immune modulating antibodies. While some of these interventions are successfully used in the treatment of hematologic malignancies (Zheng, Kros and Li, 2018) and some solid tumours (Nixon *et al.*, 2018) their application remains challenging. This is partly due to a variety of T cell intrinsic factors (e.g. a lack of target antigens, the challenge of successful trafficking into and activation within the tumour, the problem of T cell exhaustion) but also due to the immunosuppressive tumour microenvironment.

In a solid tumour malignant cells coexist in interdependence with the host stroma. This stroma comprises extracellular matrix components, vasculature and a compartment of infiltrating innate and adaptive immune cells. The interaction between cancerous and stromal cells is vital to tumour growth and development. This is not only true for structural components of the stroma (Kalluri, 2003) but also the immune cell compartment (Liu and Zeng, 2012). Tumour associated macrophages are a major type of infiltrating innate immune cell. Depending on the type of cancer they can account for up to 50 % of the total tumour cell mass (Kelly *et al.*, 1988). Being present in such large proportions, they have the potential to positively and/or negatively impact the efficacy of immune interventions.

Thus, for an increased understanding of the tumour microenvironment it is essential to decipher the different cell types present and their relative proportions to facilitate development of efficient therapeutics.

Each cell type in an organism is characterised by a specific set of expressed genes making up its transcriptome. RNA sequencing can provide valuable insight into the transcriptomics of a specific tissue. Traditional bulk high-throughput next-generation RNA sequencing techniques are useful to compare differences in the same tissue in health and disease and to map developmental changes in gene expression over time. However, sequencing libraries created with such traditional methods represent a whole population of cells and their average gene expression. This disregards cell-to-cell variability within (Shalek *et al.*, 2014) and between populations, ignoring the fact that the majority of tissue samples will be heterogenous by nature. In the case of tumour resident macrophages this issue is especially problematic, which is why in spite of extensive research very little clarity has

been achieved over what constitutes a tumour promoting versus a tumour suppressing macrophage.

One method that is emerging as a valuable tool to study the heterogeneity of cell populations is scRNA-seq. In contrast to bulk sequencing, scRNA-seq provides transcriptomic information on several thousands of single cell which can be analysed in one experiment. This allows the identification of rare cell types within a cell population that would be overlooked using bulk sequencing methods. It also allows definition of heterogeneity within a given population. In most scRNA-seq platforms, this increased understanding of cellular heterogeneity requires, by necessity, a compromise on the depth of each cell's sequencing.

10x Genomics provide a droplet-based technique using their Chromium controller which aims to capture a single cell together with a gel bead within a droplet of oil. This technique will be discussed in detail in chapter 4.

As specified in the manufacturer's protocol (10xGenomics, 2017), this technique relies on high cell viability (at least 70 %) for optimal results. Tissue dissociation during the preparation of single cell suspensions can result in high numbers of dead cells, depending on the protocol used and type of tissue digested. Lysed dead cells can release RNA which can decrease the quality of the sequencing output by creating background noise. A high proportion of dead cells has been associated with a substantial reduction in the total numbers of genes recorded per cell and thus a lack of detection of some cell populations in cluster analysis.

Thus, the primary aim of the work in this chapter was to optimise tissue digestion to extract the highest possible number of viable cells from primary tumours and other relevant tissues.

As spleens are enlarged in the animal model used in this thesis (4T1 tumour cells in BALB/c mice) and lungs are the primary target of metastasis, I focused on the digestion of those organs in addition to the primary tumour.

Results

Quality of spleen digestion and leukocyte antigen detection varies with the use of different digestion media, enzymes and the absence or presence of FBS

Spleens were excised from tumour-bearing mice and digested either according to a protocol previously applied in the group using HBSS with LiberaseTL (a collagenase-thermolysin mix) and DNase, or with HBSS replaced by full medium (RPMI, 10 % FBS) as suggested in different protocols (Stagg *et al.*, 2001) (Figure 3.1) (see chapter 2: enzymatic digestion of primary tumours and metastatic target organs).

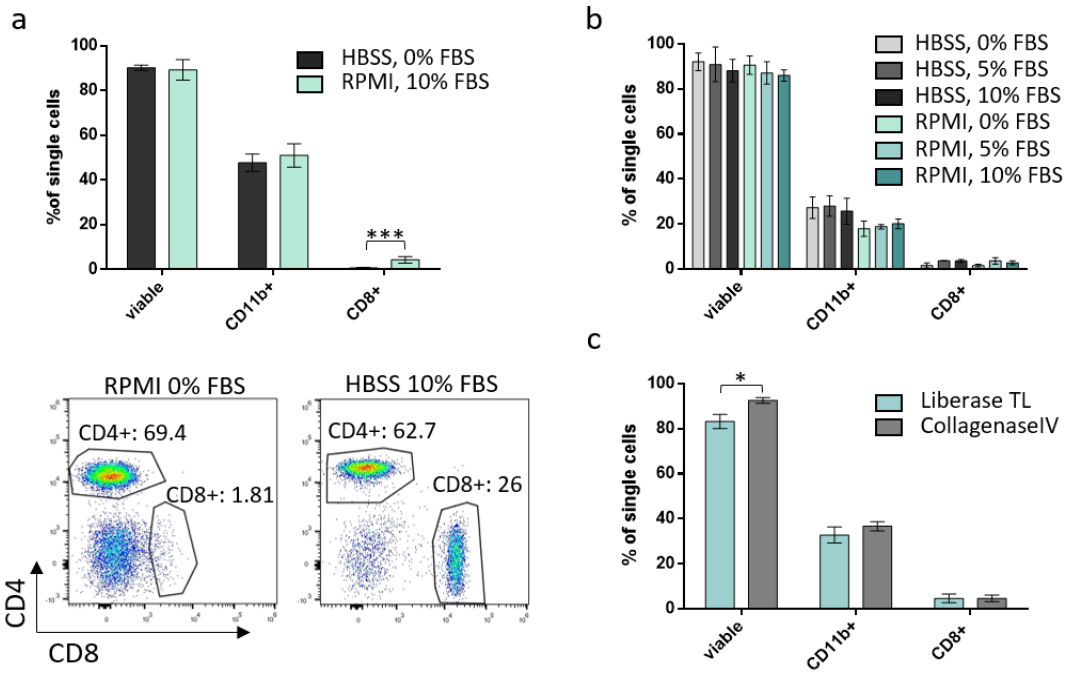

Figure 3.1: Digestion medium and enzymes used influence cell recovery and viability

a) Murine spleens were cut in half with each half digested in either full medium (RPMI, 10 % FBS) or HBSS, each containing DNase and LiberaseTL (N = 5), FACS plots are representative of 5 individual experiments, for pre-gating see supplementary figure S1; b) Murine spleens were cut in 3 parts and digested in RPMI or HBSS containing either 0, 5 or 10 % FBS as well as DNase and LiberaseTL, (N = 3);

c) Murine spleens were cut in half with each half digested in HBSS containing DNase and either LiberaseTL or Collagen IV (N = 3 individual mice). All samples were stained with a viability dye and cell surface antibodies, gating strategy see supplementary figure S1.

Data shown as mean ±SD and analysed using multiple independent student's T-test, one per row: a) p = 0.00074, T ratio: 5.29155; c) p = 0.00146, T ratio = 5.53604;

***, P ≤ 0.001**, P ≤ 0.01; *, P ≤ 0.05

In an initial experiment, single cell suspensions were recovered and stained with established cell surface markers to identify well defined immune cell populations. This stain was meant to assess cell viability and test project relevant antibodies, mainly focusing on myeloid markers but also including antibodies to cell surface receptors associated with lymphoid populations. Interestingly, while no major differences were observed in regard to cell viability and expression of most cell surface antigens, the percentage of $CD8^+$ T cells was significantly lower in the sample digested with HBSS compared to full medium (Figure 3.1a). Enzymes used for digestion may cleave cell surface markers and FBS present in full medium could have prevented this issue in the sample digested in full media. To test this hypothesis, spleens were cut into three parts and digested in either RPMI or HBSS each containing 0 %, 5 % or 10 % FBS with DNase and LiberaseTL.

Indeed, more $CD8^+$ T cells were recovered in either media supplied with FBS compared to 0% FBS. While no difference was observed in $CD8^+$ T cells between the types of media used, the proportions of $CD11b^+$ cells recovered were consistently higher after digestion in HBSS compared to RPMI (Figure 3.1b). As myeloid cells are the main focus of interest of the work in this thesis, even a small decrease of $CD11b^+$ cells could impact the scope of downstream work and should be avoided.

LiberaseTL combines Collagenase I and Collagenase II with a low concentration of Thermolysin (TL), with Collagenase I described as not optimal for myeloid cell isolation (Watkins et al., 2012). In contrast to Collagenase I and II, Collagenase IV has low tryptic activity and is commonly used to maintain receptor integrity during tissue dissociation (Worthington Biochemical Online Tissue Dissociation Guide, 2011). Thus, it was hypothesised that cell surface markers could potentially be even better conserved by the use of Collagenase IV instead of LiberaseTL. Curiously, the exchange of LiberaseTL for Collagenase IV did not affect the percentage of CD8+ or CD11b+ cells recovered. It did, however, improve the viability of the processed sample significantly (Figure 3.1c).

Hyaluronic acid is a glycosaminoglycan and major extracellular matrix component of healthy lung tissue (Lennon and Singleton, 2011). Through interaction with collagen, proteoglycans and itself it plays a key role in providing tissue integrity and elasticity (Fraser, Laurent and Laurent, 1997). To aid dissociation of hyaluronic acid in lung samples (Buhren *et al.*, 2016) and thus prevent sticking of myeloid cells to the extracellular matrix, hyaluronidase was included in the digestion protocol.

Based on experience of spleen digestion, lungs were minced and placed in a mixture of HBSS with and without FBS and either LiberaseTL or Collagenase IV (Figure 3.2a).

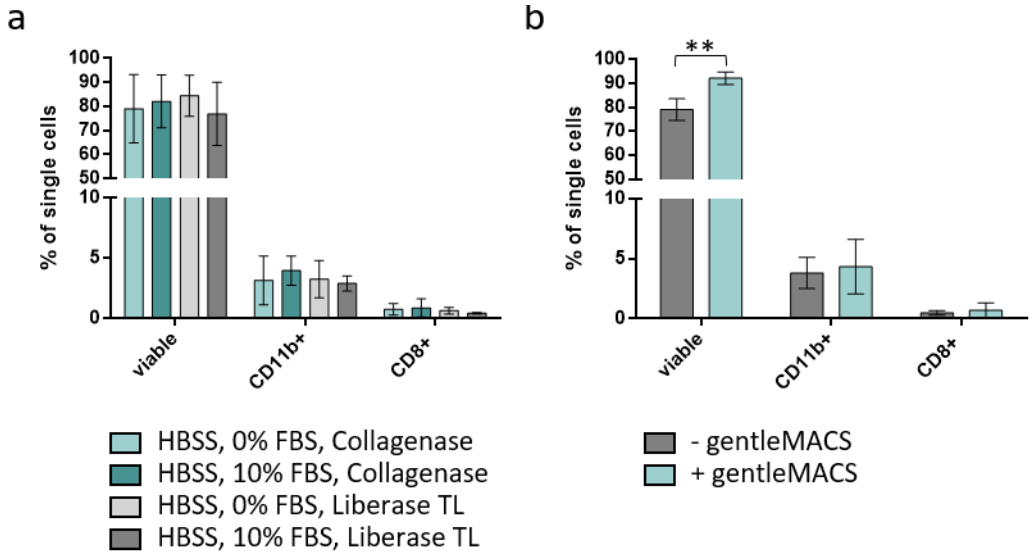

Figure 3.2: GentleMACS processing enhances single cell viability in lung dissociation

a) Murine lungs were cut in half, minced according to the protocol and digested in HBSS +/- 10 % FBS, with either LiberaseTL or Collagenase IV as well as DNase and Hyaluronidase. N = 3;

b) Murine lungs were cut in half, minced and digested in HBSS containing 10 % FBS, Collagenase IV, DNase and Hyaluronidase. Samples were processed as previously (-gentleMACS) or placed in the gentleMACS dissociator using a lung specific program developed by Miltenyi Biotech before incubation (36 seconds at 165 rounds per run (rpr) (+ gentleMACS)). N = 4 individual mice; Single cells suspensions were stained with a viability dye and cell surface antibodies.

Data shown as mean ±SD and analysed using multiple independent student's T-tests, one per row: b) p = 0.00238, T ratio = 5.03016 ;

**, $P \leq 0.01$; *, $P \leq 0.05$

No significant differences due to the medium or enzymes used in digestion were observed. Thus, I decided to continue with the same digestion conditions used for spleen dissociation (HBSS, 10% FBS and Collagenase IV) with the addition of hyaluronidase.

Cell death was high in comparison to cells recovered after spleen processing. As the use of a gentleMACS dissociator has previously been shown to positively impact cellular viability of lung samples (Jungblut *et al.*, 2009), the gentleMACS was utilised here to try and achieve similar outcomes. Indeed, treatment with a lung-specific cycle pre-programmed by the manufacturer significantly increased the proportion of live cells recovered (Figure 3.2b).

Digestion of primary tumour after 21 days of growth yields low viability that is not enhanced by use of the GentleMACS Pro Dissociator

To investigate the impact of different digestion media and methods on the dissociation of primary tumours, mammary carcinomas were harvested 21 days after tumour cell injection. Digestion generally yielded a very high proportion of dead cells, with no differences observed between incubation of the sample in HBSS with LiberaseTL or Collagenase (Figure 3.3a).

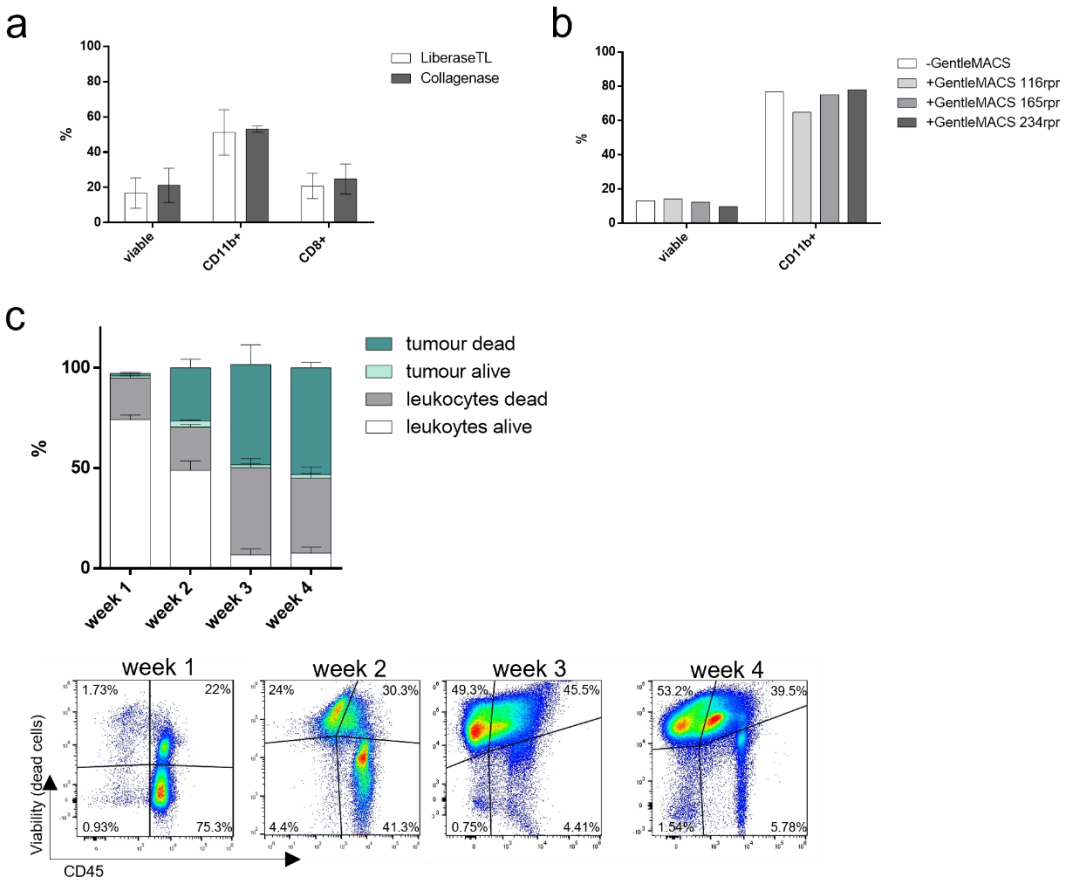

Figure 3.3: Low viability observed after tumour cell digestion is likely a result of cell death occurring during tumour progression

a) Murine tumours were digested in HBSS containing 10 % FBS, DNase and either LiberaseTL (white) or Collagenase IV (grey), N = 4 individual mice;

b) Murine tumours were digested in HBSS containing 10 % FBS, Collagenase IV and DNase. Samples were processed as previously (-GentleMACS) or placed in the gentleMACS dissociator using different tumour specific programs developed by Miltenyi Biotech before incubation (36 seconds at 116, 165 or 234 rpr), N = 1;

Single cells suspensions were stained with a viability dye staining dead cells and cell surface antibodies;

c) Murine tumours were harvested at different timepoints after tumour cell injection, processed as previously and stained with a viability dye and cell surface antibodies, N = 3 individual mice; Images show representative FACS plots of tumours digested at week 1, 2, 3 and 4 after tumour cell injection. Cell suspensions were pre-gated to exclude debris and doublets as before.

Based on the previous success with reducing cell death in lung dissociation, different gentleMACS tumour-specific programs were tested. Unfortunately, neither of these programs were associated with increased viability of recovered cells (Figure 3.3b). Additional investigation showed that a high percentage of cell death is associated with tumour progression and is thus likely not a problem of tissue dissociation, but rather due to both immune and tumour cells dying directly in the tumour microenvironment. Within the first week after injection the growing tumour was dominated by an influx of immune cells, a large percentage of which were viable. Four weeks after tumour initiation a large number of both, CD45 positive and negative cells were dead, with leukocytes accounting for roughly 50 % of the total tumour cell mass (Figure 3.3c).

To minimise the proportion of dead cells in the sample a dead cell removal kit (Dead Cell Removal Kit, Miltenyi) was used to magnetically label dead and dying cells. Indeed, comparison between the sample before (Figure 3.4, 1) and after (2) passing by a magnet revealed a reduction in the number of dead cells present. However, the portion of cells removed from the sample contained a high number of viable cells (3). Whilst this method successfully enriched the sample for live cells, the protocol requires staining of the sample for 15 minutes at room temperature for magnetic labelling. This might result in target cells shedding or internalising cell surface receptors and may cause transcriptional and molecular changes that could alter experimental outcomes. Thus, it was decided to keep cells on ice or in ice cold buffer at all times and disregard the use of the dead cell removal kit despite its success, especially since cells would be sorted before scRNA-seq thereby ensuring removal of dead cells.

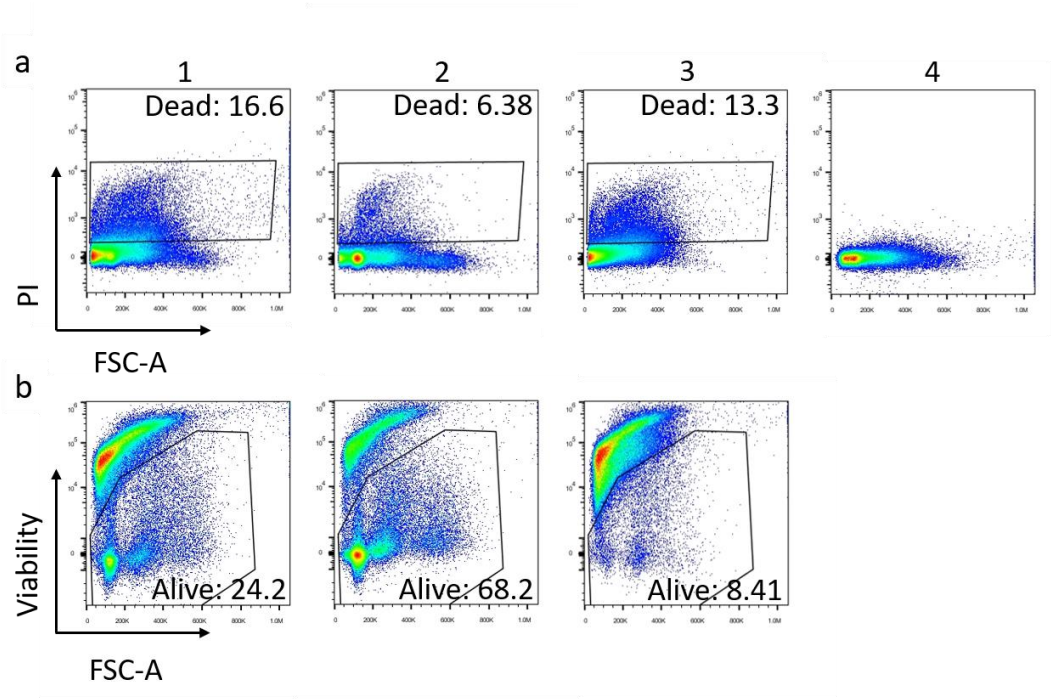

Figure 3.4: Dead cell removal kit improves sample quality

One murine tumour was minced according to the protocol and digested in HBSS, 10 % FBS, DNase and Collagenase IV before being stained with Propidium Iodide (PI) (a) or a viability dye (b). 1: Sample before dead cell removal, 2: Sample after dead cell removal, 3: Removed portion, 4: Unstained control. FACS plots obtained from one single experiment. Cell suspensions were pre-gated to exclude debris and doublets as before.

Cell sorting quality relies on stringent gating

Major immune cell populations in tumours were examined in order to develop a strategy for cell sorting. For this purpose, a primary tumour was excised after 3 weeks of growth and stained with different antibody panels. The antibodies used in these panels had all been tested before during optimisation of organ digestion.

Preliminary observation by flow cytometry showed at least three distinct $CD11b^+$ populations in the primary tumour (Figure 3.5). This included cells that were likely monocytes ($Ly6C^+$, $LY6G^-$), neutrophils ($Ly6C^+$, $LY6G^+$), and macrophages ($Ly6C^-$, $LY6G^-$, $F4/80^+$, $CD64^+$).

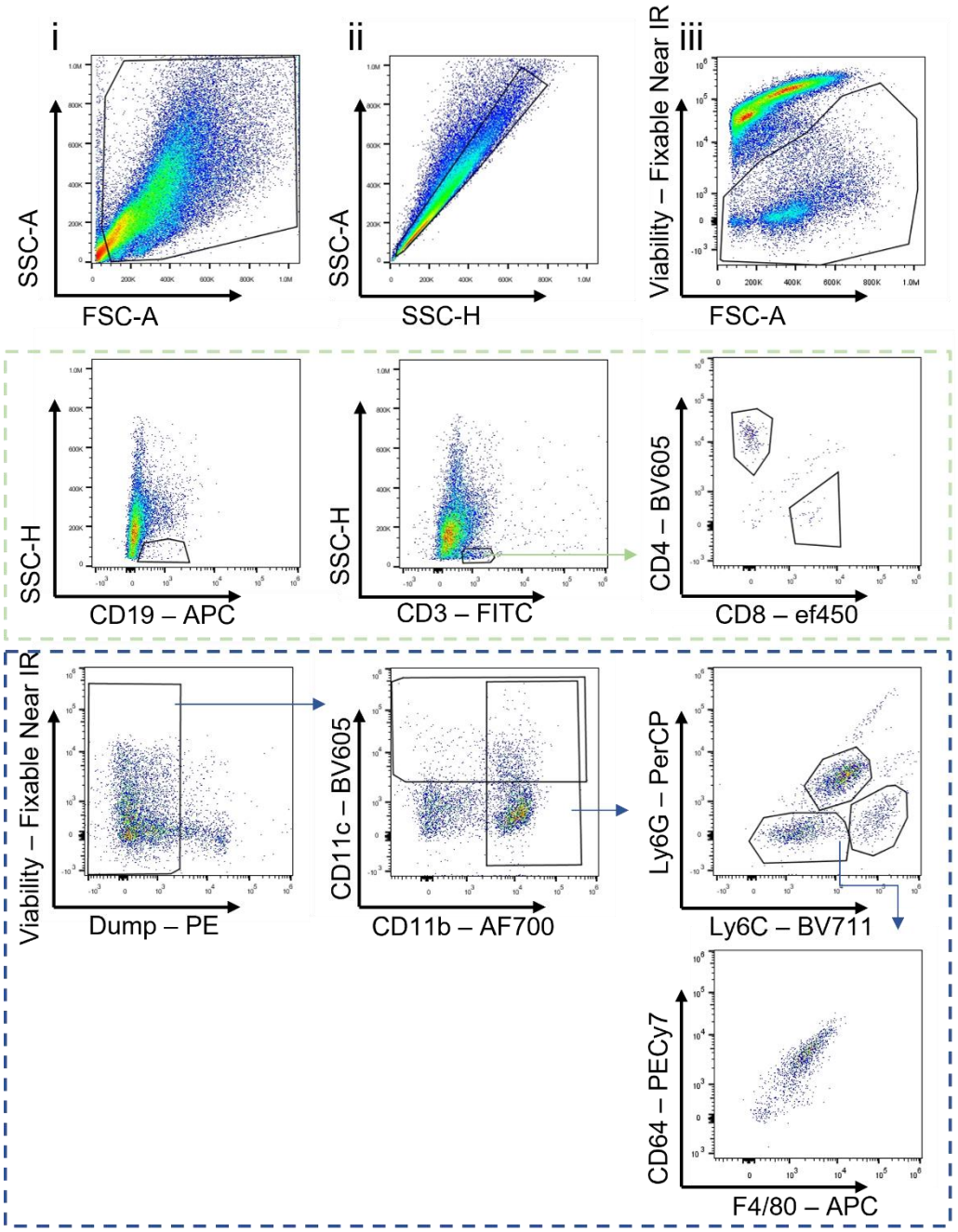

Figure 3.5: Main cell populations in the primary tumour

Murine tumours were digested according to the newly defined protocol (HBSS, 10 % FBS, DNase and Collagenase IV) and stained with a viability dye and antibodies to cell surface markers. Cells were gated based on FSC/SSC profiles (i) and doublets were excluded by plotting SSC-A against SSC-H (ii). Viable cells were gated based on low expression of the viability dye (iii) and cell populations were investigated using either a lymphoid (green) or myeloid (blue) antibody panel. Dump channel (PE) allows for exclusion of non-relevant cells staining with CD19, CD3, SiglecF, NKp46 or Terr119

Data are derived from one single experiment. FACS plots are typical of primary 4T1 tumours processed.

A time course experiment revealed the changes of these crude populations within the first 4 weeks after tumour cell injection (Figure 3.6). The total number of $CD45^+$ cells in the tumour dropped steadily over time (compare Figure 3.3c). When measured as a percentage of leukocytes, $CD11b^+$ cells remained steady for 2 weeks after injection and then dropped by roughly 50 %, recovering and increasing again after week 3.

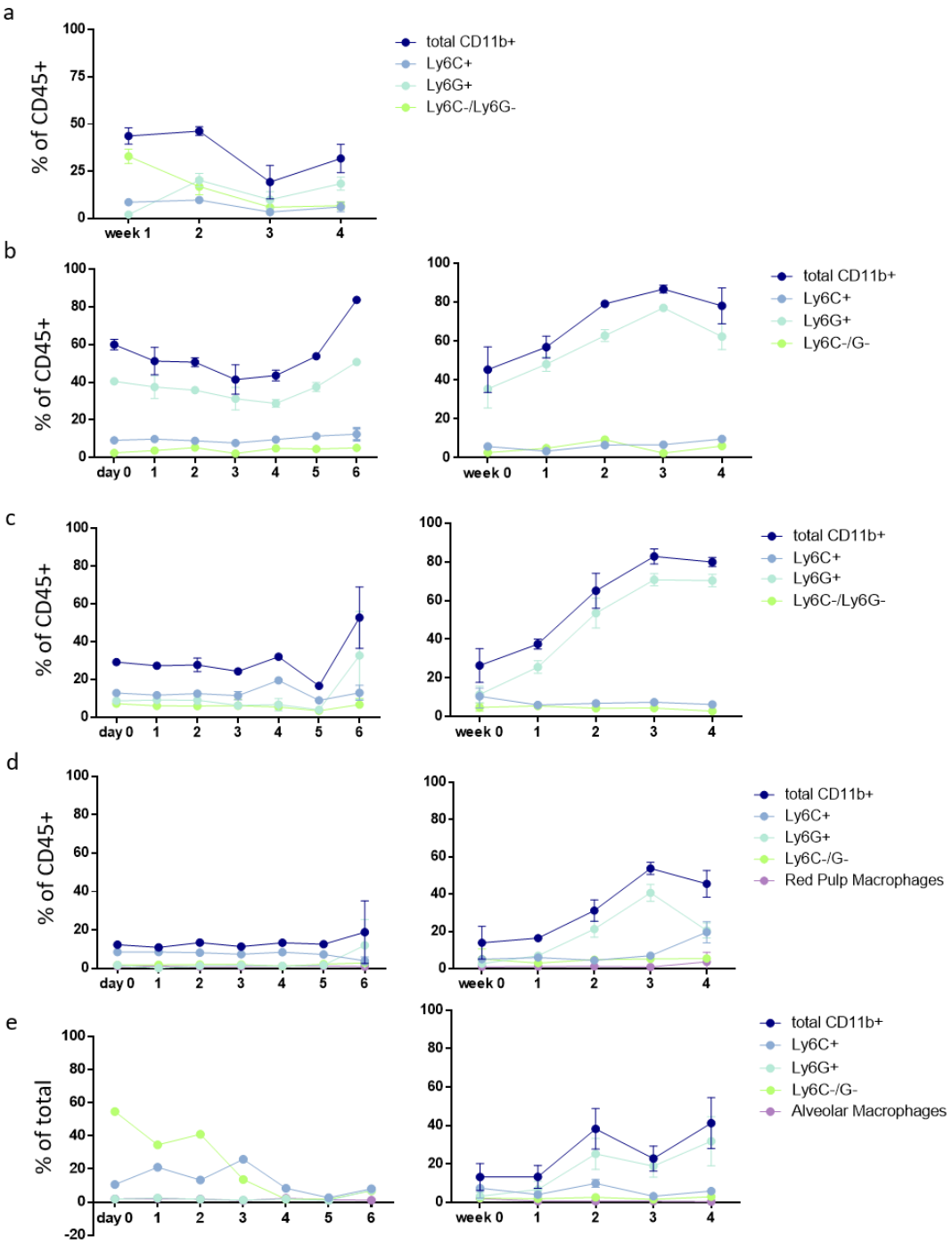

Figure 3.6: Immune cell populations change over time in the developing tumour

Tumours and organs of interest were harvested at different time points after tumour cell injection, digested as previously and stained with antibodies to cell surface markers as before. Cells extracted from (a) primary tumours, (b) blood, (c) bone marrow, (d) spleen, presented as a percentage of $CD45^{+}$ cells, and (e) lungs, presented as a percentage of total cells recovered. Day 0-6: N = 2 individual mice; Week 0/1-4: N = 3 individual mice. Data represent mean ±SD.

This change in $CD11b^+$ cells is largely driven by cells expressing Ly6G but not Ly6C, as $CD11b^+$ cells expressing only Ly6C remain stable and $CD11b^+$ cells negative for both Ly6G and Ly6C decrease within the growing tumour (Figure 3.6a).

Observing other tissues, a steady increase in $CD11b^+$, $Ly6G^+$ cells was noticed. This expansion of cells appeared earliest in the bone marrow (Figure 3.6b), between day 4 and 5 after tumour cell injection when the primary tumour is not yet palpable. $CD11b^+$, $Ly6G^+$ cells then started to increase in the blood (Figure 3.6c) and spleen (Figure 3.6d) between day 5 and 6, and finally in the lungs between 1 and 2 weeks after tumour induction (Figure 3.6e).

This first crude separation of immune cell populations informed the strategy for cell sorting prior to single cell sequencing (Figure 3.7a). While sorting provides an additional stress factor to the cells and might result in cell death, it is necessary to exclude tumour cells and already dead cells and to specifically focus on the myeloid immune cell compartment.

After gating out debris and doublets, cells were selected based on low staining with a viability dye, as well as the combined expression of CD45 with CD11b and/or CD11c in order to capture 'all' myeloid cells.

Cell sorting was performed with different tumours at four different time points to optimise the output. In the first attempt an input of 1×10^6 cells sorting for 1 hour resulted in the recovery of 250,000 cells. To increase the number of recovered cells, in the second sort 2×10^7 cells were sorted for 2 hours achieving an output of 500,000 cells. These sorted cells were stained with a second viability dye and run through a flow cytometer to assess the extent of cell death during sorting. Comparison of the cells stained with the initial viability dye pre-sort and the new viability dye post-sort revealed a proportion of cells dying during the sort (15 % of recovered cells) (Figure 3.7 b1).

In addition, flow cytometric analysis revealed a high proportion of dead cells (44.7 %) in the recovered sample that stained with the original viability dye, meaning they were slipping through the viability gate during the sort (Figure 3.7 b1). This suggested a more stringent viability gating would be required in future sorts. Re-drawing the viability gate in the third sort resulted in an output of only 300,000 cells from 5×10^7 cells initially stained, but higher purity (dead cells slipping through reduced to 7.9 %) and less debris in the recovered sample (Figure 3.7 b2), increasing the proportion of viable cells to 76.2 %.

For the final sort, 5 x 10^7 cells were stained and sorted for 1 hour. The recovered sample contained 73.4% viable cells after re-staining with a second viability dye. A fraction of this sample was run on the imagestream flow cytometer to check quality of the sorting output (Figure 3.7 c and d). The imagestream allows the visualisation of cells as they pass through the machine, which was used to check whether single cell suspensions had been achieved and to confirm the presence of expected cell populations. The rest of the sample was processed on the 10x Chromium single cell sorter and library prep were generated with the help of a dedicated research assistant (R. Raybould).

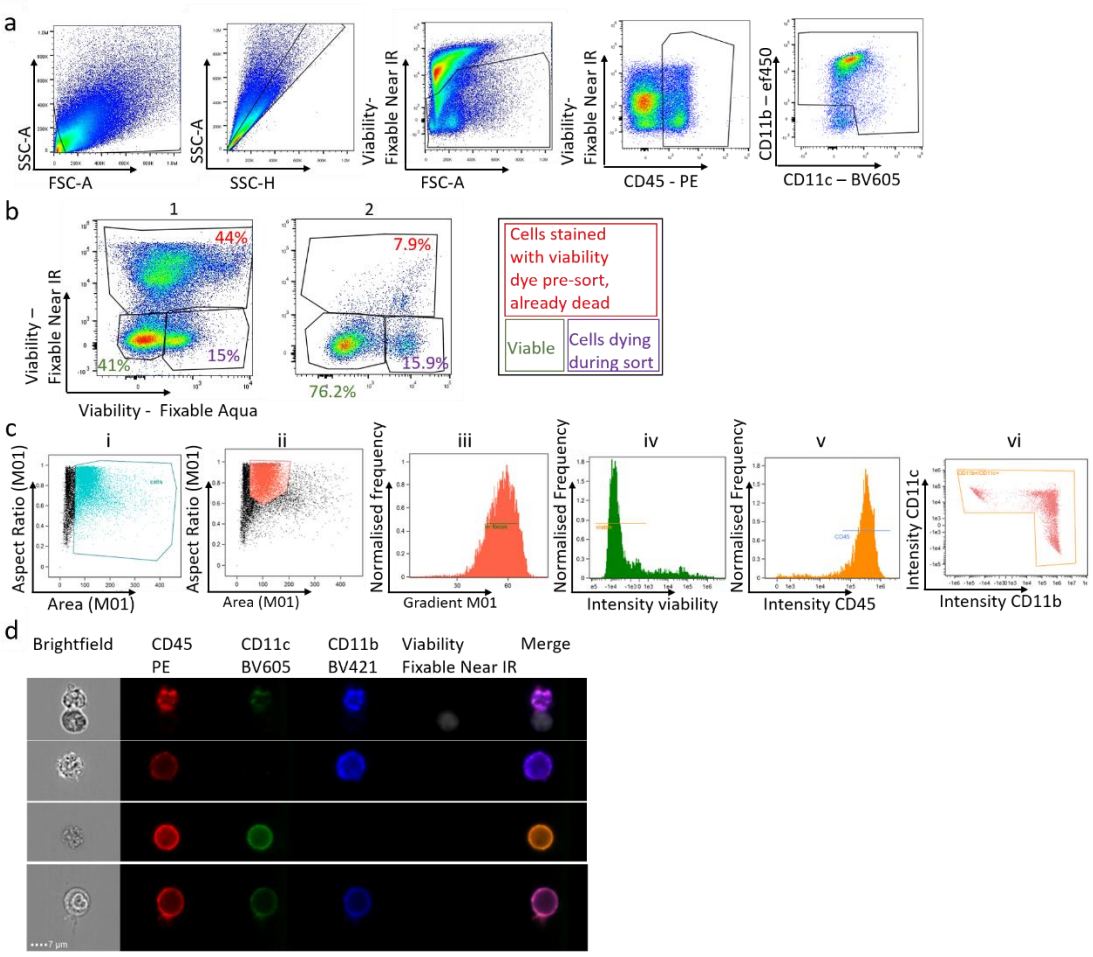

Figure 3.7: Tumour sorting strategy for scRNA-Seq based on preliminary FACS analysis

Single cell suspensions were stained with Fixable Near IR and antibodies to cell surface markers before being sorted for one hour. a) Gating strategy for cell sorting. FACS plots are representative of typical primary tumour preparations. b) Recovered cells were stained with a second viability dye (Fixable Aqua) to visualise cell death during the sort. FACS plots from 2 independent experiments show sorting output before (1) and after (2) optimising the viability gate. c and d). Recovered cells from optimised sorting were run on the imagestream flow cytometer to check quality of the sorting output and confirm the presence of cell populations. Cells were gated plotting brightfield (M01) aspect ratio against area (i). Beads appear very low in area while doublets are high. Not excluding doublets can be useful for observing cell interactions (compare d). Doublets were excluded (ii) and single cells were gated on being in focus (iii), viable (iv), expressing CD45 (v) and CD11b/CD11c (vi). As the cells were sorted based on the same strategy before running on the imagestream, one would not expect many cells falling outside of those gates. d) Representative pictures of cells recorded (note that the first row was not pre-gated on single cells, allowing to see the interaction between a leukocyte and a non-leukocyte. Data are derived from a single experiment.

Immune cell extraction from murine tissues is commonly practiced. A plethora of protocols is available, differing mainly in the types of media and enzymes used, with the application of one method over another rarely being justified (Heinlein *et al.*, 2010; Leelatian *et al.*, 2017; Rodriguez de la Fuente *et al.*, 2021). In this work I aimed to optimise the dissociation of different project relevant tissues to conserve cell surface receptors and minimise cell death. Avoiding cell death was particularly important considering the minimum viability guidelines (>70%) provided by 10x for single cell sequencing: dead cells lyse easily, releasing RNA that contributes to background noise and compromises that quality of sequenced data as discussed in this technical note (10xGenomics, 2017). A flow chart illustrates the combinations of media and enzymes trialled for organ digestion (Figure 3.8).

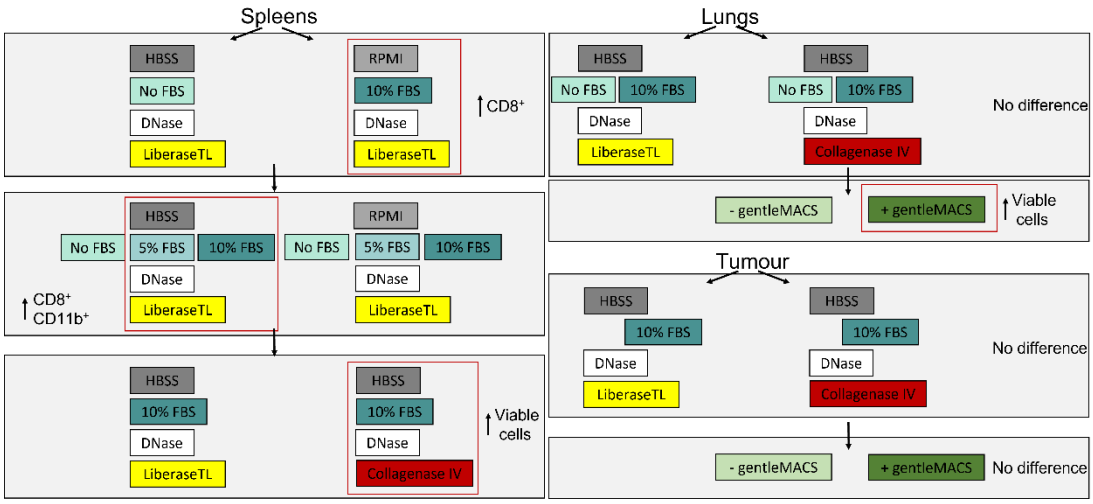

Figure 3.8: Digestion optimisation flowchart

Spleens, lungs and tumours were digested in combinations of media and enzymes as indicated. Red frames indicate a superior methods

Based on the present data, the effect of digestion media appears significant. While the initial comparison between HBSS and full media with LiberaseTL indicated a significantly better recovery of $CD8^+$ cells with RPMI, this effect probably reflects the presence (RPMI) versus absence (HBSS) of FBS. Indeed, this was confirmed when graded amounts of FBS were added to HBSS containing LiberaseTL. LiberaseTL is an enzyme mix combining purified Collagenase I and Collagenase II with a low concentration of Thermolysin. It was chosen initially as it is often a preferred enzyme blend for immune cell isolation, marketed as being

capable of improving cell viability compared to crude collagenases. This specific effect was not observed in the digestion of any type of tissue tested in this study. In fact, LiberaseTL was associated with lower viability compared to Collagenase IV. Furthermore, cell surface markers including CD8 and CD11b were lost to an equal, if not greater extent with the use of LiberaseTL compared to Collagenase IV particularly when LiberaseTL was used in HBSS without the addition of FBS. This is curious, since in comparison to other liberase formulations LiberaseTL has been shown to achieve the best recovery of $CD8^+$ cells in BALB/c mice (Goodyear *et al.*, 2014). However, in the context of this comparison, LiberaseTL was only tested against other liberase blends and not against digestion with Collagenase IV.

In general, the data highlight the different digestion requirements of different tissues and cells within and the necessity to perform tests and compare protocols and enzymes and tailor them to specific needs. Indeed, efforts are being made in tumour biology to optimise digestion of different types of tumours and share successful protocols (Slyper *et al.*, 2020)

While the digestion of spleens and lungs could be optimised achieving over 90% viability per sample, the same does not hold true for tumour dissociation.

Generally, in the animal model used for this project the tumour core becomes necrotic as the tumour increases in size. Thus, as the cancer progresses a larger percentage of cells is already dead before tumour excision and processing, explaining the low viability at the initial tumour harvest 3 weeks after injection. Potentially, the tumour could be harvested at an earlier timepoint when a much higher proportion of cells is still alive. The three week mark was chosen for two reasons: firstly, after 3 weeks of growth the tumours will have reached a reasonable size to contain a number of viable leukocytes that allows multiple flow cytometry staining panels and enables enough cells to be captured by cell sorting for single cell sequencing. Secondly, this project focusses not only on the primary tumour, but in the long term will also investigate tumour metastasis. While tumour cells may be present in the lungs of some mice earlier on, lung metastases in the majority of mice can only be detected three weeks after tumour cell injection (Yang *et al.*, 2020). Analysing the primary tumour and lung metastases at the same timepoint could be useful in future experiments.

Thus, it was decided to accept a high proportion of dead cells in the primary tumour and focus on removing them during the sample preparation for single cell sequencing.

Using a dead cell removal kit slightly enriched the sample in viable cells. However, the separation process included a staining step at room temperature adding an additional stress factor in cell processing. This could alter activation status and thus transcriptional activity of the recovered cells affecting sequencing results.

Instead, optimising the sorting strategy prior to single cell sequencing by varying the sample input, sorting times and flow cytometry gates has allowed the recovery of a single cell suspension meeting the minimum viability guidelines (>70 %) required for single cell sequencing.

Chapter 4: Identification of myeloid cell subsets in the primary tumour

Rationale

In order to understand myeloid cell infiltration and macrophage heterogeneity in the tumour microenvironment on a deeper level it is necessary to gather as much information as possible on the cells that are present during tumour development. This can be achieved by single cell RNA sequencing (scRNA-Seq) providing transcriptomic information on a large number of cells at the same timepoint.

The primary aim of the work in this chapter was to utilise data generated by scRNA-Seq to create an overview of the myeloid populations present during growth of a murine breast tumour and to capture immune cell subsets that might be overlooked with other sequencing methods.

Specific Aims

1) Identify myeloid cell populations in the primary tumour.

2) Identify specific markers associated with the aforementioned populations that allow their distinction from one another.

3) Understand how these populations evolve over time in the growing tumour to create a baseline for future manipulation experiments.

Introduction

Tumours do not develop in solitude. The proliferation of malignant cells will eventually trigger an influx of leukocytes to the site of tumour growth (de Visser, Eichten and Coussens, 2006). The immune cell infiltration of a primary cancer is highly heterogenous and the ratios of different leukocytes present direct the outcome of tumour development: leukocytes may interact with each other as well as with tumour and stromal cells to drive an anti-tumour immune response that could result in tumour cell elimination. Immune cells can, however, also negatively regulate each other and thus inhibit a potential immune response, allowing the cancer to grow and spread (Lança and Silva-Santos, 2012).

Deciphering tissue heterogeneity and thereby the proportions of different types of leukocytes within the tumour microenvironment is essential to understand the processes taking place within the primary tumour. Identifying individual immune cell subsets is necessary to specifically target certain cell types. This could potentially enable targeted manipulation of the immune response in order to drive tumour elimination.

While a lot of research has been published on different immune cell types and their role in tumour development, conclusive results are lacking. Focussing on the myeloid compartment of the immune infiltration, contradicting roles have been reported especially for macrophages: they have been shown beneficial in some primary tumours (Buddingh *et al.*, 2011; Sconocchia *et al.*, 2011), but harmful in others (Leek *et al.*, 1996b; Volodko *et al.*, 1998; Zhang *et al.*, 2013).

Due to the enormous heterogeneity of the macrophage population both in regard to their origin and function it seems highly likely that the tumour microenvironment would contain different macrophage subtypes rather than one, or a small number of, homogenous macrophage populations.

This could account for the different roles attributed to macrophages in different types of tumours, as some TAM populations could be driving inflammation and tumour progression while others might support immune effector cell function. Defining and ascribing function to distinct sub-populations has been difficult to date, as macrophage populations have been reported to share overlapping markers. In order to distinguish different subtypes of macrophages, this study aimed to investigate cellular events on the transcriptome level to find subtle differences between TAM subpopulations.

Transcriptomic analysis investigates a large set of RNA transcripts produced within a cell: while all cells share nearly identical genomes, the transcriptome will vary reflecting the phenotype and function of the individual cell type.

Traditional bulk RNA sequencing is commonly used to investigate both the presence of specific gene expression as well as its relative changes between different samples. While this method does have its application, enabling comprehensive analysis of the majority of expressed transcripts, the patterns of gene expression observed from one tissue will inevitably represent a heterogeneous mixture of distinct cell types and be skewed by variations in those populations.

This issue could be prevented by pre-sorting the cells via the selection by cell specific surface markers. However, this approach would only allow distinction between broadly different immune cell types. In the case of myeloid cells, one could select for macrophages via surface markers, such as F4/80 and CD11b. However, as the present study aimed to identify subsets within the macrophage population the markers of which are unknown, this method would not be suitable.

The introduction of single cell sequencing has provided a solution to this issue: using automated protocols, which isolate individual cells and 'barcode' all transcriptomic data from a given single cell with a sequence tag, high throughput sequencing of multiple cells can be conducted and the transcripts retrospectively assigned back to the cell of origin.

10x Genomics provide a droplet-based technique using their Chromium controller which aims to capture a single cell together with a gel bead within a droplet of oil (Figure 4.1).

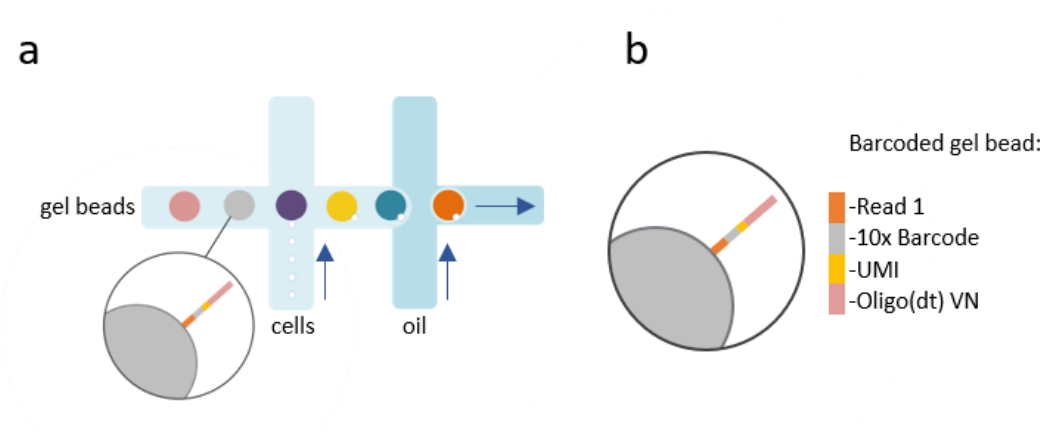

Figure 4.1: 10x Genomics Chromium sequencing overview

a) 500 to 800,000 single cells in suspension are loaded onto the Chromium Next GEM Chip. Within the controller a gel bead containing primers and barcoded oligonucleotides is combined with a single cell in a drop of oil to form a reaction vesicle. As the gel bead mix contains lysis buffer, combination of these components results in cell lysis. This frees mRNA and allows binding to the oligonucleotides. Arrows indicate direction of flow. b) Barcoded gel bead, see figure 4.2 for more detail.

Figure adapted from 10x Genomics

Single cell suspensions and gel beads are added into separate wells of the 10x Chromium Next GEM Chip. The beads and cells are combined within the controller, with a continuous flow of the mixtures being separated by oil added at intervals to form gel beads in emulsion (GEMs). Each GEM should contain one single cell at most with the remaining majority of GEMs (90-99 %) being empty, as single cells are introduced at a limiting dilution to prevent multiple cells associating within one GEM.

The gel bead mix contains lysis buffer which will lyse cells, while the enzyme mix the cells are submerged in will dissolve the gel bead. Thus, upon contact of the different components the gel bead will free its contents: an Illumina® read 1 sequencing primer, a 16 base pair 10x barcode, a 10 base pair Unique Molecular Identifier (UMI), and a 30 base pair oligo(dt) primer sequence (Figure 4.2).

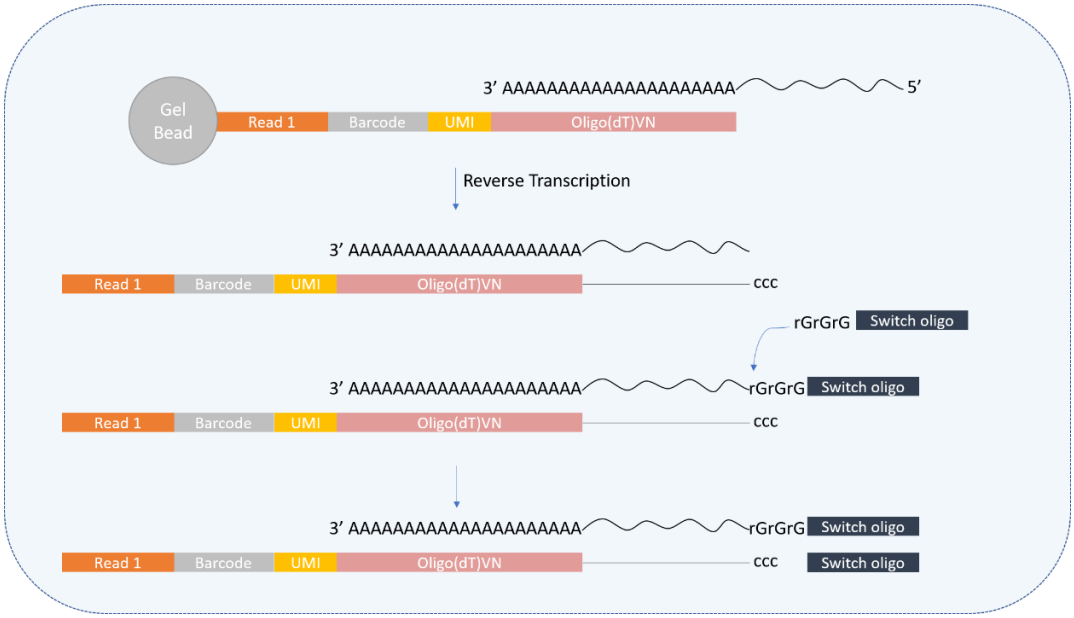

Figure 4.2: Processes within the GEM

Each gel bead is equipped with millions of copies of oligo primers containing an Illumina Read 1 sequence (orange), one of ~750,000 different 16bp barcodes (grey), a 10 nucleotide unique molecular identifier for mRNA transcript quantification (yellow) and a 30 nucleotide Oligo(dT) primer sequence to prime reverse transcription (pink).

Poly A-tailed mRNA will bind the Oligo(dT)VN sequence and reverse transcription generates full-length barcoded cDNA. Reverse transcriptase will also add untemplated C nucleotides at the 5' end that allows hybridisation of a template switch oligo. This is based on the intrinsic terminal transferase ability of Moloney murine leukaemia virus based reverse transcriptases. The template switch oligo adds a common DNA sequence used for cDNA amplification after GEMs are broken.

GEMs will be broken and the cDNA will be ready for clean-up with silane magnetic beads removing biochemical reagents and primers before amplification via PCR, library construction and sequencing (10xGenomics, 2018) (Figure 4.3).

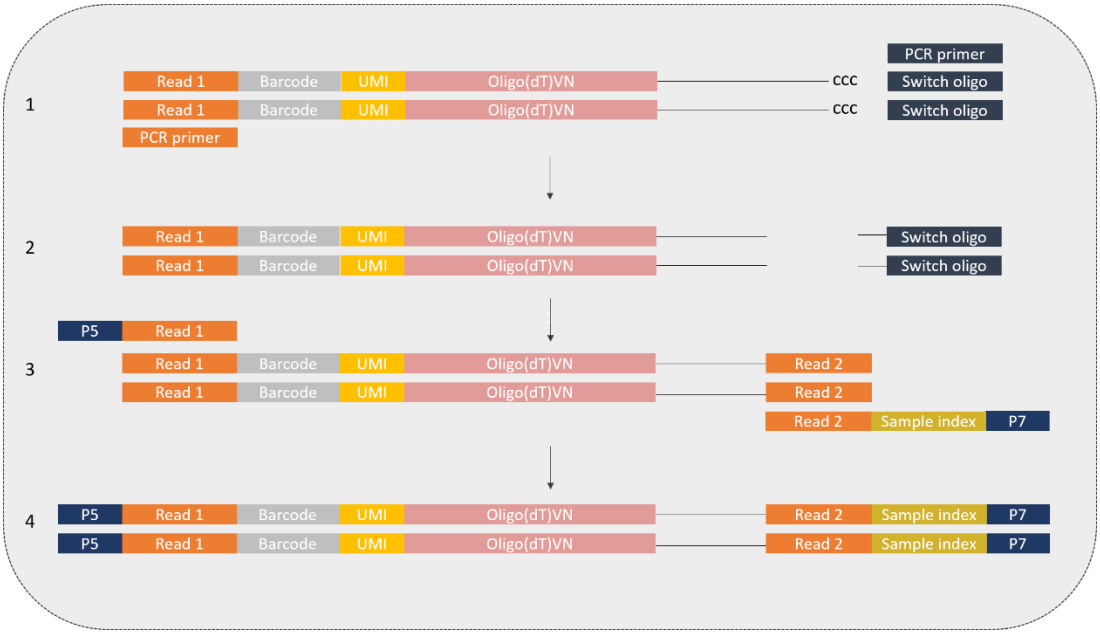

Figure 4.3: Bulk processing post GEM lysis

After GEMs are broken, the cDNA will be amplified (1) and DNA molecules are enzymatically fragmented creating molecules of 300-400 base pairs in length (2). Library preparation then adds components crucial for Illumina sequencing and downstream analysis: the illumina Read 2 adaptor is joined by adapter ligation and Illumina P5 and P7 sequences as well as the unique sample index are added in sample index PCR (3) to give the final sequencing product (4).

Figure adapted from 10x Genomics

This technique allows the identification of rare cell populations within any tissue and the quantification of their relative gene expression. While the 10x Genomics Chromium platform sequencing is a relatively low depth compared to bulk RNA sequencing, it does allow several thousands of cells to be analysed at once. Thus, it is ideal for examining the constituents of a heterogenous population. The primary aim of this part of the study was to utilise single cell RNA sequencing to identify markers corresponding to distinct macrophage subsets that could be used in flow cytometry and histology to create an overview of the myeloid cells infiltrating primary tumours over time.

Single cell sequencing identifies subsets of myeloid cells in the growing tumour

Single cell sequencing was performed on cells extracted and pooled from 3 individual 4T1 tumours grown in female BALB/c mice and harvested on day 21 post tumour cell inoculation. 5 x 10^7 cells were stained with antibodies to cell surface markers (CD45, CD11b, CD11c) and a viability marker as discussed in the previous chapter and purified by cell sorting on FACSAria™ III for 1 hour (Figure 4.4).

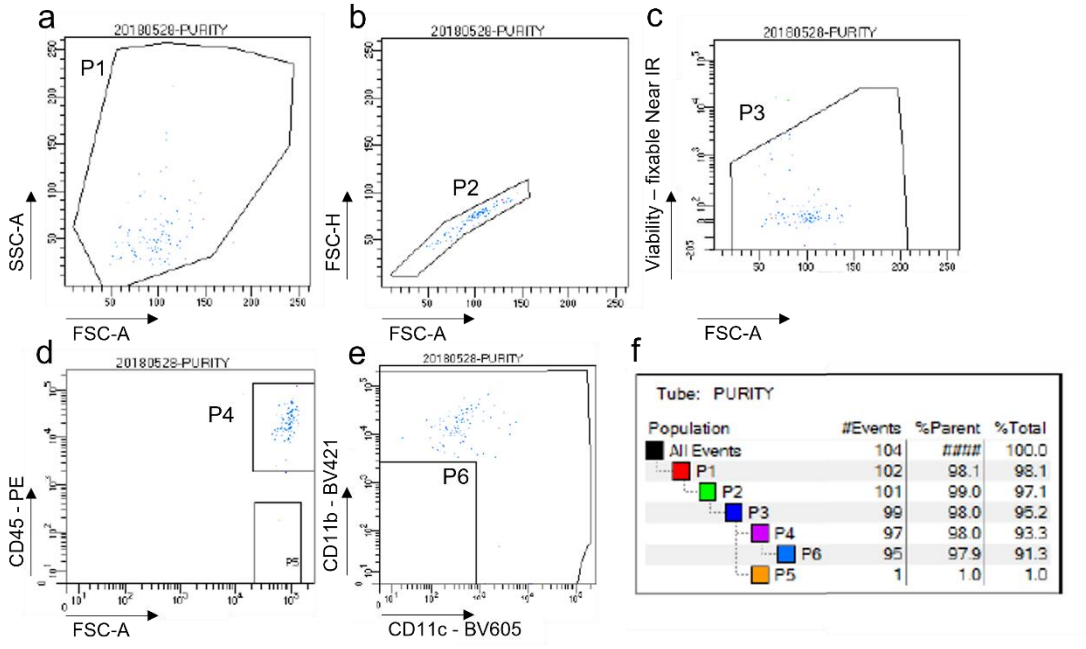

Figure 4.4: Purity of cells for single cell sequencing after cell sorting

A sample of 104 cells purified on FACSAria™ III was re-run to assess purity. a-e) Cells falling into the gates excluding debris (a, P1 = 98.1%), doublets (b, P2 = 99%), dead cells (c, P3 = 98%) and staining for CD45 (d, P4 = 98%) and CD11b/CD11c (e, P6 = 97.9%); f) Numbers and % of events recoded in the specific gates. N = 1

From this output 2 x 10,000 cells (sample 1 and 2) were loaded to different wells of a Chromium chip and processed on the 10x Chromium single cell sorter (v2 Chemistry). Post GEM clean-up and amplification were conducted by a dedicated research assistant (R. Raybould) according to the manufacturer's protocol. cDNA content was measured via Qubit assay as 0.304 ng/µl for sample 1 and 0.356 ng/µl for sample 2. cDNA was amplified for 10 cycles and post amplification quality was checked with the Agilent Bioanalyzer High Sensitivity chip. The sample was run undiluted as recommended for low RNA content

(Figure 4.5). The electropherogram of an ideal sample should show one marker peak each at the beginning and end of the curve, a flat baseline and a peak of DNA at appropriate size as shown in figure 4.5 1. Degraded DNA would show as jagged baseline to the left of the main DNA peak indicating the presence of smaller DNA fragments(Vitale, 2001; Jabsom, 2010).

1

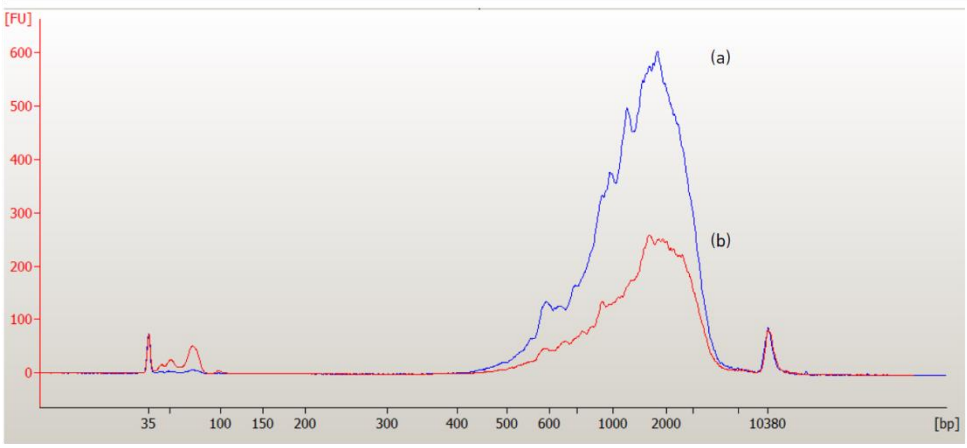

2 a

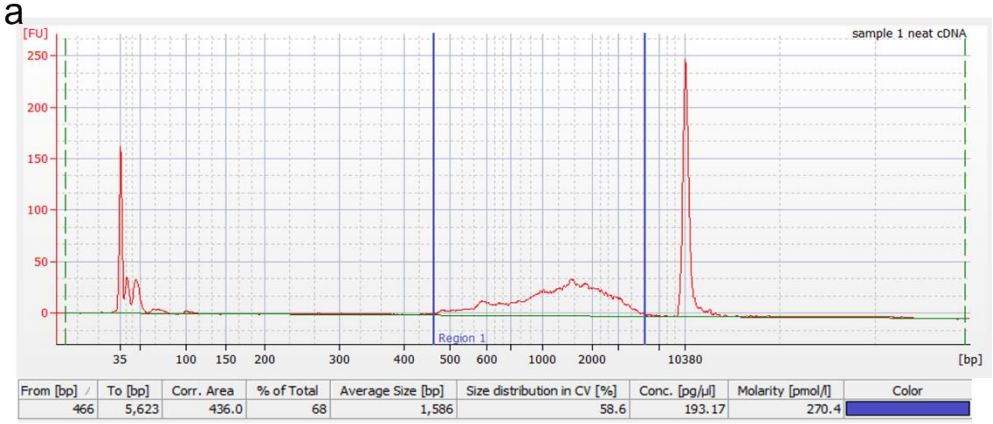

From [bp]	To [bp]	Corr. Area	% of Total	Average Size [bp]	Size distribution in CV [%]	Conc. [pg/µl]	Molarity [pmol/l]	Color
466	5,623	436.0	68	1,586	58.6	193.17	270.4	

b

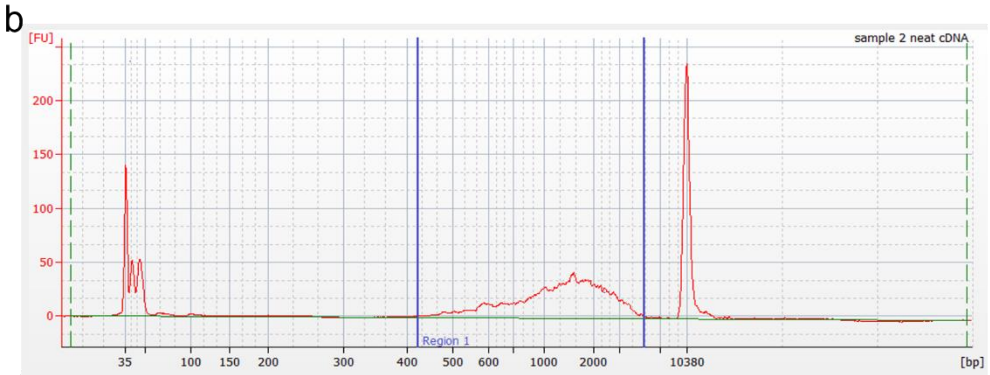

From [bp]	To [bp]	Corr. Area	% of Total	Average Size [bp]	Size distribution in CV [%]	Conc. [pg/µl]	Molarity [pmol/l]	Color
422	5,487	496.2	66	1,546	57.1	217.73	311.9	

Figure 4.5: cDNA quality check on the 2100 Bioanalyzer prior to sequencing

1: Typical electropherogram of PCR amplified DNA libraries as published in the manufacturer's protocol. Trace (a) follows a 1:5 dilution while trace (b) illustrates running undiluted product which is necessary when little RNA is present in the input cells. The peaks at 35 and 10380 basepairs are upper and lower markers that enable alignment of the sample with a ladder of known DNA sizes run beforehand to determine the size of DNA fragments. 2: cDNA generated from 3 pooled 4T1 tumours run undiluted, sample 1 (a) and sample 2 (b) are technical replicates of 10,000 single cells each. The correction area (436.0 for sample 1, 496.2 for sample 2) is defined as the total area under the peak within the region defined by blue borders.

The output showed a small peak of cDNA in the region between 400 and 6,000 basepairs corresponding to the target DNA for sequencing.

As sample 1 and 2 were technical replicates, both sample libraries were pooled and sequenced together by Wales Gene Park using paired-end sequencing and single indexing. Post sequencing data processing was performed using Cell Ranger pipelines as recommended by 10x Genomics.

A t-SNE map of the populations was created using Cell Ranger and visualised with loupe cell browser software. t-SNE stands for t-Distributed Stochastic Neighbour Embedding, a technique applying dimensionality reduction to a given dataset. This aims to reduce high dimensional data (i.e. a dataset where the number of features is significantly higher than the number of observations) to low dimensional space (typically a two-dimensional map) for easy visualisation. First, the probability of similarity of individual points in high dimensional and corresponding low dimensional space is calculated. Next, the algorithms aim to minimise the difference between those probabilities in higher and lower dimensional space to best visualise the data points in lower dimensional space. This way t-SNE is able to map high dimensional data to a lower dimensional space preserving the local structure while revealing the global structure of a dataset and creating clusters based on the similarity of data points with multiple features (Maaten and Hinton, 2008).

In order to identify immune cell populations, the most highly expressed genes in every cluster were investigated (Figure 4.6). This allowed the detection of a small population of T (cluster 9, 2%) and B cells (cluster 8, 1 %) as well as mast cells (cluster 5, 2 %) and dendritic cells (DCs) (clusters 10, 11 and 7, 4 %) among a population of neutrophils (1, 6 %), cells clustering with neutrophils that could not be further identified (2-4, 47 %) and monocyte/macrophage type cells (6, 12-15; 36 %) (Figure 4.6a).

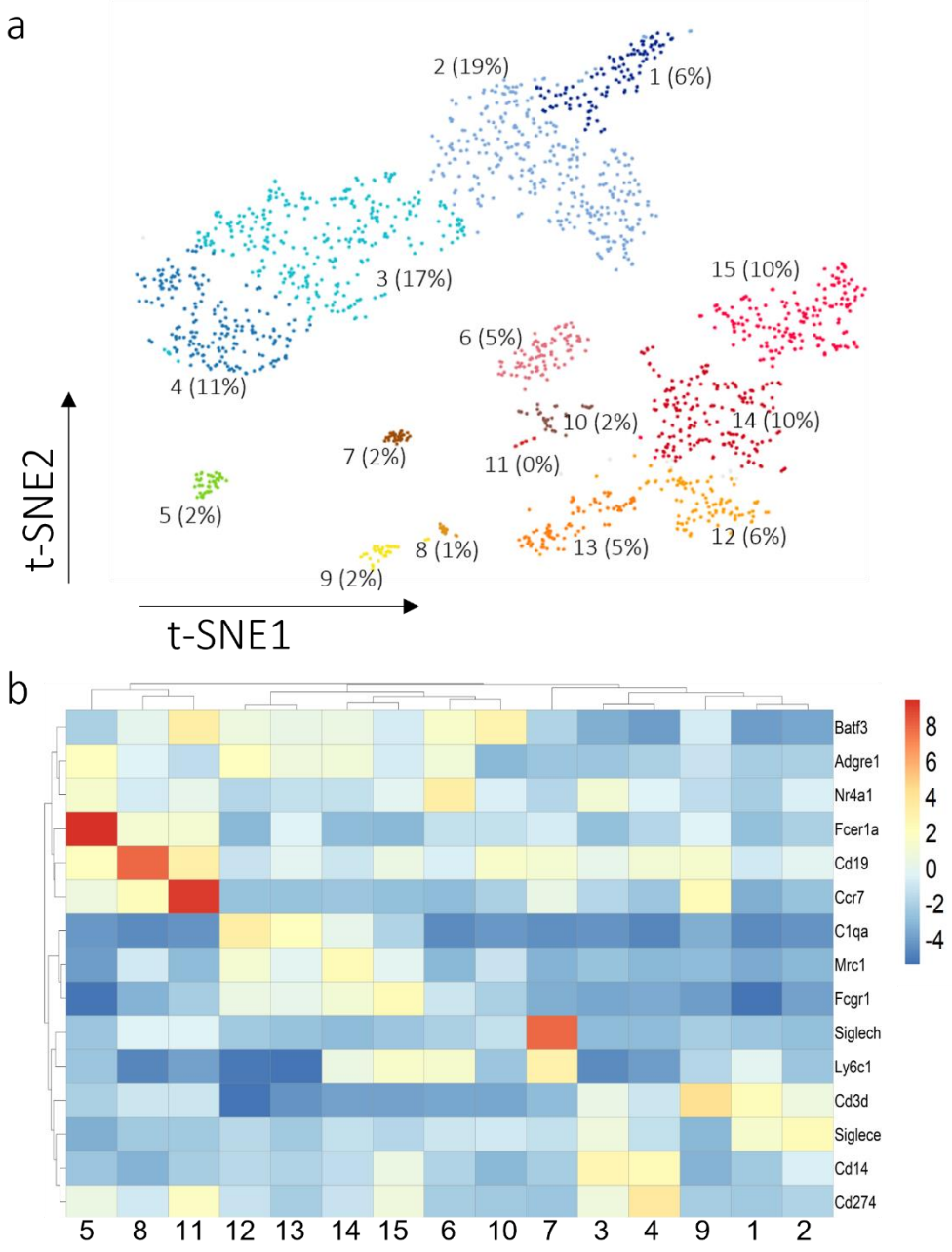

Figure 4.6: Cloupe analysis allows the identification of different cell clusters

a) t-Distributed Stochastic Neighbor Embedding (t-SNE) projection of viable, $CD45^+$, $CD11b^+/CD11c^+$ cells sorted from 3 pooled murine 4T1 tumours harvested 3 weeks after tumour cell injection. Cells are grouped into 15 clusters, cluster number and % of cells in each cluster are indicated. Each dot represents a single cell. b) Heatmap illustrating average expression of selected marker genes (rows) among clusters indicated in (a) (columns). Scale illustrates colour scale for fold change values in log2 base. Red indicates increased gene expression, blue decreased gene expression. N = 1645 cells

Marker genes of interest were selected based on existing literature: T cells (9) were identified based on their unique expression of *Cd3d*, B cells (8) expressed *Cd19*, mast cells (5) *Fcer1*, dendritic cells (10/11) *Batf3* and plasmacytoid DCs (7) *Siglech* (Figure 4.6 b).

Cd3d codes for the delta chain of the T cell co-receptor CD3 expressed mainly by T cells (Gil *et al.*, 2011); Cd19 encodes the CD19 antigen essential in B cell development (Wang, Wei and Liu, 2012); Fcer1 encodes FC epsilon receptor 1 expressed on mast cells, which binds IgE and enables degranulation and effector function (Rios and Kalesnikoff, 2015); Batf3 is a transcription factor essential for the development of conventional DCs (Theisen *et al.*, 2019); Siglech encodes the sialic acid-binding lectin SiglecH which is expressed by plasmacytoid DCs and routinely used to identify these cells (Swiecki *et al.*, 2014).

Three populations of cells clustering with neutrophils were classified based to their transcriptomic similarity to neutrophils, but they could be distinguished from each other by specific gene expression. Neutrophils (1) showed expression of transcripts for *Ly6c1, Ly6g* and *Siglece*. Population 2 markedly expressed *Siglece* but not *Ly6c1* and limited amounts of *Ly6g*. Populations 3 and 4 both were found to express *Cd14* to a higher extent than most other cell populations, with population 3 being low but population 4 being high for *Cd274* (encodes PDL1) expression. The endotoxin receptor CD14 is predominately expressed by myeloid cells and often regarded as a monocyte/macrophage specific surface marker. While this indicates that populations 3 and 4 could be of myeloid origin, CD14 has also been shown to be expressed by bone-marrow derived DCs (Mahnke *et al.*, 1997) and neutrophils (Haziot, Tsuberi and Goyert, 1993). Also, M-MDSCs have been suggested to express CD14 (Tian *et al.*, 2015). Since cell populations 2, 3 and 4 could not be defined and did not cluster with monocytes and macrophage subsets, they are referred to as 'populations associated with neutrophils' for the remainder of the study.

Similarly, monocyte and macrophage populations could be split into separate clusters: monocytes (6) showed a unique combined expression of *Ly6c1* and *Nr4a1*. They likely represent a mixture of inflammatory Ly6C$^+$ monocytes and patrolling Ly6C$^-$ monocytes that have been shown to rely on the transcription factor Nr4a1 for development from bone marrow precursors (Geissmann, Jung and Littman, 2003; Hanna *et al.*, 2011).

The bulk of the macrophage populations could be divided by expression of *Ly6c1* and *Adgre1* (encoding F4/80): populations 14 and 15 were found to express *Ly6c1*, with 15

being negative for *Adgre1* and 14 showing some expression. Since mature macrophages express F4/80, this indicates that populations 14 and 15 might be derived from monocytes and represent a more immature macrophage phenotype. Populations 12 and 13 both showed a high expression of *C1qa* distinguishing them from all other populations, with cluster 12 being positive and cluster 13 negative for *Mrc1* (encoding CD206) (Figure 4.6 b). The top 10 significantly upregulated genes for each cluster are shown in supplementary figure S2.

Importantly, when it comes to defining negative expression of a single gene, the sequencing depth of 10x has to be considered: for this sample the median capture of genes per cell was 1,129, which is not atypical for 10x. The level of gene expression between individual cells, even of the same population, is highly variable as is gene expression within a single cell at different timepoints (Marinov *et al.*, 2014). The estimated number of protein coding genes in humans is roughly 20,000, with likely similar numbers in mice (Abdellah *et al.*, 2004). Even considering cells only express a fraction of these genes at any given time, capturing just over 1,000 genes is only sufficient to detect the highest expressed genes within a cell. Thus, while gene expression can flag up as 'negative' from the sequencing data and will be referred to as such in this chapter, many of the genes may in fact be expressed at lower levels.

In order to validate macrophage sub-clusters, the subset of cells characterised as macrophages by t-SNE clustering was processed by Uniform Manifold Approximation and Projection (UMAP) using Seurat package in R. The UMAP algorithm is similar to t-SNE for data visualisation, but preserves the global structure better, so that relationships between clusters are visualised more meaningful (Mcinnes, Healy and Melville, 2020). This analysis gave broadly similar clusters (Supplementary Figures S3 and S4).

Single cell sequencing data informs flow cytometry gating strategy

Based on mRNA expression data three antibody panels were created to be able to distinguish different immune cell populations via flow cytometry. This process is illustrated in figure 4.7: tumour immune populations can be split into an *Fcγr1* negative (neutrophils and populations 2-4, 1) and a positive side (monocytes and macrophages, 2). Genes that were found to be able to separate different populations of neutrophils and related and monocytic cells are shown in the panels.

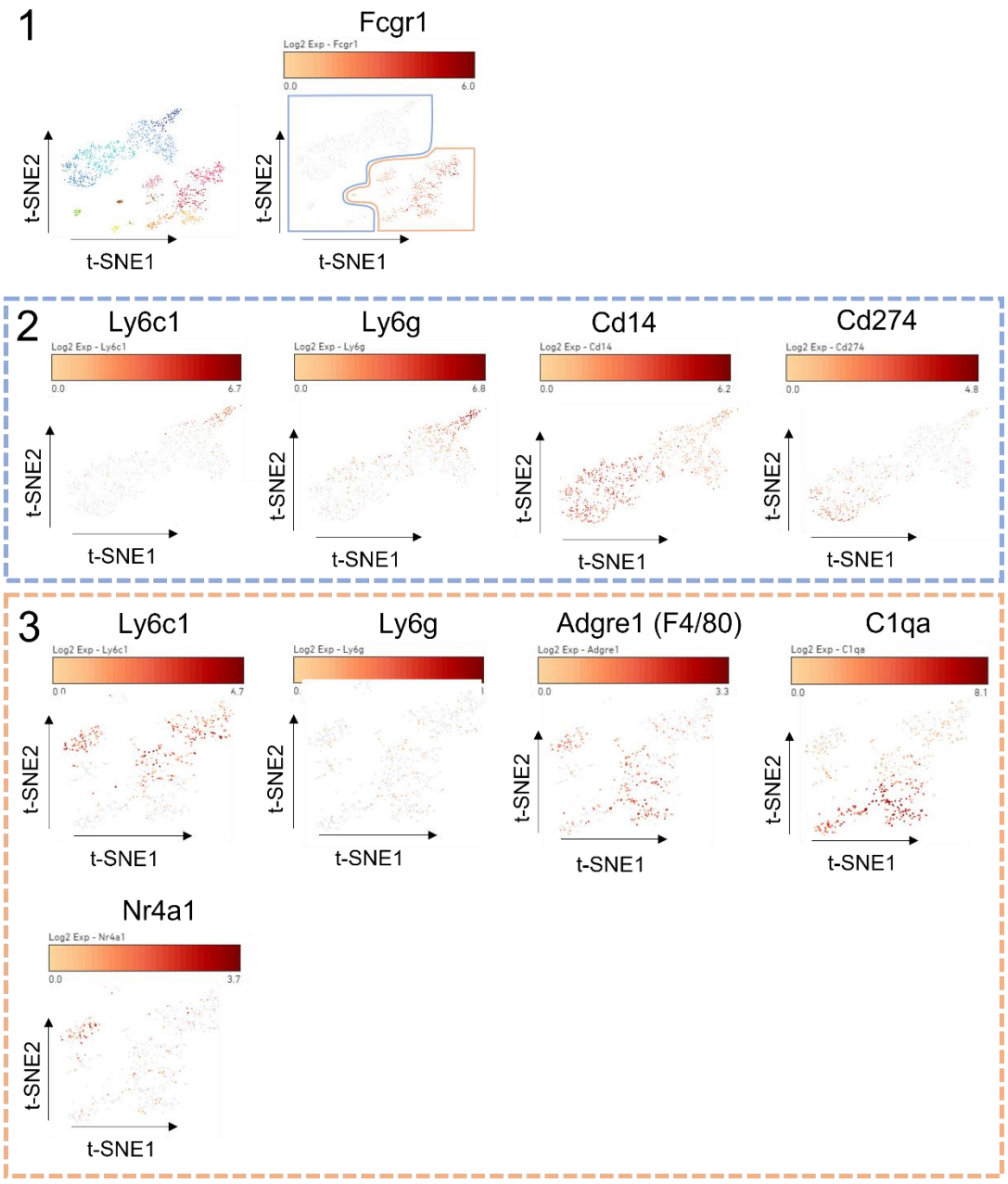

Figure 4.7: Gene expression data visualised by cloupe software was utilised to create flow cytometry antibody panels

1) t-SNE plot of the whole cell output illustrates separation of the clusters based on the expression of Fcγr1. 2) focusses on the Fcγr1 negative cell portion and 3) on the Fcγr1 positive section. The extent of gene expression of selected markers is indicated with red standing for high, and white for low expression. N = 1645 cells

Figure 4.8 shows the flow cytometry gating strategy applied based on the same markers:

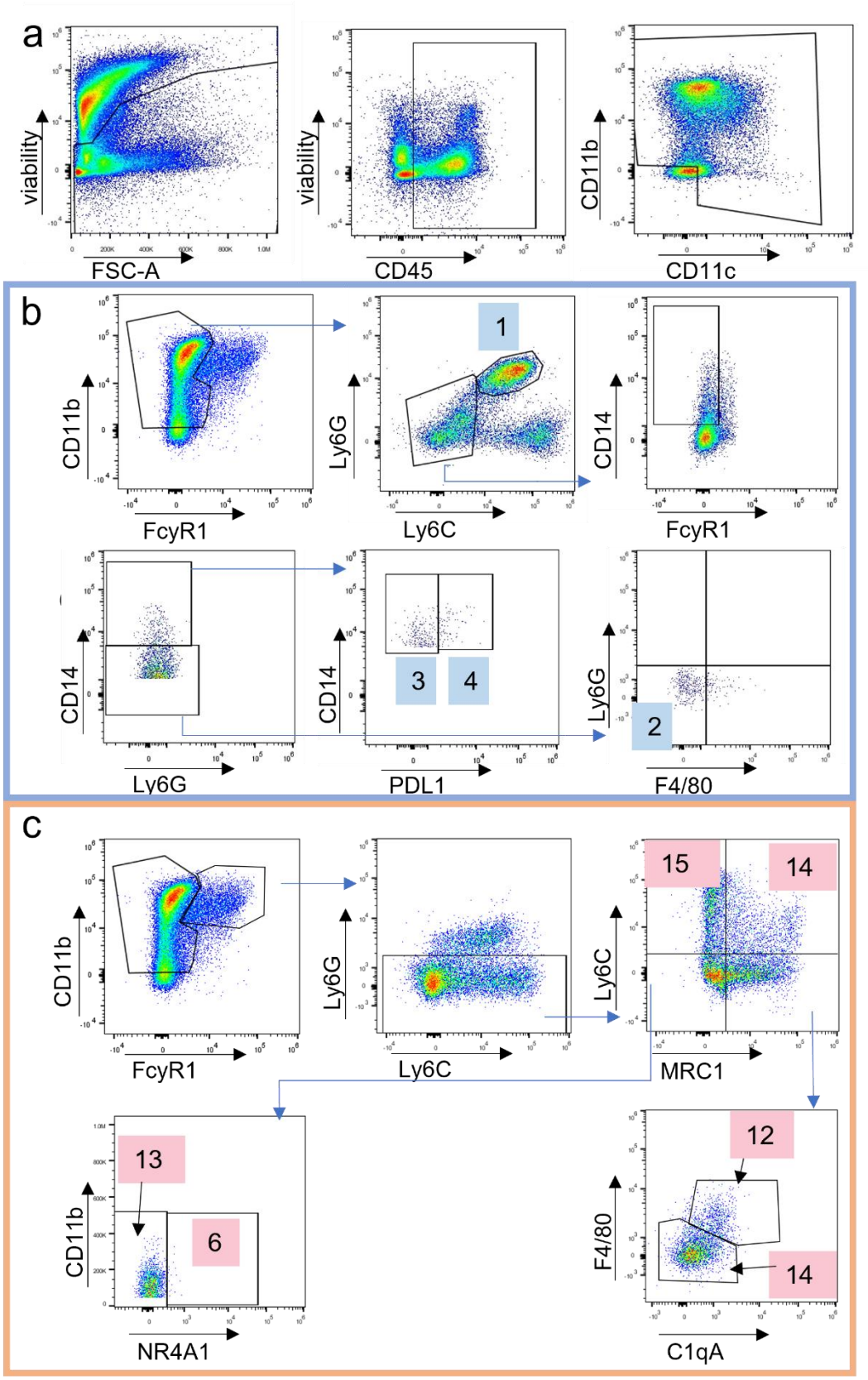
a
viability
FSC-A
viability
CD45
CD11b
CD11c
b
CD11b
FcyR1
1
Ly6G
Ly6C
CD14
FcyR1
CD14
Ly6G
CD14
3
4
PDL1
Ly6G
2
F4/80
c
CD11b
FcyR1
Ly6G
Ly6C
15
14
Ly6C
MRC1
13
CD11b
6
NR4A1
12
F4/80
14
C1qA

Figure 4.8: Gating strategy to identify macrophage and neutrophil type populations by flow cytometry

a) Cells extracted from 4T1 tumours 3 weeks after tumour cell injection were gated to remove debris and doublets as before (not shown). Cells were then selected based on low expression of a viability dye before being gated on the expression of CD45 and CD11b/CD11c and further gated according to strategy b or c. The CD11b/CD11c gate was drawn bigger on purpose to not lose relevant cells with low expression.

b) Gating strategy for neutrophils and associated populations: cells were selected based on the lack of expression of FcγR1. Neutrophils (1) express Ly6C and Ly6G. Ly6C negative cells were gated on CD14 and the positive population split into high and low CD14 expression. CD14 high cells were separated by the expression of PDL1 (3/4). CD14 low cells were gated on being negative for F4/80 (2).

c) Gating strategy for the identification of macrophage type cells: FcγR1 positive cells were selected and split by expression of Ly6C and MRC1 (14, 15). $Ly6C^-$ $MRC1^-$ cells were again split by expression of NR4A1: NR4A1 positive (6) or negative (13). $Ly6C^-$ $MRC1^+$ were split by expression of C1qA and F4/80: $C1qA^+$ $F4/80^+$ (12) and $C1qA^-$ $F4/80^-$ (14). FACS plots representative of typical 4T1 tumours harvested 21 days after tumour cell injection.

As cells for flow cytometry analysis were taken directly from the tumour and not sorted before gating, debris and doublets were gated out at the beginning. Cells were then selected based on low staining with a viability dye, as well as on their expression of CD45, CD11b and/or CD11c to mimic conditions of cell sorting performed prior to sequencing (Figure 4.8 a).

For gating on the populations associated with neutrophils, cells were chosen based on the lack of expression of FcγR1 (Figure 4.8 b). Population 1 expressed Ly6G and Ly6C and could be distinguished easily. The remaining Ly6C negative cells then were gated on the expression of CD14 which was highly transcribed in population 3 and 4 and low in population 2. The presence of PDL1 then distinguished between 3 and 4, while the CD14 low population was defined based on being negative for Ly6C and F4/80.

In contrast, the monocyte/macrophage populations did express FcγR1 and were selected based on expression of this marker (Figure 4.8 c). Gating Ly6C against MRC1 was used to identify population 15 ($Ly6C^+$ $MRC1^-$) and the part of population 14 expressing Ly6C and MRC1 (compare Table 4.1). $Ly6C^-$, $MRC1^-$ cells include $NR4A1^+$ monocytes (6) and $NR4A1^-$ population 13 which can be differentiated by NR4A1. $Ly6C^-$ $MRC1^+$ cells can be split into $F4/80^+$ $C1qA^+$ population 12 and $F4/80^-$ $C1qA^-$ remains of population 14. Importantly,

NR4A1$^-$ monocytes which express high levels of Ly6C could not be distinguished from population 15 at this point, due to the continuous stain on flow cytometry. Only after completion of most of the work summarised in this thesis could these populations be separated based on protein expression of Ly6B and CD62L in monocytes but not TAMs (Figure 4.9).

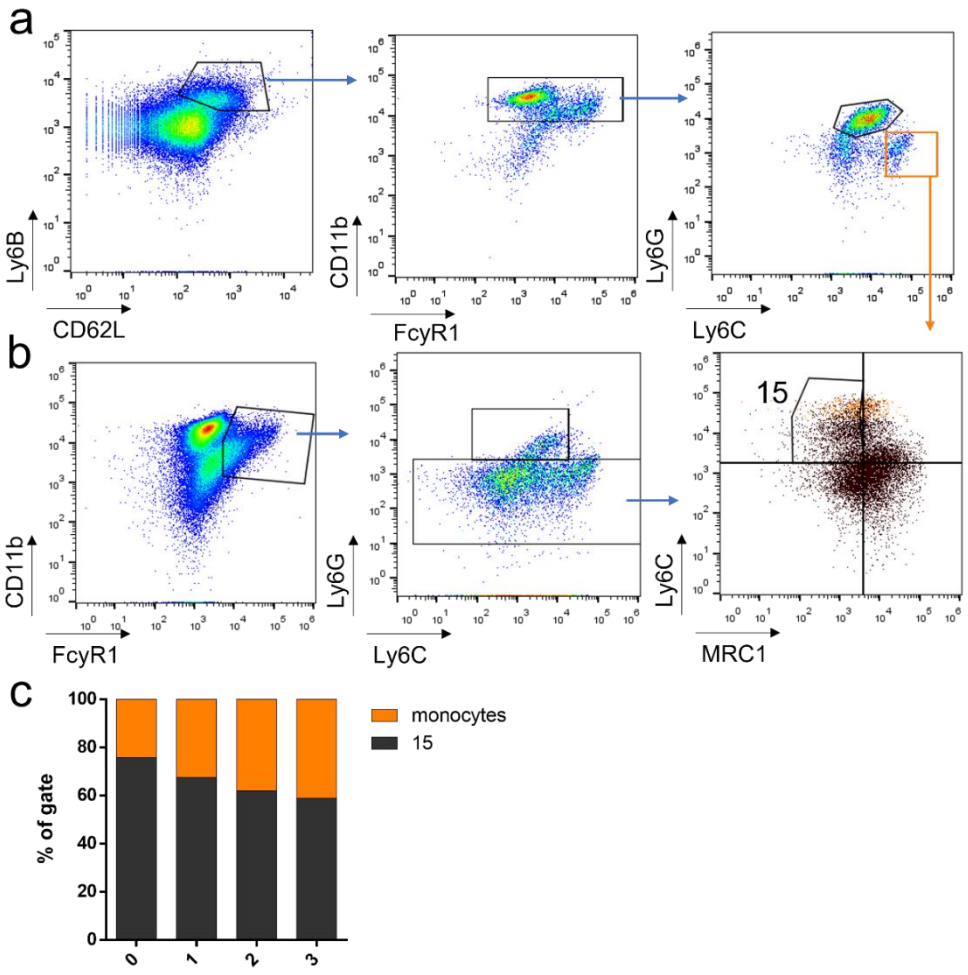

Figure 4.9: TAM population 15 and monocytes can be distinguished by visualising Ly6B vs CD62L

4T1 tumours harvested 3 weeks after tumour cell induction were processed and stained with relevant antibodies. a) After gating out debris, doublets, dead cells and tumour cells as previously illustrated, cells were gated on expression of Ly6B and CD62L. The Ly6B$^+$ CD62L$^+$ portion was gated on CD11b and FcyR1 and monocytes were distinguished as Ly6C$^+$ Ly6G$^-$. b) The same cells as above were gated as usual (CD11b$^+$ FcyR1$^+$ Ly6C$^+$ Ly6G$^-$) with population 15 identified as Ly6C$^+$ MRC1$^-$ as previously shown. Black and orange plot shows monocytes (orange) in the gate used to distinguish macrophage populations. c) Percentage of monocytes (orange) and macrophages belonging to population 15 (black) of total Ly6C$^+$ MRC1$^-$ cells as gated above in 4 individual samples (0-3). N = 4

This technique allowed the identification of all myeloid cells and cells clustering with neutrophils with two separate FACS panels. For fluorescent minus one (FMO) controls of main antibodies used see supplementary figure S5). All other missing populations were of lesser interest for this study and gated with two additional panels shown in the supplements (supplementary figure S6). The two populations of DCs identified in the sequencing data differed in the expression of CCR7, indicating their migratory potential. For the purpose of this study, all DCs were grouped together as population 10/11. The main unique protein marker combinations used to identify the different populations are summarised in Table 4.1:

Cell population	Unique protein marker combination					
1 (neutrophils)	CD11b	FcγR1	Ly6C	Ly6G		
2	CD11b	FcγR1	CD14	Ly6G	F4/80	
3	CD11b	FcγR1	CD14	CD274		
4	CD11b	FcγR1	CD14	CD274		
5 (mast cells)	FceR1	CD3	CD19	SiglecF	CD11b	
6 (monocytes)	CD11b	FcγR1	Ly6C	NR4A1		
7 (pDCs)	SiglecH	MHCII	Ly6C			
8 (B cells)	CD19					
9 (T cells)	CD3					
10/11 (DCs)	CD11c	MHCII				
12 (macrophages)	CD11b	FcγR1	Ly6C	C1qA	F4/80	MRC1
13 (macrophages)	CD11b	FcγR1	Ly6C	C1qA	F4/80	MRC1
14 (macrophages)	CD11b	FcγR1	Ly6C	C1qA	F4/80	MRC1
15 (macrophages)	CD11b	FcγR1	Ly6C	C1qA	F4/80	MRC1

Table 4.1: Unique protein markers for the identification of different cell clusters by flow cytometry

Table summarising the main unique protein markers used for the identification of immune cell subsets by flow cytometry. These markers were derived from Cloupe analysis. Blue colour indicates cells are negative for a specific marker, orange colour indicates cells are positive for the specific marker, yellow indicates cells can be positive or negative.

Expression profiles were validated in tumour samples

Given the high cost of single cell sequencing, I wanted to be able to use the unique protein markers identified by the sequencing data to characterise immune cell populations throughout the remainder of the study. This workflow is illustrated in figure 4.10. The flow cytometry panels defined above that are based on single cell sequencing data were validated by application to 24 individual 4T1 tumours spread over 6 different experiments. The comparability of populations observed across different experiments indicated that the panels could be taken forward to reliably identify immune cell populations in future studies. Since then, the panels have successfully been applied to over 150 individual 4T1 tumours across different experiments.

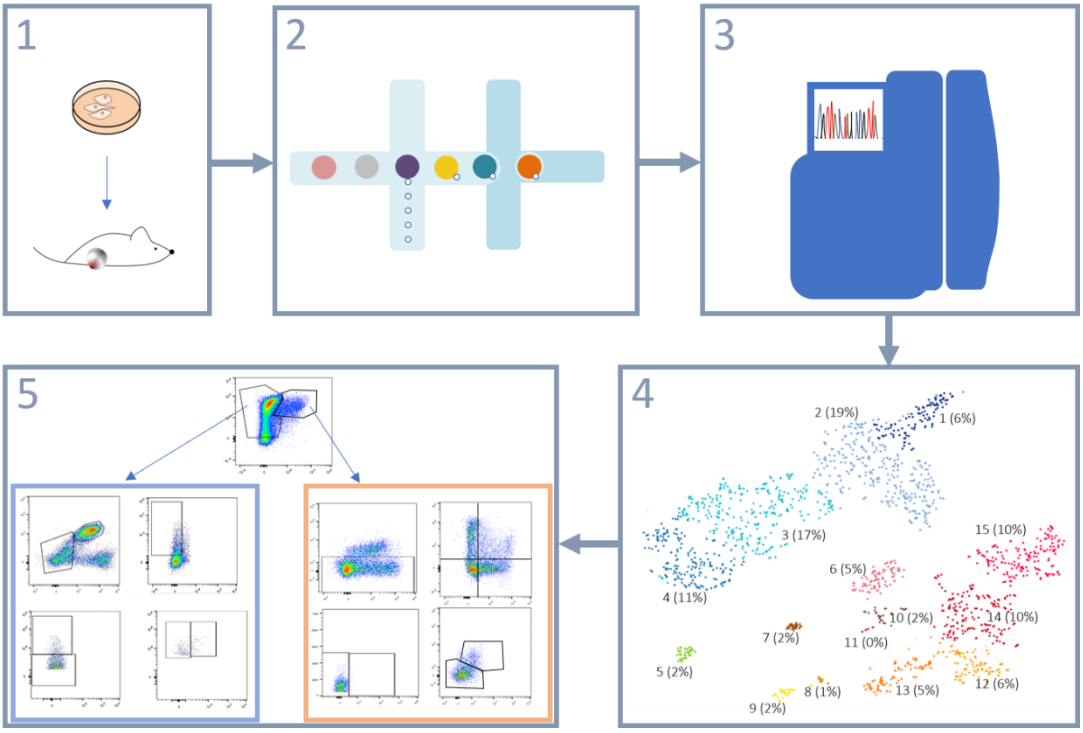

Figure 4.10: Workflow of the creation of flow cytometry panels to analyse the tumour immune infiltrate populations

4T1 tumour cells were subcutaneously injected at 1 x 10^5 cells per mouse (1). Tumours were grown for 21 days before cells were sorted and single, viable leukocytes expressing CD11b and/or CD11c underwent single cell sequencing (2 and 3). Single cell sequencing data were analysed with Cloupe software (4), determining immune cell populations that were validated by Flow cytometry (5).

Flow cytometric analysis allows an overview of how immune cell subsets change during 4T1 tumour growth

In order to observe how immune cell populations change over time in the growing tumour a time course experiment was conducted where mice were injected on the same day and tumours were harvested 1, 2, 3 and 4 weeks after tumour cell injection (Figure 4.11).

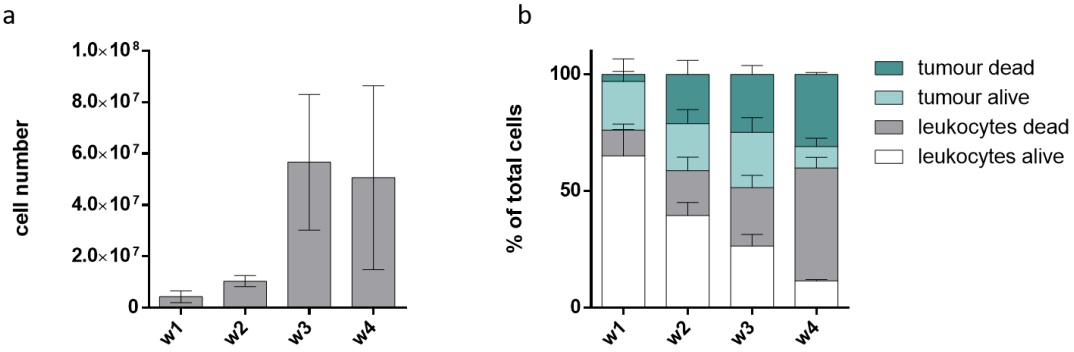

Figure 4.11: Overview of change in tumour associated immune cell populations over the course of 4 weeks

a) Total number of cells recovered from 4T1 tumours at week 1 (w1) to week 4 (w4), b) Percentages of dead (grey) and alive (white) leukocytes and dead (dark blue) and alive (light blue) tumour cell from cells isolated. Leukocytes gates are based on expression of CD45, tumour cells are CD45 negative. N = 3/group, Bars and error bars show mean ±SD, Data representative of 2 individual experiments.

a) Data were analysed with one-way ANOVA: f = 4.385, p = 0.042, R square = 0.6291; b) Data were analysed with two-way RM ANOVA: weeks: F(3,6) = 0.9738, p = 0.4647; cell types: F (3,6) = 17.25, p = 0.0024; interaction: F (9,18) = 22.71, p < 0.0001;

The total cell number extracted from processed samples was quite low in the first two weeks before tumours grew rapidly until week three. Of the recovered cells a higher proportion was found to be dead as the tumour progressed. This cell death included both immune and tumour cells and was likely due to a central necrosis that typically started to develop in the tumour between week two and three. In the two-way RM ANOVA comparing cell types across weeks, the comparison of percentage of total cells between weeks was not significant, as expected, since all percentages add up to 100. The comparison between cell types compared the average of the different cell types across the weeks with each other and was significant (p = 0.0024), meaning that there was a difference in the percentages of cell types. The most important comparison was interaction,

comparing different cell types between different weeks. This value was highly significant ($p < 0.0001$), showing that the percentage of dead and alive tumour cells and leukocytes differed between the weeks.

Investigating the immune cell populations according to their earlier classifications, it could be observed that neutrophils (1) increased up until week 3, both in a percentage of viable leukocytes (Figure 4.12 1a) as well as in actual numbers (4.12 1b), before dropping again between week 3 and 4. The other populations clustering with neutrophils (2-4) remained stable over time.

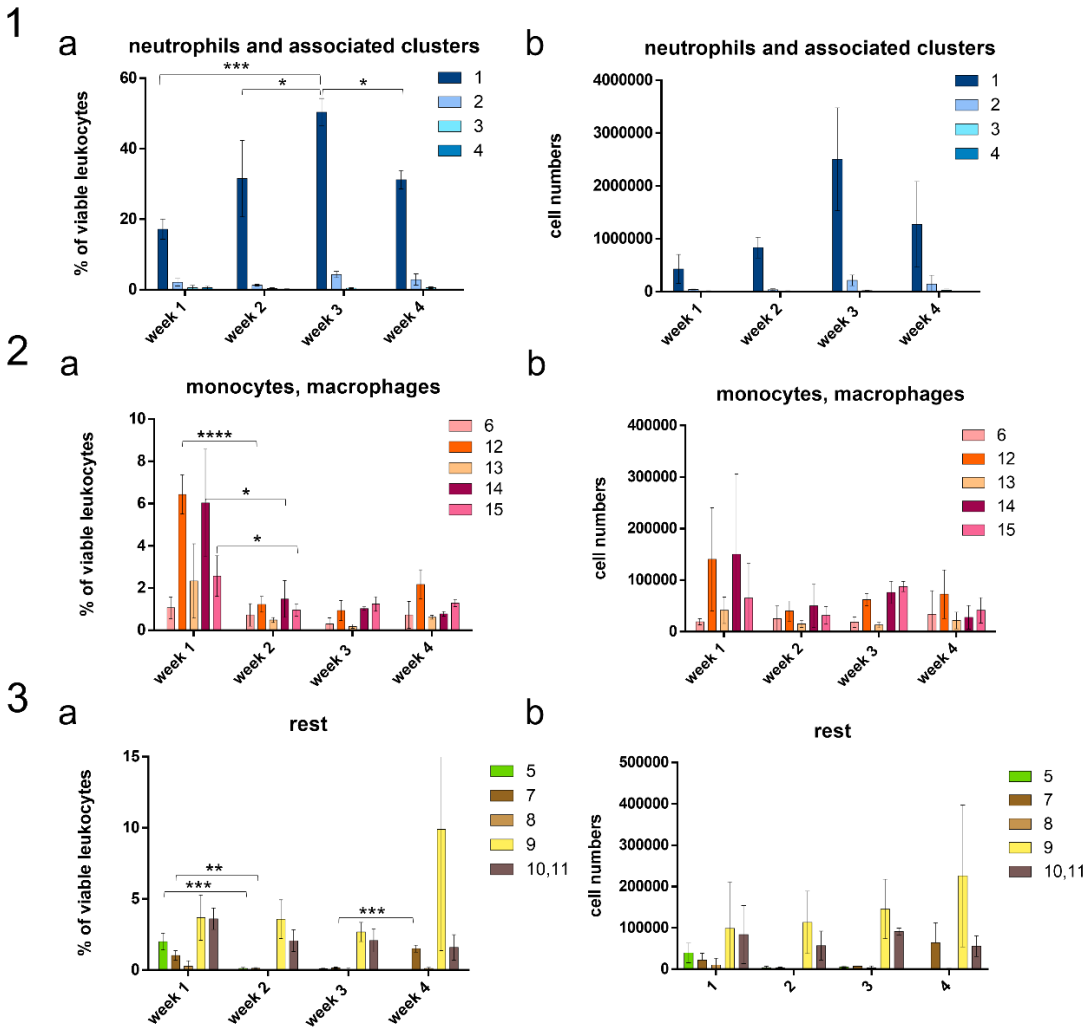

Figure 4.12: Overview of change in tumour associated immune cell populations over the course of 4 weeks

Graphs illustrate the change in leukocyte populations as extracted from 4T1 tumours injected in Balb/c mice 1-4 weeks after tumour induction. Populations are numbered according to sequencing clusters and are grouped into populations clustering with neutrophils (1), macrophage type cells (2) and rest (3). Graphs show cells as a percentage of viable leukocytes (a) and cell numbers (b). N = 3/group, Bars and error bars represent mean with SD;

Data were analysed with one way ANOVA, means were compared by Tukey's multiple comparison test: (1) a) 1: p = 0.0012, R square = 0.8499; 2-4: ns; (2) a) 6: ns; 12: p < 0.0001, R square = 0.9458; 13: ns; 14: p = 0.0042, R square = 0.7926; 15: p = 0.0254, R square = 0.6687; (3) a) 5: p < 0.0001, R square = 0.9818; 7: p < 0.0001, R square = 0.9219; 8-10 = ns;

****, $P \leq 0.0001$; P***, $P \leq 0.001$; **, $P \leq 0.01$; *, $P \leq 0.05$

Within the macrophage clusters (Figure 4.12 2a and b) the biggest change was observed for populations 12 and 14, the numbers of which dropped by about 60 % between the first two weeks. Population 15 also decreased between week one and two. After this initial drop, all populations remained relatively stable. Monocytes (6) did not significantly change in numbers or percentage of total viable leukocytes during the period of observation.

Of the remaining clusters (Figure 4.12 3a and b) a significant decrease in population 5 (mast cells) as well as population 7 (plasmacytoid dendritic cells) was observed between week one and two. Population 7 increased again between week three and four.

Neutrophils and some TAMs cluster in the tumour centre

In order to investigate whether the different macrophage and neutrophil-associated populations were evenly distributed throughout the tumour tissue or clustered in preferred niches, sections of tumour tissue were stained with cluster relevant antibodies as shown in table 4.2:

Cell population	**Unique protein marker combination**		
fluorophore	FITC/AF488	PE/AF555	APC/AF647
1 (neutrophils)	Ly6G	CD45	Ly6C
2	FcγR1	LY6G	SiglecE
3	FcγR1	CD274	CD14
4	FcγR1	CD274	CD14
6 ($NR4A1^+$ monocytes)	CD11b	NR4A1	Ly6C
12 (macrophages)	C1qA	CD45	F4/80
13 (macrophages)	C1qA	CD45	F4/80
14 (macrophages)	CD11b	MRC1	Ly6C
6/15 ($NR4A1^-$ monocytes and macrophages)	Ly6G	CD45	Ly6C

Table 4.2: Unique protein markers for the identification of different cell clusters by histology

Table summarising the main unique protein markers used for the identification of immune cell subsets by histology. These markers were derived from Cloupe analysis. Blue colour indicates cells are negative for a specific marker, orange colour indicates cells are positive for the specific marker.

Figure 4.13 shows neutrophil associated populations in whole tumour scans (1) and details (2):

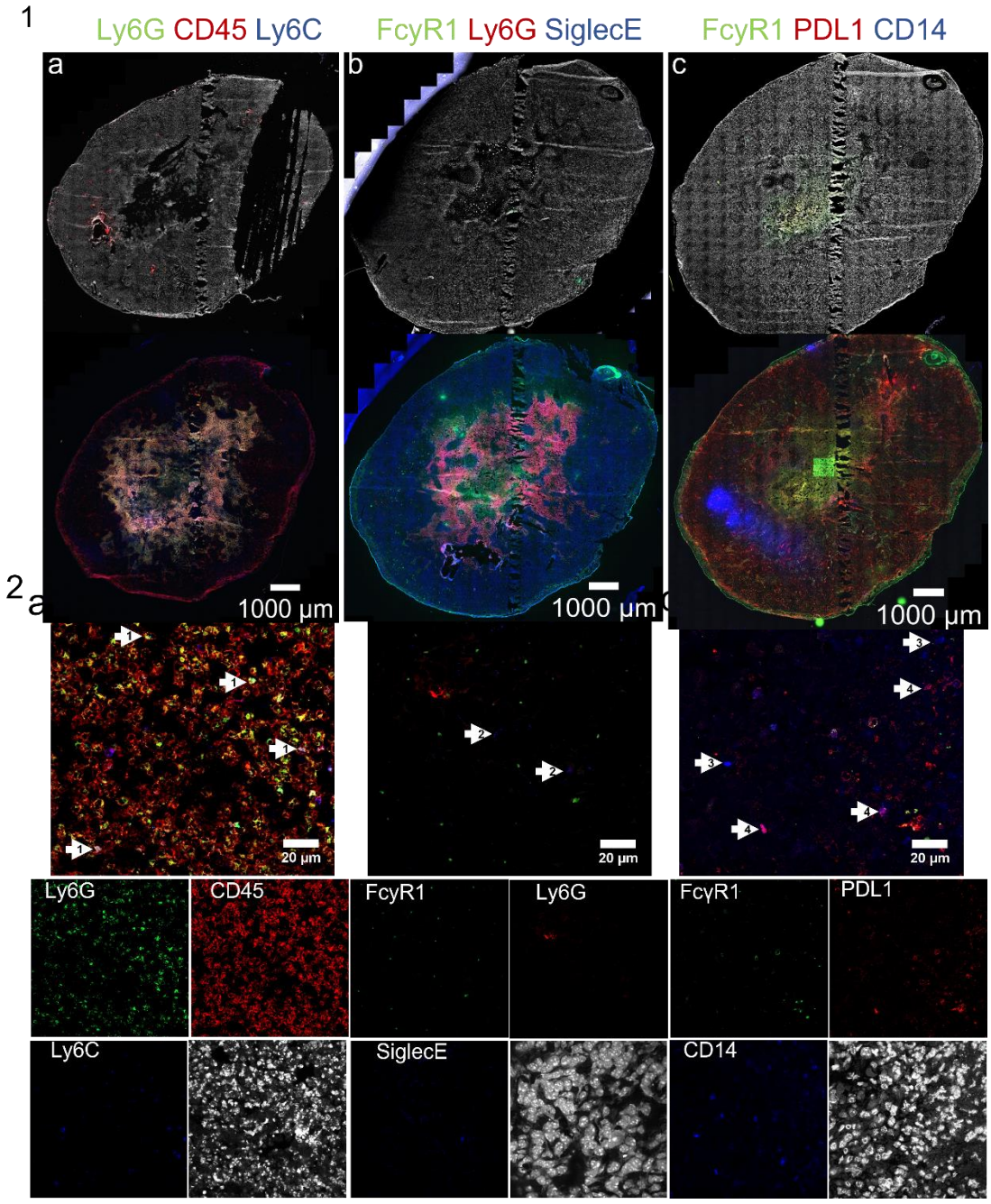

Figure 4.13: Neutrophils and associated cell populations in the primary tumour

4T1 tumours harvested 3 weeks after tumour cell induction were cut into 7 µm sections and stained with relevant antibodies and isotypes (see methods for isotypes).

a) Ly6G – AF488, CD45 – PE, Ly6C – AF647, b) FcyR1 – FITC, Ly6G – PE, SiglecE – AF647, c) FcyR1 – FITC, CD274 – PE, CD14 – AF647 All sections were stained with Hoechst (1 µg/ml) (only shown in isotype pictures). Scale bars: 100 µm for whole tumour sections (1), 20 µm for subsections (2). Images are representative of 4 individual tumours/experiments.

Figure 4.14 shows macrophage populations in whole tumour scans (1) and details (2):

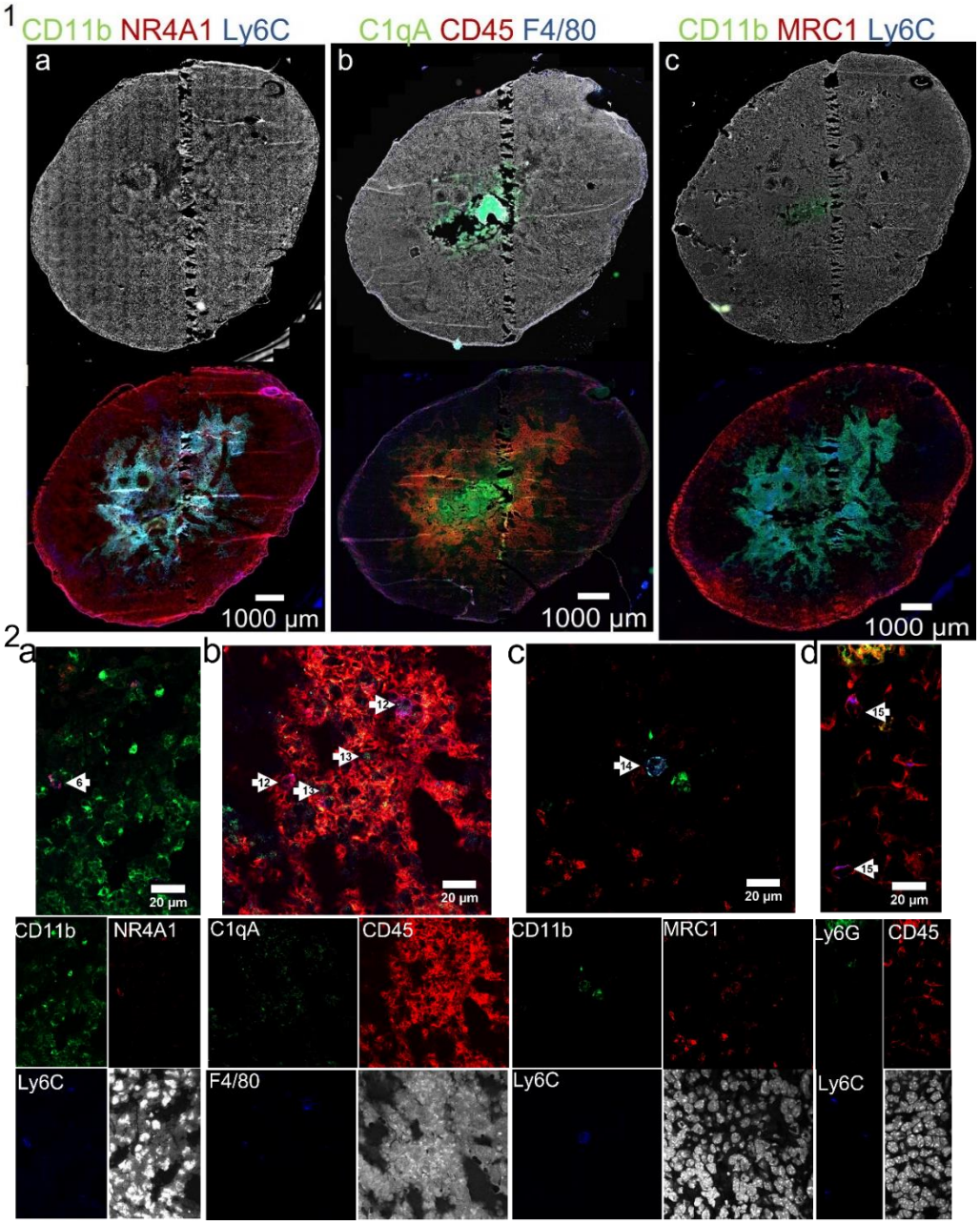

Figure 4.14: Macrophage populations in the primary tumour

4T1 tumours harvested 3 weeks after tumour cell induction were cut into 7 µm sections and stained with relevant antibodies and isotypes (see methods for isotypes).

1: a) CD11b – FITC, NR4A1 – AF555, Ly6C – AF647, b) C1qA – FITC, CD45 – PE, F4/80 – APC, c) CD11b – FITC, MRC1 – PE, Ly6C – AF647; 2: a-c as above, d) Ly6G – FITC, CD45 – PE, Ly6C – AF647; All sections were stained with Hoechst (1 µg/ml). Scale bars: full tumour 100 µm (1), selected sections 20 µm (2), images are representative of 4 individual tumours/experiments.

To analyse cellular location an ellipse was fitted to the tumour sample. Length and width of the ellipse were measured, and an ellipse of half the length and width was created in the tumour centre to represent the central region, while everything outside was termed tumour periphery (Figure 4.15, 1).

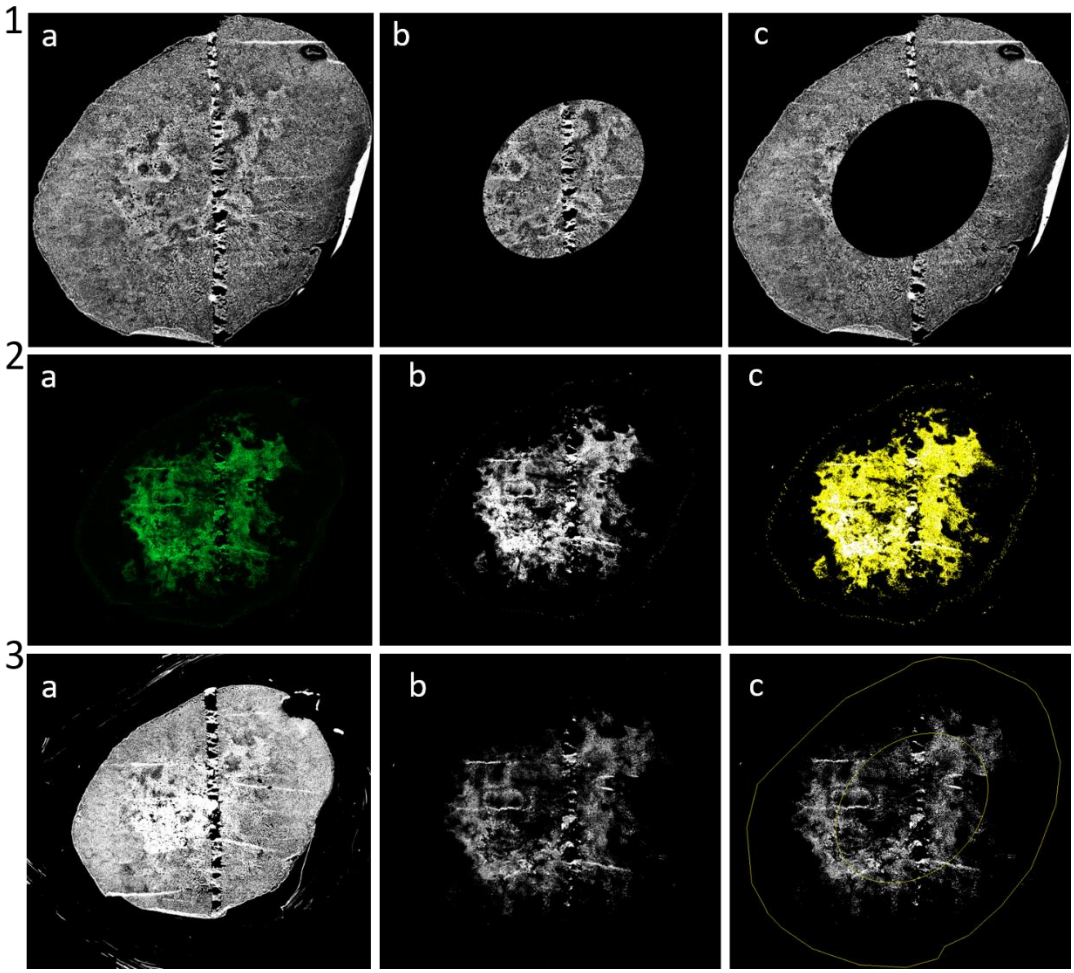

Figure 4.15: Analysis of spatial distribution of identified immune cell populations in the primary tumour

4T1 tumours harvested 3 weeks after tumour cell induction were cut into 7 µm sections and stained with relevant antibodies and isotypes (see methods) and Hoechst.
1) Width and height of the whole tumour section (a) were divided by 2 to create an ellipse representing the tumour core (b), with the outside representing tumour periphery (c).
2) To determine the percentage area of staining covered in the different regions, images were converted to 8bit (a), before a threshold was applied to the staining in every channel recorded and converted to binary (b). This was then used to create a region of interest (ROI) for each channel (c). 3) All the ROIs were applied to the Hoechst stain which was converted to binary (a), revealing the area of interest (b). The different tumour regions were then applied and percentage of area covered was measured (c).
Images are representative of 4 individual tumours/experiments.

These subregions are not strict biological entities but rather used to enable image analysis. To investigate cell localisation, the percentage area of staining covered in the different regions was determined, using the above described combination of markers (table 4.2) to identify different cell types (figure 4.15, 2). Images were converted to 8bit before a threshold was applied to the staining in every channel recorded and the picture was converted to binary. The threshold was then used to create a selection that could be applied to the whole tumour section stained with Hoechst and the percentage area of the selection covering tumour centre and periphery could be measured (3).

Analysis of the different cell types (Figure 4.16) showed that neutrophils (a,1) expressing Ly6G, CD45 and Ly6C tended to cluster in the core of the tumour.

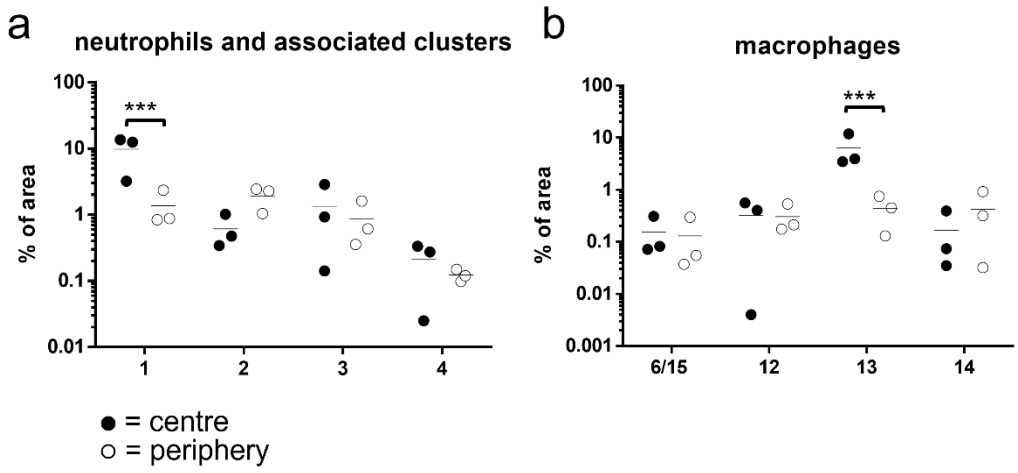

Figure 4.16: Analysis of spatial distribution of neutrophils and associated populations and macrophages in the primary tumour

4T1 tumours harvested 3 weeks after tumour cell induction were cut into 7um sections and stained with relevant antibodies and isotypes (see methods). All sections were stained with Hoechst (1 µg/ml). Plots show percentage area of centre and periphery as identified in figure 4.15 covered by cells stained with antibodies in combinations outlined in table 4.2. a) shows neutrophils and associated clusters, b) shows macrophages. N = 3

Data show mean and were analysed using multiple t tests, one per cell type, statistical significance determined using Holm-Sidak method, alpha = 5.00%. a) 1: p = 0.000183, t ratio = 4.83394; b) 13: p = 0.00050, t ratio = 4.346;

P***, $P \leq 0.001$; **, $P \leq 0.01$; *, $P \leq 0.05$;

Population 2 expressing SiglecE but neither FcyR1 or Ly6G showed a slight tendency towards the tumour periphery, albeit not significant. Populations 3 and 4 (3: $CD14^+$, $FcyR1^-$, $PDL1^-$; 4: $CD14^+$, $PDL1^+$, $FcyR1^-$) did not show a preferential location. In regard to macrophage populations (b) only population 13 ($C1qA^+$, $CD45^+$, $F4/80^-$) was enriched in the tumour core, with all other populations distributed throughout the tumour.

Single cell sequencing data suggests functional differences in TAM populations

Since one of the macrophage populations (population 13) clustered in the tumour centre, it was investigated whether this preferential localisation was reflected by differences in gene expression between the populations. Ingenuity pathway analysis (IPA) performed on genes extracted from cloupe software flagged up functional differences between the four macrophage clusters.

Populations 12, 13 and 14 showed increased expression of genes associated with inflammatory responses, while population 15 showed decreased expression of genes involved in inflammation. In contrast, cluster 15 showed enhanced expression of genes associated with phagocytosis and genes related to cellular movement, which were reduced in the other populations.

Sequencing data were not deep enough to visualise whole pathways in IPA.

Thus, following this initial lead, genes up or down-regulated by at least a log2 fold change between different TAM populations were plotted (Figure 4.17 a and b).

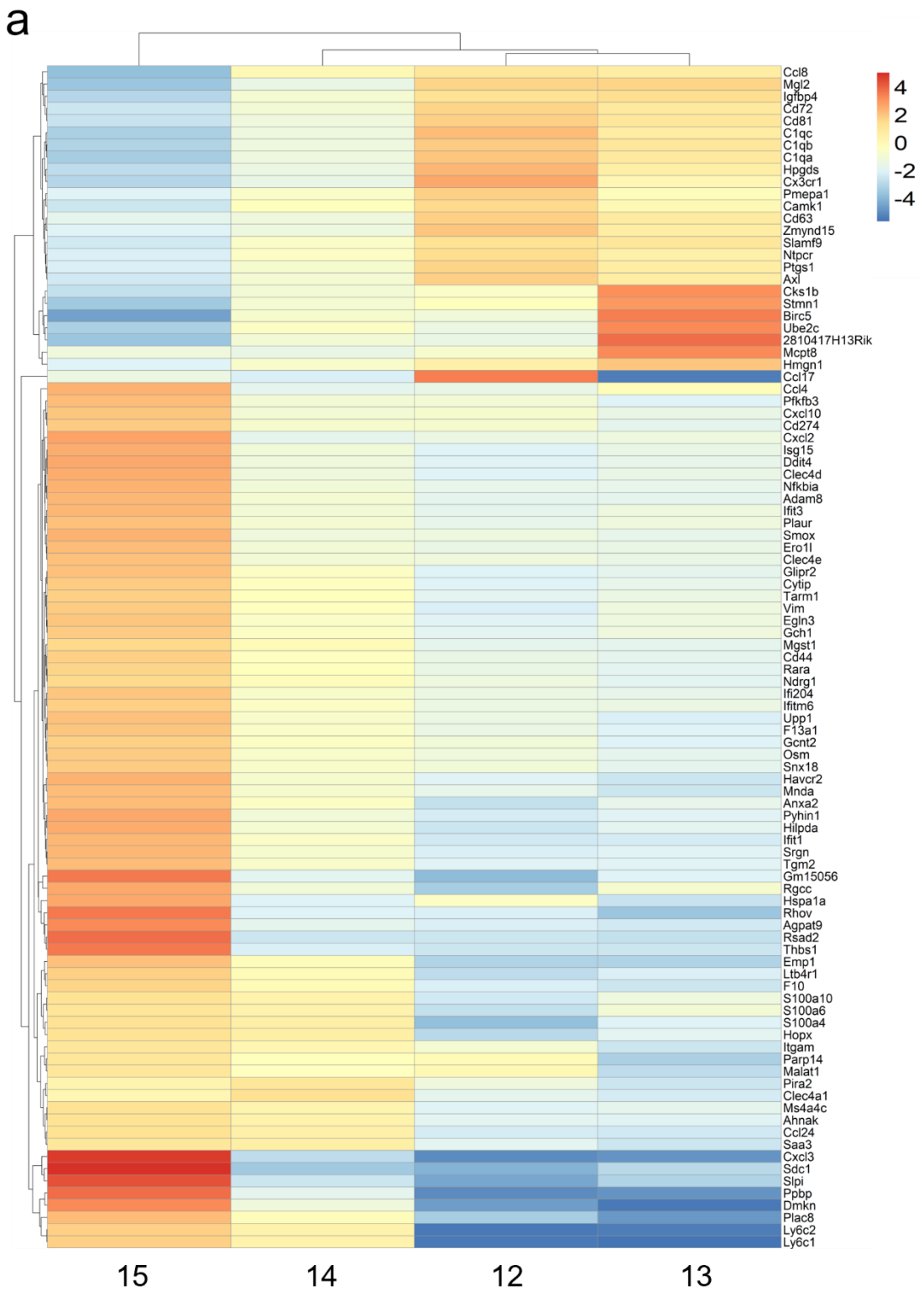

b

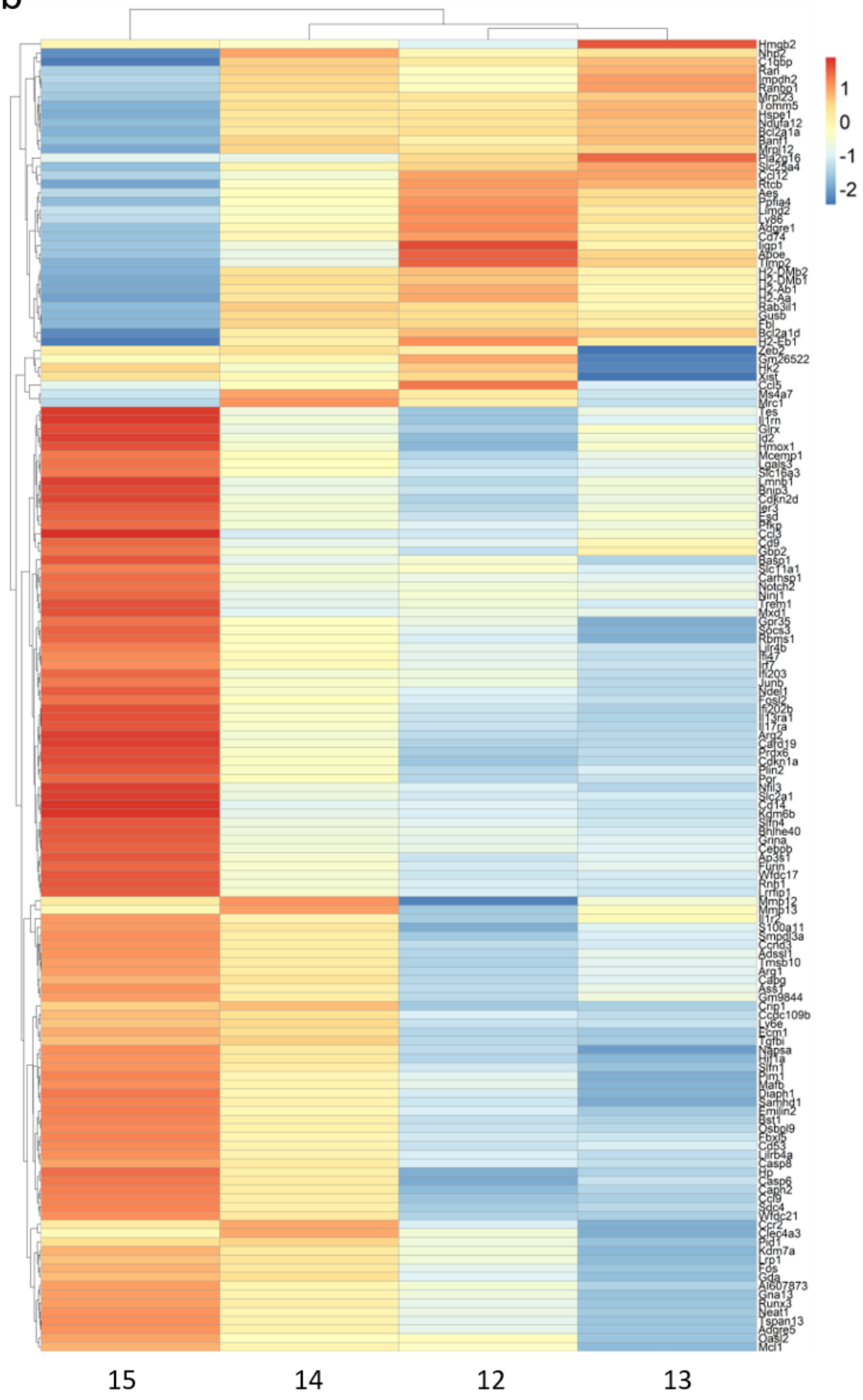

Figure 4.17: Heatmap illustrating differential gene expression in different TAM populations

scRNA-Seq data were used to create heatmaps of log2 fold difference in gene expression between populations 12-15 as characterised earlier. a) Hierarchical clustering of genes with a standard deviation above 1.5, b) Hierarchical clustering of genes with a standard deviation between 1 and 1.5; Heatmaps were constructed with R software, red indicates higher expression values, blue indicates lower expression values.

Indeed, population 15 appeared to be the most distinct, with population 14 being closest related to 15, while 12 and 13 also shared similar gene expression patterns. Several genes were expressed differently between the subsets: amongst other genes population 12 and 13 differed in the expression of a number of long non coding RNAs including *Malat1*, *H19* and *Xist*, the relevance of which is not yet clear. Population 14 and 15 showed differences in gene expression levels in a variety of genes illustrated in Figure 4.15: markedly, population 14 showed low expression of the genes involved in phagocytotic pathways highly expressed in population 15.

Population 15, being the most distinct population showed uniquely increased expression of genes associated with phagocytosis including transglutaminase 2 (*Tgm2*) and *Cd44* (Nadella *et al.*, 2015), Interferon stimulated gene 15 (*Isg15*) (Yángüez *et al.*, 2013), *Slpi* (Odaka *et al.*, 2003) and galectin 3 (*Lgals3*) (Voss *et al.*, 2017). It was also marked by the upregulation of the glycolysis pathway (*Pfkb3*, *Slc16a3*, *Pfkp*, *Slc2a1*, *Hif1a*) which has been shown to be enhanced during proinflammatory activation (Viola *et al.*, 2019).

In general, genes highly up or down regulated in population 15, and to a lesser extend population 14, specifically include those associated with monocyte-derived macrophages exposed to hypoxia *in vitro* (Fang *et al.*, 2009).

In a fast-growing tumour, increased oxygen demand can result in hypoxia and hypoxia-induced alterations in immune cell transcriptomes. Likely, hypoxic regions would be present in the core of a tumour, with cells exposed to hypoxia upregulating Hif-1α expression which acts as a master regulator of cellular responses to hypoxia. This is not in line with population 15 being evenly distributed throughout the tumour, so the presence of Hif-1α in whole tumour sections was investigated. To ensure Hif-1α could be detected, 4T1 cells were exposed to hypoxic conditions (1 % O_2) *in vitro* for 24 hours (Figure 4.18 1).

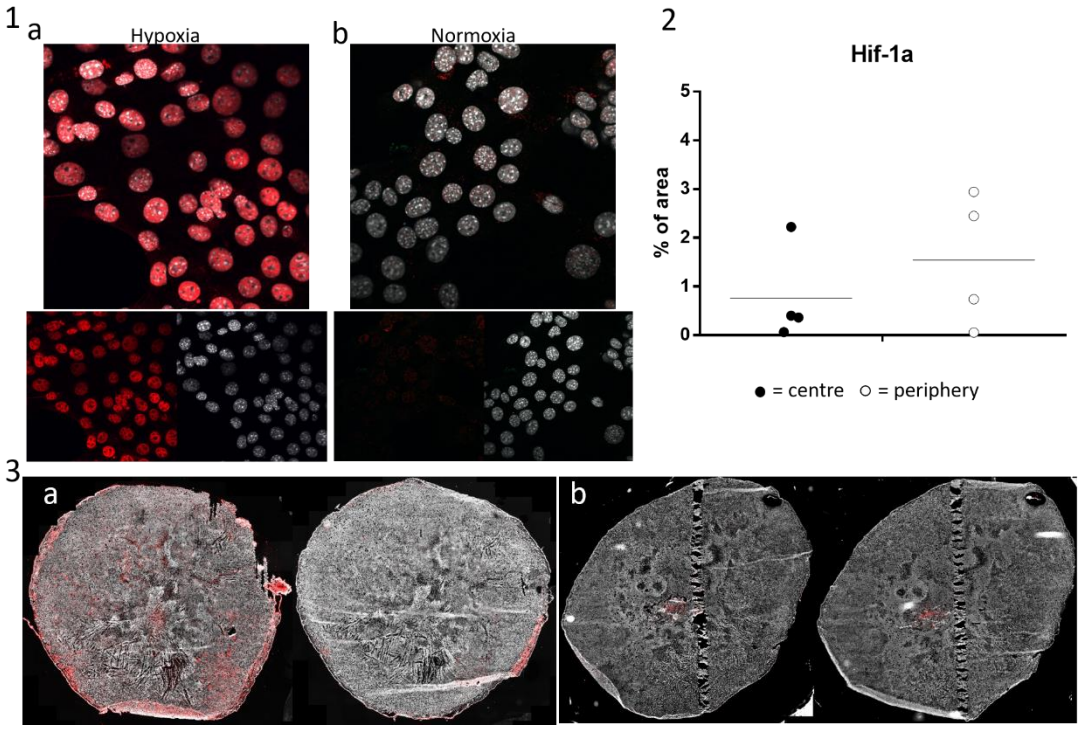

Figure 4.18: Hif-1α expression differs among tumours and is not restricted to the tumour core

1) 4T1 tumour cells were cultured in Hypoxia (1 % O_2, a) or Normoxia (20 % O_2, b) for 24 hours before they were fixed and stained with anti-Hif-1α antibody and Hoechst.

2) Percentage area of centre and periphery of whole tumour sections covered by Hif-1α staining was recorded and compared. N = 4

3) Example of Hif-1α and isotype staining in a tumour with relatively high (a) and low (b) Hif-1α detection. Images are representative of 4 individual tumours.

Investigating Hif-1α expression in the primary tumour, it became clear than tumours differ in the extent of Hif-1α that can be detected three weeks post tumour cell inoculation, and that Hif-1α is not preferentially expressed in the tumour core. Given that there was no difference detected in the area of whole tumour section covered by TAM populations in a tumour with high vs low hypoxia, it is unlikely that hypoxia is the main influence on the observed differential TAM phenotypes.

TAM populations do not resemble M1 or M2 type macrophages

TAMs are often thought of as a specialised class of M2 type macrophages, with efforts towards repolarisation into M1 types linked to increased anti-tumour immune responses.

Thus, it was investigated whether TAM populations identified in this study fall into either the M1 or the M2 category. Comparing log2 fold change values of gene expression in TAM populations to markers proposed to be up-regulated in M1 (Figure 4.19 a) or M2 type macrophages (b) (Jablonski *et al.*, 2015) revealed that TAM populations do not fall at either end of the polarisation spectrum, but rather have a mixed phenotype.

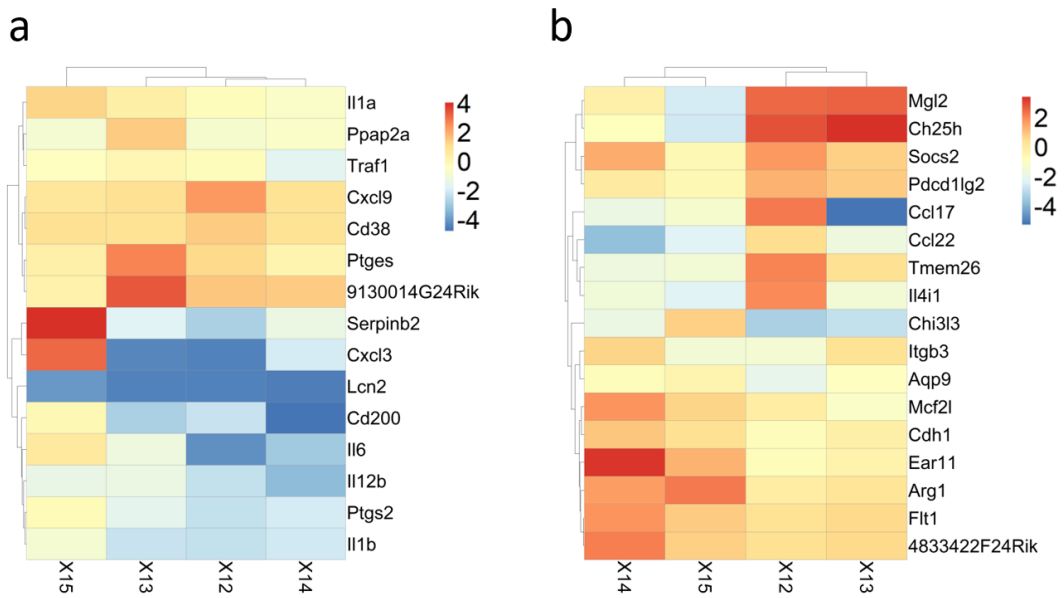

Figure 4.19: TAM populations co-express markers of M1 and M2 macrophages

log2 fold difference in gene expression between TAM populations and other immune cell populations identified by scRNA-Seq were used to create heatmaps of gene expression characteristic of M1 (a) and M2 (b) macrophages. X12-X15 correspond to macrophage populations 12-15. Heatmaps were constructed with R software, red indicates higher expression values, blue indicates lower expression values.

The lack of depth of single cell sequencing does not allow to conclude that genes with very low expression are in fact not expressed, since expression might just not be detected. Nevertheless, all TAM populations co-expressed genes of M1 and M2 typical markers. The same was true when investigating the protein expression of typical M1 and M2 markers (Martinez *et al.*, 2008) (Figure 4.20).

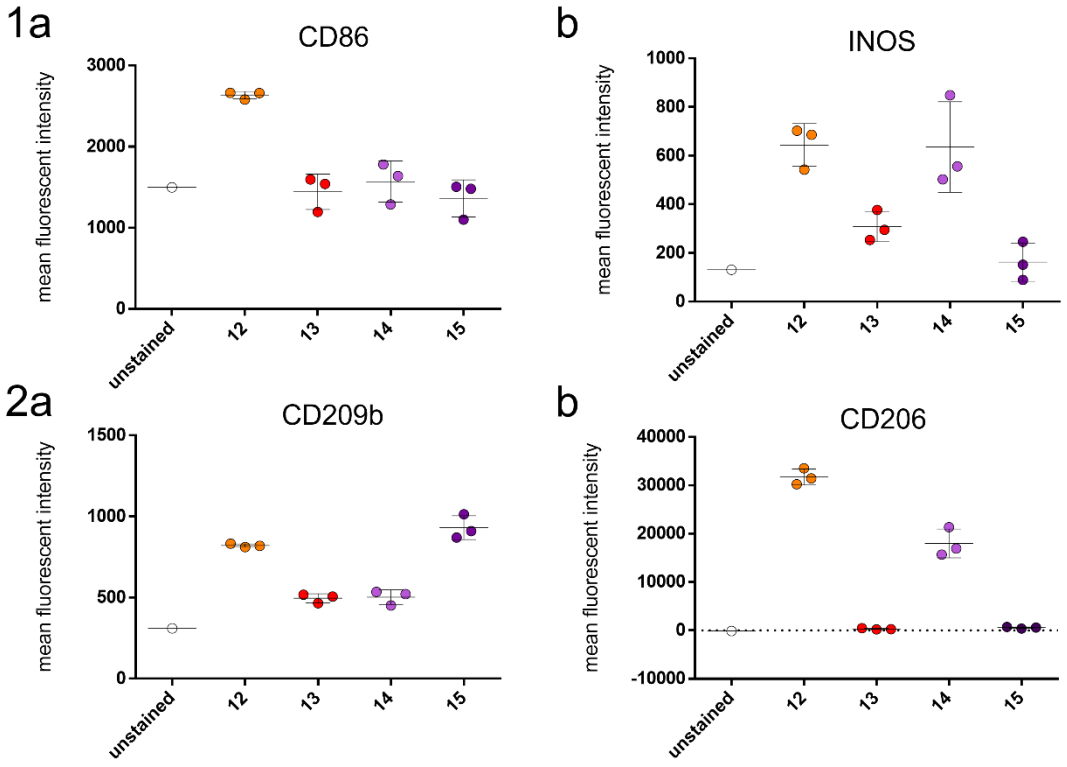

Figure 4.20: TAMs comprise markers of both, traditional M1 and M2 macrophages

4T1 tumours harvested 3 weeks after tumour cell induction were processed as described earlier and stained with relevant antibodies.

Mean fluorescent intensity comparing M1 (a) and M2 (b) associated markers: CD86, INOS, CD209b and CD206 expression of an unstained sample and different macrophage populations (12-15), N = 1 for unstained, 3 distinct tumours for the rest;

Data were analysed with one way ANOVA, means were compared to each other by Turkey's multiple comparison test. 1a: $p = 0.0002$, R square = 0.9057; b: $p < 0.0001$, R square = 0.9636; 2a: $p = 0.0018$, R square = 0.8325; b: $p < 0.0001$, R square = 0.9888;

Population 12 expressed the M1 associated co-stimulatory CD86 and INOS, but also M2 associated CD209b and CD206. Population 13 showed low or no expression of all these markers. Population 14 expressed M1 typical INOS but also M2 typical CD209b and CD206 and population 15 only expressed CD209b.

Macrophage origin is unclear

The origin of the distinct macrophage populations was unclear at this point. The sequencing data suggested that especially population 15, but potentially also 14 could be recently derived from incoming monocytes, as both populations were marked by the

expression of *Ccr2* and *Ly6c1*, with population 15 additionally expressing *Cd14*. In contrast, population 12 expressed *Adgre1* and *Cx3cr1*, and both, 12 and 13 expressed various H2-complex genes suggesting they might be either tissue resident type cells or fully differentiated activated monocyte-derived macrophages. Aiming to prevent the recruitment of monocytes into the primary tumour by administration of antibody binding CCL2 either before or after tumour cell inoculation was unsuccessful, both in reducing the numbers of any immune cells in the tumours, as well as in reducing tumour growth (Figure 4.21).

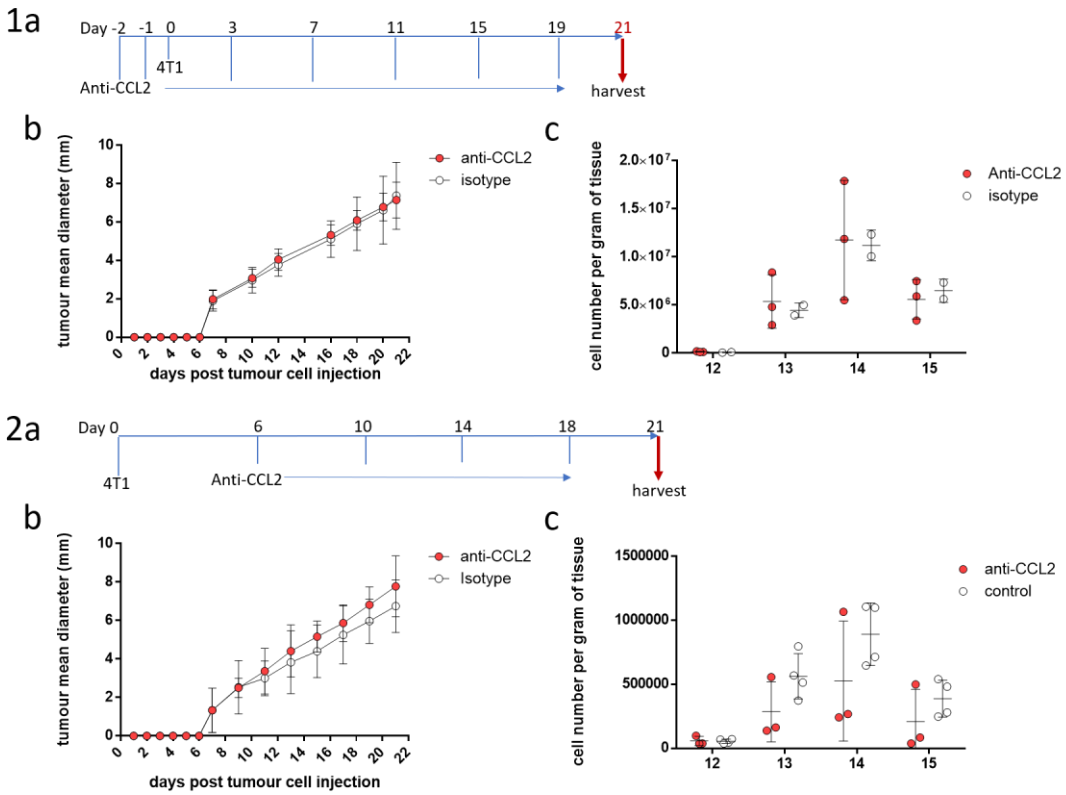

Figure 4.21: i.p. injection of anti-CCL2 antibody does not reduce TAM populations

1 a) Mice were injected i.p. with anti-CCL2 or isotype antibody on day -2 and -1 prior tumour cell inoculation. Antibody injections were repeated every 4 days. Tumours were collected on day 21 after tumour cell inoculation. Growth curve (b) and total number of TAM subsets per gram of tumour tissue recovered, N = 3 for treatment, 2 for isotypes; 2 a) Mice were injected i.p. with anti-CCL2 or isotype antibody once tumours became palpable. Antibody injections were repeated every 4 days. Tumours were collected on day 21 after tumour cell inoculation. Growth curve (b) and total number of TAM subsets per gram of tumour tissue recovered, N = 3 for treatment, 4 for isotypes;

Discussion

Single cell sequencing

For single cell sequencing, tumour cell dissociations were pooled from 3 individual female BALB/c mice (10-12 weeks of age) that had been injected with 4T1 tumour cells on the same day. This was meant to not only increase the number of viable cells available for sequencing at the end of tumour processing, but also to overcome inter-individual differences that might occur between the mice. Arguably, pooling three different tumours could contort the representation of populations that are present. However, those three mice were genetically identical, age matched and kept in the same cage so no great differences were expected. As observed in later experiments analysed by flow cytometry, despite presenting with the same initial clusters of immune cells individual tumours did sometimes contain an unusually high number of B or T cells. If one such tumour had been used for sequencing on its own, this cell population might have been overrepresented. Generally, however, this study was interested mainly in myeloid populations which appeared to be relatively stable between different mice observed throughout experiments. Ideally, three different samples would have been processed and sequenced in parallel. This, however, was not feasible due to financial constraints and the difficulty of isolating a sufficient number of viable cells expressing the aforementioned markers to be recovered after cell sorting (compare chapter 3). Thus, to bypass this issue, a strategy for identification of the populations identified by single cell sequencing by flow cytometry was designed and validated by successful application to 24 individual tumours before application to 150 individual tumours from different experimental settings over the course of the study.

Sample processing

Total cDNA content as measured by Qubit assay was low for both samples, with 0.304 ng/µl measured for sample 1 and 0.356 ng/µl for sample 2. A low yield of cDNA could possibly be the result of faulty processing or loss of cDNA during clean-up steps. To rule out technical error the experiment was repeated with a different set of tumours processed in the same way, yielding comparably low results (0.56 ng/µl for sample 1 and 0.48 ng/µl for sample 2). Thus, it was concluded that the low amount of cDNA recovered might actually represent a generally low mRNA content in analysed cells.

cDNA amplification after GEM lysis was conducted in a total of 10 cycles. This was calculated from an input number of 10,000 cells/well which, based on a 60 % capture rate, equates to 10 cycles as recommended by the manufacturer. This recommendation is based on a need to balance the number of cycles needed to generate enough DNA for library construction while keeping PCR amplification artefacts low. The post-cDNA amplification quality check revealed peaks of short fragment size. These peaks <100 base pairs were indicative of primer carryover that is normal and does not affect later sequencing (Biswas and Sharma, 2018).

Clustering

t-SNE clustering was performed with the 10x Genomics Cell Ranger software and yielded four distinct subsets of macrophages. Macrophage associated cell IDs were extracted and UMAP clustering was applied using Seurat package in R software to cluster the cells independently.

UMAP analysis revealed three clusters, one of which each corresponded to macrophage populations 14 and 15 as identified by Cell Ranger, while a third one combined cells from clusters 12 and 13 (supplementary figure S3). Changing the parameters increased the number of clusters observed, resulting in a split of this third cluster into clusters resembling 12 and 13, but also sub-clustering what corresponded to population 15 into two different clusters (supplementary figure S4). Generally, UMAP clustering did support Cell Ranger t-SNE clustering in that broadly the same clusters were detected. The difference observed between the two clustering methods and indeed between the different parameters chosen for UMAP clustering illustrates the challenge of single cell sequencing analysis, where cells can be clustered into increasing numbers of marginally different populations by parameter alteration. Any clustering suggested by the algorithm will need to be biologically validated. The merging of clusters 12 and 13 into one big cluster is not entirely surprising given the close similarity in gene expression between these two clusters. Since 12 and 13 could be differentiated by protein expression in flow cytometry, it was decided to persevere with this distinction for the purpose of the experiments in this thesis, as it would allow the detection of any potentially meaningful changes in either of the two parts of the C1qA positive macrophage population that might have been lost by grouping them together.

Single cell sequencing data suggested the presence of multiple subsets of undefined populations clustering with neutrophils as well as different types of macrophages among other established immune cell populations. While cells for sequencing purposes were sorted based on the cell surface expression of CD11b and CD11c to focus on myeloid cells, other cell types also express these markers (X. Liu *et al.*, 2015), (Vinay and Kwon, 2010). Thus, the populations and their ratios identified through sequencing do not reflect the total immune cell infiltration in the 4T1 tumour.

While repeated sequencing was not feasible, the data obtained by single cell sequencing were validated by the creation of flow cytometry panels based on markers identified with the sequencing data. The same populations identified through sequencing could also be identified with flow cytometry across 24 4T1 tumours from distinct experiments which validated the use of those panels for future studies, where they have successfully been applied to 150 individual 4T1 tumours across different experiments.

Gene expression analysis identified at least four distinct subsets of macrophages. The concept of multiple variants of macrophages in the tumour microenvironment is not new: this is reflected by the idea of M1 and M2 type macrophages coinciding within tumour tissue which are often suggested to suppress and support tumour growth respectively (Medrek *et al.*, 2012). In the 4T1 tumour context, Movahedi and colleagues (Kiavash Movahedi *et al.*, 2010) discovered two types of TAMs: MHCII high TAMs characterised by the upregulation of M1 markers, and MHCII low TAMs characterised by M2 marker expression. This pattern could not be observed in the present study. While MHCII high (12, 13) and low (14, 15) populations were detected, they did not fall into M1/M2 categories. Indeed, investigating markers characteristic of M1 and M2 type cells, TAM populations were found to express markers assigned to both ends of the polarisation spectrum. These data are in line with studies from other tumour models: in a model of lung cancer at least four different monocyte/macrophage subsets were identified based on transcriptional profiling, neither of which preferentially expressed M1 or M2 associated markers (Poczobutt *et al.*, 2016). Similar results have also been reported in human breast cancer (Azizi *et al.*, 2018a) and glioma (Müller *et al.*, 2017).

While the M1/M2 classification is still widely used in the field it is a rather outdated and oversimplified view of macrophage function. There is also a lack of consensus on reliable M1 or M2 related markers in mice (Jablonski *et al.*, 2015; Orecchioni *et al.*, 2019) and

humans (Martinez *et al.*, 2006; Kaneda, Cappello, *et al.*, 2016; Rostam *et al.*, 2017). Thus, while certain TAM subsets might express different markers that are often associated with either M1 or M2 macrophages this does not characterise them as inflammatory or resolution type cells. Since macrophage targeting approaches focussing on the reprogramming into M1 type cells in cancer do show promising results in preclinical settings (Kaneda, Cappello, *et al.*, 2016; Peng *et al.*, 2017; Bart *et al.*, 2020; Wyatt Shields *et al.*, 2020), it is likely that some of the pro-inflammatory actions usually assigned to M1 type macrophages are beneficial in supporting tumour rejection.

Ignoring M1/M2 based phenotypes, 4T1 TAMs have also been categorised based on their expression of podoplanin (Bieniasz-Krzywiec *et al.*, 2019). However, podoplanin was not detected in single cell sequencing in the present study and its expression at the protein level was not investigated.

While sequencing was not deep enough to fully dissect the phenotype and function of identified TAM populations, one TAM subtype (15) was associated with markers related to cellular movement. Combined with the expression of monocyte-typical *Ccr2*, *Ly6c1* and *Cd14*, which made it difficult to separate this macrophage population from *Ly6c1*$^{+}$*Nr4a1*$^{-}$ monocytes, the data suggest that population 15 might be a population recently differentiated from tumour infiltrating monocytes. In contrast to the increased expression of genes associated with phagocytic capacities, all other populations were associated with increased gene expression related to inflammatory processes but not phagocytosis.

Histological analysis

Histological analysis revealed that neutrophils and TAM population 13 preferentially clustered close to the tumour core, while the other subsets showed no preferential location in the tumour.

In lung carcinomas it has been shown that MHCII low TAMs reside in hypoxic areas and MCHII high TAMs cluster in normoxic tumour regions (Laoui *et al.*, 2014). In the present study, two populations of TAMs (12, 13) highly expressed MHCII but they did not cluster together, since population 12 was evenly distributed throughout the tumour and 13 clustered in the tumour centre. Also, while analysis of gene expression profiles especially for population 15 flagged up genes up- or downregulated in monocyte derived macrophages exposed to hypoxia *in vitro* (Fang *et al.*, 2009), population 15 did not cluster with areas of hypoxia. In general, areas of hypoxia were only detected in one of the three

tumours investigated. This is interesting, since tumours were of similar size and had been collected on the same day post 4T1 inoculation. Tumours with and without areas of hypoxia did not differ in their immune cell content. Thus, while the tissue microenvironment is likely to influence macrophage gene expression, hypoxia likely is not the main influence on TAM phenotype. Clearly the sample size is too small for conclusive results. Still, the data are in line with a study by Laoui and colleagues where altering tumour internal oxygen levels did not affect relative macrophage numbers and expression of M2 markers in tumour cores.

TAM origin

Investigating the origin of TAM populations by blockade of CCL2 via anti-CCL2 antibody did not alter TAM populations. This could mean that none of the TAM populations discovered in the present study were monocyte derived. This is, however, unlikely, given the expression of monocyte-typical *Ccr2*, *Ly6c1* and *Cd14* in population 15 and data reported by Movahedi and colleagues (Kiavash Movahedi *et al.*, 2010) showing that TAMs were derived form Ly6C high monocytes. Anti-CCL2 antibody treatment followed a protocol applied by Li and colleagues (Li *et al.*, 2013), resulting in reduced 4T1 tumour growth. Importantly, Li and colleagues did not investigate whether or not a reduction of TAMs or monocytes was achieved by this treatment. Also, interestingly, while not testing this concept in 4T1 tumours, Li and colleagues found that anti-CCL2 therapy was only effective when delivered once MCA tumours were already established but not when used prior to tumour cell inoculation. This points toward an important role of monocytes, and potentially monocyte-derived macrophages in the initial stage of tumour formation.

Delivering antibody treatment following the same protocol, in the present experiment three TAM populations were decreased in two out of three mice. Thus, the sample size should be increased to investigate whether an effect could be present. In line with other findings of this study, population 12 which expressed markers of tissue resident cell types was not decreased, however, the closely related population 13 was, as were the potentially monocyte-derived 14 and 15.

Using a computational approach, it was attempted to investigate the origin of macrophage populations clustering together (12/13, 14/15) via the pseudotime modelling analysis: the pseudotime algorithm aligns single cells along a timeline according to continuous changes in gene transcription, suggesting a path of how different cell types most likely develop relative to each other (Haghverdi *et al.*, 2016).

Different sets of parameters were trialled in the pseudotime analysis to investigate whether macrophage populations develop independently or whether one population reflects a transitional phase. Different parameters used to test this hypothesis reported different results. As there appears to be no consensus on which parameters should be used to correctly model macrophage development, no conclusion could be reached at this point. Additionally, as one needs to set a starting point for the trajectory, in this case monocytes, it can not be investigated whether clusters 14/15 and 12/13 are indeed derived from monocytes or are resident macrophage cell types.

In conclusion, the work summarised in this chapter identified three distinct immune cell populations clustering with neutrophils and four distinct macrophage populations in the 4T1 model of breast cancer that differ in gene expression and spatial distribution. These distinct populations have not been identified before. The TAMs identified conform to neither the M1 nor the M2 spectrum of polarisation, sharing markers of both types. Due to their transcriptional and spatial differences it is reasonable to hypothesise that these different populations would affect tumour development in different ways and that they would respond in unique ways to therapeutic intervention.

Chapter 5: Manipulation of immune cell populations

Rationale

The multiple roles of TAMs in tumour development and progression suggest that they may be exploited for anti-cancer therapy. The hypothesis is that some of the TAM populations discovered in chapter 4 could aid tumour progression, while others could help tumour control. Directly targeting myeloid cells in the tumour microenvironment may affect each of the TAM populations differently, resulting in different treatment outcomes. Further, little is known about the effects of Treg manipulation on TAM content, especially regarding the multiple populations described earlier in this work.

After establishing the presence of different types of TAMs in the typical development of a mouse model of breast cancer shown in chapter 4, the primary aim of the work in this chapter was to investigate how manipulation of immune cell subsets can affect these TAM populations and whether there are correlates with changes in tumour growth and metastasis.

Specific Aims

1) Interfere with myeloid populations directly to investigate their role in tumour progression and metastasis.

2) Determine how regulatory T cell depletion / inactivation affects tumour myeloid cell populations.

3) Examine the potential benefit of combining Treg depletion with TAM manipulation.

Introduction

The immune infiltrate of the primary tumour includes a variety of cell types, some of which are known to actively interfere with anti-tumour responses and therapeutics. Such cells can be part of the innate immune system, including TAMs, as well as adaptive immune cells such as regulatory T cells.

Interaction between Tregs and TAMs in the tumour microenvironment

Tregs are crucial to maintain normal tissue homeostasis (Sakaguchi *et al.*, 2001) but also play a critical role in intra-tumour immune suppression, interfering with anti-tumour therapies in human patients (Curiel *et al.*, 2004; Hobeika *et al.*, 2011) and murine models (Onda, Kobayashi and Pastan, 2019). Tregs in the tumour microenvironment likely interact with antigen presenting cells including TAM populations inducing an immune tolerant state that prevents effector T cell activation and anti-tumour immune responses. Such interactions have been demonstrated *in vitro* (Taams *et al.*, 2005) and *in vivo* (Maloy *et al.*, 2003; Mahajan *et al.*, 2006), albeit to date not in the tumour context.

Treg/TAM interactions are not one-sided: TAMs have been shown to promote Treg entry into tumour tissues (Curiel *et al.*, 2004) and even support *de novo* induction of Tregs from conventional $CD4^+$ T cells (Schmidt *et al.*, 2016).

As both TAMs and Tregs are known to be able to produce and respond to anti-inflammatory mediators, it is likely that those two populations would influence and potentiate each other. Indeed, a high number of TAMs displaying M2 characteristics in the tumour microenvironment correlated with the accumulation of $FOXP3^+$ Tregs and poor survival in laryngeal squamous cell carcinoma (Sun *et al.*, 2017). *In vitro* evidence supports the idea that those macrophages promote *de novo* induction of Tregs which in turn induce a TAM phenotype in monocytes. Importantly, reducing either population within the tumour *in vivo* decreased the other, and targeting both simultaneously improved efficacy regarding tumour growth inhibition and prolongation of survival in a mouse model of squamous cell carcinoma (Sun *et al.*, 2017).

While this suggests that macrophages and Tregs influence each other, the authors focused on M2 type macrophages, which they identified by expression of CD163. Cells expressing M2 type markers were detected in the myeloid infiltrate of 4T1 tumours as illustrated in the previous chapter. However, findings of the present study showed that all identified

TAMs expressed a mixture of markers associated with the M1/M2 phenotype. In addition, different types of cancer might harbour different macrophage populations.

Thus, the experiments described in this chapter aimed to investigate the effect of Treg manipulation on all macrophage type cells present in the 4T1 tumour microenvironment.

Targeting Tregs and TAMs in the 4T1 tumour microenvironment

Macrophages in the tumour microenvironment can potentially be inhibited with various methods:

Interfering with CSF1R signalling – GW2580

The importance of CSF1R signalling for macrophage survival, proliferation and motility has been discussed earlier. Interfering with CSF1R signalling using small molecule inhibitors such as GW2580 has been associated with varying results in different tumour models: while GW2580 treatment in an oncogene driven mammary tumour decreased F4/80 high but not MHCII high macrophages (Tymoszuk *et al.*, 2014) the opposite was observed in a model of pancreatic ductal adenocarcinoma (PDAC) (Mitchem *et al.*, 2013).
The effect of GW2580 treatment on different macrophage types identified in the 4T1 model and its potential effect on primary tumour and metastasis progression have not been evaluated to date.

Clodrosomes

While CSF1R interference does not necessarily deplete macrophages, this may be achieved by the use of liposomal clodronate, which, once ingested by phagocytotic cells, causes apoptosis. In murine models this method has been widely used to deplete macrophages in different tissues and contexts (Fritz *et al.*, 2014; Griesmann *et al.*, 2017; Opperman *et al.*, 2019).

Current data suggest not only an interplay but also a dependency between Tregs and TAMs that may have therapeutic potential. Thus, interfering with Tregs in the tumour context would likely affect TAM populations which could potentially impact tumour outcome. Different mechanisms blocking Treg function have been described in the context of cancer:

PI-3065

PI-3065 is a selective inhibitor of the PI3K p110δ subunit expressed by all immune cells. In the 4T1 model, treatment of mice with PI-3065 was associated with reduced growth of the primary tumour and decreased metastasis. This effect was not caused by inhibition of 4T1

tumour cells which lack p110δ expression, but likely due to Treg inhibition (Ali *et al.*, 2014). While conventional T cells seem to be protected from p110δ inhibition by the expression of other class I isoforms, other immune cells including B cells, macrophages and neutrophils also express p110δ and could also be affected by this type of therapy.

In macrophages, the PI3K-AKT pathway has been implicated in regulating activation status and inflammatory responses (Sharif *et al.*, 2019). Inhibition of PI3Kγ has been shown to reprogram TAMs into pro-inflammatory phenotypes capable of restoring $CD8^+$ T cell activation and cytotoxicity against tumour cells in murine models (Kaneda, Messer, *et al.*, 2016). In contrast, the role of p110δ is less well explored: macrophages from mice expressing inactive p110δ display difficulties in the crossing of basement membranes and collagen IV degradation in a model of systemic lupus (Suárez-Fueyo *et al.*, 2014). Further, p110δ is primarily activated in macrophages in response to CSF1R signalling and its inhibition was associated with reduced macrophage tissue infiltration and extracellular matrix degradation *in vitro* (Mouchemore *et al.*, 2013). While these data point towards an effect of p110δ inhibition on macrophages, the outcomes of blocking p110δ signalling in macrophages in the tumour context, especially the multiple populations of TAMs identified in the previous chapter, are not understood.

DEREG mice

While PI3Kδ inhibition might have off-target effects by acting on macrophages and other immune cell populations, DEREG mice can be used to specifically deplete Tregs without directly targeting other cell types. DEREG mice express the diphtheria toxin (DT) receptor under control of the *Foxp3* promotor. DT mediated Treg depletion has been associated with primary tumour regression in different types of cancer (Klages *et al.*, 2010; Teng *et al.*, 2010; Fisher *et al.*, 2017). Interfering with Treg function has been described to promote tumour control; however, these studies have not focused on the effect such therapies could have on macrophages in the tumour microenvironment. In addition, Treg manipulation methods are rarely combined with strategies inhibiting TAM populations.

Few studies have focussed on macrophage inhibition or depletion in the 4T1 tumour context. My research has identified different types of tumour infiltrating macrophages; the effects of macrophage manipulation therapy on these subsets need to be investigated. Thus, the aim of the work in this chapter was to study the effect of macrophage and Treg manipulation, on their own and in combination, on all TAM populations described in the

previous chapter. I also aimed investigate the wider implications this manipulation has on tumour growth and metastasis.

Intraperitoneally injected clodronate liposome is insufficient for 4T1 TAM depletion

Clodronate liposomes were used to investigate the effect of macrophage depletion on 4T1 tumour growth. Based on previous experiences in the group, different doses (25, 50 and 100 µl/mouse) were trialled to investigate safety and efficacy of the treatment (Figure 5.1).

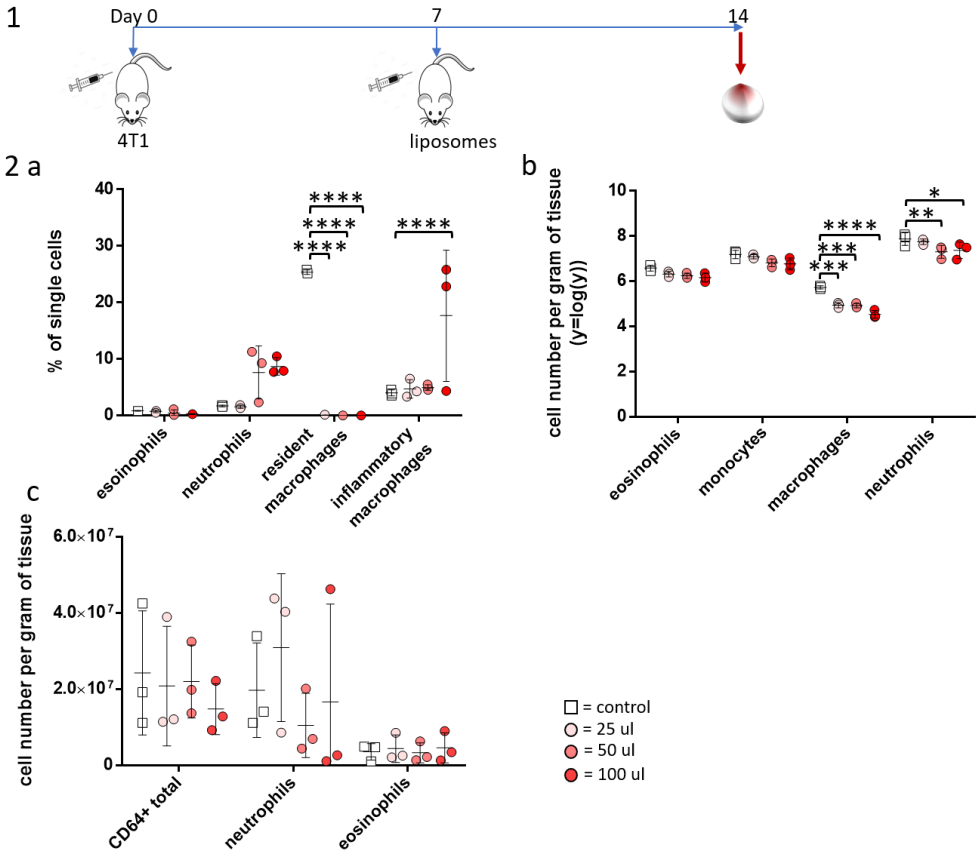

Figure 5.1: i.p. injection of clodronate liposomes depletes peritoneal macrophages

1) Mice were injected i.p. with different doses of clodronate liposomes or empty liposomes (controls) 7 days after tumour cell inoculation. Tumours, spleens and peritoneal lavage were collected on day 14 after tumour cell inoculation;

2) Immune cell types in (a) peritoneal lavage as % of single cells recovered, (b) spleens as total cell number per gram of tissue and (c) primary tumours as total cell numbers per gram of tissue. N = 3 for all conditions, Graphs show means ± SD.

a) and c) Data were analysed by two-way RM ANOVA with Tukey's multiple comparisons test, b) Data were log transformed (y=Log(y)) and analysed by two-way RM ANOVA with Tukey's multiple comparisons test: a) doses: $F(3, 8) = 9.592$, $p = 0.005$, cell types: $F(3, 24) = 11.64$, $p < 0.0001$, interaction: $F(9,24) = 18.28$, $p < 0.0001$; b) doses: $F(3, 8) = 7.999$, $p = 0.00086$, cell types: $F(3, 24) = 1337$, $p < 0.0001$, interaction: $F(9,24) = 8.933$, $p < 0.0001$;

****, $P \leq 0.0001$; ***, $P \leq 0.001$; **, $P \leq 0.01$; *, $P \leq 0.05$

In the peritoneum (2a) the different doses of clodronate showed equal efficacy in depletion of resident macrophages, with the medium and high dose associated with recruitment of neutrophils and inflammatory macrophages. In the spleen (2b) all cell types followed a trend of dose dependent reduction, with no neutrophil infiltration associated with higher doses. All doses reduced macrophage numbers, but could not achieve complete depletion. In the tumour (2c) clodronate treatment did not have any effect. In the analysis of all datasets by two-way RM ANOVA cell types came up as a significantly different factor (a: $p < 0.0001$, b: $p < 0.0001$, c: $p = 0.01$) which is due to the presence of different cell types in different proportions at the relevant site. Doses were a significant factor in peritoneal lavage (a: $p = 0.005$) and spleen (b: $p = 0.00086$) and interaction flagged significant in lavage (a: $p < 0.0001$) and spleen (b: $p < 0.0001$).

Due to the lack of effect observed in the primary tumour it was hypothesised that liposomes might have been taken up by macrophages in the peritoneal cavity and potentially other organs before being able to reach the tumour site. Thus, an even higher dose of 150 µl of clodronate liposomes per mouse was injected every 5 days throughout tumour development to investigate whether and how this high dose of liposomal clodronate would affect tumour infiltrating macrophages and primary tumour development (Figure 5.2).

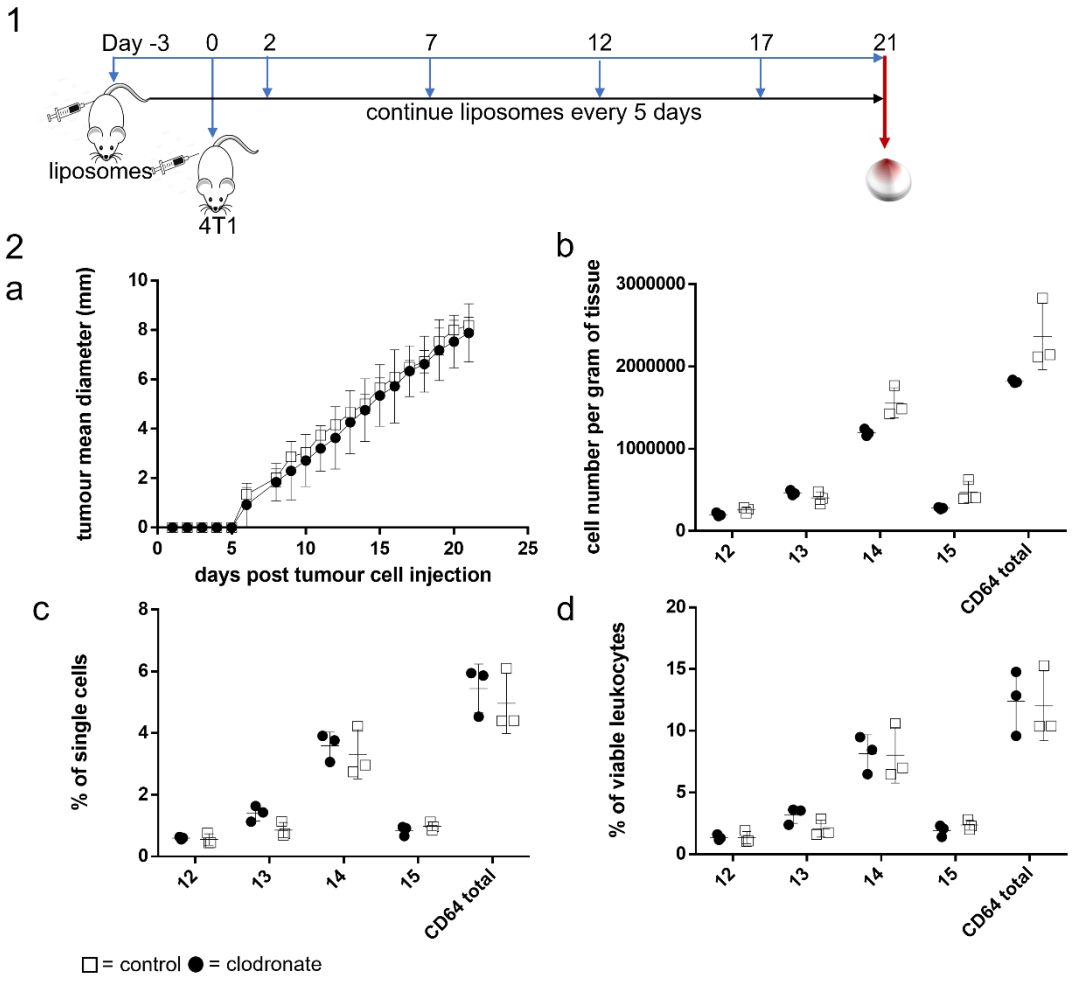

Figure 5.2: i.p. injection of clodronate liposomes fails to deplete 4T1 TAMs

1) Mice were injected i.p. with different doses of clodronate liposomes or empty liposomes (controls) 3 days prior to tumour cell inoculation. Injections were repeated every 5 days. Tumours were collected on day 21 after tumour cell inoculation.

2) a) Growth curve of tumours in mice receiving injections with empty (white squares, control) or clodronate (black circles) liposomes. b-d) macrophage subsets (12-15) and total number of $CD64^+$ immune cells as cell number per gram of tumour tissue (b), % of single cells (c) or % of viable leukocytes (d) recovered.

N = 3 for all conditions, graphs show means ± SD;

Primary tumour growth was not affected by repeated i.p. administration of 150 µl clodronate liposomes (2a). Neither were most immune cell populations in the tumour and lungs (Figure 5.2 and 5.3).

When calculated as numbers per gram of tumour tissue, TAM populations 14 and 15 looked like they might be affected by clodronate treatment (figure 5.2 b). This was, however, not evident when calculating the cells as a percentage of single cells (c) or viable leukocytes (d). Thus, if chlodronate liposomes were having an effect on macrophage numbers, it was very mild and insufficient given that the objective was to study macrophage depletion. Again, this lack of depletion could have been due to lack of localisation of liposomes to the tumour. Injection of a higher dose of clodronate liposomes was not considered safe based on previous experiments.

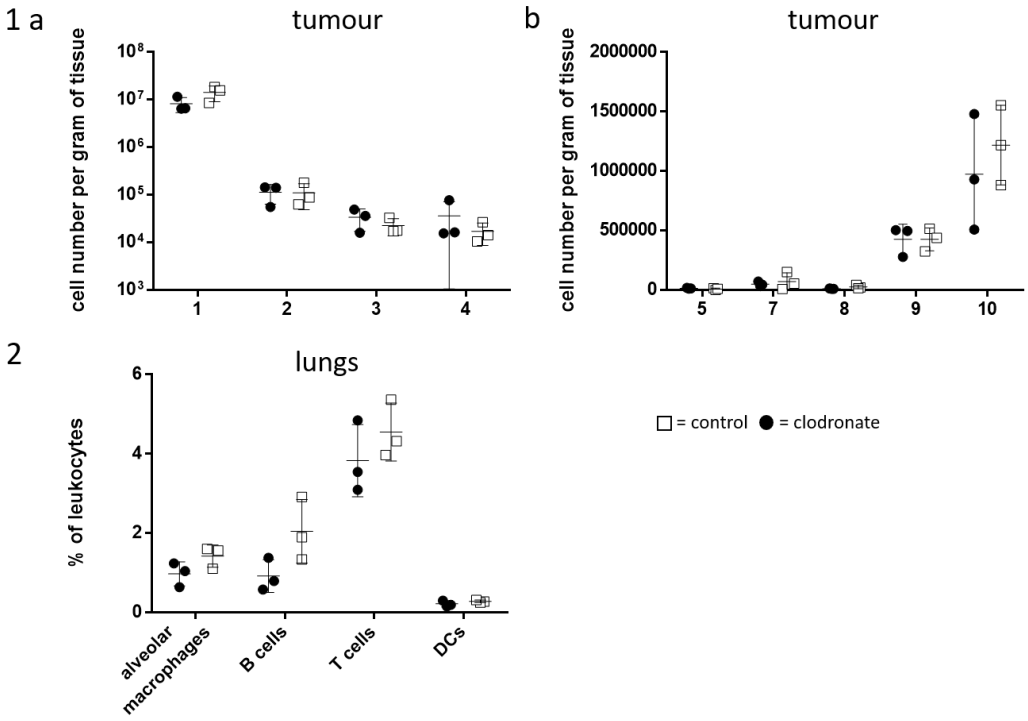

Figure 5.3: i.p. injection of clodronate liposomes does not affect other cell populations in tumour and lungs

Mice were injected i.p. with clodronate liposomes at different doses or empty liposomes (controls) 3 days prior tumour cell inoculation. Injections were repeated every 5 days. Tumours, were harvested on day 21 after tumour cell inoculation

1) a) Populations of neutrophils (1) and associated cells (2-4); b) populations of mast cells (5), pDCs (7), B cells (8), T cells (9) and DCs (10) in primary tumours as cell number per gram of tumour tissue. 2) Populations of immune cells in lungs as % of leukocytes. N = 3 for all conditions, Graphs show means ± SD.

Blocking CSF1R signalling reduces macrophage proliferation *in vitro* and *in vivo*

The CSF1R inhibitor GW2580 was used to trial a different method of macrophage reduction and its potential impact on tumour growth. GW2580 efficacy was tested *in vitro*: bone marrow was collected and left to adhere for 24 hours. Non-adherent cells were collected, plated at 200,000 cells per well, differentiated into macrophages *in vitro* and cultured in the presence of CSF1 and different doses of GW2580 for 24 hours (Figure 5.4). Since Dimethyl Sulfoxide (DMSO) is used in the preparation of GW2580 for oral gavage, one extra control was included of DMSO alone in the highest concentration used in GW2580 preparation to ensure no off-target effect of DMSO on macrophages could be observed.

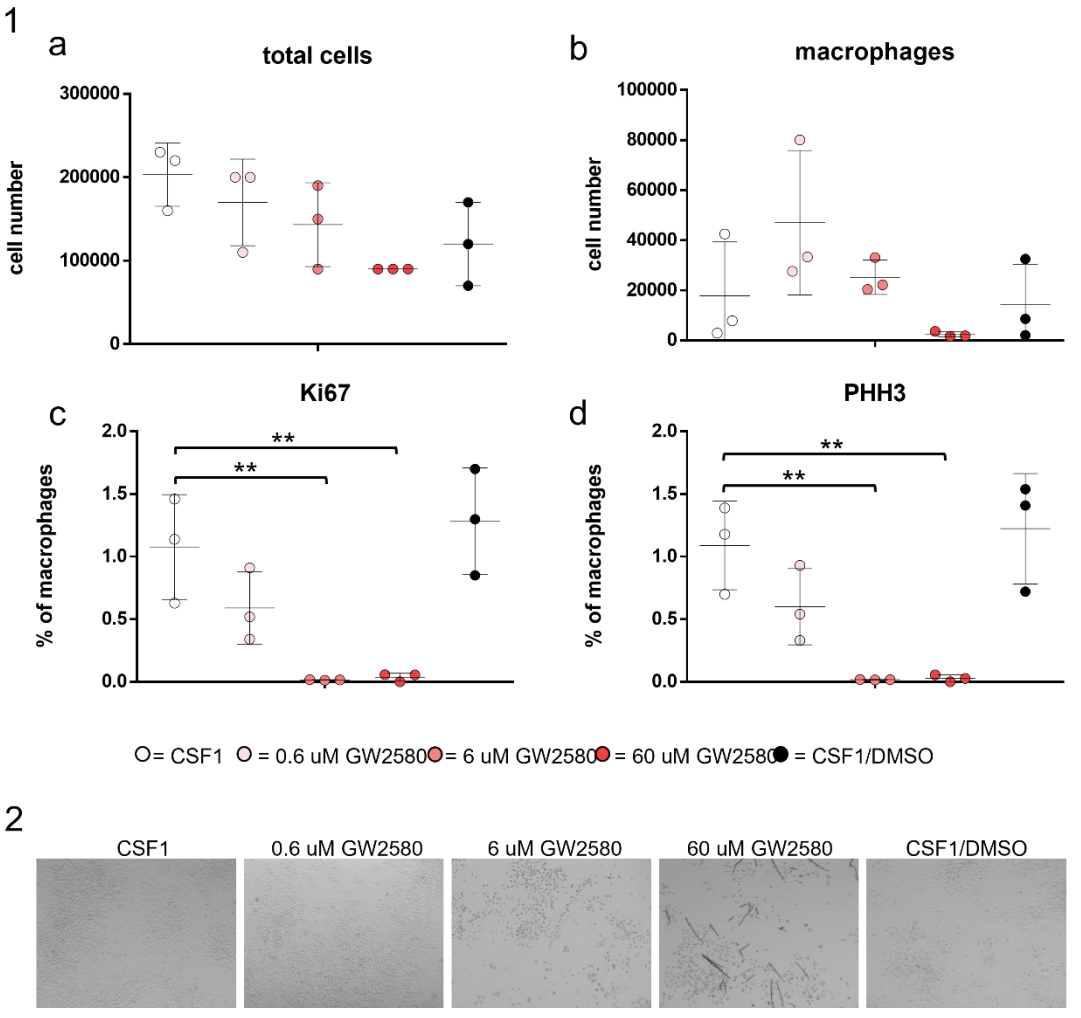

Figure 5.4: GW2580 treatment *in vitro* reduces macrophage proliferation

Bone marrow derived cells were plated in wells at 200,000 cells per well and differentiated into macrophages via CSF1. Bone marrow derived macrophages were treated with CSF1 only (white circle), CSF1 and DMSO in the highest concentration used for GW2580 preparations (CSF1/DMSO, black) or CSF1 plus GW2580 at 0.6 µM, 6 µM and 60 µM for 24 hours. Cells were harvested and stained for flow cytometry.

1) a) Number of total cells recovered from plates, b) total macrophages ($CD11b^+$, $F480^+$) recovered, c) percentage of macrophages positive for Ki67 and d) percentage of macrophages positive for PHH3; N = 3 for technical replicates, all cells were derived from one mouse. Graphs show means ± SD. Data were analysed with one way ANOVA, means were compared to the control (CSF1) by Dunnett's multiple comparison test: c) p = 0.0009, R square = 0.821; d) p = 0.0008, R square = 0.8246

2) Microscopy images of monocyte-derived macrophage wells before harvest: pictures are representative of 3 individual wells;

****, $P \leq 0.0001$; P***, $P \leq 0.001$; **, $P \leq 0.01$; *, $P \leq 0.05$

The data suggest a generally lower number of total cells recovered from wells treated with the highest dose of inhibitor that can likely be attributed to cell death, as only about half of the plated cells were recovered. Microscopy images show the appearance of crystal like structures in wells treated with 60 µM GW2580 (5.3 2). These crystals are not reported in the literature and it was unclear how and why they developed. Comparing macrophage proliferation, the lowest dose of inhibitor (0.6 µM) was associated with a slight reduction in both proliferation markers Ki67 and PHH3, although this trend was not statistically significant. Both the medium (6 µM) and high (60 µM) dose significantly reduced proliferation in monocyte derived macrophages and no crystal formation was observed in wells treated with the medium dose.

Based on these findings and data published on *in vivo* use of GW2580 (Conway *et al.*, 2005) the inhibitor was tested *in vivo* in a model of zymosan induced peritonitis at a concentration of 160 mg/kg every 24 hours corresponding approximately to a plasma concentration of 5.6 µM as discussed later. Macrophages were gated according to Figure 5.5.

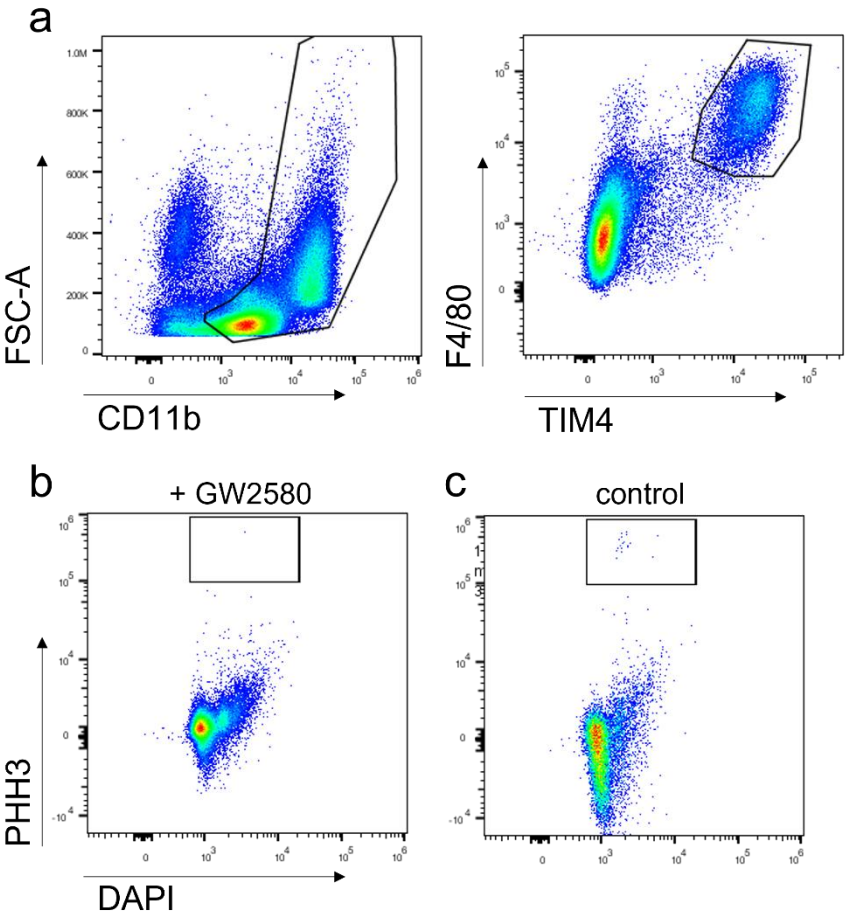

Figure 5.5: Gating for macrophage proliferation after GW2580 treatment *in vivo*

a) After removing debris and doublets as before, cells were gated based on expression of CD11b, F4/80 and TIM4. b and c) Macrophages (F4/80+ TIM4+) were gated based on PHH3 to determine cell proliferation. b) shows expression of PHH3 in GW2580 treated cells, c) shows expression of PHH3 in untreated controls. FACS plots are representative of 5 individual mice.

Oral gavage of 160 mg/kg GW2580 was associated with reduced numbers of macrophages recovered, as well as with reduced macrophage proliferation based on expression of PHH3 (Figure 5.6).

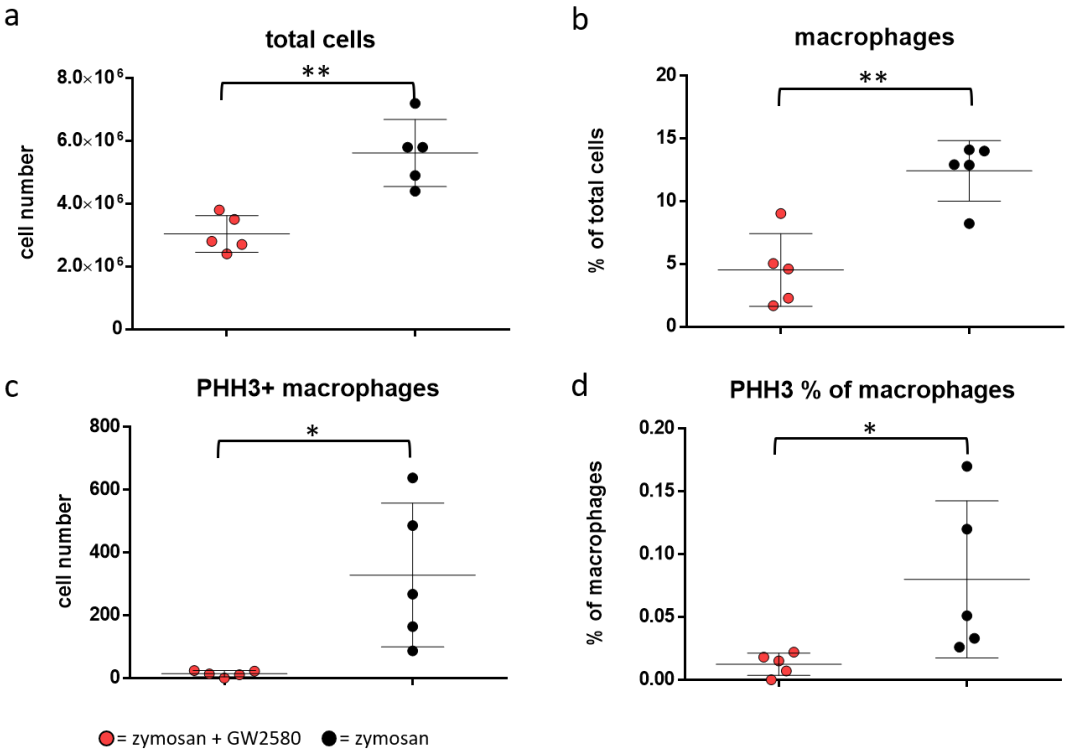

Figure 5.6: GW2580 treatment *in vivo* reduces macrophage proliferation

Mice were treated with 160 ml/kg GW2580 (red circle) or vehicle (black circle) 24 hours before i.p. injection of zymosan. GW2580 treatment was continued once a day until harvest 48 hours after zymosan injection. Peritoneal lavages were stained for flow cytometry. a) Number of total cells recovered from lavages, b) % of macrophages from total cells recovered, c) total numbers of $PHH3^{+}$ macrophages, d) percentage of macrophages positive for PHH3; N = 5 for both groups, Data are means ± SD. Data were analysed using two-tailed Student's T test: a: p = 0.0015, R square = 0.7369, b: p = 0.0016, R square = 0.7325, c: p = 0.0154, R square = 0.5405, d: p = 0.0438, R square = 0.4167

**, $P \leq 0.01$; *, $P \leq 0.05$

Blocking CSF1R signalling does not affect primary tumour progression but metastasis

In order to investigate the effect of GW2580 induced macrophage blockade on breast tumour development, mice bearing 4T1 tumours were treated with 160 mg/kg GW2580 as illustrated in figure 5.7 1.

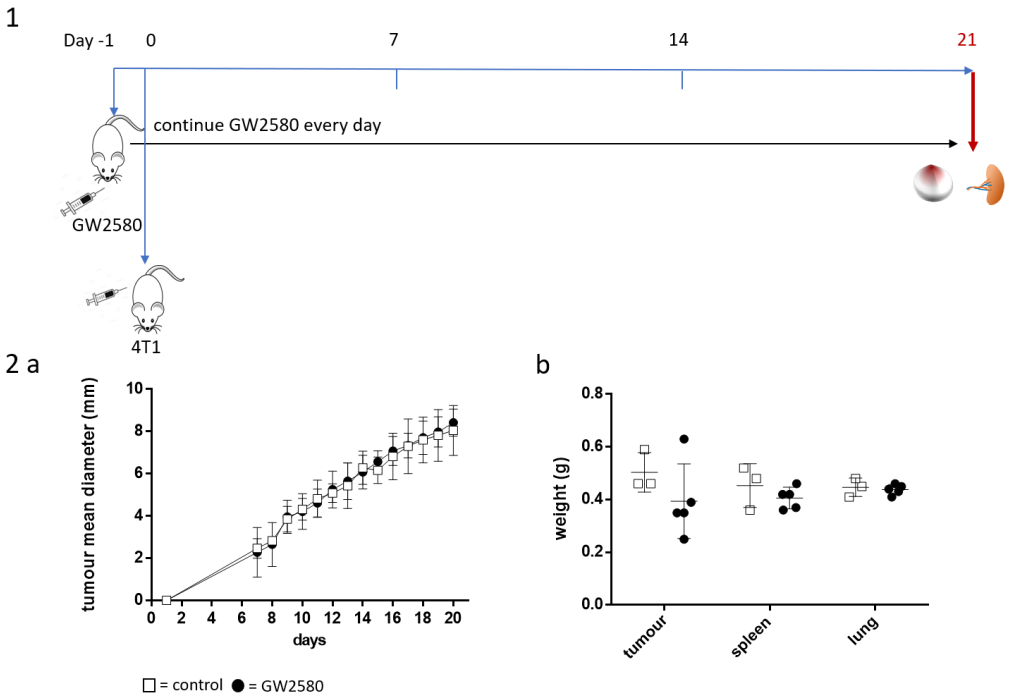

Figure 5.7: GW2580 treatment does not cause tumour regression

1) Mice were treated with oral gavage with 160 mg/kg GW2580 or PBS (control) one day before injection of 4T1 cells. Gavage treatment was continued once per day and tumours and relevant organs were harvested on day 21 after 4T1 inoculation. 2) Growth curve (a) and organ weights (b) of GW2580 treated mice (black circles) or controls (white squares, control), n = 3 for controls, 5 for treatment; Graphs show means ± SD.

GW2580 treatment did not affect tumour growth or weights of any organs recovered (5.7 2). Investigating subsets of immune cells identified in the previous chapter, GW2580 treatment was associated with reduced tumour infiltration with all TAM subsets (12-15), as well as dendritic cells (10/11) and B cells (8) (Figure 5.8).

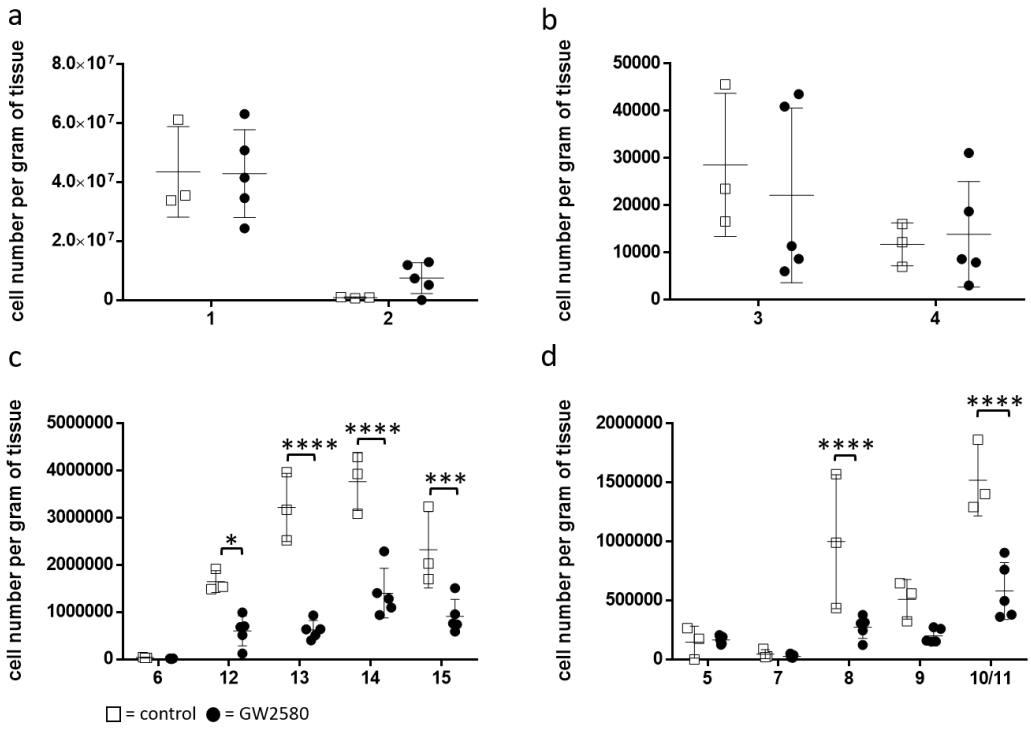

Figure 5.8: GW2580 reduces populations of TAMs, lymphocytes and dendritic cells in the tumour

Mice were treated with 160 mg/kg GW2580 or PBS (control) by oral gavage. Graphs show numbers of immune cell subsets identified in the previous chapter as total cell number per gram of tumour tissue. a) and b) show neutrophils (1) and associated populations (2-4), c) shows NR4A1$^+$ monocytes (6) and macrophage populations (12-15), d) shows mast cells (5), plamacytoid DCs (7), B cells (8), T cells (9) and DCs (10/11).

N = 3 for controls, 5 for treatment; Graphs show means ± SD. Cell numbers were analysed by two-way RM ANOVA with Sidak's multiple comparisons test:

c) treatment: F (1, 6) = 67.4, p = 0.0002; cell types: F (4, 24) = 46.53, p < 0.0001; interaction: F (4, 24) = 13.72 p < 0.0001;

d) treatment: F (1, 6) = 23.15, p = 0.003; cell types: F (4, 24) = 35.65, p < 0.0001; interaction: F (4, 24) = 9.756, p < 0.0001;

****, $P \leq 0.0001$; P***, $P \leq 0.001$; **, $P \leq 0.01$; *, $P \leq 0.05$

Since T cells appeared to be reduced in GW2580 treated mice, albeit not significantly, I also investigated T cell subpopulations; GW2580 treated tumours had significantly less $CD4^+$ conventional T cells, with no differences observed in $CD8^+$ conventional T cells and $CD4^+$ Tregs (see supplementary figure S7).

While growth of the primary tumour was not affected by TAM reduction, macrophages do play various roles in carcinogenesis in addition to primary tumour development and are also important for the metastatic process. Thus, it was hypothesised that the inhibition of macrophages could influence lung metastasis. Indeed, decreased lung metastasis in GW2580 treated mice compared to controls was observed (Figure 5.9 1b).

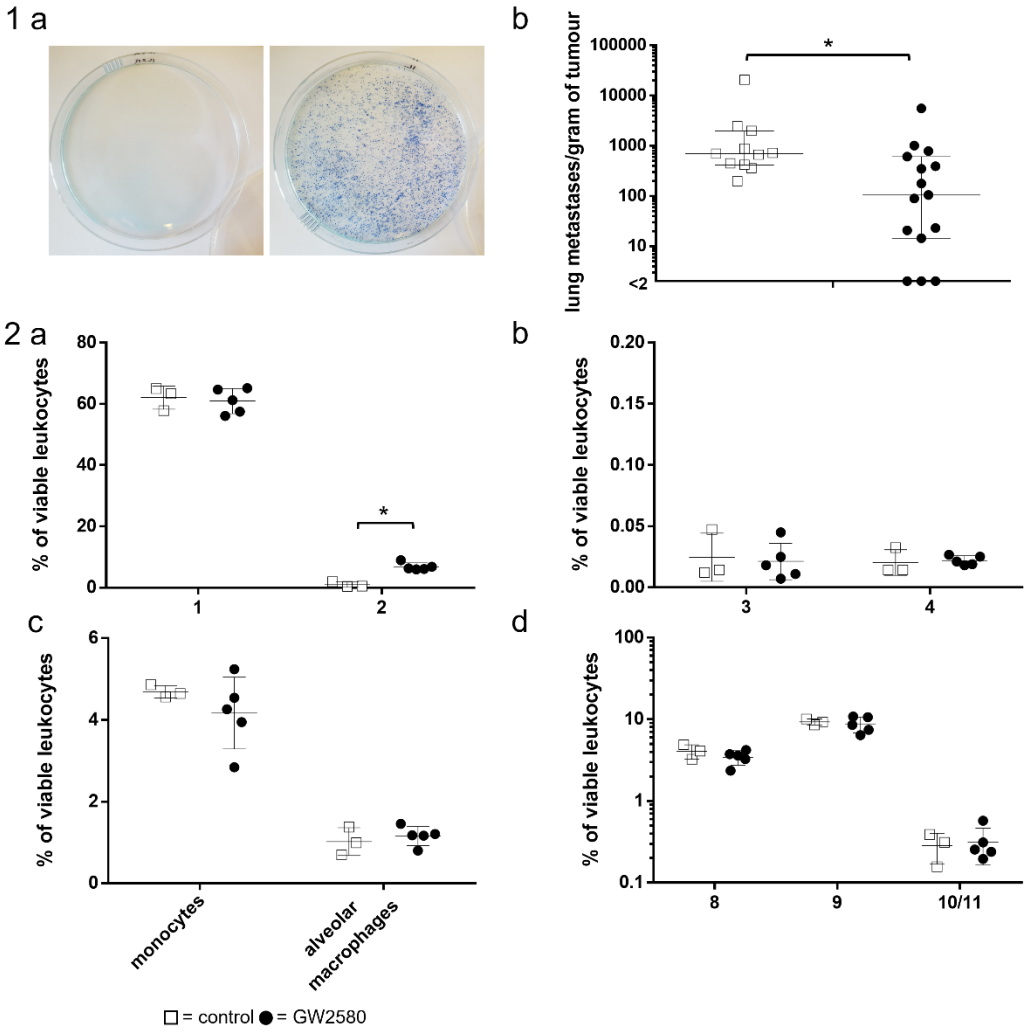

Figure 5.9 : GW2580 treatment affects lung metastasis

Mice bearing 4T1 tumours were treated with 160 mg/kg GW2580 or PBS (control) as previously described. On the day of harvest lungs were digested and cell suspensions split into 2 parts. Part 1 was plated for clonogenic assay, part 2 was stained for flow cytometry.

1) Analysis of metastatic burden of 4T1 lungs: a) representative images of no metastasis vs metastasis 2 weeks after plating of lung cell suspensions. b) Number of lung metastases per gram of tumour from GW2580 treated mice (black circle) or controls (white square); n = 11 for controls, 15 for treatment. Graph shows median and interquartile range. <2 denotes tumours where not metastatic foci were detected.

2) Immune cell subsets as % of viable leukocytes recovered from lung tissue. a) and b) show neutrophils (1) and associated populations (2-4), c) shows monocytes and alveolar macrophages ($Cd11c^+$, $F4/80^+$), d) shows B cells (8), T cells (9) and DCs (10/11), N = 3 for controls, 5 for treatment. All graphs show means ± SD.

Macrophage populations in the lungs were not affected by GW2580 treatment, nor were most other immune cell populations. The only difference was observed in population 2 (clustering with neutrophils), the numbers of which were significantly increased in lungs of GW2580 treated mice compared to controls (5.9 2a). A similar trend was observed in tumour data (see 5.8 a), however, in the primary tumour this increase was not statistically significant.

Since a decrease in macrophage populations did not affect primary tumour growth, I hypothesised that an increase in macrophage populations could have a different outcome. As Treg suppress macrophages and Treg reduction was associated with increased TAM numbers in an MC38 tumour models (Gyori *et al.*, 2018), I wanted to investigate the effect of Treg inhibition on previously identified TAM numbers and tumour growth in the 4T1 model.

PI-3065 slows primary tumour growth, reduces spleen size and affects TAM population numbers

To determine the effect of Treg inhibition on primary tumour growth mice were treated with the PI3Kδ inhibitor PI-3065 as illustrated in figure 5.10 1. Comparison of tumour growth throughout the experiment showed a significant difference in tumour size between PI-3065 treated and vehicle treated mice on the day of harvest (5.10 2).

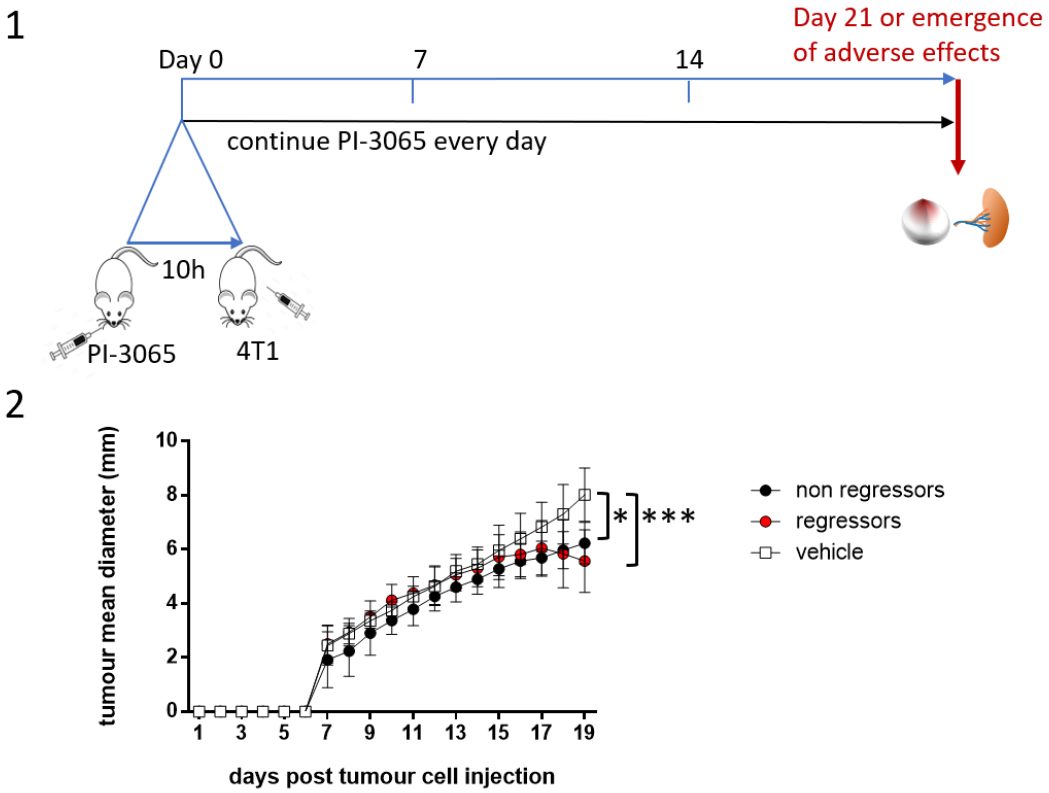

Figure 5.10: PI-3065 treatment reduces tumour growth and splits mice into tumour regressors vs non regressors

1) Mice received oral gavage with PI-3065 10 hours prior to injection of 4T1 cells, with treatment continuing once per day. Tumours and spleens were collected at day 21 or earlier if a humane endpoint was reached.

2) Growth curve of tumours in mice receiving injections with vehicle (white squares) or PI-3065 (circles). Red circles indicate mice that regressed tumours, black circles illustrate mice that did not regress tumours. Tumours were collected on day 19 after 4T1 injection. N = 8 for vehicles, 20 for treatment (9 regressors, 11 non regressors). Data shown are means ± SD. Data were analysed with Kruskal-Wallis test, individual groups were compared using Dunn's multiple-comparisons test: p = 0.0009, H = 14.10

***, $P \leq 0.001$; **, $P \leq 0.01$; *, $P \leq 0.05$

Furthermore, mice treated with PI-3065 could be separated into two groups based on their response to treatment: mice in which the primary tumour decreased in size were classified as regressors while in non-regressors a decrease in tumour size was not observed. Some of the non-regressor tumours stagnated, while others continued to grow, albeit slower than those in vehicle treated mice. This phenomenon had been reported by the group before (Hughes *et al.*, 2020).

Comparing organ weights after harvest, PI-3065 treated mice had smaller tumours and spleens compared to vehicle treated ones, albeit only statistically significant for regressor mice (Figure 5.11 a and b). While non-regressor spleens appeared to be smaller than vehicle ones, when plotting tumour weight against spleen weight no difference was detected between vehicle and PI-3065 treated spleens (5.11 c).

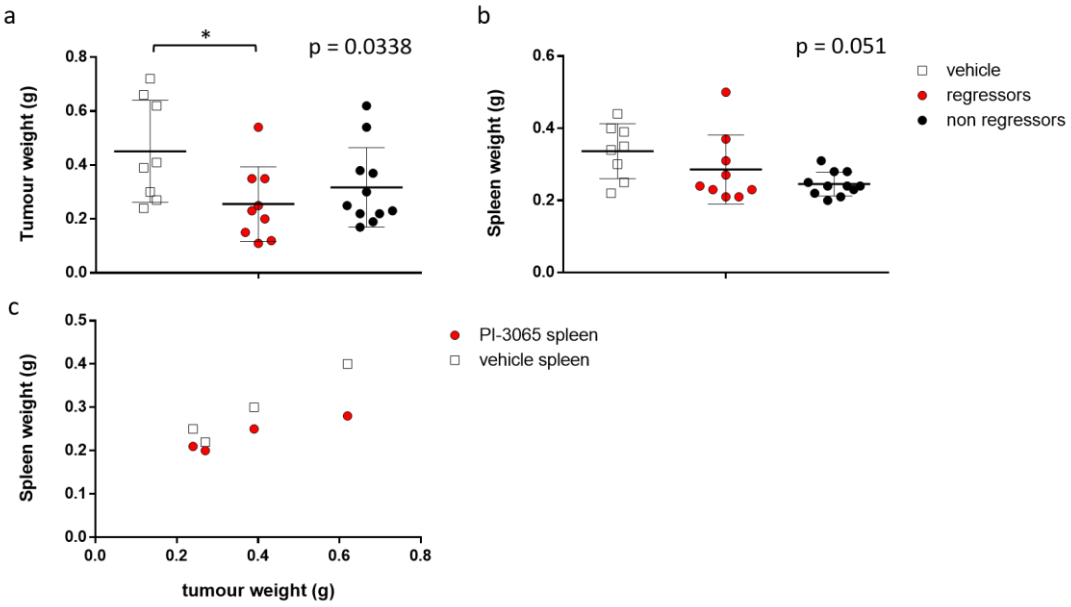

Figure 5.11: Tumour and spleen weights in PI-3065 and vehicle treated mice

a) Tumour weight, b) spleen weight and c) tumour weight vs spleen weight of mice that received oral gavage with PI-3065 or vehicle. N = 8 for vehicles, 20 for treatment (9 regressors, 11 non regressors); a) and b) show means ± SD. Data were analysed by Kruskal-Wallis test, individual groups were compared using Dunn's multiple-comparisons test: a) p = 0.0338 , H = 6.775, asterisk relates to post-hoc test; b) p = 0.051, H = 5.953; c) linear regression: vehicle: p = 0.0084, R square = 0.7125; regressor: p = 0.161, R square = 0.2598; non regressor: p = 0.0264, R square = 0.01782; slopes are equal (p = 0.4246); *, $P \leq 0.05$

Investigating the immune cell populations identified in the previous chapter showed no significant change in tumour resident neutrophils (Figure 5.12 a (1)) as well as neutrophil-associated populations 2 (b) and 3 (c) but an increased number of cells belonging to population 4 (d) in PI-3065 treated regressors compared to vehicle treated mice.

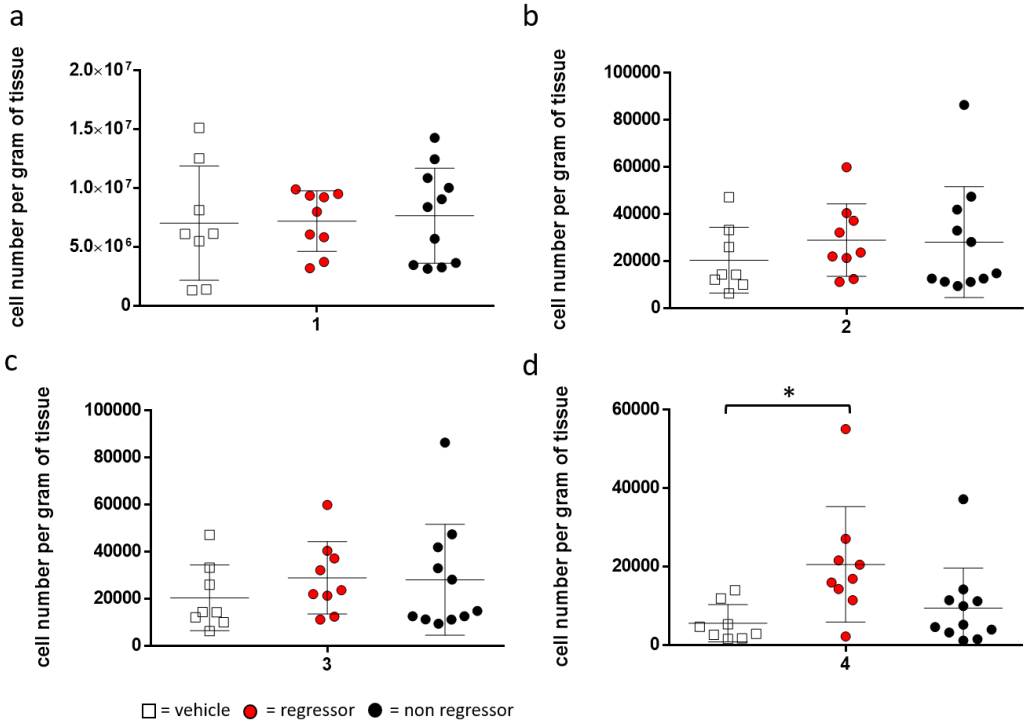

Figure 5.12: PI-3065 did not significantly impact most tumour infiltrating populations clustering with neutrophils

Mice bearing 4T1 tumours were treated with PI-3065 or vehicle as previously described. Tumours were collected on day 19 after 4T1 inoculation. Graphs show numbers of a) neutrophils (1), cells belonging to population b) 2, c) 3, d) 4 per gram of tumour tissue. N = 8 for vehicles, 20 for treatment (9 regressors, 11 non regressors). Graphs are means ± SD. Data were analysed by Kruskal-Wallis test, individual groups were compared using Dunn's multiple-comparisons test: d) p = 0.0118, H = 8.993;

*, $P \leq 0.05$

Investigating cell numbers of tumour infiltrating monocytes and TAM populations identified in the previous chapter, regressing tumours and non-regressing tumours differed in TAM population cell numbers (Figure 5.13).

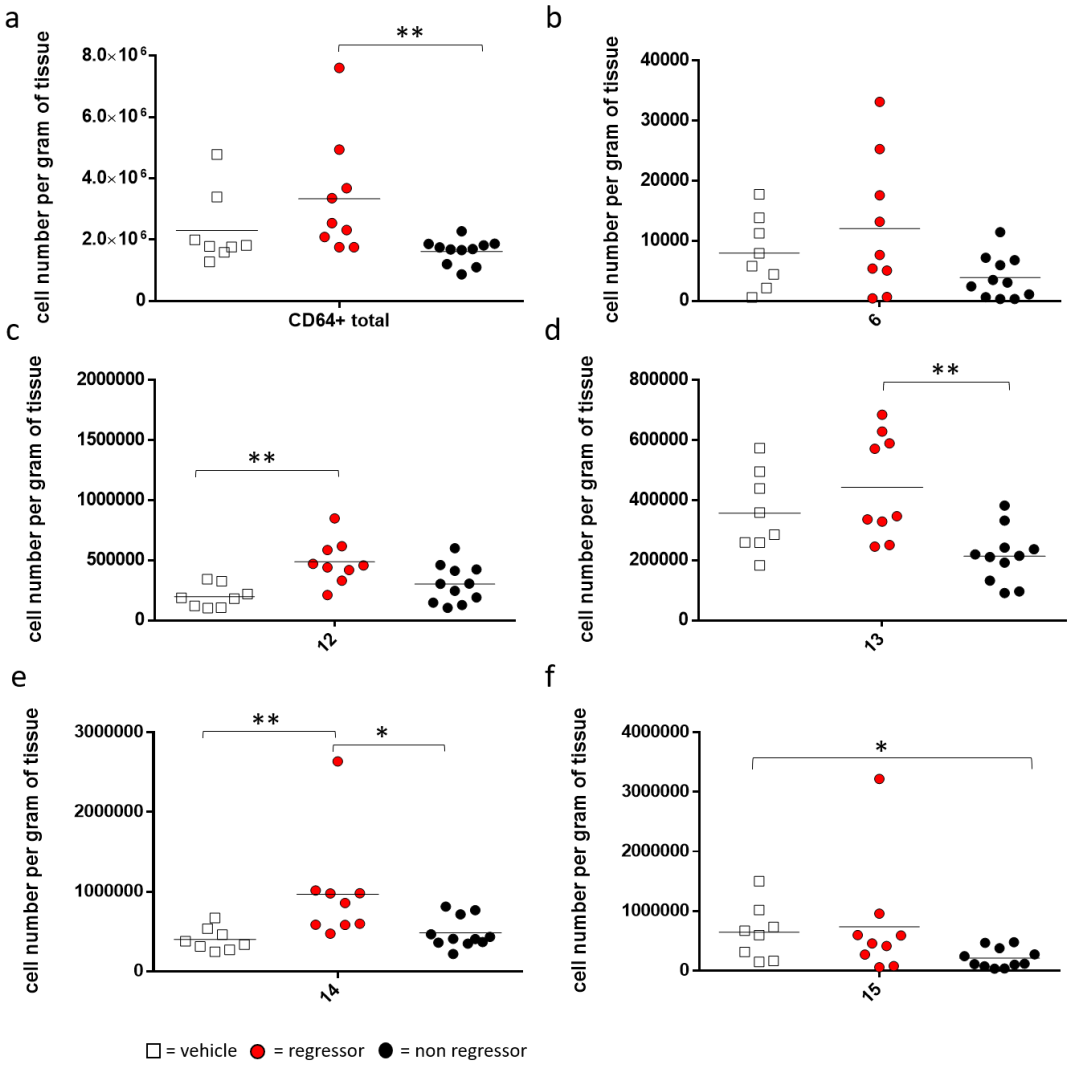

Figure 5.13: PI-3560 affects tumour infiltrating monocyte/macrophage populations

Mice bearing 4T1 tumours were treated with PI-3065 or vehicle as previously described. Tumours were harvested on day 19 after 4T1 inoculation. Graphs show numbers of a) total $CD64^+$ cells, b) $NR4A1^+$ monocytes (6), cells belonging to macrophage population c) 12, d) 13, e) 14, f) 15 per gram of tumour tissue. N = 8 for vehicles, 20 for treatment (9 regressors, 11 non-regressors); Graphs show means ± SD. Data were analysed with Kruskal-Wallis test, individual groups were compared using Dunn's multiple-comparisons test: a: p = 0.0093, H = 9.348; c: p = 0.0041, H = 11.01; d: p = 0.003, H = 11.6; e: p = 0.0024, H = 12.09; f: p = 0.0259, H = 7.309;

**, $P \leq 0.01$ *, $P \leq 0.05$

While populations 12 (c) and 14 (e) were increased in regressing tumours even compared to controls, populations 13 (d) and 15 (f) were similar between controls and regressors, but significantly decreased in non-regressors. Regressing tumours also had higher numbers of T cells compared to non-regressors (Figure 5.14).

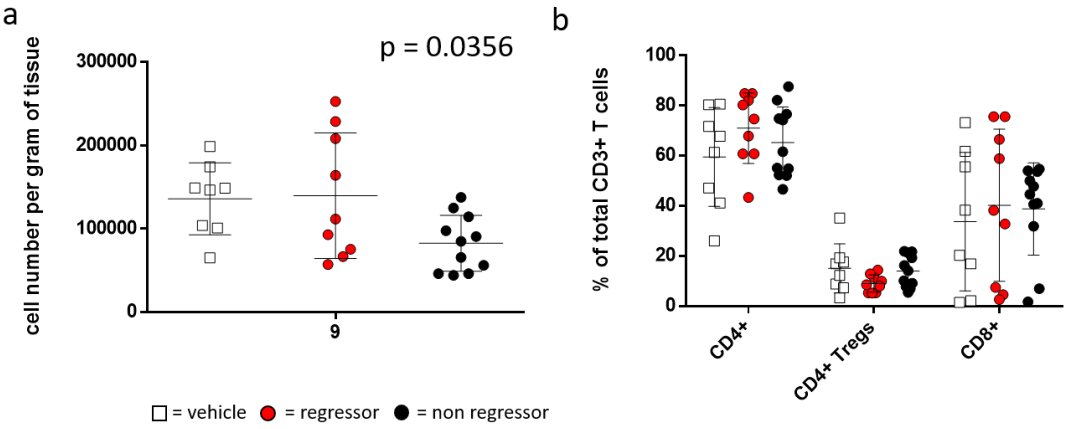

Figure 5.14: PI-3560 affects tumour infiltrating T cells

Mice bearing 4T1 tumours were treated with PI-3065 or vehicle as previously described. Tumours were harvested on day 19 after 4T1 inoculation. Graphs show numbers of a) total T cells per gram of tumour tissue and b) different types of T cells as a % of total T cells. N = 8 for vehicles, 20 for treatment (9 regressors, 11 non regressors); Graphs show means ± SD. Data were analysed with Kruskal-Wallis test, individual groups were compared using Dunn's multiple-comparisons test: a: p = 0.0356, H = 6.673;

Comparing different types of $CD3^+$ T cells, no difference was found between conventional $CD4^+$, $CD8^+$ T cells and Tregs in the different tumours. No difference in cell numbers per gram of tumour was found in all other populations including B cells, mast cells, plasmacytoid dendritic cells and dendritic cells comparing treatment to controls (see supplementary figure S8).

Treg depletion causes regression of the primary tumour and increase in spleen size

PI-3065 interferes with Treg function but does not necessarily impact Treg numbers. Thus, I wanted to investigate the effect of DT induced Treg depletion in DEREG mice on tumour associated immune cell populations. I hypothesised that Treg depletion would result in an increase of TAM populations and $CD8^+$ T cells and reduced tumour growth.

Indeed, treatment of DEREG mice with DT as illustrated in figure 5.15 1 resulted in the regression of primary tumours (2a) associated with a significant reduction of Tregs in tumour (3a) and spleen (3b). Cell numbers were calculated per gram of tissue to compensate for the increased weight of DT treated spleens.

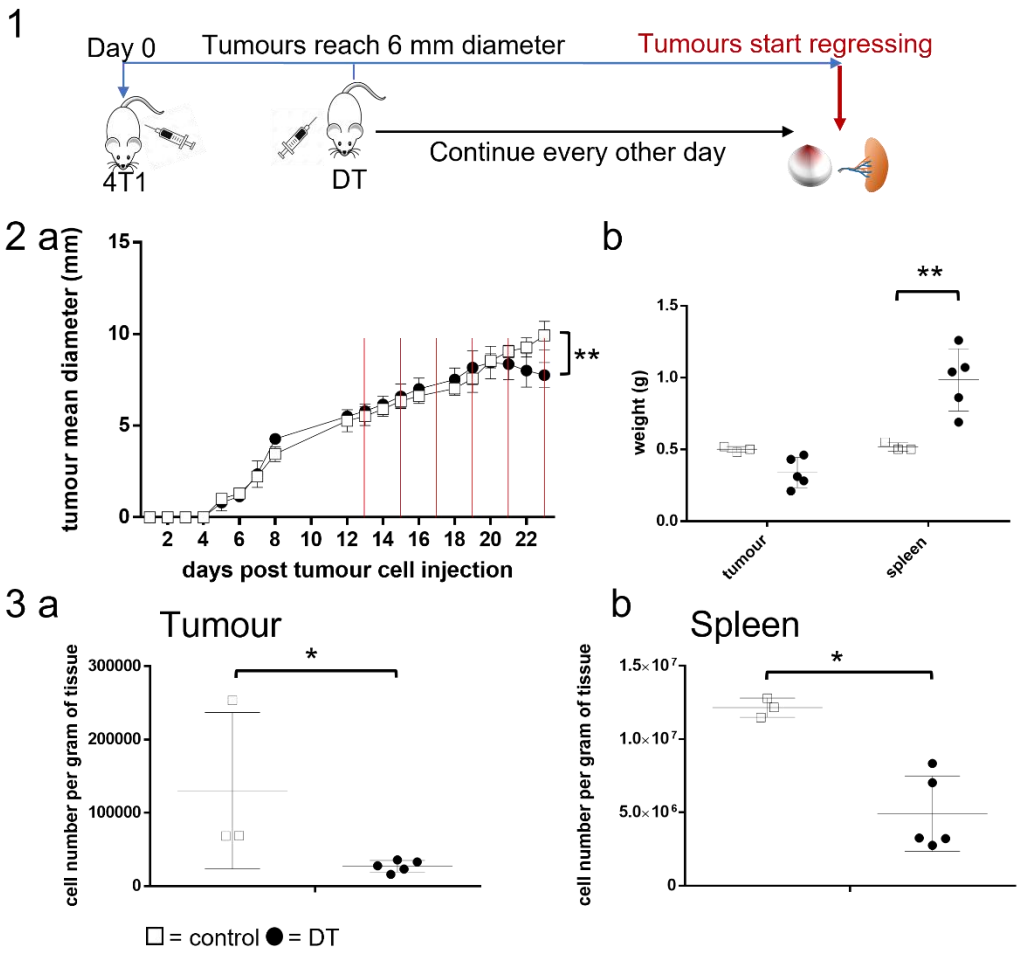

Figure 5.15: DT treatment in DEREG mice reduces Tregs and causes tumour regression

1) Mice were injected s.c. with 4T1 cells. Once tumours reached an average of 6 mm in diameter treatment with DT was commenced and injections were continued every other day. Tumours were collected once regression was observed in all tumours.

2) a) Growth curve of DEREG mice (black circles, DEREG) or DEREG- littermate controls (white squares, control) injected with DT: DT injections are illustrated by red lines. Tumours were harvested on day 23 after 4T1 inoculation. b) Tumour and spleen weights on day of harvest;

3) Numbers of $CD4^+$, $FOXP3^+$ Tregs per gram of tissue in a) tumours and b) spleens. N = 3 for controls, 5 for treatment. Data shown are means ± SD.

2: a) Tumour size was compared on the day of harvest p = 0.0063 (unpaired Student's T test, R square = 0.7372); b) Tumour and spleen weights were analysed by two-way RM ANOVA with Sidak's multiple comparisons test: treatment: F (1, 6) = 3.834, p = 0.098; tissue type: F (1, 6) = 25.18, p = 0.0024; interaction: F (1, 6) = 22.71, p = 0.0031;

3: Treg numbers were compared on the day of harvest by Mann-Whitney test a) p = 0.0357; b) p = 0.0357

**, P ≤ 0.01; *, P ≤ 0.05, ns = non-significant

In contrast to PI-3065 treatment where spleen weights were decreased, Treg depletion with DT was associated with a highly significant increase in spleen weights (5.15 2b). Both, the 4T1 tumour model as well as Treg depletion are known to drive splenomegaly and increased immature splenic granulocytes defined as being Ly6C^{+}, Ly6G^{+} (DuPre´, Redelman and Hunter, 2007), (Lee, Wang and Kim, 2009). Thus, it was hypothesised that this further increase in spleen size could be driven by expansion of the same cell type. Interestingly however, no change in this immature population could be detected in spleens from DT treated DEREG vs DEREG^{-} mice (Figure 5.16 b).

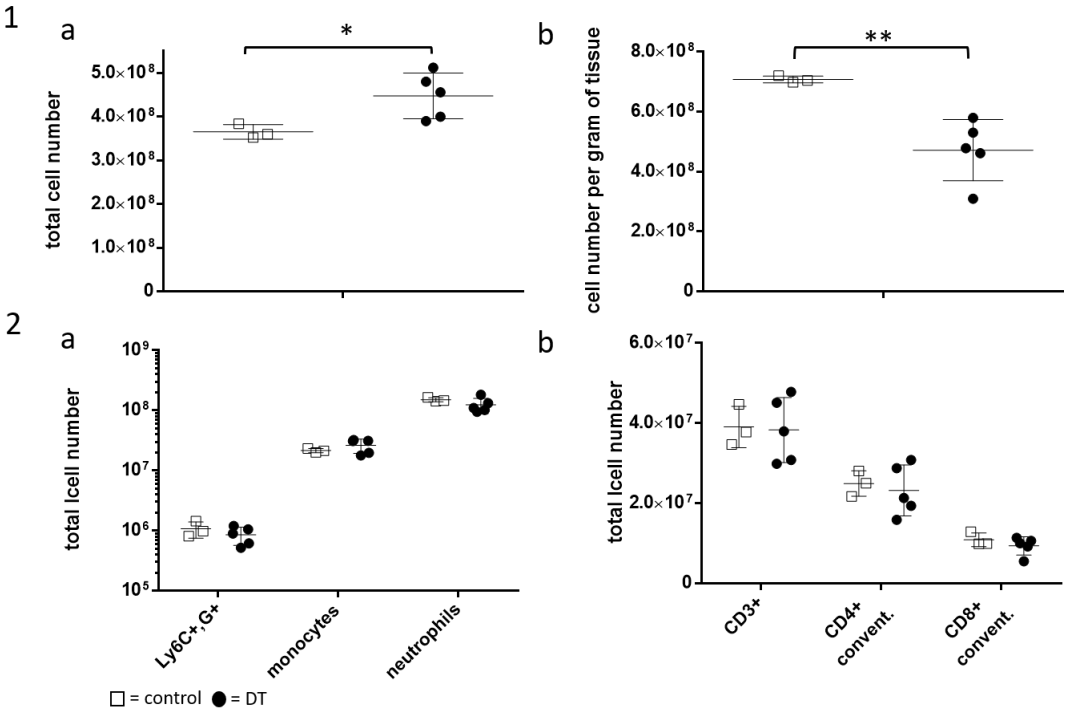

Figure 5.16: DT mediated Treg-depletion is not associated with immature granulocyte or effector T cell expansion

DEREG (DT) and DEREG- (control) mice bearing 4T1 tumours were treated with DT as previously described. Tumours were harvested on day 23 after 4T1 inoculation. 1: Spleen cell numbers from DT treated DEREG+ and control mice as total cell number recovered (a) and cell number per gram of spleen tissue (b)

2: Graphs show total numbers of CD11b+ Ly6C+ Ly6G+ (Ly6C+,G+), CD11b+ Ly6C+ Ly6G- (mono/macs) and CD11b+ Ly6C- Ly6G+ (neutrophils) cells (a) and total number of CD3+ as well as CD3+ CD4+ (CD4+ convent.) and CD3+ CD8+ (CD8+ convent.) T cells. N = 3 for controls, 5 for treatment, Graphs show means ± SD.

1: Cell numbers were analysed by unpaired T tests with Welch's correction; a: p = 0.021 R square = 0.6730, b: p = 0.0062, R square = 0.8628

**, P ≤ 0.01; *, P ≤ 0.05

Also, intriguingly, while slightly more total cells were recovered form the spleens of DT treated DEREG mice compared to controls, per gram of tissue extracted DEREG spleens had less cells recovered than control mice. There was no difference detected in conventional $CD4^+$ and $CD8^+$ T cells in treated vs non-treated spleens.

Treg depletion driven tumour regression is associated with decreased infiltration of most immune cell populations

Investigating immune cell populations as defined in the previous chapter it could be observed that Treg depletion by DT was associated with a reduction in the cell numbers of most infiltrating immune cell populations per gram of tumour tissue (Figure 5.17).

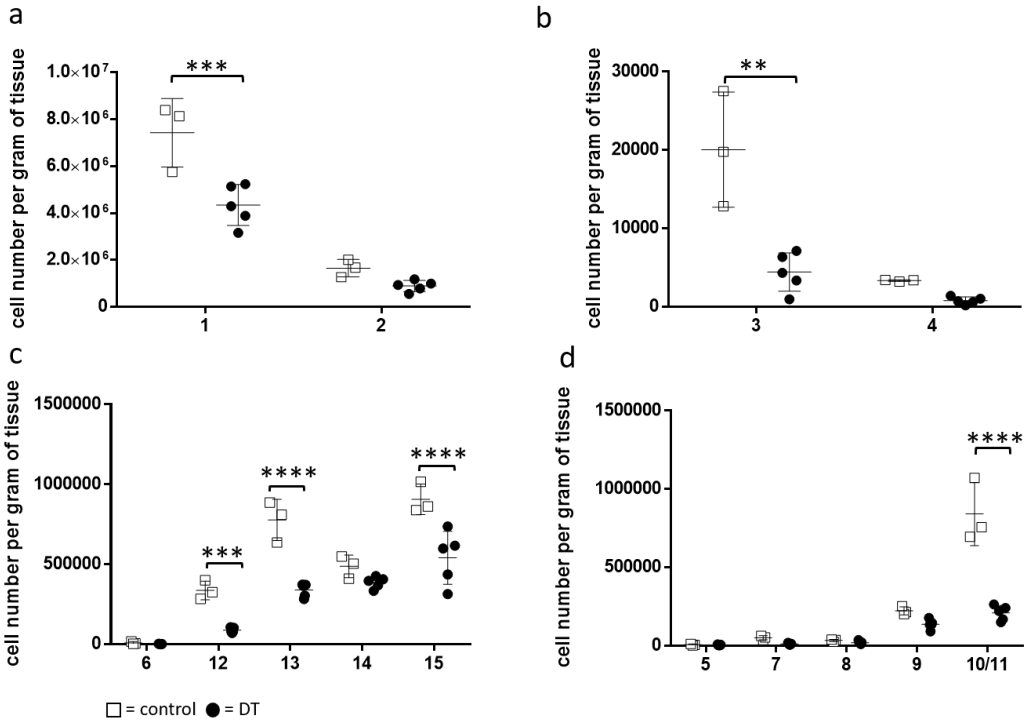

Figure 5.17: DT mediated Treg depletion affects most tumour infiltrating immune cell populations

DEREG (DT) and DEREG- (control) mice bearing 4T1 tumours were treated with DT as previously described. Tumours were harvested on day 23 after 4T1 inoculation. Graphs show numbers of immune cell subsets identified in the previous chapter as total cell number per gram of tumour tissue. a) and b) show neutrophils (1) and associated populations (2-4), c) shows NR4A1+ monocytes (6) and macrophage populations (12-15), d) shows mast cells (5), plamacytoid DCs (7), B cells (8), T cells (9) and DCs (10/11), N = 3 for controls, 5 for treatment. Graphs show means ± SD. Cell numbers were analysed by two-way RM ANOVA with Sidak's multiple comparisons test:

a) treatment: $F(1, 6) = 16.03$, $p = 0.0071$; cell types: $F(1, 6) = 183.8$, $p < 0.0001$; interaction: $F(1, 6) = 11.65$, $p = 0.0143$;

b) treatment: $F(1, 6) = 25.74$, $p = 0.0023$; cell types: $F(1, 6) = 38.15$, $p = 0.0008$; interaction: $F(1, 6) = 15.74$, $p = 0.0074$;

c) treatment: $F(1, 6) = 51.72$, $p = 0.0004$; cell types: $F(1, 6) = 120.9$, $p < 0.0001$; interaction: $F(1, 6) = 45.55$, $p < 0.0001$;

While this depletion of Tregs seemed to drive tumour regression, it was unclear whether that was due to a reduction in infiltrating macrophage cell types or whether the macrophage reduction was caused by tumour regression. Investigating effector T cells, no difference was found in $CD8^+$ T cells in DT treated DEREG vs control mice.

Combination of DEREG and GW2580 does not combine the benefits of individual treatments

As Treg depletion via DT was associated with a reduction in tumour growth and GW2580 treatment with a decrease in lung metastasis, I hypothesised that a combination of both treatments might also combine both benefits (Figure 5.18). Comparing the combination of GW2580 plus DT in DEREG mice to controls, I observed a plateauing of tumour growth within a few days of treatment. However, treated tumours started to grow again even though treatment was continued.

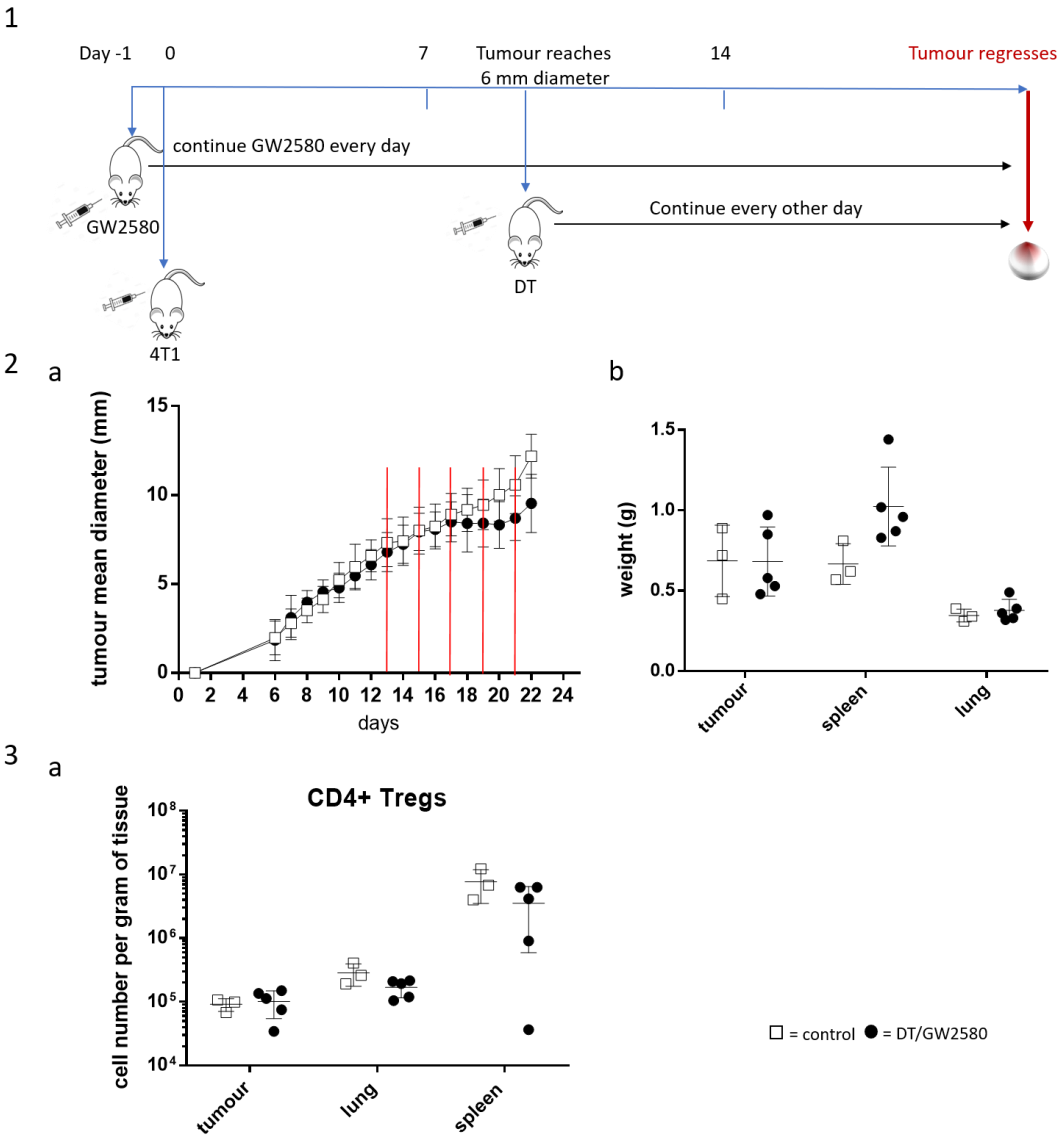

Figure 5.18: Combination of GW2580 and DT treatment only initially slows tumour growth

1) Mice were treated with oral gavage with GW2580 or PBS (control) one day before injection of 4T1 cells. GW2580 treatment was continued once per day. Once tumours reached an average of 6 mm in diameter treatment with DT was commenced and injections were continued every other day. Tumours were harvested once a humane endpoint was reached or at 28 days after 4T1 inoculation. 2) Growth curve (a) and organ weights (b) of DEREG and DEREG$^-$ mice bearing 4T1 tumours treated with DT and GW2580 (DT/GW2580, black circle) or vehicle (control, white square). Tumours were harvested on day 21 after 4T1 inoculation. Red lines illustrate DT treatment. 3) a) Numbers of CD4$^+$ Tregs in tumours, lungs and spleens of DT/GW2580 treated DEREG or control DEREG$^-$ mice; N = 3 for controls, 5 for treatment, Graphs show means ± SD.

Tumour and lung weights were comparable between treated and control mice. As observed with DT treatment on its own, spleens of mice treated with DT/GW2580 appeared bigger than those of control mice, although in this experiment the difference was not statistically significant. While after DT treatment on its own the numbers of $CD4^+$ Tregs were significantly reduced in spleens of tumour bearing mice, this was not observed in spleens, lungs and tumours of mice receiving a combination of DT and GW2580. From experiments using both treatment options individually, I had hypothesised a significant change in most of the immune cell populations identified in the previous chapter upon treatment combination. This was, however, not the case (Figure 5.19).

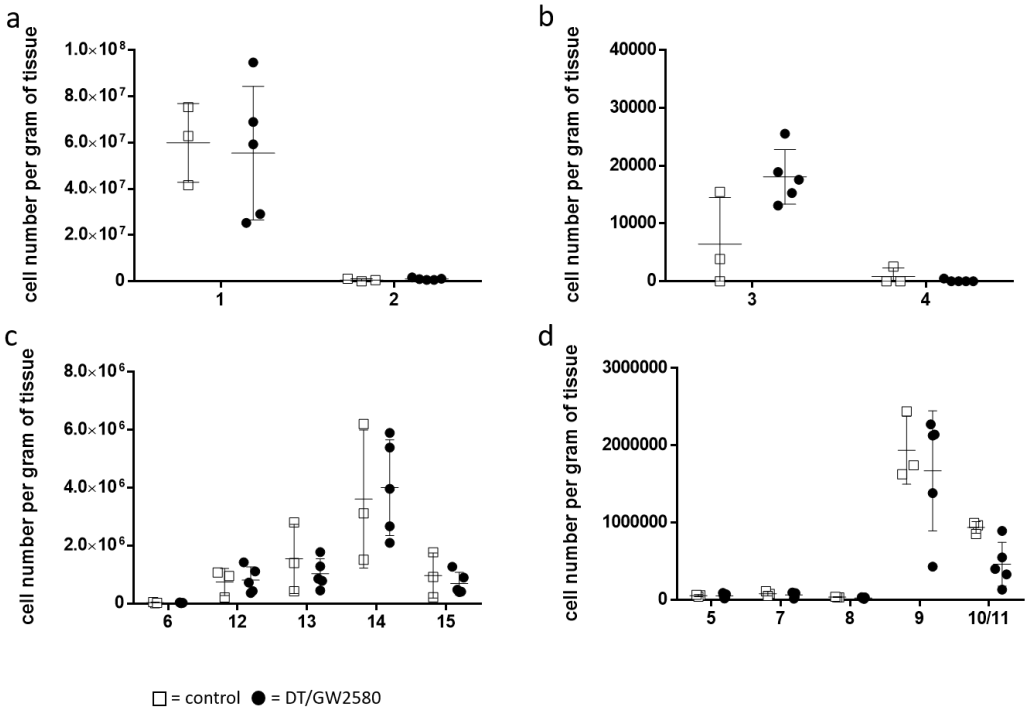

Figure 5.19: Combination of DT and GW2580 is associated with a loss of changes in populations observed with either treatment on its own

DEREG and $DEREG^-$ mice bearing 4T1 tumours were treated with DT and GW2580 (DT/GW2580, black circle) or vehicle (control, white square). Tumours were harvested on day 21 after 4T1 inoculation. Graphs show numbers of immune cell subsets identified in the previous chapter as total cell number per gram of tumour tissue. a) and b) show neutrophils (1) and associated populations (2-4), c) shows $NR4A1^+$ monocytes (6) and macrophage populations (12-15), d) shows mast cells (5), plasmacytoid DCs (7), B cells (8), T cells (9) and DCs (10/11), N = 3 for controls, 5 for treatment; Graphs show means ± SD. Data were analysed by two-way RM ANOVA with Sidak's multiple comparisons test.

DT treatment on its own was associated with a decrease in neutrophils and associated population compared to controls. This effect was completely lost upon combination with GW2580. When looking at macrophage targeting, GW2580 treatment alone reduced all TAM populations, while DT treatment on its own reduced macrophage populations 12, 13 and 15. Upon combined GW2580 and DT treatment, these effects were lost. Similarly, both GW2580 treatment and DT mediated Treg depletion on their own reduced DCs, which was not observed upon treatment combination.

Investigating lung metastasis, no difference was found in the same immune cell populations in the lungs of DT/GW2580 treated vs control mice (Figure 5.20).

While the combination of DT and GW2580 treatment was initially associated with reduced primary tumour growth, the growth curve showed that in contrast to the DT only treated mice where tumours regressed, DT/GW2580 tumours only plateaued but did resume growth. The same results were also observed in another experiment starting DT treatment at an earlier timepoint and thus smaller size of the tumours (average of 4 mm in diameter) (see supplementary figure S9).

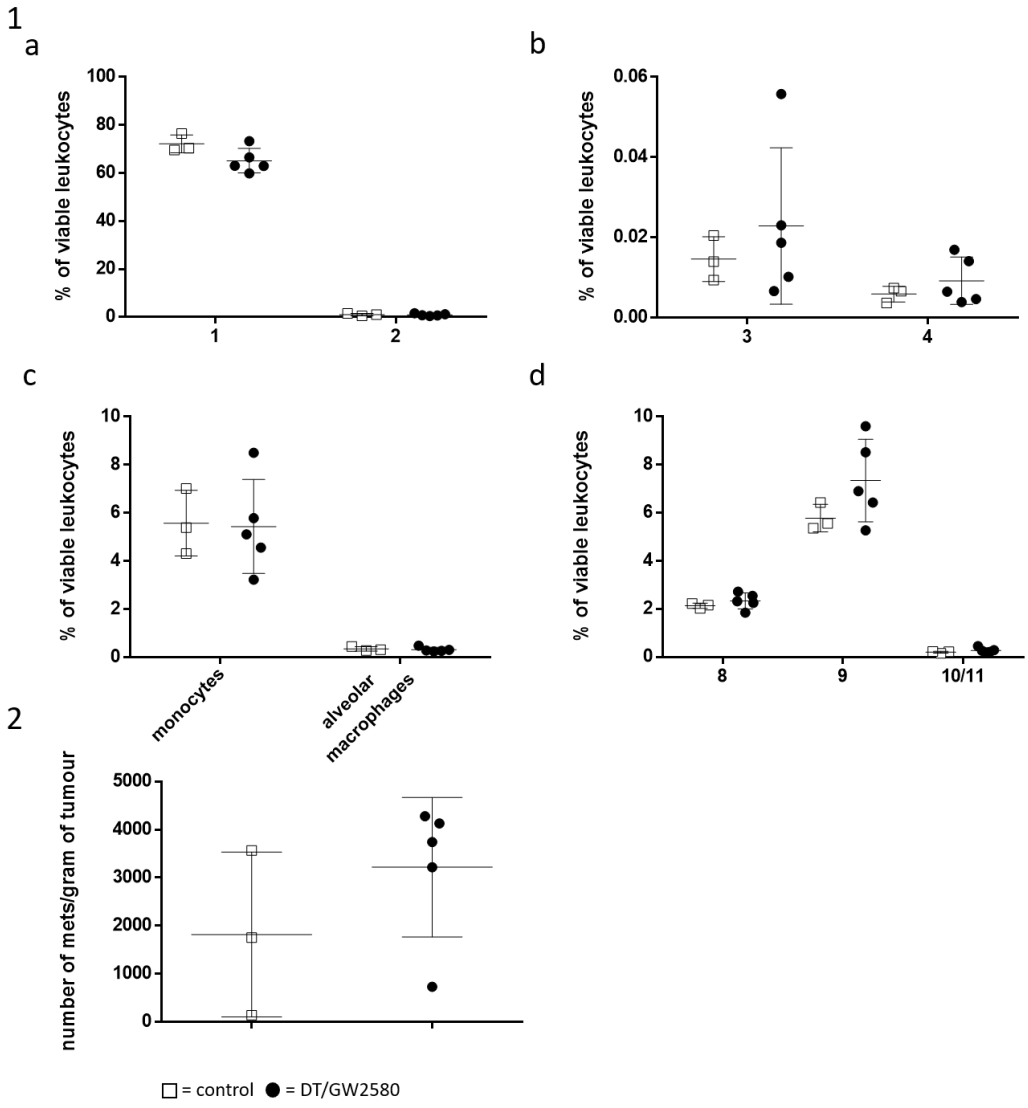

Figure 5.20: Combination of DT and GW2580 does not affect lung metastasis

DEREG and DEREG$^-$ mice bearing 4T1 tumours were treated with DT and GW2580 (DT/GW2580, black circle) or vehicle (control, white square). Tumours were harvested on day 21 after 4T1 inoculation.

1: Numbers of immune cell subsets as total cell number per gram of lung tissue. a) and b) show neutrophils (1) and associated populations (2-4), c) shows monocytes and alveolar macrophages, d) shows B cells (8), T cells (9) and DCs (10/11).

2: Number of lung metastases per gram of tumour;

N = 3 for controls, 5 for treatment, Data are means ± SD.

Discussion

Clodronate liposomes

In contrast to published evidence of 4T1 TAM depletion and primary tumour control by i.p.. injection of clodronate liposomes (Jang *et al.*, 2020), the same effect could not be observed in the present study. This lack of effect could have been due to lack of localisation of liposomes to the tumour. Theoretically, this could be tested with the injection and visualisation of fluorescent liposomes. Alternatively, other injection strategies such as intravenous or intratumoural injections could be explored to enhance tumour delivery of the liposomes. Of note, i.v. injection of clodronate liposomes has been shown to reduce primary 4T1 tumour growth, even though TAM numbers were not evaluated (M. Liu *et al.*, 2015). Intratumoural injections failed to deplete 4T1 TAMs (Tsan and Gao, 2005). Due to the relative success with GW2580, the use of liposomes was discontinued.

GW2580

In vitro testing illustrated the efficacy of GW2580 in reducing macrophage proliferation at concentrations of 6 µM and 60 µM. 60 µM was associated with the appearance of crystal like structures that were observed in three replicates of the same concentration but not other concentrations or the vehicle GW2580 was dissolved in. Whilst the origin of the crystal aggregates was unclear and there was no prior evidence of them in the literature, their presence ruled out the use of this dose for *in vivo* experiments.

Conway and colleagues measured plasma levels of GW2580 in mice after oral administration of 80 mg/kg GW2580 showing a maximal plasma concentrations of 5.6 µM lasting for 4 hours after dosing (Conway *et al.*, 2005). This corresponds roughly to the middle concentration of 6 µM used for *in vitro* testing. After this initial peak, the plasma concentration decreased to roughly 2 µM between 4 and 8 hours after gavage, and further below 1 µM within the next 4 hours. While some researchers have used a single daily dose of GW2580, other papers have suggested a dosing of GW2580 every 12 hours (Crespo *et al.*, 2011). Considering the half-life of the drug *in vivo*, such a regime would certainly maintain a more stable level of plasma GW2580. However, the present experiment involved daily treatment of the mice for at least three weeks, making this option unfeasible. Several groups have also achieved macrophage depletion with a single dose of 160 mg/kg (Priceman *et al.*, 2010), (Swierczak *et al.*, 2014).

According to Conway and colleagues, GW2580 completely inhibits the ability of CSF1 to induce growth of mouse myeloid cells at a concentration of 0.8-1 µM *in vitro*. Based on the fact that quadrupling the dose from 20 to 80 mg/kg also quadrupled the initial peak of plasma concentration (1.4 and 5.6 µM respectively) (Conway *et al.*, 2005), it is likely that increasing the dose to 160 mg/kg would cause an initial peak of over 10 µM. As the initial peak at 5.6 µM decreased to just below 1 µM after 12 hours for the 80 mg/kg dose, it is further likely that this level would be reached after roughly 24 hours with the doubled dose. Indeed, it was reported that 160 mg/kg once daily resulted in a plasma concentration remaining greater than 1 µM for 24 hours ensuring continuous CSF1R inhibition (Priceman *et al.*, 2010).

In the present study, treatment of mice with GW2580 was associated with reduced TAM numbers, but did not affect primary tumour progression.

This is in line with other studies: GW2580 treatment of mice bearing 4T1.2 tumours was not associated with any change in primary tumour growth compared to controls (Swierczak *et al.*, 2014). However, Swierczak and colleagues observed a significant increase in lung metastasis along with an increase in neutrophil numbers both in primary tumours and lungs of GW2580 treated mice. This was not the case in the present study. While both experiments used the same regime of inhibitor dosing, the present study inoculated mice with 4T1 tumour cells subcutaneously close to the mammary glands, while Swierczak and colleagues injected 4T1.2 cells directly into the mammary glands. The 4T1.2 line is derived from the 4T1 line and preferentially metastasises to the bones and lungs, but not to the liver (Lelekakis *et al.*, 1999). While at the present time no study has directly compared the kinetics of 4T1 to 4T1.2 primary tumours and metastasis, it might be possible that there are differences in lung metastasis in those two models that could explain the different outcomes.

In addition to decreasing TAM number, GW2580 treatment also significantly reduced DC and B cell numbers while showing a trend toward reduced T cell numbers. GW2580 has been shown to reduce monocyte derived DCs in primary tumours and block tumour-specific T cell proliferation in draining lymph nodes (Kuhn, Yang and Ronchese, 2015), which could explain this effect. As DCs act as antigen presenting cells and thus are important for the activation of T cells which then drive tumour cell rejection, a reduction of both these populations in the tumour environment would not be helpful in anti-tumour immunity. Thus, use of a macrophage specific depletion method that does not affect DCs

may be more beneficial to support tumour rejection. The lower number of B cells in Treg depleted tumours could be a direct consequence of reduced tumour growth resulting in less tertiary lymphoid structures that can recruit lymphocytes. This would need to be investigated.

The data on lung metastasis suggest a reduction after GW2580 treatment. Ideally, the sample size needs to be increased. Alveolar macrophage numbers were not affected by GW2580 gavage. Indeed, alveolar macrophages have been reported to differentiate via GM-CSF early in life (Guilliams *et al.*, 2013) and have even been found to be present and functional in the lungs of GM-CSF and CSF1 deficient mice, suggesting that they might not rely on these growth factors (Lieschke *et al.*, 1994).

The only population altered in the lungs of GW2580 treated mice was population 2 which was significantly increased in lungs of treated mice. This population which clustered closely with neutrophils was characterised based the expression of CD11b and SiglecE, but not FcγR1, Ly6C, Ly6G, F4/80 and only low CD14.

The data on SIGLECE expression in the tumour context are controversial: SigE-/- mice have been suggested to better clear tumour cells after injection. However, while loss of SiglecE delayed tumour development, once tumours appeared they grew faster and ended up being bigger than controls (Läubli *et al.*, 2014). The paper focussed on SiglecE expression in myelomonocytic cells, which are immature cells that can differentiate into neutrophils, monocytes, macrophages and DCs. Based on the paper, it seems likely that at a later stage of the tumour (i.e. the point of harvest), an increase in cells expressing SiglecE would be associated with increased tumour progression. This is curious, as the data suggest a reduction of metastatic cells in lungs of mice treated with the inhibitor, along with an increase in SiglecE expressing cells. It is, however, very possible that other tumour associated cells also express SiglecE that are not accounted for in this thesis, so that SiglecE expression on cell of population number 2 might not be the decisive factor. Indeed, considering the importance of macrophages in the metastatic process, a reduction of TAMs in the primary tumour alone (as observed after treatment with GW2580) could potentially significantly affect lung metastasis.

PI-3065

Use of PI-3065 in the 4T1 model showed a statistically significant reduction in growth of the primary tumour compared to controls, with the treatment group splitting into two

subtypes: tumour growth slowing down (non-regressors) and tumour regression (regressors). This had been reported before by the group (Lauder *et al.*, 2020), together with the observation that 4T1 specific $CD8^+$ T cells are expanded only in regressing tumours. The group also found increased infiltration of tumours with conventional $CD8^+$ and $CD4^+$ T cells. In the present study only an overall significant change in total T cells could be detected, with non-regressing tumours showing a trend toward reduced T cell numbers. Comparing the sample size of the present study to that of Lauder and colleagues, it is more likely that these observations reflect the small number of mice analysed in the present study and more tumours would have needed to be analysed in order to observe significant effects.

Comparing the weights of tumours and spleens, both types of tissues where smaller in treated mice compared to controls regardless of tumour regression status even though this only reached statistical significance in regressing tumours. This was expected, as it has been observed before that spleen size in the 4T1 model positively correlates to size of the primary tumour, suggesting that spleens would be smaller in treatment groups due to tumour regression.

Comparing the two subgroups of mice receiving PI-3065 treatment on the day of harvest, differences were observed in the number of cells belonging to population 4 which was increased in regressors but not in non-regressors compared to controls. Population 4 clustered with neutrophils and was initially characterised based on the expression of CD14 and CD274. CD274, also known as PD-L1, interacts with PD1 expressed on T cells, negatively regulating T cell activation. PD1 is expressed by activated and exhausted conventional T cells as well as by a fraction of Tregs where ligation reinforces FOXP3 expression (Stathopoulou *et al.*, 2018). As the action of PD-L1 generally blocks T cell effector function and stabilises Treg populations, it seems curious that an increased number of cells expressing PDL1 would be associated with reduced tumour growth. This increase could, however, be due to increased immune activation evidenced by increased T cell infiltration into the tumour driving counter measures to balance immune responses. Also, it is very possible that cells from population 4 do express other functional markers that were overlooked in this experiment and could affect tumour growth in different ways.

PI-3065 treatment also impacted macrophage numbers: Goulielmaki and colleagues blocked p110δ in p110δ-expressing MDA-MB-231 tumours in BALB/c nude which lack T cells. They showed that p110δ inhibition prevented tumour growth and reduced

macrophage localisation into the tumour independently of Treg inhibition (Goulielmaki *et al.*, 2018). In the present study, regressing tumours had higher numbers of all macrophages subsets than controls and non-regressors. This difference could be due to the tumour model, since in contrast to MDA-MB-231, 4T1 cells do not express p110δ themselves. In the 4T1 model, the increased number of TAMs could be the result of a reduction of Treg function which would normally act to suppress TAMs. It would be interesting to follow 4T1 tumour growth and PI-3065 injection in athymic nude mice to evaluate a T cell independent effect on tumour control.

Due to the fact that the action of PI-3065 on macrophages is currently not understood and p110δ inhibition might also affect other immune cell populations, the DEREG model of Treg depletion was chosen to specifically target Tregs in the tumour microenvironment.

DEREG mice

DT treatment of DEREG mice carrying 4T1 tumours was associated with a reduction of Tregs and the regression of primary tumours. This effect has previously been reported by Hughes and colleagues (Hughes *et al.*, 2020). In this experiment the authors started DT treatment as soon as tumours were palpable and reported complete tumour regression in some mice. Starting DT treatment at this timepoint could potentially have a stronger effect on tumour growth, as Tregs are depleted early and can not negatively affect anti-tumour immunity. However, a complete tumour regression was not desired at this point as tumour tissue was needed to analyse the immune cell infiltrate and observe effects of decreased tumour growth especially on macrophage populations. Thus, it was decided to start DT treatment once tumours had reached an average size of 6 mm in diameter. While the growth curve clearly showed a initial regression of DT treated tumours it is not known whether a complete regression would have been achieved starting DT treatment at this later timepoint.

Tumour regression would have been expected to cause a decrease in spleen weights. However, spleen weights of DT treated mice were significantly increased compared to those of controls. This was probably a direct effect of Treg depletion, as it has been shown that Tregs suppress splenic extramedullary myelopoiesis stimulated by conventional T cells (Lee, Wang and Kim, 2009). Interestingly however, when calculated as cell numbers per gram of spleen tissue, there was no preferential expansion of immature myeloid cells defined as $CD11b^+$, $Ly6C^+$ and $Ly6G^+$. It is possible that expanding cells in DT spleens were at more immature stages not yet expressing CD11b. Such cells could be detected by staining

for CD117 (Wu *et al.*, 2018). Also, since compared to control spleens DT treated DEREG$^+$ spleens had less cells per gram of spleen tissue, it is likely that spleens of treated mice contained a higher proportion of extracellular matrix.

It has been shown that partial depletion of Tregs in the 4T1 model induces effector CD8$^+$ T cells that express high levels of CD11c and low levels of PD1 in tumour draining lymph nodes. These cells have been shown to migrate into the tumour and kill DCs, thereby regulating the local anti-tumour response (Goudin *et al.*, 2016). In the present experiment tumour T cell stains did not contain antibodies detecting CD11c or PD1 so it was impossible to say whether such cells were present in the sample. DT treatment was, however, associated with a decrease in tumour resident DCs.

In regard to other immune cell populations identified in the work presented in the previous chapter, decreased numbers of populations associating with neutrophils and nearly all macrophage populations were observed.

Curiously, no increase in T cells in tumours and spleens of DT treated DEREG mice was observed, which is not in line with previous findings, as it has been shown that Treg depletion increases the numbers of CD8$^+$ T cells in primary tumours (Chaput *et al.*, 2007). While Chaput and colleagues used anti-CD25 mAb to achieve Treg depletion, the effects on Tregs would be expected to be similar compared to DT treatment in the DEREG model. However, while the use of anti-CD25 mAb completely depletes Tregs, this likely is not the case in the DEREG model.

The DEREG model has been created using bacterial artificial chromosome (BAC) transgenesis which can be incomplete in terms of transgene expression. Thus, DT treatment only results in depletion of 95-98 % of FOXP3$^+$ Tregs (Lahl *et al.*, 2007). While this does prevent mice from developing lethal autoimmune conditions observed in FOXP3-DTR knock-in mice (Kim *et al.*, 2009) it is possible that over time those surviving FOXP3$^+$ Tregs proliferate and accumulate reducing the desired effect of Treg depletion. Indeed, it has been shown that Treg depletion caused a homeostatic rebound of those cells due to reduced apoptosis and induced proliferation dependent on IL-2 and co-stimulation (Pierson *et al.*, 2013). Further, it has been reported that prolonged treatment of DEREG mice with DT (>2 weeks) resulted in the production of anti-DT antibodies that were able to at least partially interfere with DT induced FOXP3 Treg depletion (Junhua Wang *et al.*, 2016). Also, it has been shown that while DT mediated Treg depletion can result in complete tumour

regression when administered to mice bearing small tumours, efficacy of this treatment was reduced as tumour burden increased (Fisher *et al.*, 2017).

GW2580 in DEREG mice

Based on the fact that DT treatment reduced primary tumour growth, and GW2580 treatment might decrease metastasis, it was hypothesised that a combination of both therapeutics could combine both benefits. This was, however, not the case in the present study. While combination therapy initially resulted in a plateauing of primary tumour growth, treated tumours continued to grow again after a few days. The number of lung metastases per gram of tumour was not different in treated compared to untreated mice, although the sample size should be increased.

In line with this, most populations that were affected by treatment with GW2580 and DT alone did not show a difference to controls upon treatment combination. This was especially curious in regard to TAM populations which were decreased by either treatment on its own, suggesting that the two treatments somehow cancel out their respective effects. It would be interesting to analyse tumours at the plateauing stage to see whether or not immune populations more closely resemble the patterns observed in DT treatment alone. This could also give an indication as to which cells are involved in driving growth retardation.

Sun and colleagues reported reduced tumour growth when inhibiting Tregs and macrophages together. They intraperitoneally injected a CCR4 antagonist to prevent trafficking of Tregs into to tumour and gadolinium chloride to cause M2 type macrophage (defined by expressing CD163) apoptosis. Gadolinium chloride forms mineral emboli in capillaries when injected i.v. and is taken up by mononuclear phagocytes where it inhibits calcium mobilisation damaging the plasma membrane. While the group did not show data of macrophage reduction, they stated that M2 macrophages were reduced by roughly 80 % in the tumour. CD163 was not expressed by any of the TAM populations investigated in the present work, and, as described in chapter 4, all TAM subsets expressed a mixture of M1 and M2 associated markers. Nevertheless, Sun et al.'s data support the idea that some TAM populations could be beneficial, and an attempt at reducing all macrophages subsets in the tumour would not achieve tumour regression.

Conclusion

The contributions of macrophages and Tregs to tumour growth are intertwined. While CSF1R inhibition reduced TAMs, it also reduced DCs and leukocytes and failed to establish primary tumour control, even if a reduction in metastasis was observed. TAM and DC reduction was also a result of Treg depletion in DEREG^{+} mice, all of which regressed their tumours.

In contrast, p110δ inhibition increased TAM populations and T cells in mice that controlled the tumours, but not mice that failed to do so. The differential effect of Treg depletion via DEREG/DT and PI-3065 treated mice on TAMs suggests that PI-3065 might affect macrophages independently of Treg contribution and this should be studied in detail.

Treatment with GW2580 and DT in DEREG mice was expected to combine the effects of both individual treatments, reducing TAMs and controlling the primary tumour and metastasis. The failure of the combined treatment to do so was curious, especially since both treatments individually lowered TAM numbers.

The present data suggest that neither a general reduction nor increase in the TAM department is desirable on its own. Reliable markers must be identified for the different TAM populations to allow the specific targeting of individual populations. Further, macrophage specific effects should be studied in the absence of T cells to fully understand the role of macrophages in tumour growth and metastasis.

Chapter 6: General discussion

Earlier research

Macrophages are essential cells of the innate immune system. They are vital for homeostasis and in the response to pathogens, but are also believed to play a pivotal role in cancer. Depending on the type of malignancy, macrophages can make up the majority of the immune cell infiltrate and have been assigned various roles in tumour progression, including the promotion of inflammation, angiogenesis and metastasis. Thus, in most types of solid cancer a high macrophage infiltration has been reported to correlate with worse prognosis (Zhang *et al.*, 2012). This, however, seems to depend on the type of macrophage present: macrophages are highly heterogeneous, a concept that also applies to TAMs (Cassetta *et al.*, 2019). Most work in breast cancer has focused on the ratio of M1 and M2 macrophages for diagnostic purpose: a high ratio of M1 type TAMs in ER^+ breast cancer has been associated with increased overall survival, although it is not clear how M1 macrophages were defined in this context (Teschendorff *et al.*, 2007). In $HER2^+$ breast cancer, a high infiltration of $CD163^+$ macrophages (termed M2-like) in the tumour centre was associated with poor prognosis, but increased $iNOS^+$ TAMs (M1-like) combined with a high number of $CD8^+$ T cells in the centre correlated with improved survival (Honkanen *et al.*, 2019). However, correcting for tumour subtype and TAM location, Gwak and colleagues showed that TAM levels only had prognostic value in hormone receptor positive subtypes (Gwak *et al.*, 2015).

Triple negative breast cancer is the most challenging form to treat. Mouse models have revealed that TAMs interfere with therapeutics (Santoni *et al.*, 2018) and have suggested TAM depletion or re-education as a therapeutic option. Importantly, most studies broadly defined TAMs as M1 or M2 based on the expression of selected cell surface markers, whilst suggesting that M1 type TAMs are beneficial and M2 types are detrimental. Since TAMs likely do not fall into either of these categories, a global targeting of all TAMs for depletion or re-education purposes is likely to interfere with beneficial TAM subsets.

Thus, the purpose of the work in this thesis was to investigate the myeloid immune cell population in the 4T1 model of TNBC, to understand the phenotypes of different TAM subpopulations, how these cells are affected by immune targeted interventions and their relationship with tumour growth and regression.

Findings and limitations

Four distinct subsets of macrophages are present in the developing 4T1 tumour

The research summarised in this thesis suggests the presence of four distinct TAM populations in addition to monocytes in the 4T1 model of breast cancer.
In t-SNE projections of single cell sequencing from viable $CD45^+$ $CD11b^+$/$CD11c^+$ cells from 4T1 tumour preparations, monocytes clustered away from macrophages and expressed a mixture of *Ly6c1* and *Nr4a1.* Four types of macrophages (12, 13, 14, 15) clustered together.

In flow cytometric analysis, $NR4A1^+$ monocytes could be distinguished from macrophage subsets, but Ly6C high monocytes could not be separated from macrophage population 15 ($Ly6C^+$, $C1qA^-$, $F4/80^-$, $MRC1^-$). Only after completion of most experiments did we distinguish monocytes and population 15 macrophages by expression of Ly6B and CD62L on monocytes but not macrophages. Thus, while the relative percentages of monocytes and macrophages within population 15 could be determined in control tumours, whether and how these proportions change with different manipulation methods is unclear at this point and would need to be determined in additional studies.

In t-SNE projections and by flow cytometry macrophage populations separated based on gene and protein expression of Ly6C and F4/80: populations 14 and 15 expressed Ly6C, with 15 being negative for F4/80 and 14 showing some expression. While being most related in gene expression, population 14 and 15 differed in their expression of genes associated with phagocytosis, which were highly expressed only in population 15 (*Tgm2*, *CD44*, *Isg1*, *Slpi*, *Lgals3*) and those associated with antigen presentation (*H2-DMb2*, *H2-DMb1*, *H2-Ab1*, *H2-Aa*, *H2-b1*) expressed in population 14 but not 15. Antigen presentation genes were also highly expressed in populations 12 and 13. Both populations showed a high expression of C1q distinguishing them from all other immune cell populations, with cluster 12 being positive and cluster 13 negative for MRC1 (CD206).

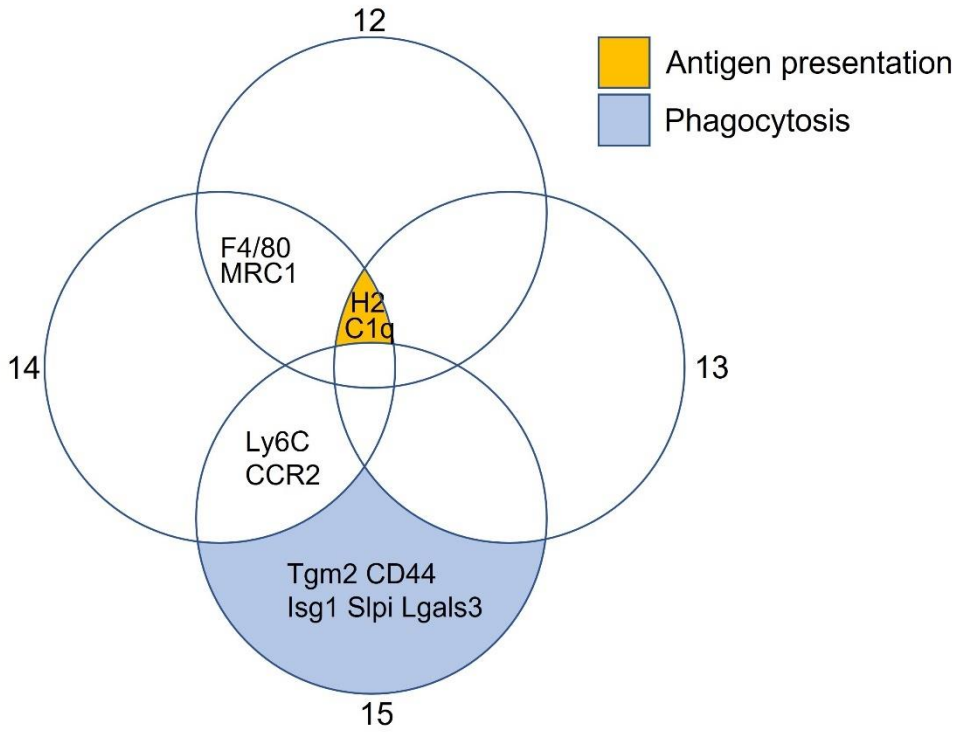

Figure 6.1: Gene expression and putative pathways in different TAM populations

Venn diagram showing unique and shared genes and potential pathways active in different TAM populations. 12-15 indicated TAM subsets;

Deciphering TAM subtypes in TNBC, and breast cancer in general, is an area of active research. Single cell sequencing of human breast cancers identified three different types of TAMs in ER^- tumours: all of them highly expressed HLA-DR, CD86 and CD84, with two of the populations sharing similar gene expression and clustering closer together, and one population – characterised by high expression of PD-L1 and CD38 – clustering farther away (Wagner *et al.*, 2019). This ubiquitous expression of MHCII by TAMs was not in line with results from the present study, where TAM populations 14 and especially 15 were associated with reduced H2-complex genes.

Via flow cytometric separation of cell types by differential expression of MHCII and Ly6C, Movahedi and colleagues (K. Movahedi *et al.*, 2010) identified MHCII positive and low subsets of TAMs in the 4T1 model. The group described MHCII high TAMs as $Ly6C^-$, $F4/80^+$, MRC1 low, which could reflect population 12 identified by the work in this thesis. Their MHCII low TAM population still expressed F4/80 and MRC1, which could correspond to population 14 discovered in the present study. In line with Movahedi's findings, MHCII high

TAMs (12) in the present study expressed higher levels of *Cx3cr1* while MHCII low populations (14) expressed higher levels of *Ccr2.* In addition to those populations relating to subtypes identified by Movahedi (12 and 14), the present study also identified a $Ly6C^{+}$ population of TAMs (population 15) as well as a population characterised by low expression of F4/80 but increased expression of the C1q subunits (population 13).

C1q is a component of the complement system, binding antibodies complexed with antigen and initiating the classical pathway of the complement cascade that culminates in cell destruction and inflammation (Nayak *et al.*, 2012). If antibodies are bound to tumour cells, activation of the complement cascade could result in tumour cell lysis. Importantly however, expression of membrane regulators including CD46, CD55 and CD59 by tumour cells can prevent this activation (Donin *et al.*, 2003). Expression of such regulators has been documented in a variety of cancers, including the TNBC cell line MCA-MB0231-HM, where it was linked to increased tumour growth (Ouyang *et al.*, 2016). There are currently no data available on the expression of membrane regulators by 4T1 tumour cells.

Independently of membrane regulators, in clear-cell renal cell carcinoma (CCRCC) models, TAMs producing C1q have been linked to unfavourable prognosis, as tumour cells produce complement products and initiate the complement pathway on intra-tumour antibody complexes driving inflammation and T-cell exhaustion (Roumenina *et al.*, 2019). Consistent with this, C1q deficient (*$C1qa^{-/-}$)* mice showed enhanced survival in the B16 melanoma model compared to wild-type mice (Bulla *et al.*, 2016).

In contrast, in the BALB-neuT model of HER2-positive breast cancer C1q deficiency was associated with increased tumour progression, with its effects suspected to be due to a direct action on tumour cells by activation of the oncosuppressor WWOX causing tumour cell apoptosis (Bandini *et al.*, 2016). In line with this, meta-analysis of human data showed that high C1qa levels were associated with favourable prognosis in basal-like and HER2-positive breast cancer, but with a pro-tumour role in lung adenocarcinoma and CCRCC (Mangogna *et al.*, 2019). The specific effect of TAM derived C1q in TNBC is unclear.

Activation of the complement cascade also generates factors such as C3a and C5a which have been linked to increased CCL2 production and macrophage infiltration in the MCA model of breast cancer (Bonavita *et al.*, 2015). Interestingly, while inhibition of the C3a receptor (C3aR) via the antagonist SB290157 slowed primary 4T1 tumour growth (Rolfe *et al.*, 2021), no significant change in primary tumour growth but reduced metastasis to the lungs of 4T1 breast cancer cells was observed in $C3aR^{-/-}$ mice (Shu *et al.*, 2020). This

discrepancy might be due to the non-selective nature of SB290157, which has been shown to also depress C5a-dependent ERK signalling in macrophages (Li *et al.*, 2020).

Another marker differentiating the TAM populations was MRC1, which was expressed by populations 12 and 14 but not 13 and 15. In human breast cancer of different molecular subtypes $MRC1^-$ $MHCII^+$ TAMs were associated with poor patients survival, while $MRC1^+$ TAMs were associated with increased $CD8^+$ T cell infiltration (Strack *et al.*, 2020). In the present study, population 13 was identified as $MRC1^-$ $MHCII^+$, while populations 12 and 14 expressed MRC1 and population 15 expressed neither MHCII nor MRC1.

In contrast to all other TAM populations, cluster 15 was associated with increased gene expression relating to phagocytosis, including genes coding for CD14 and most importantly CD209, the expression of which has been shown to directly correlate with particle uptake in macrophages (Schulz *et al.*, 2019). In theory, phagocytic cells can engulf tumour cells and link innate and adaptive immunity evoking anti-tumour T cell responses. Importantly, however, tumour cells have evolved the expression of anti-phagocytic checkpoints such as CD47, preventing phagocytosis (Chao *et al.*, 2010). In TNBC CD47 expression was associated with poor prognosis (Yuan *et al.*, 2019) and anti-CD47 antibody administration increased macrophage phagocytosis of the human colon cancer cell line DLD1 *in vitro*, priming $CD8^+$ T cell responses (Tseng *et al.*, 2013). While CD47 can prevent TAMs from engulfing cancer cells, TAMs can still clear dying or apoptotic cells supporting the resolution of inflammation. Thus, phagocytic macrophages could be beneficial in the tumour environment.

On the other hand, macrophage uptake of tumour cells has been suggested to potentially transform them into tumour like cells, integrating tumour cell genetic material into their DNA while maintaining macrophage cell surface markers that would allow them to evade immune recognition and facilitate tumour spread (Zhang *et al.*, 2017). Myeloid cells containing tumour derived material and expressing markers associated with epithelial cells (EpCAM) have been detected in human circulation (Adams *et al.*, 2014, 2016); whether they truly play a role in metastasis is not clear.

Trastuzumab is used in clinical treatment of breast cancer, binding HER2 and promoting macrophage activation: the drug was shown to induce antibody dependent phagocytosis of $HER2^+$ breast cancer cells by human macrophages, causing macrophage mediated suppression of natural killer (NK) cell and $CD8^+$ T cell proliferation and antibody dependent cytotoxicity against the tumour cells *in vitro*. These results were replicated with $CD20^+$ Raji

lymphoma cells and rituximab, which binds CD20, and prevention of phagocytosis abrogated inhibitory effects (Su *et al.*, 2018). Again, these data suggest that the uptake of tumour cells by macrophages could aid tumour development by suppressing anti-tumour immunity.

All TAM populations identified in the work summarised in this thesis could potentially have pro- and anti-tumour functions. It is not currently possible to infer their action in the primary tumour based solely on gene expression and existing literature. It is likely that variations in gene expression influencing distinct functional pathways with relevance to tumour progression, metastasis or immune recognition decide whether a type of TAM would be beneficial or harmful, and such variations would be heavily influenced by TAMs' close environment.

TAM subsets share M1 and M2 markers

In the 4T1 model, Movahedi and colleagues (Kiavash Movahedi *et al.*, 2010) identified MHCII high and low subgroups of TAMs, which were associated with the expression of M1 and M2 type macrophage markers respectively. The group defined M1 marker genes as *Nos2* (INOS), *Ptgs2* and *Cd11c* and M2 markers as *Arg1*, *Cd163*, *Stab1* and *Mrc1.*

Gene expression profiles in the identified TAM populations did not correlate with subtypes identified by Movahedi and colleagues. In fact, the present study showed that all TAM populations identified co-expressed genes and proteins of M1/M2 polarisation states as identified by Jablonski and colleagues (Jablonski *et al.*, 2015). Indeed, this is in line with other studies: in single cell sequencing of human breast cancer, researchers identified different macrophage populations with a positive correlation between the expression of M2-type and M1-type markers (Azizi *et al.*, 2018b). Importantly, the overlap of genes associated with M1 and M2 polarisation between Movahedi and Jablonski is minimal (*Ptgs2*, *Il1b*, *Il6* and *Il12b* for M1 and *Arg1* for M2) illustrating the difficulty in assigning genes to these highly polarised phenotypes. M1 and M2 macrophage subtypes are based on *in vitro* polarisation of macrophages with LPS or IL-4 respectively and many markers cannot be translated into the *in vivo* setting (Orecchioni *et al.*, 2019). This results in a lack of consensus in the definition of M1/M2 polarisation types and can create confusion when comparing different studies, arguing for the eradiation of this outdated classification system.

Distinct subsets of myeloid cells cluster in distinct regions of the primary tumour

Neutrophils and macrophage population 13 clustered in the tumour centre, while the other macrophage populations were spread throughout the tumour. The location of TAM populations was not associated with hypoxia as detected by Hif1α staining, and indeed significant hypoxia was only detected in one out of three tumours investigated. Importantly, the sample size is too small to draw any conclusions.

Spatial location of TAMs regardless of hypoxia has been implicated to correlate with their role: single cell sequencing of tumours in a murine model of mammary adenocarcinoma (MMTV-PyMT) revealed a TAM subset expressing Lyve-1 in the proximity of blood vessels that supported tumour growth (Opzoomer *et al.*, 2021). Lyve-1 mRNA was not detected in the sequencing data in the present study, although sequencing depth might have been too shallow. Additionally, blood vessels were not stained for in histological sections and thus it could not be determined whether specific TAM subpopulations clustered in close proximity.

Origin of distinct subsets is unclear

Genes expressed by the different TAM populations indicated that 14 and 15 (*Ly6c*$^{+}$, *Adgre* low, *Cc14*$^{+}$, *Ccr2*$^{+}$) might be derived from monocytes and represent a more immature macrophage phenotype. In an attempt to dissect the origins of TAM populations, anti-mouse CCL2 antibody was injected i.p. to block monocyte recruitment into the tumour, hypothesising that this would reduce the numbers of monocyte derived macrophages in the primary tumour. Following a protocol that has led to reduced tumour growth in the same animal model (Li *et al.*, 2013), two out of three mice injected with the antibody showed a reduction in macrophage subtypes 13, 14 and 15 but no change in tumour growth. Due to low numbers and a lack of power, this reduction in macrophages was not significant and the experiment would need to be repeated to confirm whether or not macrophage reductions can be achieved. Also, even in the 2 tumours that had reduced TAM numbers, primary tumour growth was not affected by anti-CCL2 antibody injection. This is curious, as reduced primary tumour growth was achieved by Li and colleagues in the same model. One reason could be the potential use of a different version of the 4T1 model: it is unclear from the above study whether 4T1 tumour cells were injected s.c. or orthotopically. Those two states of the model have been shown to differ in primary tumour growth and metastasis (Zhang *et al.*, 2018). In general, orthotopic tumour models have been shown to contain less functional blood vessels (Fung *et al.*, 2015), differ in TAM

composition and react differently to chemotherapy (Devaud *et al.*, 2014). Thus, it is feasible that they would react differently to CCL2 blockade.

In conclusion, neither the data from CCL2 antibody experiments nor a computational approach using pseudotime modelling could support or contradict the hypothesis that populations 14 and 15 depend on monocyte influx.

Global increase or reduction of all macrophage populations likely does not aid 4T1 tumour control

Global reductions in TAM numbers were achieved by blocking CSF1R signalling with GW2580, reducing metastatic burden in the lungs. This points towards a role of TAMs in metastasis, which indeed is supported by previous research (Luo *et al.*, 2006; Qian *et al.*, 2009b; Kitamura *et al.*, 2015; Linde *et al.*, 2018).

In different tumour models, CSF1R modulation has been associated with different results: while blockade by BLZ945 in the MMTV-PyMT model of breast cancer caused decreased primary tumour growth, this study reported reduced TAMs but also increased $CD8^+$ T cells (Strachan *et al.*, 2013) which was not the case in the present study, where TAM numbers were decreased but tumour growth and $CD8^+$ T cells were unaffected . The group did not investigate lung metastasis. In contrast, in a study of PyMT cancer in *Csf1*^{op} mice, the absence of CSF1 did not affect primary tumour growth but delayed pulmonary metastasis (Lin *et al.*, 2001). This is in line with results observed after CSF1R inhibition by GW2580 in the present study.

A global reduction of macrophages was also observed upon depletion of Tregs via DT administration in DEREG mice, which resulted in reduced tumour growth. In the present study, Treg depletion was not associated with increased $CD8^+$ T cells in the primary tumour. Treg depletion in the same way in the MCA model was shown to reduce primary tumour growth and increase $CD8^+$ T cells, even if in some cases $CD8^+$ depletion did not affect suppressed tumour growth, suggesting that control of tumour growth does not entirely depend on $CD8^+$ T cells (Teng *et al.*, 2010).

Both, individual GW2580 treatment and Treg depletion also reduced DCs in the primary tumour, with GW2580 additionally reducing B cells (see chapter 5, figure 5.7) and DT treatment reducing neutrophil infiltration (figure 5.17). Since Treg depletion but not GW2580 was associated with primary tumour reduction, it is possible that neutrophils play a role in primary tumour growth. Intra-tumour neutrophils have been associated with

reduced overall survival in different histological types of cancer, although this meta-analysis did not include studies of breast cancer (Shen *et al.*, 2014).

Interestingly, combining GW2580 and Treg depletion by DT, aiming to reduce both TAMs and Tregs at the same time, was not associated with any changes in immune cell populations compared to controls and only transiently reduced primary tumour growth. Since tumour immune cell content was only assessed after the initial plateauing phase of primary tumour growth and once tumours had started to grow again, it is likely that at the initial point of growth stagnation the tumour microenvironment would have been different to that of control tumours. Thus, it would be important to investigate which changes in immune cell populations are associated with the reduced growth and why and how these alterations are then lost.

In contrast to those treatments, PI3Kδ inhibition via PI-3065 resulted in reduced tumour growth, with regressing tumours associated with consistently higher TAM infiltration than non-regressing tumours. This is reflected by a study by Usman and colleagues, where PI3K inhibition via GDC-0941 increased TAM infiltration in the 4T1 model (Usman *et al.*, 2018).

It is curious that Treg depletion in DEREG mice resulted in reduced TAM numbers and Treg inhibition via the PI3Kδ inhibitor increased TAM infiltration. However, PI3Kδ is expressed by a variety of immune cells and its inhibition can also affect other cell types including conventional T cells (Okkenhaug *et al.*, 2002), B cells (Clayton *et al.*, 2002) neutrophils (Sadhu *et al.*, 2003), natural killer cells (Kim *et al.*, 2007) and myeloid cells (Shimizu-Hirota *et al.*, 2012). Thus, the TAM increase observed after PI3Kδ inhibition might not be an effect of Treg reduction but could be due to the PI-3065 directly affecting other cell types.

Future perspective

The work presented in this thesis has identified types of TAMs that have not previously been described in the 4T1 model of breast cancer. Flow cytometry data supported single cell sequencing derived distinction of four TAM populations in the 4T1 tumour. Considering the lack of depth experienced with 10x Genomics sequencing that prevented IPA and deeper analysis of gene expression, a different method of single cell sequencing should be trialled to gain more detailed information. One option would be Clontech ICELL8 (Goldstein *et al.*, 2017) detecting double the number of genes, or Fluidigm C1 96 (Gong, Do and Ramakrishnan, 2018) detecting up to three times the number of genes detected by 10x Chromium in a study published as a preprint (Wang *et al.*, 2019). Additionally, sequencing

should be performed in other TNBC mouse models as well to investigate the stability of TAM populations across different models. Further, spatial transcriptomic techniques are now available that allow analysis of single cell gene expression across a frozen tissue section. These approaches provide information on gene expression and spatial location of a cell simultaneously (Rao *et al.*, 2021), and could provide additional insight into the different TAM populations relative to the tumour.

The data gathered in this study were not sufficient to draw conclusions about the specific functions of the different TAM populations and their importance in tumour progression and metastasis. The data do, however, clearly suggest that a global TAM reduction on its own reduces metastatic burden, but does not result in control or regression of the primary tumour. This finding is important, as the primary tumour can often be surgically removed, while metastases remain the primary cause of tumour related death (Chaffer and Weinberg, 2011). The lack of effect of global TAM depletion on primary tumour growth is in line with research in human TNBC where $CD163^+$ TAMs have been associated with worse prognosis, but no correlation was found between the overall number of $CD68^+$ TAMs and disease outcome (Jamiyan *et al.*, 2020). Since CD68 is a pan macrophage marker, these data suggest that a general infiltration of the tumour with TAMs is not necessarily harmful, and only certain subsets of TAMs are linked to tumour progression. Indeed, $CD68^+$ TAM counts were not associated with survival in a large cohort of 1322 invasive breast cancer patients, although no distinction was made between cancer types based on hormone receptor expression (Mahmoud *et al.*, 2012). Thus, in the future it will be essential to find specific targeting methods to selectively deplete individual TAM populations to investigate their role in tumour development and metastasis. It will also be important to investigate whether the identified TAM populations or populations with similar functions can also be detected in human patients. For therapeutic purpose it is likely if one or more TAM subsets prove beneficial in arresting tumour development, re-education of other subsets to match their phenotype could be superior to depletion of harmful subsets, as cell death could negatively affect the tumour microenvironment.

The data further suggest that a combination of interventions targeting Tregs and TAMs at the same time needs to be carefully planned, considering the complete loss of the observed individual beneficial effects upon combination of GW2580 and Treg depletion.

For future experiments, it would be interesting to compare the immune cell infiltration of tumours receiving the combined treatment at an earlier timepoint to investigate what

drives the initial stalling of tumour growth and the subsequent loss of beneficial effects. In general, it will be important to confirm the presence of the TAM populations discovered in the 4T1 and other TNBC models, as well as define roles of individual TAM populations discovered in the present study for the development of novel therapeutics. It will also be vital to be able to target individual TAM populations specifically without affecting macrophages systemically, either by targeting specific markers that are not shared by peripheral macrophages or by sequestering potential therapeutics in the primary tumour.

In conclusion, the work summarised in this thesis aimed to explore TAM subsets in an unbiased way by investigating how they are affected by known treatment regimes (CSFR1 inhibition and Treg-depletion) in order to infer key functions in the tumour microenvironment (tumour progression vs immunity). Single cell sequencing was performed on untreated tumours to identify the baseline subpopulations and different treatments were used to try to determine deviations from the baseline. Since all four TAM populations identified were equally affected by different treatments, it was impossible to infer which subpopulation would be associated with tumour growth and which with tumour regression. Importantly, a general depletion of all macrophages was only beneficial for controlling lung metastasis, while in combination with Treg depletion it compromised the otherwise effective control of primary tumour growth.

References

10xGenomics (2017) 'Technical Note - Removal of Dead Cells from Single Cell Suspensions Improves Performance for 10x Genomics Single Cell Application', *Document Number CG000130*. Available at: https://assets.ctfassets.net/an68im79xiti/4tVumiyINGgAeoCg8SiWGG/1cf0888200d668142612c8d3f3679cf4/CG000130_10x_Technical_Note_DeadCell_Removal_RevA.pdf.

10xGenomics (2018) 'PROTOCOL STEP 4 – Library Construction Chromium™ Single Cell 3' Reagent Kits v2 User Guide', *Document Number CG00052*. 10x Genomics. Available at: https://assets.ctfassets.net/an68im79xiti/UhAMGmlaEMmYMaA4A4Uwa/274a813b81e42cba81345d49380432d7/CG00052_SingleCell3_ReagentKitv2UserGuide_RevD.pdf (Accessed: 8 May 2018).

Abdellah, Z. *et al.* (2004) 'Finishing the euchromatic sequence of the human genome', *Nature*. Nature Publishing Group, 431(7011), pp. 931–945. doi: 10.1038/nature03001.

Adams, D. L. *et al.* (2014) 'Circulating giant macrophages as a potential biomarker of solid tumors', *Proceedings of the National Academy of Sciences of the United States of America*. National Academy of Sciences, 111(9), pp. 3514–3519. doi: 10.1073/pnas.1320198111.

Adams, D. L. *et al.* (2016) 'Circulating cancer-associated macrophage-like cells differentiate malignant breast cancer and benign breast conditions', *Cancer Epidemiology Biomarkers and Prevention*. American Association for Cancer Research Inc., 25(7), pp. 1037–1042. doi: 10.1158/1055-9965.EPI-15-1221.

Ahmad, S. *et al.* (2017) 'Differential PI3Kδ Signaling in CD4 $^{+}$ T-cell Subsets Enables Selective Targeting of T Regulatory Cells to Enhance Cancer Immunotherapy', *Cancer Research*, 77(8), pp. 1892–1904. doi: 10.1158/0008-5472.CAN-16-1839.

Ali, K. *et al.* (2014) 'Inactivation of PI(3)K p110δ breaks regulatory T-cell-mediated immune tolerance to cancer', *Nature*, 510(7505), pp. 407–411. doi: 10.1038/nature13444.

Allan, S. E. *et al.* (2007) 'Activation-induced FOXP3 in human T effector cells does not suppress proliferation or cytokine production', *international Immunology*, 19(4), pp. 345–354. Available at: https://academic.oup.com/intimm/article/19/4/345/691439 (Accessed: 18 March 2020).

Allen, W. E. *et al.* (1998) 'A role for Cdc42 in macrophage chemotaxis', *Journal of Cell Biology*. The Rockefeller University Press, 141(5), pp. 1147–1157. doi: 10.1083/jcb.141.5.1147.

Alon, T. *et al.* (1995) 'Vascular endothelial growth factor acts as a survival factor for newly formed retinal vessels and has implications for retinopathy of prematurity', *Nature Medicine*. Nature Publishing Group, 1(10), pp. 1024–1028. doi: 10.1038/nm1095-1024.

Amit, M. and Gil, Z. (2013) 'Macrophages increase the resistance of pancreatic adenocarcinoma cells to gemcitabine by upregulating cytidine deaminase', *OncoImmunology*. Landes Bioscience, 2(12), p. e27231. doi: 10.4161/onci.27231.

Annunziato, F. *et al.* (2002) 'Phenotype, localization, and mechanism of suppression of CD4+CD25+ human thymocytes', *Journal of Experimental Medicine*. The Rockefeller University Press, 196(3), pp. 379–387. doi: 10.1084/jem.20020110.

Antony, P. A. *et al.* (2005) ' CD8 + T Cell Immunity Against a Tumor/Self-Antigen Is Augmented by CD4 + T Helper Cells and Hindered by Naturally Occurring T Regulatory Cells ', *The Journal of Immunology*. The American Association of Immunologists, 174(5), pp. 2591–2601. doi: 10.4049/jimmunol.174.5.2591.

Apostolou, I. and Von Boehmer, H. (2004) 'In vivo instruction of suppressor commitment in naive T cells', *Journal of Experimental Medicine*. The Rockefeller University Press, 199(10), pp. 1401–1408. doi: 10.1084/jem.20040249.

Arce Vargas, F. *et al.* (2017) 'Fc-Optimized Anti-CD25 Depletes Tumor-Infiltrating Regulatory T Cells and Synergizes with PD-1 Blockade to Eradicate Established Tumors', *Immunity*. Cell Press, 46(4), pp. 577–586. doi: 10.1016/j.immuni.2017.03.013.

Arock, M. *et al.* (1996) 'Interleukin-10 inhibits cytokine generation from mast cells', *European Journal of Immunology*. John Wiley & Sons, Ltd, 26(1), pp. 166–170. doi: 10.1002/eji.1830260126.

Atochina, O. *et al.* (2001) 'A Schistosome-Expressed Immunomodulatory Glycoconjugate Expands Peritoneal Gr1+ Macrophages That Suppress Naive CD4+ T Cell Proliferation Via an IFN-γ and Nitric Oxide-Dependent Mechanism', *The Journal of Immunology*. American Association of Immunologists, 167(8), pp. 4293–4302. doi: 10.4049/JIMMUNOL.167.8.4293.

Azizi, E. *et al.* (2018a) 'Single-Cell Map of Diverse Immune Phenotypes in the Breast Tumor Microenvironment', *Cell*. Cell Press, 174(5), pp. 1293-1308.e36. doi: 10.1016/j.cell.2018.05.060.

Azizi, E. *et al.* (2018b) 'Single-Cell Map of Diverse Immune Phenotypes in the Breast Tumor Microenvironment', *Cell*. Cell Press, 174(5), pp. 1293-1308.e36. doi: 10.1016/j.cell.2018.05.060.

Azorin, P. *et al.* (2018) 'Distinct expression profiles and functions of Kindlins in breast cancer', *Journal of Experimental and Clinical Cancer Research*. BioMed Central Ltd., 37(1), pp. 1–15. doi: 10.1186/s13046-018-0955-4.

Bader, J. E. *et al.* (2018) 'Macrophage depletion using clodronate liposomes decreases tumorigenesis and alters gut microbiota in the AOM/DSS mouse model of colon cancer', *American Journal of Physiology-Gastrointestinal and Liver Physiology*. American Physiological Society, 314(1), pp. G22–G31. doi: 10.1152/ajpgi.00229.2017.

Baghdadi, M. *et al.* (2018) 'High co-expression of IL-34 and M-CSF correlates with tumor progression and poor survival in lung cancers', *Scientific Reports*. Nature Publishing Group, 8(1), pp. 1–10. doi: 10.1038/s41598-017-18796-8.

Baker, A. H. *et al.* (1993) 'Expression of the colony-stimulating factor 1 receptor in B lymphocytes.', *Oncogene*, 8(2), pp. 371–8. Available at: http://www.ncbi.nlm.nih.gov/pubmed/8426743 (Accessed: 1 April 2020).

Bandini, S. *et al.* (2016) 'The non-inflammatory role of C1q during Her2/neu-driven mammary carcinogenesis', *OncoImmunology*. Taylor and Francis Inc., 5(12). doi: 10.1080/2162402X.2016.1253653.

Baras, A. S. *et al.* (2016) 'The ratio of CD8 to Treg tumor-infiltrating lymphocytes is associated with response to cisplatin-based neoadjuvant chemotherapy in patients with muscle invasive urothelial carcinoma of the bladder', *OncoImmunology*. Taylor and Francis Inc., 5(5). doi: 10.1080/2162402X.2015.1134412.

Bardel, E. *et al.* (2008) ' Human CD4 + CD25 + Foxp3 + Regulatory T Cells Do Not Constitutively Express IL-35 ', *The Journal of Immunology*. The American Association of Immunologists, 181(10), pp. 6898–6905. doi: 10.4049/jimmunol.181.10.6898.

Barrera, P. *et al.* (2000) 'Synovial macrophage depletion with clodronate-containing liposomes in rheumatoid arthritis', *Arthritis & Rheumatism*. John Wiley & Sons, Ltd, 43(9), pp. 1951–1959. doi: 10.1002/1529-0131(200009)43:9<1951::AID-ANR5>3.0.CO;2-K.

Bart, V. M. T. *et al.* (2020) 'Macrophage Reprogramming for Therapy', *Immunology*. John Wiley & Sons, Ltd, p. imm.13300. doi: 10.1111/imm.13300.

Bartelmez, S. H. *et al.* (1989) 'Interleukin 1 plus interleukin 3 plus colony-stimulating factor 1 are essential for clonal proliferation of primitive myeloid bone marrow cells.', *Experimental hematology*, 17(3), pp. 240–5. Available at: http://www.ncbi.nlm.nih.gov/pubmed/2783913 (Accessed: 2 April 2020).

Beck, A. H. *et al.* (2009) 'The macrophage colony-stimulating factor 1 response signature in breast

carcinoma', *Clinical Cancer Research*. American Association for Cancer Research, 15(3), pp. 778–787. doi: 10.1158/1078-0432.CCR-08-1283.

Begg, S. K. *et al.* (1993) 'Delayed hematopoietic development in osteopetrotic (op/op) mice.', *The Journal of experimental medicine*. The Rockefeller University Press, 177(1), pp. 237–42. Available at: http://www.ncbi.nlm.nih.gov/pubmed/8418205 (Accessed: 25 March 2019).

Behnes, C. L. *et al.* (2014) 'Tumor-associated macrophages are involved in tumor progression in papillary renal cell carcinoma', *Virchows Archiv*. Springer, 464(2), pp. 191–196. doi: 10.1007/s00428-013-1523-0.

Bergmann, C. *et al.* (2008) 'T regulatory type 1 cells in squamous cell carcinoma of the head and neck: mechanisms of suppression and expansion in advanced disease', *Clinical cancer research : an official journal of the American Association for Cancer Research*. Clin Cancer Res, 14(12), pp. 3706–3715. doi: 10.1158/1078-0432.CCR-07-5126.

Beury, D. W. *et al.* (2014) 'Cross-talk among myeloid-derived suppressor cells, macrophages, and tumor cells impacts the inflammatory milieu of solid tumors', *Journal of Leukocyte Biology*, 96(6), pp. 1109–1118. doi: 10.1189/jlb.3A0414-210R.

Bieniasz-Krzywiec, P. *et al.* (2019) 'Podoplanin-Expressing Macrophages Promote Lymphangiogenesis and Lymphoinvasion in Breast Cancer', *Cell Metabolism*. Cell Press, 30(5), pp. 917-936.e10. doi: 10.1016/j.cmet.2019.07.015.

Biewenga, J. *et al.* (1995) 'Macrophage depletion in the rat after intraperitoneal administration of liposome-encapsulated clodronate: Depletion kinetics and accelerated repopulation of peritoneal and omental macrophages by administration of freund's adjuvant', *Cell and Tissue Research*. Springer-Verlag, 280(1), pp. 189–196. doi: 10.1007/BF00304524.

Biswas, M. and Sharma, S. (2018) 'Sample Quality Control in Agilent NGS Solutions', *Agilent Technologies Application Note*, publicatio. Available at: https://www.agilent.com/cs/library/applications/application-ngs-electrophoresis-samplequalitycontrol-tapestation-5994-0127en-agilent.pdf.

Black, W. C. and Welch, H. G. (1993) 'Advances in Diagnostic Imaging and Overestimations of Disease Prevalence and the Benefits of Therapy', *New England Journal of Medicine*. Massachusetts Medical Society , 328(17), pp. 1237–1243. doi: 10.1056/NEJM199304293281706.

Boissonnas, A. *et al.* (2010) 'Foxp3+ T Cells Induce Perforin-Dependent Dendritic Cell Death in Tumor-Draining Lymph Nodes', *Immunity*. Cell Press, 32(2), pp. 266–278. doi: 10.1016/j.immuni.2009.11.015.

Bonavita, E. *et al.* (2015) 'PTX3 Is an Extrinsic Oncosuppressor Regulating Complement-Dependent Inflammation in Cancer', *Cell*. Cell Press, 160(4), pp. 700–714. doi: 10.1016/J.CELL.2015.01.004.

Boocock, C. A. *et al.* (1989) 'Colony-stimulating factor-1 induces rapid behavioural responses in the mouse macrophage cell line, BAC1.2F5', *Journal of Cell Science*, 93(3).

Borsig, L. *et al.* (2001) 'Heparin and cancer revisited: Mechanistic connections involving platelets, P-selectin, carcinoma mucins, and tumor metastasis', *Proceedings of the National Academy of Sciences of the United States of America*. National Academy of Sciences, 98(6), pp. 3352–3357. doi: 10.1073/pnas.061615598.

Bots, M. and Medema, J. P. (2006) 'Granzymes at a glance', *Journal of Cell Science*. The Company of Biologists Ltd, 119(24), pp. 5011–5014. doi: 10.1242/jcs.03239.

Bowman, R. L. *et al.* (2016) 'Macrophage Ontogeny Underlies Differences in Tumor-Specific Education in Brain Malignancies', *Cell Reports*. Cell Press, 17(9), pp. 2445–2459. doi: 10.1016/J.CELREP.2016.10.052.

Bronte, V. *et al.* (2016) 'Recommendations for myeloid-derived suppressor cell nomenclature and

characterization standards', *Nature Communications 2016 7:1*. Nature Publishing Group, 7(1), pp. 1–10. doi: 10.1038/ncomms12150.

Bucana, C. *et al.* (1976) 'Morphological evidence for the translocation of lysosomal organelles from cytotoxic macrophages into the cytoplasm of tumor target cells.', *Cancer research*. American Association for Cancer Research, 36(12), pp. 4444–58. Available at: http://www.ncbi.nlm.nih.gov/pubmed/187323 (Accessed: 23 July 2019).

Buchrieser, J., James, W. and Moore, M. D. (2017) 'Human Induced Pluripotent Stem Cell-Derived Macrophages Share Ontogeny with MYB-Independent Tissue-Resident Macrophages.', *Stem cell reports*. Elsevier, 8(2), pp. 334–345. doi: 10.1016/j.stemcr.2016.12.020.

Buddingh, E. P. *et al.* (2011) 'Tumor-Infiltrating Macrophages Are Associated with Metastasis Suppression in High-Grade Osteosarcoma: A Rationale for Treatment with Macrophage Activating Agents', *Clinical Cancer Research*, 17(8), pp. 2110–2119. doi: 10.1158/1078-0432.CCR-10-2047.

Buhren, B. A. *et al.* (2016) 'Hyaluronidase: from clinical applications to molecular and cellular mechanisms.', *European journal of medical research*. BioMed Central, 21, p. 5. doi: 10.1186/s40001-016-0201-5.

Bulfoni, M. *et al.* (2016) 'In patients with metastatic breast cancer the identification of circulating tumor cells in epithelial-to-mesenchymal transition is associated with a poor prognosis', *Breast Cancer Research*. BioMed Central, 18(1), p. 30. doi: 10.1186/s13058-016-0687-3.

Bulla, R. *et al.* (2016) 'C1q acts in the tumour microenvironment as a cancer-promoting factor independently of complement activation', *Nature Communications 2016 7:1*. Nature Publishing Group, 7(1), pp. 1–11. doi: 10.1038/ncomms10346.

Burchill, M. A. *et al.* (2008) 'Linked T Cell Receptor and Cytokine Signaling Govern the Development of the Regulatory T Cell Repertoire', *Immunity*. Cell Press, 28(1), pp. 112–121. doi: 10.1016/j.immuni.2007.11.022.

Burgess, A. and Metcalf, D. (1980) 'The nature and action of granulocyte-macrophage colony stimulating factors', *Blood*. American Society of Hematology, 56(6), pp. 947–958. doi: 10.1182/blood.V56.6.947.947.

Burnet, F. M. (Frank M. (1970) *Immunological surveillance.* Oxford New York: Pergamon Press. Available at: https://www.worldcat.org/title/immunological-surveillance/oclc/170002 (Accessed: 29 April 2019).

Byrne, P. V., Guilbert, L. J. and Stanley, E. R. (1981) 'Distribution of cells bearing receptors for a colony-stimulating factor (CSF-1) in murine tissues', *Journal of Cell Biology*. The Rockefeller University Press, 91(3 I), pp. 848–853. doi: 10.1083/jcb.91.3.848.

Cai, J. *et al.* (2019) 'Tumor-associated macrophages derived TGF-β-induced epithelial to mesenchymal transition in colorectal cancer cells through Smad2,3-4/Snail signaling pathway', *Cancer Research and Treatment*. Korean Cancer Association, 51(1), pp. 252–256. doi: 10.4143/crt.2017.613.

Camerer, E. *et al.* (2004) 'Platelets, protease-activated receptors, and fibrinogen in hematogenous metastasis', *Blood*, 104(2), pp. 397–401. doi: 10.1182/blood-2004-02-0434.

Cao, X. *et al.* (2007) 'Granzyme B and Perforin Are Important for Regulatory T Cell-Mediated Suppression of Tumor Clearance', *Immunity*. Cell Press, 27(4), pp. 635–646. doi: 10.1016/j.immuni.2007.08.014.

Casazza, A. *et al.* (2013) 'Impeding macrophage entry into hypoxic tumor areas by Sema3A/Nrp1 signaling blockade inhibits angiogenesis and restores antitumor immunity.', *Cancer cell*. Elsevier, 24(6), pp. 695–709. doi: 10.1016/j.ccr.2013.11.007.

Cassetta, L. *et al.* (2019) 'Human Tumor-Associated Macrophage and Monocyte Transcriptional

Landscapes Reveal Cancer-Specific Reprogramming, Biomarkers, and Therapeutic Targets', *Cancer Cell*, 35(4), pp. 588-602.e10. doi: 10.1016/j.ccell.2019.02.009.

Catlett-Falcone, R. *et al.* (1999) 'Constitutive activation of Stat3 signaling confers resistance to apoptosis in human U266 myeloma cells', *Immunity*. Cell Press, 10(1), pp. 105–115. doi: 10.1016/S1074-7613(00)80011-4.

Cecchini, M. G. *et al.* (1994) 'Role of colony stimulating factor-1 in the establishment and regulation of tissue macrophages during postnatal development of the mouse', *Development*. The Company of Biologists, 120(6), pp. 1357–1372. doi: 10.1242/DEV.120.6.1357.

Celada, A. and Maki, R. A. (1992) 'Transforming growth factor-beta enhances the M-CSF and GM-CSF-stimulated proliferation of macrophages.', *The Journal of Immunology*, 148(4).

Chaffer, C. L. and Weinberg, R. A. (2011) 'A perspective on cancer cell metastasis', *Science*, 331(6024), pp. 1559–1564. doi: 10.1126/SCIENCE.1203543.

Chang, M. Y. *et al.* (1998) 'Human monocyte-derived macrophages secrete two forms of proteoglycan- macrophage colony-stimulating factor that differ in their ability to bind low density lipoproteins', *Journal of Biological Chemistry*. American Society for Biochemistry and Molecular Biology, 273(26), pp. 15985–15992. doi: 10.1074/jbc.273.26.15985.

Chao, M. P. *et al.* (2010) 'Calreticulin is the dominant pro-phagocytic signal on multiple human cancers and is counterbalanced by CD47', *Science Translational Medicine*. American Association for the Advancement of Science, 2(63), pp. 63ra94-63ra94. doi: 10.1126/scitranslmed.3001375.

Chapoval, A. I. *et al.* (1998) 'CSF-1 (M-CSF) differentially sensitizes mononuclear phagocyte subpopulations to endotoxin in vivo: a potential pathway that regulates the severity of Gram-negative infections', *Journal of Leukocyte Biology*. Federation of American Societies for Experimental Biology, 63(2), pp. 245–252. doi: 10.1002/jlb.63.2.245.

Chaput, N. *et al.* (2007) 'Regulatory T Cells Prevent CD8 T Cell Maturation by Inhibiting CD4 Th Cells at Tumor Sites', *The Journal of Immunology*. The American Association of Immunologists, 179(8), pp. 4969–4978. doi: 10.4049/jimmunol.179.8.4969.

Charo, I. F. and Ransohoff, R. M. (2006) 'The Many Roles of Chemokines and Chemokine Receptors in Inflammation', *New England Journal of Medicine*. Massachusetts Medical Society, 354(6), pp. 610–621. doi: 10.1056/NEJMra052723.

Chaturvedi, V. *et al.* (2011) 'Cutting Edge: Human Regulatory T Cells Require IL-35 To Mediate Suppression and Infectious Tolerance', *The Journal of Immunology*. The American Association of Immunologists, 186(12), pp. 6661–6666. doi: 10.4049/jimmunol.1100315.

Chen, Jingqi *et al.* (2011) 'CCL18 from Tumor-Associated Macrophages Promotes Breast Cancer Metastasis via PITPNM3', *Cancer Cell*. Cell Press, 19(4), pp. 541–555. doi: 10.1016/j.ccr.2011.02.006.

Chen, W. J. *et al.* (2003) 'Conversion of Peripheral CD4+CD25- Naive T Cells to CD4+CD25+ Regulatory T Cells by TGF-β Induction of Transcription Factor Foxp3', *Journal of Experimental Medicine*. The Rockefeller University Press, 198(12), pp. 1875–1886. doi: 10.1084/jem.20030152.

Chen, Z. *et al.* (2017) 'Cellular and Molecular Identity of Tumor-Associated Macrophages in Glioblastoma', *Cancer Research*, 77(9), pp. 2266–2278. doi: 10.1158/0008-5472.CAN-16-2310.

Clayton, E. *et al.* (2002) 'A Crucial Role for the p110δ Subunit of Phosphatidylinositol 3-Kinase in B Cell Development and Activation', *The Journal of Experimental Medicine*. The Rockefeller University Press, 196(6), p. 753. doi: 10.1084/JEM.20020805.

Cochain, C. *et al.* (2010) 'Regulation of monocyte subset systemic levels by distinct chemokine receptors controls post-ischaemic neovascularization', *Cardiovascular Research*. Narnia, 88(1), pp. 186–195. doi: 10.1093/cvr/cvq153.

Collison, L. W. *et al.* (2007) 'The inhibitory cytokine IL-35 contributes to regulatory T-cell function',

Nature. Nature Publishing Group, 450(7169), pp. 566–569. doi: 10.1038/nature06306.

Conway, J. G. *et al.* (2005) 'Inhibition of colony-stimulating-factor-1 signaling in vivo with the orally bioavailable cFMS kinase inhibitor GW2580.', *Proceedings of the National Academy of Sciences of the United States of America*. National Academy of Sciences, 102(44), pp. 16078–83. doi: 10.1073/pnas.0502000102.

Correale, P. *et al.* (2010) 'Regulatory (FoxP3+) T-cell Tumor Infiltration Is a Favorable Prognostic Factor in Advanced Colon Cancer Patients Undergoing Chemo or Chemoimmunotherapy', *Journal of Immunotherapy*, 33(4), pp. 435–441. doi: 10.1097/CJI.0b013e3181d32f01.

Coussens, L. M. *et al.* (2000) 'MMP-9 Supplied by Bone Marrow–Derived Cells Contributes to Skin Carcinogenesis', *Cell*. Cell Press, 103(3), pp. 481–490. doi: 10.1016/S0092-8674(00)00139-2.

Crespo, O. *et al.* (2011) 'Tyrosine kinase inhibitors ameliorate autoimmune encephalomyelitis in a mouse model of multiple sclerosis', *Journal of Clinical Immunology*. NIH Public Access, 31(6), pp. 1010–1020. doi: 10.1007/s10875-011-9579-6.

Curiel, T. J. *et al.* (2004) 'Specific recruitment of regulatory T cells in ovarian carcinoma fosters immune privilege and predicts reduced survival', *Nature Medicine*. Nature Publishing Group, 10(9), pp. 942–949. doi: 10.1038/nm1093.

D'Armiento, J. *et al.* (1992) 'Collagenase expression in the lungs of transgenic mice causes pulmonary emphysema', *Cell*. Cell, 71(6), pp. 955–961. doi: 10.1016/0092-8674(92)90391-O.

Dai, X.-M. *et al.* (2004) 'Incomplete restoration of colony-stimulating factor 1 (CSF-1) function in CSF-1–deficient Csf1op/Csf1op mice by transgenic expression of cell surface CSF-1', *Blood*, 103, pp. 1114–1123. Available at: http://www.bloodjournal.org/content/103/3/1114?sso-checked=true.

Dameron, K. M. *et al.* (1994) 'Control of angiogenesis in fibroblasts by p53 regulation of thrombospondin-1', *Science*, 265(5187), pp. 1582–1584. doi: 10.1126/science.1978757.

Danna, E. A. *et al.* (2004) 'Surgical removal of primary tumor reverses tumor-induced immunosuppression despite the presence of metastatic disease.', *Cancer research*, 64(6), pp. 2205–11. Available at: http://www.ncbi.nlm.nih.gov/pubmed/15026364 (Accessed: 12 April 2018).

Dao, T. *et al.* (2019) 'Depleting T regulatory cells by targeting intracellular Foxp3 with a TCR mimic antibody', *OncoImmunology*. Taylor and Francis Inc., 8(7). doi: 10.1080/2162402X.2019.1570778.

Darrasse-Jèze, G. *et al.* (2009) 'Feedback control of regulatory T cell homeostasis by dendritic cells in vivo', *Journal of Experimental Medicine*. The Rockefeller University Press, 206(9), pp. 1853–1862. doi: 10.1084/jem.20090746.

Davidson, T. S. *et al.* (2007) ' Cutting Edge: IL-2 Is Essential for TGF-β-Mediated Induction of Foxp3 + T Regulatory Cells ', *The Journal of Immunology*. The American Association of Immunologists, 178(7), pp. 4022–4026. doi: 10.4049/jimmunol.178.7.4022.

Davies, L. C. *et al.* (2013) 'Distinct bone marrow-derived and tissue-resident macrophage lineages proliferate at key stages during inflammation', *Nature Communications*. Europe PMC Funders, 4. doi: 10.1038/ncomms2877.

Davis, M. I. *et al.* (2011) 'Comprehensive analysis of kinase inhibitor selectivity', *Nature Biotechnology 2011 29:11*. Nature Publishing Group, 29(11), pp. 1046–1051. doi: 10.1038/nbt.1990.

Delemarre, F. G. A. *et al.* (1990) 'Repopulation of Macrophages in Popliteal Lymph Nodes of Mice After Liposome-Mediated Depletion', *Journal of Leukocyte Biology*. John Wiley & Sons, Ltd, 47(3), pp. 251–257. doi: 10.1002/jlb.47.3.251.

Dennis, K. L. *et al.* (2015) 'T-cell expression of IL10 is essential for tumor immune surveillance in the small intestine', *Cancer immunology research*. NIH Public Access, 3(7), p. 806. doi: 10.1158/2326-6066.CIR-14-0169.

Devaud, C. *et al.* (2014) 'Tissues in different anatomical sites can sculpt and vary the tumor microenvironment to affect responses to therapy', *Molecular Therapy*. Nature Publishing Group, 22(1), pp. 18–27. doi: 10.1038/MT.2013.219/ATTACHMENT/008F67AB-390A-40A3-B2AD-6E3B8734EF7C/MMC1.PDF.

Dexter, D. L. *et al.* (1978) 'Heterogeneity of tumor cells from a single mouse mammary tumor.', *Cancer research*, 38(10), pp. 3174–81. Available at: http://www.ncbi.nlm.nih.gov/pubmed/210930 (Accessed: 12 April 2018).

Diakonova, M., Bokoch, G. and Swanson, J. A. (2002) 'Dynamics of cytoskeletal proteins during Fcγ receptor-mediated phagocytosis in macrophages', *Molecular Biology of the Cell*. American Society for Cell Biology, 13(2), pp. 402–411. doi: 10.1091/mbc.01-05-0273.

Ding, J. *et al.* (2016) 'CSF1 is involved in breast cancer progression through inducing monocyte differentiation and homing', *International Journal of Oncology*. Spandidos Publications, 49(5), pp. 2064–2074. doi: 10.3892/ijo.2016.3680.

Doedens, A. L. *et al.* (2010) 'Macrophage expression of hypoxia-inducible factor-1α suppresses T-cell function and promotes tumor progression', *Cancer Research*, 70(19), pp. 7465–7475. doi: 10.1158/0008-5472.CAN-10-1439.

Donin, N. *et al.* (2003) 'Complement resistance of human carcinoma cells depends on membrane regulatory proteins, protein kinases and sialic acid', *Clinical and Experimental Immunology*. John Wiley & Sons, Ltd, 131(2), pp. 254–263. doi: 10.1046/j.1365-2249.2003.02066.x.

Dunn, G. P. *et al.* (2002) 'Cancer immunoediting: from immunosurveillance to tumor escape', *Nature Immunology*. Nature Publishing Group, 3(11), pp. 991–998. doi: 10.1038/ni1102-991.

duPre', S. A. and Hunter, K. W. (2007) 'Murine mammary carcinoma 4T1 induces a leukemoid reaction with splenomegaly: Association with tumor-derived growth factors', *Experimental and Molecular Pathology*, 82(1), pp. 12–24. doi: 10.1016/j.yexmp.2006.06.007.

DuPre´, S. A., Redelman, D. and Hunter, K. W. (2007) 'The mouse mammary carcinoma 4T1: characterization of the cellular landscape of primary tumours and metastatic tumour foci', *International Journal of Experimental Pathology*, 88(5), pp. 351–360. doi: 10.1111/j.1365-2613.2007.00539.x.

Ehrlich, P. (1909) 'Ueber den jetzigen Stand der Karzinomforschung', *Ned Tijdschr Geneeskd*, 5, pp. 273–290. Available at: https://www.pei.de/EN/institute/paul-ehrlich/publications/publications-of-paul-ehrlich-node.html.

Espinosa, I. *et al.* (2014) 'Stromal signatures in endometrioid endometrial carcinomas', *Modern Pathology*. Nature Publishing Group, 27(4), pp. 631–639. doi: 10.1038/modpathol.2013.131.

Fallarino, F. *et al.* (2003) 'Modulation of tryptophan catabolism by regulatory T cells', *Nature Immunology*. Nature Publishing Group, 4(12), pp. 1206–1212. doi: 10.1038/ni1003.

Fang, H.-Y. *et al.* (2009) 'Hypoxia-inducible factors 1 and 2 are important transcriptional effectors in primary macrophages experiencing hypoxia.', *Blood*. Howard Hughes Medical Institute, 114(4), pp. 844–59. doi: 10.1182/blood-2008-12-195941.

Felix, R. *et al.* (1994) 'Role of colony-stimulating factor-1 in bone metabolism', *Journal of Cellular Biochemistry*. John Wiley & Sons, Ltd, 55(3), pp. 340–349. doi: 10.1002/jcb.240550311.

Fisher, S. A. *et al.* (2017) 'Transient Treg depletion enhances therapeutic anti-cancer vaccination':, *Immunity, inflammation and disease*. Wiley-Blackwell, 5(1), pp. 16–28. doi: 10.1002/iid3.136.

Fleisch, H. (1989) 'Bisphosphonates: a new class of drugs in diseases of bone and calcium metabolism.', *Recent results in cancer research. Fortschritte der Krebsforschung. Progrès dans les recherches sur le cancer*, pp. 1–28. doi: 10.1007/978-3-642-83668-8_1.

Fleming, V. *et al.* (2018) 'Targeting myeloid-derived suppressor cells to bypass tumor-induced

immunosuppression', *Frontiers in Immunology*. Frontiers Media S.A., 9(MAR), p. 398. doi: 10.3389/FIMMU.2018.00398/BIBTEX.

Folkman, J. (1984) 'Angiogenesis', in. Springer, Boston, MA, pp. 412–428. doi: 10.1007/978-1-4613-2825-4_42.

Fontenot, J. D., Gavin, M. A. and Rudensky, A. Y. (2017) 'Foxp3 programs the development and function of CD4+CD25+ regulatory T cells', *Journal of Immunology*. American Association of Immunologists, 198(3), pp. 986–992. doi: 10.1038/ni904.

Forssell, J. *et al.* (2007) 'High Macrophage Infiltration along the Tumor Front Correlates with Improved Survival in Colon Cancer', *Clinical cancer research : an official journal of the American Association for Cancer Research*. American Association for Cancer Research, 13(5), pp. 1472–1479. doi: 10.1158/1078-0432.ccr-06-2073.

Fox, C. J., Hammerman, P. S. and Thompson, C. B. (2005) 'Fuel feeds function: Energy metabolism and the T-cell response', *Nature Reviews Immunology*. Nature Publishing Group, pp. 844–852. doi: 10.1038/nri1710.

Francis, J. N., Till, S. J. and Durham, S. R. (2003) 'Induction of IL-10+CD4+CD25+T cells by grass pollen immunotherapy', *Journal of Allergy and Clinical Immunology*. Mosby Inc., 111(6), pp. 1255–1261. doi: 10.1067/mai.2003.1570.

Fraser, H. M. and Lunn, S. F. (2000) 'Angiogenesis and its control in the female reproductive system', *British Medical Bulletin*, 56(3), pp. 787–797. doi: 10.1258/0007142001903364.

Fraser, J. R., Laurent, T. C. and Laurent, U. B. (1997) 'Hyaluronan: its nature, distribution, functions and turnover.', *Journal of internal medicine*, 242(1), pp. 27–33. Available at: http://www.ncbi.nlm.nih.gov/pubmed/9260563 (Accessed: 25 April 2019).

Freytag, S. *et al.* (2018) 'Comparison of clustering tools in R for medium-sized 10x Genomics single-cell RNA-sequencing data', *F1000Research*. NLM (Medline), 7, p. 1297. doi: 10.12688/f1000research.15809.2.

Fritz, J. M. *et al.* (2014) 'Depletion of tumor-associated macrophages slows the growth of chemically induced mouse lung adenocarcinomas', *Frontiers in Immunology*. Frontiers Media S.A., 5(NOV), p. 587. doi: 10.3389/fimmu.2014.00587.

Fu, X. T. *et al.* (2015) 'Macrophage-secreted IL-8 induces epithelial-mesenchymal transition in hepatocellular carcinoma cells by activating the JAK2/STAT3/Snail pathway', *International Journal of Oncology*. Spandidos Publications, 46(2), pp. 587–596. doi: 10.3892/ijo.2014.2761.

Fung, A. S. *et al.* (2015) 'The effect of chemotherapeutic agents on tumor vasculature in subcutaneous and orthotopic human tumor xenografts', *BMC Cancer*. BioMed Central Ltd., 15(1), pp. 1–10. doi: 10.1186/S12885-015-1091-6/FIGURES/5.

Gabrilovich, D. I. (2017) 'Myeloid-Derived Suppressor Cells', *Cancer Immunology Research*. American Association for Cancer Research, 5(1), pp. 3–8. doi: 10.1158/2326-6066.CIR-16-0297.

Galy, A. H., Spits, H. and Hamilton, J. A. (1993) 'Regulation of M-CSF production by cultured human thymic epithelial cells.', *Lymphokine and cytokine research*, 12(5), pp. 265–70. Available at: http://www.ncbi.nlm.nih.gov/pubmed/8260534 (Accessed: 1 April 2020).

Gao, F. *et al.* (2019) 'Local T regulatory cells depletion by an integrated nanodrug system for efficient chem-immunotherapy of tumor', *Science China Chemistry*. Science in China Press, 62(9), pp. 1230–1244. doi: 10.1007/s11426-019-9507-x.

Gao, J. J. and Swain, S. M. (2018) 'Luminal A Breast Cancer and Molecular Assays: A Review', *The Oncologist*. Alphamed Press, 23(5), pp. 556–565. doi: 10.1634/theoncologist.2017-0535.

Gatenby, R. A. and Gillies, R. J. (2004) 'Why do cancers have high aerobic glycolysis?', *Nature Reviews Cancer*. Nature Publishing Group, 4(11), pp. 891–899. doi: 10.1038/nrc1478.

Geiger, R. *et al.* (2016) 'L-Arginine Modulates T Cell Metabolism and Enhances Survival and Anti-tumor Activity', *Cell*. Cell Press, 167(3), pp. 829-842.e13. doi: 10.1016/j.cell.2016.09.031.

Geissmann, F. *et al.* (2010) 'Development of monocytes, macrophages, and dendritic cells.', *Science (New York, N.Y.)*. American Association for the Advancement of Science, 327(5966), pp. 656–61. doi: 10.1126/science.1178331.

Geissmann, F., Jung, S. and Littman, D. R. (2003) 'Blood monocytes consist of two principal subsets with distinct migratory properties', *Immunity*. Cell Press, 19(1), pp. 71–82. doi: 10.1016/S1074-7613(03)00174-2/ATTACHMENT/2F665FE9-3116-429E-9AB0-E24CFCFC4415/MMC3.JPG.

Geller, D. A. and Billiar, T. R. (1998) 'Molecular biology of nitric oxide synthases', *Cancer and Metastasis Reviews*. Springer, pp. 7–23. doi: 10.1023/A:1005940202801.

Gil, J. *et al.* (2011) 'A leaky mutation in CD3D differentially affects αβ and γδ T cells and leads to a Tαβ–Tγδ+B+NK+ human SCID', *The Journal of Clinical Investigation*. American Society for Clinical Investigation, 121(10), pp. 3872–3876. doi: 10.1172/JCI44254.

Girardi, M. *et al.* (2003) 'The Distinct Contributions of Murine T Cell Receptor (TCR)γδ $^{+}$ and TCRαβ $^{+}$ T Cells to Different Stages of Chemically Induced Skin Cancer', *The Journal of Experimental Medicine*, 198(5), pp. 747–755. doi: 10.1084/jem.20021282.

Giraudo, E., Inoue, M. and Hanahan, D. (2004) 'An amino-bisphosphonate targets MMP-9-expressing macrophages and angiogenesis to impair cervical carcinogenesis.', *The Journal of clinical investigation*. American Society for Clinical Investigation, 114(5), pp. 623–33. doi: 10.1172/JCI22087.

Goldstein, L. D. *et al.* (2017) 'Massively parallel nanowell-based single-cell gene expression profiling', *BMC Genomics*. BioMed Central Ltd., 18(1). doi: 10.1186/S12864-017-3893-1.

Gong, H., Do, D. and Ramakrishnan, R. (2018) 'Single-Cell mRNA-Seq Using the Fluidigm C1 System and Integrated Fluidics Circuits', *Methods in molecular biology (Clifton, N.J.)*. Methods Mol Biol, 1783, pp. 193–207. doi: 10.1007/978-1-4939-7834-2_10.

Goodyear, A. W. *et al.* (2014) 'Optimization of murine small intestine leukocyte isolation for global immune phenotype analysis', *Journal of Immunological Methods*. doi: 10.1016/j.jim.2014.01.014.

Gordon, S. (2007) 'The macrophage: Past, present and future', *European Journal of Immunology*, 37(S1), pp. S9–S17. doi: 10.1002/eji.200737638.

Goswami, S. *et al.* (2005) 'Macrophages Promote the Invasion of Breast Carcinoma Cells via a Colony-Stimulating Factor-1/Epidermal Growth Factor Paracrine Loop', *Cancer Research*, 65(12), pp. 5278–5283. doi: 10.1158/0008-5472.CAN-04-1853.

Goudin, N. *et al.* (2016) 'Depletion of Regulatory T Cells Induces High Numbers of Dendritic Cells and Unmasks a Subset of Anti-Tumour CD8+CD11c+ PD-1lo Effector T Cells.', *PloS one*. Public Library of Science, 11(6), p. e0157822. doi: 10.1371/journal.pone.0157822.

Goulielmaki, E. *et al.* (2018) 'Pharmacological inactivation of the PI3K p110δ prevents breast tumour progression by targeting cancer cells and macrophages', *Cell Death & Disease*. Nature Publishing Group, 9(6), p. 678. doi: 10.1038/s41419-018-0717-4.

Govinden, R. and Bhoola, K. D. (2003) 'Genealogy, expression, and cellular function of transforming growth factor-β', *Pharmacology and Therapeutics*. Elsevier Inc., pp. 257–265. doi: 10.1016/S0163-7258(03)00035-4.

Griesmann, H. *et al.* (2017) 'Pharmacological macrophage inhibition decreases metastasis formation in a genetic model of pancreatic cancer', *Gut*. BMJ Publishing Group, 66(7), pp. 1278–1285. doi: 10.1136/gutjnl-2015-310049.

Grossman, W. J., Verbsky, J. W., Tollefsen, B. L., *et al.* (2004) 'Differential expression of granzymes A and B in human cytotoxic lymphocyte subsets and T regulatory cells', *Blood*. American Society of Hematology, 104(9), pp. 2840–2848. doi: 10.1182/blood-2004-03-0859.

Grossman, W. J., Verbsky, J. W., Barchet, W., *et al.* (2004) 'Human T Regulatory Cells Can Use the Perforin Pathway to Cause Autologous Target Cell Death', *Immunity*. Cell Press, 21(4), pp. 589–601. doi: 10.1016/j.immuni.2004.09.002.

Groux, H. *et al.* (1997) 'A CD4+ T-cell subset inhibits antigen-specific T-cell responses and prevents colitis', *Nature*. Nature, 389(6652), pp. 737–742. doi: 10.1038/39614.

Guilliams, M. *et al.* (2013) 'Alveolar macrophages develop from fetal monocytes that differentiate into long-lived cells in the first week of life via GM-CSF', *Journal of Experimental Medicine*. J Exp Med, 210(10), pp. 1977–1992. doi: 10.1084/jem.20131199.

Guth, A. M. *et al.* (2013) 'Liposomal clodronate treatment for tumour macrophage depletion in dogs with soft-tissue sarcoma', *Veterinary and Comparative Oncology*. NIH Public Access, 11(4), pp. 296–305. doi: 10.1111/j.1476-5829.2012.00319.x.

Gwak, J. M. *et al.* (2015) 'Prognostic value of tumor-associated macrophages according to histologic locations and hormone receptor status in breast cancer', *PLoS ONE*. Public Library of Science, 10(4), p. e0125728. doi: 10.1371/journal.pone.0125728.

Gyori, D. *et al.* (2018) 'Compensation between CSF1R+ macrophages and Foxp3+ Treg cells drives resistance to tumor immunotherapy', *JCI insight*. NLM (Medline), 3(11). doi: 10.1172/jci.insight.120631.

Haghverdi, L. *et al.* (2016) 'Diffusion pseudotime robustly reconstructs lineage branching', *Nature Methods*. Nature Publishing Group, 13(10), pp. 845–848. doi: 10.1038/nmeth.3971.

Hamilton, G. *et al.* (2016) 'Small cell lung cancer: Recruitment of macrophages by circulating tumor cells', *OncoImmunology*. Taylor and Francis Inc., 5(3). doi: 10.1080/2162402X.2015.1093277.

Han, J. M., Patterson, S. J. and Levings, M. K. (2012) 'The Role of the PI3K Signaling Pathway in CD4+ T Cell Differentiation and Function', *Frontiers in Immunology*. Frontiers Media SA, 3. doi: 10.3389/fimmu.2012.00245.

Hanahan, D. and Weinberg, R. A. (2011) 'Hallmarks of Cancer: The Next Generation', *Cell*, 144(5), pp. 646–674. doi: 10.1016/j.cell.2011.02.013.

Hanna, R. N. *et al.* (2011) 'The transcription factor NR4A1 (Nur77) controls bone marrow differentiation and survival of Ly6C− monocytes', *Nature Immunology*. NIH Public Access, 12(8), p. 778. doi: 10.1038/NI.2063.

Hascitha, J. *et al.* (2016) 'Analysis of Kynurenine/Tryptophan ratio and expression of IDO1 and 2 mRNA in tumour tissue of cervical cancer patients', *Clinical Biochemistry*. Elsevier Inc., 49(12), pp. 919–924. doi: 10.1016/j.clinbiochem.2016.04.008.

Haziot, A., Tsuberi, B. Z. and Goyert, S. M. (1993) 'Neutrophil CD14: biochemical properties and role in the secretion of tumor necrosis factor-alpha in response to lipopolysaccharide.', *The Journal of Immunology*, 150(12).

Heinlein, C. *et al.* (2010) 'A rapid and optimization-free procedure allows the in vivo detection of subtle cell cycle and ploidy alterations in tissues by flow cytometry', *Cell Cycle*. Taylor & Francis, 9(17), p. 3584. doi: 10.4161/CC.9.17.12831.

Helm, O. *et al.* (2014) 'Tumor-associated macrophages exhibit pro- and anti-inflammatory properties by which they impact on pancreatic tumorigenesis', *International Journal of Cancer*, 135(4), pp. 843–861. doi: 10.1002/ijc.28736.

Herembert, T. *et al.* (1997) 'Control of vascular smooth-muscle cell growth by macrophage-colony-stimulating factor.', *Biochemical Journal*, 325(1), pp. 123–128.

Hieshima, K. *et al.* (1997) 'A novel human CC chemokine PARC that is most homologous to macrophage-inflammatory protein-1 alpha/LD78 alpha and chemotactic for T lymphocytes, but not for monocytes.', *Journal of immunology (Baltimore, Md. : 1950)*. American Association of

Immunologists, 159(3), pp. 1140–9. Available at: http://www.ncbi.nlm.nih.gov/pubmed/9233607 (Accessed: 23 March 2020).

Hiratsuka, S. *et al.* (2002) 'MMP9 induction by vascular endothelial growth factor receptor-1 is involved in lung-specific metastasis', *Cancer Cell*. Cell Press, 2(4), pp. 289–300. doi: 10.1016/S1535-6108(02)00153-8.

Hiratsuka, S. *et al.* (2006) 'Tumour-mediated upregulation of chemoattractants and recruitment of myeloid cells predetermines lung metastasis', *Nature Cell Biology*. Nature Publishing Group, 8(12), pp. 1369–1375. doi: 10.1038/ncb1507.

Hobeika, A. C. *et al.* (2011) 'Depletion of human regulatory T cells.', *Methods in molecular biology (Clifton, N.J.)*. Humana Press, Totowa, NJ, 707, pp. 219–231. doi: 10.1007/978-1-61737-979-6_14.

Hockel, M. and Vaupel, P. (2001) 'Tumor Hypoxia: Definitions and Current Clinical, Biologic, and Molecular Aspects', *JNCI Journal of the National Cancer Institute*. Narnia, 93(4), pp. 266–276. doi: 10.1093/jnci/93.4.266.

Hoelzinger, D. B. *et al.* (2010) 'Blockade of CCL1 Inhibits T Regulatory Cell Suppressive Function Enhancing Tumor Immunity without Affecting T Effector Responses', *The Journal of Immunology*. The American Association of Immunologists, 184(12), pp. 6833–6842. doi: 10.4049/jimmunol.0904084.

Hollmén, M. *et al.* (2016) 'G-CSF regulates macrophage phenotype and associates with poor overall survival in human triple-negative breast cancer', *OncoImmunology*. Taylor and Francis Inc., 5(3). doi: 10.1080/2162402X.2015.1115177.

Holmgren, L. *et al.* (1999) 'Horizontal Transfer of DNA by the Uptake of Apoptotic Bodies', *Blood*. Content Repository Only!, 93(11), pp. 3956–3963. doi: 10.1182/BLOOD.V93.11.3956.

Hong, S., Dissing-Olesen, L. and Stevens, B. (2016) 'New insights on the role of microglia in synaptic pruning in health and disease.', *Current opinion in neurobiology*. NIH Public Access, 36, pp. 128–34. doi: 10.1016/j.conb.2015.12.004.

Honkanen, T. J. *et al.* (2019) 'Prognostic and predictive role of tumour-associated macrophages in HER2 positive breast cancer', *Scientific Reports*. Nature Publishing Group, 9(1), p. 10961. doi: 10.1038/s41598-019-47375-2.

Huang, C. T. *et al.* (2004) 'Role of LAG-3 in regulatory T cells', *Immunity*. Elsevier, 21(4), pp. 503–513. doi: 10.1016/j.immuni.2004.08.010.

Hughes, E. *et al.* (2020) 'Primary breast tumours but not lung metastases induce protective anti-tumour immune responses after Treg-depletion', *Cancer Immunology, Immunotherapy*. Springer Science and Business Media Deutschland GmbH, 69(10), pp. 2063–2073. doi: 10.1007/s00262-020-02603-x.

Hunter, M. *et al.* (2009) 'Survival of monocytes and macrophages and their role in health and disease', *Frontiers in Bioscience*. NIH Public Access, 14(11), pp. 4079–4102. doi: 10.2741/3514.

Iannello, A. *et al.* (2016) 'Immunosurveillance and immunotherapy of tumors by innate immune cells.', *Current opinion in immunology*. NIH Public Access, 38, pp. 52–8. doi: 10.1016/j.coi.2015.11.001.

Inaba, T. *et al.* (1992) 'Expression of M-CSF receptor encoded by c-fms on smooth muscle cells derived from arteriosclerotic lesion.', *The Journal of biological chemistry*, 267(8), pp. 5693–9. Available at: http://www.ncbi.nlm.nih.gov/pubmed/1531986 (Accessed: 1 April 2020).

Inaba, T. *et al.* (2010) 'Indoleamine 2,3-dioxygenase expression predicts impaired survival of invasive cervical cancer patients treated with radical hysterectomy', *Gynecologic Oncology*. Academic Press, 117(3), pp. 423–428. doi: 10.1016/j.ygyno.2010.02.028.

Jablonski, K. A. *et al.* (2015) 'Novel markers to delineate murine M1 and M2 macrophages', *PLoS ONE*. Public Library of Science, 10(12). doi: 10.1371/journal.pone.0145342.

Jabsom (2010) 'Bioanalyzer Interpretation Bioanalyzer RNA Total Eukaryote 2100 Nano Information gathered from USU and Agilent website 2010'.

Jagannathan-Bogdan, M. and Zon, L. I. (2013) 'Hematopoiesis.', *Development (Cambridge, England)*. Company of Biologists, 140(12), pp. 2463–7. doi: 10.1242/dev.083147.

Jamiyan, T. *et al.* (2020) 'CD68- and CD163-positive tumor-associated macrophages in triple negative cancer of the breast', *Virchows Archiv 2020 477:6*. Springer, 477(6), pp. 767–775. doi: 10.1007/S00428-020-02855-Z.

Jang, J. H. *et al.* (2020) 'Breast Cancer Cell–Derived Soluble CD44 Promotes Tumor Progression by Triggering Macrophage IL1β Production', *Cancer Research*. American Association for Cancer Research, 80(6), pp. 1342–1356. doi: 10.1158/0008-5472.CAN-19-2288.

Jing, Y. *et al.* (2011) 'Epithelial-Mesenchymal Transition in tumor microenvironment', *Cell & Bioscience*. BioMed Central, 1(1), p. 29. doi: 10.1186/2045-3701-1-29.

Jinushi, M. *et al.* (2011) 'Tumor-associated macrophages regulate tumorigenicity and anticancer drug responses of cancer stem/initiating cells', *Proceedings of the National Academy of Sciences of the United States of America*. National Academy of Sciences, 108(30), pp. 12425–12430. doi: 10.1073/pnas.1106645108.

Jones, E. *et al.* (2002) 'Depletion of CD25+ regulatory cells results in suppression of melanomagrowth and induction of autoreactivity in mice', *Cancer Immunity*. Academy of Cancer Immunology, 5, pp. 1–12.

Jordan, M. S. *et al.* (2001) 'Thymic selection of CD4+CD25+ regulatory T cells induced by an agonist self-peptide', *Nature Immunology*. Nature Publishing Group, 2(4), pp. 301–306. doi: 10.1038/86302.

Jungblut, M. *et al.* (2009) 'Standardized Preparation of Single-Cell Suspensions from Mouse Lung Tissue using the gentleMACS Dissociator', *Journal of Visualized Experiments*, (29). doi: 10.3791/1266.

Juntilla, M. M. *et al.* (2007) 'Akt1 and Akt2 are required for αβ thymocyte survival and differentiation', *Proceedings of the National Academy of Sciences of the United States of America*. National Academy of Sciences, 104(29), pp. 12105–12110. doi: 10.1073/pnas.0705285104.

Kalluri, R. (2003) 'Basement membranes: structure, assembly and role in tumour angiogenesis', *Nature Reviews Cancer*. Nature Publishing Group, 3(6), pp. 422–433. doi: 10.1038/nrc1094.

Kandel, J. *et al.* (1991) 'Neovascularization is associated with a switch to the export of bFGF in the multistep development of fibrosarcoma', *Cell*. Cell Press, 66(6), pp. 1095–1104. doi: 10.1016/0092-8674(91)90033-U.

Kaneda, M. M., Cappello, P., *et al.* (2016) 'Macrophage PI3Kγ drives pancreatic ductal adenocarcinoma progression', *Cancer Discovery*. American Association for Cancer Research Inc., 6(8), pp. 870–885. doi: 10.1158/2159-8290.CD-15-1346.

Kaneda, M. M., Messer, K. S., *et al.* (2016) 'PI3Kγ 3 is a molecular switch that controls immune suppression', *Nature*. Nature Publishing Group, 539(7629), pp. 437–442. doi: 10.1038/nature19834.

Kaplan, D. H. *et al.* (1998) 'Demonstration of an interferon gamma-dependent tumor surveillance system in immunocompetent mice.', *Proceedings of the National Academy of Sciences of the United States of America*. National Academy of Sciences, 95(13), pp. 7556–61. Available at: http://www.ncbi.nlm.nih.gov/pubmed/9636188 (Accessed: 26 April 2019).

Kaplan, R. N. *et al.* (2005) 'VEGFR1-positive haematopoietic bone marrow progenitors initiate the pre-metastatic niche', *Nature*. Nature Publishing Group, 438(7069), pp. 820–827. doi: 10.1038/nature04186.

Kawamura, S. and Ohteki, T. (2018) 'Monopoiesis in humans and mice', *International Immunology*. Oxford University Press, pp. 503–509. doi: 10.1093/intimm/dxy063.

Kawata, M. *et al.* (2012) 'TGF-β-induced epithelial-mesenchymal transition of A549 lung adenocarcinoma cells is enhanced by pro-inflammatory cytokines derived from RAW 264.7 macrophage cells', *The Journal of Biochemistry*, 151(2), pp. 205–216. doi: 10.1093/jb/mvr136.

Kelly, P. M. *et al.* (1988) 'Macrophages in human breast disease: a quantitative immunohistochemical study.', *British journal of cancer*, 57(2), pp. 174–7. Available at: http://www.ncbi.nlm.nih.gov/pubmed/2833921 (Accessed: 12 April 2018).

Khan, G. N. *et al.* (2017) 'Heterogeneous Cell Types in Single-cell-derived Clones of MCF7 and MDA-MB-231 Cells | Enhanced Reader', *Anticancer Research*, 37(2343–2354).

Kheir, W. A. *et al.* (2005) 'A WAVE2-Abi1 complex mediates CSF-1-induced F-actin-rich membrane protrusions and migration in macrophages', *Journal of Cell Science*. The Company of Biologists Ltd, 118(22), pp. 5369–5379. doi: 10.1242/jcs.02638.

Kim, J. *et al.* (2009) ' Cutting Edge: Depletion of Foxp3 + Cells Leads to Induction of Autoimmunity by Specific Ablation of Regulatory T Cells in Genetically Targeted Mice ', *The Journal of Immunology*. The American Association of Immunologists, 183(12), pp. 7631–7634. doi: 10.4049/jimmunol.0804308.

Kim, J. M., Rasmussen, J. P. and Rudensky, A. Y. (2007) 'Regulatory T cells prevent catastrophic autoimmunity throughout the lifespan of mice', *Nature Immunology*. Nat Immunol, 8(2), pp. 191–197. doi: 10.1038/ni1428.

Kim, N. *et al.* (2007) 'The p110delta catalytic isoform of PI3K is a key player in NK-cell development and cytokine secretion', *Blood*. American Society of Hematology, 110(9), pp. 3202–3208. doi: 10.1182/BLOOD-2007-02-075366.

Kim, Y.-B. *et al.* (2017) 'Interaction of macrophages with apoptotic cells inhibits transdifferentiation and invasion of lung fibroblasts.', *Oncotarget*. Impact Journals, LLC, 8(68), pp. 112297–112312. doi: 10.18632/oncotarget.22737.

Kitamura, T. *et al.* (2015) 'CCL2-induced chemokine cascade promotes breast cancer metastasis by enhancing retention of metastasis-associated macrophages', *Journal of Experimental Medicine*. The Rockefeller University Press, 212(7), pp. 1043–1059. doi: 10.1084/JEM.20141836.

Klages, K. *et al.* (2010) 'Selective depletion of Foxp3+ regulatory T cells improves effective therapeutic vaccination against established melanoma', *Cancer Research*. American Association for Cancer Research, 70(20), pp. 7788–7799. doi: 10.1158/0008-5472.CAN-10-1736.

Klimp, A. H. *et al.* (2001) 'Expression of cyclooxygenase-2 and inducible nitric oxide synthase in human ovarian tumors and tumor-associated macrophages.', *Cancer research*, 61(19), pp. 7305–9. Available at: http://www.ncbi.nlm.nih.gov/pubmed/11585770 (Accessed: 26 September 2019).

Kok, K., Geering, B. and Vanhaesebroeck, B. (2009) 'Regulation of phosphoinositide 3-kinase expression in health and disease', *Trends in Biochemical Sciences*. Elsevier Ltd, pp. 115–127. doi: 10.1016/j.tibs.2009.01.003.

Kowanetz, M. *et al.* (2010) 'Granulocyte-colony stimulating factor promotes lung metastasis through mobilization of Ly6G+Ly6C+ granulocytes.', *Proceedings of the National Academy of Sciences of the United States of America*. National Academy of Sciences, 107(50), pp. 21248–55. doi: 10.1073/pnas.1015855107.

Kryczek, I. *et al.* (2006) 'B7-H4 expression identifies a novel suppressive macrophage population in human ovarian carcinoma', *Journal of Experimental Medicine*. The Rockefeller University Press, 203(4), pp. 871–881. doi: 10.1084/jem.20050930.

Kuehnemuth, B. *et al.* (2018) 'CCL1 is a major regulatory T cell attracting factor in human breast cancer', *BMC Cancer*. BioMed Central Ltd., 18(1). doi: 10.1186/s12885-018-5117-8.

Kuhn, S., Yang, J. and Ronchese, F. (2015) 'Monocyte-derived dendritic cells are essential for CD8+ T

cell activation and antitumor responses after local immunotherapy', *Frontiers in Immunology*. Frontiers Research Foundation, 6(NOV), p. 584. doi: 10.3389/fimmu.2015.00584.

Kumar, V. *et al.* (2017) 'Cancer-Associated Fibroblasts Neutralize the Anti-tumor Effect of CSF1 Receptor Blockade by Inducing PMN-MDSC Infiltration of Tumors.', *Cancer cell*. NIH Public Access, 32(5), pp. 654-668.e5. doi: 10.1016/j.ccell.2017.10.005.

Kuo, D. Y. S. *et al.* (2010) 'Paclitaxel plus oxaliplatin for recurrent or metastatic cervical cancer: A New York Cancer Consortium Study', *Gynecologic Oncology*. Academic Press, 116(3), pp. 442–446. doi: 10.1016/j.ygyno.2009.10.082.

Kusmartsev, S. and Gabrilovich, D. I. (2002) 'Immature myeloid cells and cancer-associated immune suppression', *Cancer Immunology, Immunotherapy*, 51(6), pp. 293–298. doi: 10.1007/S00262-002-0280-8.

Lahl, K. *et al.* (2007) 'Selective depletion of Foxp3+ regulatory T cells induces a scurfy-like disease', *Journal of Experimental Medicine*. The Rockefeller University Press, 204(1), pp. 57–63. doi: 10.1084/jem.20061852.

Lahl, K. and Sparwasser, T. (2011) 'In vivo depletion of FoxP3+ Tregs using the DEREG mouse model.', *Methods in molecular biology (Clifton, N.J.)*. Humana Press, Totowa, NJ, 707, pp. 157–172. doi: 10.1007/978-1-61737-979-6_10.

Laimer, K. *et al.* (2011) 'Expression and prognostic impact of indoleamine 2,3-dioxygenase in oral squamous cell carcinomas', *Oral Oncology*. Pergamon, 47(5), pp. 352–357. doi: 10.1016/j.oraloncology.2011.03.007.

Lança, T. and Silva-Santos, B. (2012) 'The split nature of tumor-infiltrating leukocytes: Implications for cancer surveillance and immunotherapy', *OncoImmunology*. Taylor & Francis, pp. 717–725. doi: 10.4161/onci.20068.

Laoui, D. *et al.* (2014) 'Tumor Hypoxia Does Not Drive Differentiation of Tumor-Associated Macrophages but Rather Fine-Tunes the M2-like Macrophage Population', *Cancer Research*, 74(1), pp. 24–30. doi: 10.1158/0008-5472.CAN-13-1196.

Läubli, H. *et al.* (2014) 'Engagement of myelomonocytic Siglecs by tumor-associated ligands modulates the innate immune response to cancer', *Proceedings of the National Academy of Sciences of the United States of America*. National Academy of Sciences, 111(39), pp. 14211–14216. doi: 10.1073/pnas.1409580111.

Lauder, S. N. *et al.* (2020) 'Enhanced antitumor immunity through sequential targeting of PI3Kδand LAG3', *Journal for ImmunoTherapy of Cancer*. BMJ Publishing Group, 8(2). doi: 10.1136/jitc-2020-000693.

Lee, J. H., Wang, C. and Kim, C. H. (2009) ' FoxP3 + Regulatory T Cells Restrain Splenic Extramedullary Myelopoiesis via Suppression of Hemopoietic Cytokine-Producing T Cells ', *The Journal of Immunology*. The American Association of Immunologists, 183(10), pp. 6377–6386. doi: 10.4049/jimmunol.0901268.

Leek, R. D. *et al.* (1996a) 'Association of macrophage infiltration with angiogenesis and prognosis in invasive breast carcinoma.', *Cancer research*. American Association for Cancer Research, 56(20), pp. 4625–9. Available at: http://www.ncbi.nlm.nih.gov/pubmed/8840975 (Accessed: 26 March 2019).

Leek, R. D. *et al.* (1996b) 'Association of macrophage infiltration with angiogenesis and prognosis in invasive breast carcinoma.', *Cancer research*. American Association for Cancer Research, 56(20), pp. 4625–9. Available at: http://www.ncbi.nlm.nih.gov/pubmed/8840975 (Accessed: 23 July 2019).

Leelatian, N. *et al.* (2017) 'Preparing Viable Single Cells from Human Tissue and Tumors for Cytomic Analysis Current Protocols in Molecular Biology UNIT 25C.1', *Current protocols in molecular biology*. NIH Public Access, 118, p. 25C.1.1. doi: 10.1002/CPMB.37.

Lehenkari, P. P. *et al.* (2002) 'Further insight into mechanism of action of clodronate: Inhibition of mitochondrial ADP/ATP translocase by a nonhydrolyzable, adenine-containing metabolite', *Molecular Pharmacology*, 61(5), pp. 1255–1262. doi: 10.1124/mol.61.5.1255.

Lelekakis, M. *et al.* (1999) 'A novel orthotopic model of breast cancer metastasis to bone', *Clinical and Experimental Metastasis*. Clin Exp Metastasis, 17(2), pp. 163–170. doi: 10.1023/A:1006689719505.

Lennon, F. E. and Singleton, P. A. (2011) 'Role of hyaluronan and hyaluronan-binding proteins in lung pathobiology', *American Journal of Physiology-Lung Cellular and Molecular Physiology*. American Physiological Society Bethesda, MD, 301(2), pp. L137–L147. doi: 10.1152/ajplung.00071.2010.

Van Lent, P. L. E. M. *et al.* (1993) 'In vivo role of phagocytic synovial lining cells in onset of experimental arthritis', *American Journal of Pathology*. American Society for Investigative Pathology, 143(4), pp. 1226–1237.

Li, J., Zhang, Y.-P. and Kirsner, R. S. (2003) 'Angiogenesis in wound repair: Angiogenic growth factors and the extracellular matrix', *Microscopy Research and Technique*, 60(1), pp. 107–114. doi: 10.1002/jemt.10249.

Li, M. *et al.* (2013) 'A role for CCL2 in both tumor progression and immunosurveillance', *OncoImmunology*. Taylor & Francis, 2(7). doi: 10.4161/onci.25474.

Li, X. J. *et al.* (2012) 'As an independent unfavorable prognostic factor, IL-8 promotes metastasis of nasopharyngeal carcinoma through induction of epithelial-mesenchymal transition and activation of AKT signaling', *Carcinogenesis*. Oxford Academic, 33(7), pp. 1302–1309. doi: 10.1093/carcin/bgs181.

Li, X. X. *et al.* (2020) 'The "C3aR Antagonist" SB290157 is a Partial C5aR2 Agonist', *Frontiers in Pharmacology*. Frontiers Media SA, 11. doi: 10.3389/FPHAR.2020.591398.

Li, Y. *et al.* (2015) 'Osteopontin-expressing macrophages in non-small cell lung cancer predict survival', *Annals of Thoracic Surgery*. Elsevier USA, 99(4), pp. 1140–1148. doi: 10.1016/j.athoracsur.2014.11.054.

Lidor, Y. J. *et al.* (1993) 'Constitutive production of macrophage colony-stimulating factor and interleukin-6 by human ovarian surface epithelial Cells', *Experimental Cell Research*, 207(2), pp. 332–339. doi: 10.1006/excr.1993.1200.

Lieschke, G. J. *et al.* (1994) 'Mice lacking both macrophage- and granulocyte-macrophage colony-stimulating factor have macrophages and coexistent osteopetrosis and severe lung disease', *Blood*. American Society of Hematology, 84(1), pp. 27–35. doi: 10.1182/blood.v84.1.27.27.

Lin, C.-Y. *et al.* (2006) 'Macrophage activation increases the invasive properties of hepatoma cells by destabilization of the adherens junction', *FEBS Letters*. No longer published by Elsevier, 580(13), pp. 3042–3050. doi: 10.1016/J.FEBSLET.2006.04.049.

Lin, E. Y. *et al.* (2001) 'Colony-stimulating factor 1 promotes progression of mammary tumors to malignancy.', *The Journal of experimental medicine*. The Rockefeller University Press, 193(6), pp. 727–40. Available at: http://www.ncbi.nlm.nih.gov/pubmed/11257139 (Accessed: 26 March 2019).

Lin, E. Y. *et al.* (2006) 'Macrophages Regulate the Angiogenic Switch in a Mouse Model of Breast Cancer', *Cancer Res.* American Association for Cancer Research, 66(23), pp. 11238–11246. doi: 10.1158/0008-5472.can-06-1278.

Lin, E. Y. *et al.* (2007) 'Vascular endothelial growth factor restores delayed tumor progression in tumors depleted of macrophages', *Molecular Oncology*. John Wiley & Sons, Ltd, 1(3), pp. 288–302. doi: 10.1016/j.molonc.2007.10.003.

Lin, H. *et al.* (2008) 'Discovery of a cytokine and its receptor by functional screening of the extracellular proteome', *Science (New York, N.Y.)*. Science, 320(5877), pp. 807–811. doi: 10.1126/SCIENCE.1154370.

Lin, N. U. *et al.* (2012) 'Clinicopathologic features, patterns of recurrence, and survival among women with triple-negative breast cancer in the National Comprehensive Cancer Network', *Cancer*. John Wiley & Sons, Ltd, 118(22), pp. 5463–5472. doi: 10.1002/cncr.27581.

Linde, N. *et al.* (2018) 'Macrophages orchestrate breast cancer early dissemination and metastasis', *Nature Communications 2017 9:1*. Nature Publishing Group, 9(1), pp. 1–14. doi: 10.1038/s41467-017-02481-5.

Liu, C.-Y. *et al.* (2013) 'M2-polarized tumor-associated macrophages promoted epithelial–mesenchymal transition in pancreatic cancer cells, partially through TLR4/IL-10 signaling pathway', *Laboratory Investigation*. Nature Publishing Group, 93(7), pp. 844–854. doi: 10.1038/labinvest.2013.69.

Liu, J. *et al.* (2011) 'Tumor-associated macrophages recruit CCR6+ regulatory T cells and promote the development of colorectal cancer via enhancing CCL20 production in mice', *PLoS ONE*. Public Library of Science, 6(4). doi: 10.1371/journal.pone.0019495.

Liu, M. *et al.* (2015) 'Macrophages support splenic erythropoiesis in 4T1 tumor-bearing mice', *PLoS ONE*. Public Library of Science, 10(3). doi: 10.1371/journal.pone.0121921.

Liu, X. *et al.* (2015) 'B cells expressing CD11b effectively inhibit CD4+ T-cell responses and ameliorate experimental autoimmune hepatitis in mice', *Hepatology*, 62(5), pp. 1563–1575. doi: 10.1002/hep.28001.

Liu, Y. and Zeng, G. (2012) 'Cancer and innate immune system interactions: translational potentials for cancer immunotherapy.', *Journal of immunotherapy (Hagerstown, Md. : 1997)*. NIH Public Access, 35(4), pp. 299–308. doi: 10.1097/CJI.0b013e3182518e83.

Liu, Z. *et al.* (2009) 'Tumor Regulatory T Cells Potently Abrogate Antitumor Immunity', *Journal of immunology (Baltimore, Md. : 1950)*. NIH Public Access, 182(10), p. 6160. doi: 10.4049/JIMMUNOL.0802664.

Loyher, P.-L. *et al.* (2018) 'Macrophages of distinct origins contribute to tumor development in the lung.', *The Journal of experimental medicine*. Rockefeller University Press, 215(10), pp. 2536–2553. doi: 10.1084/jem.20180534.

Lu, X. *et al.* (2019) 'Macrophage colony-stimulating factor mediates the recruitment of macrophages in triple negative breast cancer', *International Journal of Biological Sciences*. Ivyspring International Publisher, 15(13), pp. 2859–2871. doi: 10.7150/ijbs.39063.

Lund, J. M. *et al.* (2008) 'Coordination of early protective immunity to viral infection by regulatory T cells', *Science*. Howard Hughes Medical Institute, 320(5880), pp. 1220–1224. doi: 10.1126/science.1155209.

Lundgren, K., Nordenskjöld, B. and Landberg, G. (2009) 'Hypoxia, Snail and incomplete epithelial–mesenchymal transition in breast cancer', *British Journal of Cancer*, 101(10), pp. 1769–1781. doi: 10.1038/sj.bjc.6605369.

Luo, Y. *et al.* (2006) 'Targeting tumor-associated macrophages as a novel strategy against breast cancer', *The Journal of Clinical Investigation*. American Society for Clinical Investigation, 116(8), pp. 2132–2141. doi: 10.1172/JCI27648.

Maaten, L. van der and Hinton, G. (2008) 'Visualizing Data using t-SNE', *Journal of Machine Learning Research*, 9(Nov), pp. 2579–2605. Available at: http://www.jmlr.org/papers/v9/vandermaaten08a.html (Accessed: 15 April 2019).

Mackaness, G. B. (1962) 'Cellular resistance to infection.', *The Journal of experimental medicine*. The Rockefeller University Press, 116(3), pp. 381–406. Available at: http://www.ncbi.nlm.nih.gov/pubmed/14467923 (Accessed: 12 April 2018).

Magnani, C. F. *et al.* (2011) 'Killing of myeloid APCs via HLA class I, CD2 and CD226 defines a novel

mechanism of suppression by human Tr1 cells', *European Journal of Immunology*, 41(6), pp. 1652–1662. Available at: https://onlinelibrary.wiley.com/doi/full/10.1002/eji.201041120.

Mahajan, D. *et al.* (2006) 'CD4+CD25+ regulatory T cells protect against injury in an innate murine model of chronic kidney disease', *Journal of the American Society of Nephrology*. American Society of Nephrology, 17(10), pp. 2731–2741. doi: 10.1681/ASN.2005080842.

Mahmoud, S. M. A. *et al.* (2012) 'Tumour-infiltrating macrophages and clinical outcome in breast cancer', *Journal of Clinical Pathology*. BMJ Publishing Group, 65(2), pp. 159–163. doi: 10.1136/JCLINPATH-2011-200355.

Mahnke, K. *et al.* (1997) 'CD14 is Expressed by Subsets of Murine Dendritic Cells and Upregulated by Lipopolysaccharide', *Advances in Experimental Medicine and Biology*. Springer, Boston, MA, 417, pp. 145–159. doi: 10.1007/978-1-4757-9966-8_25.

Makarenkova, V. P. *et al.* (2006) 'CD11b+/Gr-1+ Myeloid Suppressor Cells Cause T Cell Dysfunction after Traumatic Stress', *The Journal of Immunology*. American Association of Immunologists, 176(4), pp. 2085–2094. doi: 10.4049/JIMMUNOL.176.4.2085.

Maloy, K. J. *et al.* (2003) 'CD4+CD25+ TR cells suppress innate immune pathology through cytokine-dependent mechanisms', *Journal of Experimental Medicine*. The Rockefeller University Press, 197(1), pp. 111–119. doi: 10.1084/jem.20021345.

Mangogna, A. *et al.* (2019) 'Is the Complement Protein C1q a Pro- or Anti-tumorigenic Factor? Bioinformatics analysis involving human carcinomas', *Frontiers in Immunology*. Frontiers Media S.A., 10(MAY), p. 865. doi: 10.3389/fimmu.2019.00865.

Marconi, C. *et al.* (2008) 'Tumoral and macrophage uPAR and MMP-9 contribute to the invasiveness of B16 murine melanoma cells', *Clinical & Experimental Metastasis*. Springer Netherlands, 25(3), pp. 225–231. doi: 10.1007/s10585-007-9136-0.

Marie, J. C., Liggitt, D. and Rudensky, A. Y. (2006) 'Cellular Mechanisms of Fatal Early-Onset Autoimmunity in Mice with the T Cell-Specific Targeting of Transforming Growth Factor-β Receptor', *Immunity*. Elsevier, 25(3), pp. 441–454. doi: 10.1016/j.immuni.2006.07.012.

Marinov, G. K. *et al.* (2014) 'From single-cell to cell-pool transcriptomes: Stochasticity in gene expression and RNA splicing', *Genome Research*. Cold Spring Harbor Laboratory Press, 24(3), pp. 496–510. doi: 10.1101/gr.161034.113.

Martin, A. L. *et al.* (2008) 'Selective Regulation of CD8 Effector T Cell Migration by the p110γ Isoform of Phosphatidylinositol 3-Kinase', *The Journal of Immunology*. The American Association of Immunologists, 180(4), pp. 2081–2088. doi: 10.4049/jimmunol.180.4.2081.

Martinez, F. O. *et al.* (2006) 'Transcriptional Profiling of the Human Monocyte-to-Macrophage Differentiation and Polarization: New Molecules and Patterns of Gene Expression', *The Journal of Immunology*. The American Association of Immunologists, 177(10), pp. 7303–7311. doi: 10.4049/jimmunol.177.10.7303.

Martinez, F. O. *et al.* (2008) 'Macrophage activation and polarization', *Frontiers in Bioscience*. Front Biosci, pp. 453–461. doi: 10.2741/2692.

Maxwell, P. H. *et al.* (1999) 'The tumour suppressor protein VHL targets hypoxia-inducible factors for oxygen-dependent proteolysis', *Nature*. Nature Publishing Group, 399(6733), pp. 271–275. doi: 10.1038/20459.

Mcinnes, L., Healy, J. and Melville, J. (2020) 'UMAP: Uniform Manifold Approximation and Projection for Dimension Reduction'.

Medrek, C. *et al.* (2012) 'The presence of tumor associated macrophages in tumor stroma as a prognostic marker for breast cancer patients', *BMC Cancer*, 12. doi: 10.1186/1471-2407-12-306.

Mellor, A. L. and Munn, D. H. (2004) 'IDO expression by dendritic cells: Tolerance and tryptophan

catabolism', *Nature Reviews Immunology*. Nature Publishing Group, pp. 762–774. doi: 10.1038/nri1457.

Mersin, H. *et al.* (2008) 'The prognostic importance of triple negative breast carcinoma', *Breast*. Churchill Livingstone, 17(4), pp. 341–346. doi: 10.1016/j.breast.2007.11.031.

Metz, R. *et al.* (2012) 'IDO inhibits a tryptophan sufficiency signal that stimulates mTOR: A novel IDO effector pathway targeted by D-1-methyl-tryptophan', *OncoImmunology*. Taylor & Francis, 1(9), pp. 1460–1468. doi: 10.4161/onci.21716.

Milas, L. *et al.* (1987) 'Macrophage content of murine sarcomas and carcinomas: associations with tumor growth parameters and tumor radiocurability.', *Cancer research*. American Association for Cancer Research, 47(4), pp. 1069–75. Available at: http://www.ncbi.nlm.nih.gov/pubmed/3802091 (Accessed: 25 September 2019).

Mills, C. D. *et al.* (2000) 'M-1/M-2 macrophages and the Th1/Th2 paradigm.', *Journal of immunology (Baltimore, Md. : 1950)*. American Association of Immunologists, 164(12), pp. 6166–73. doi: 10.4049/jimmunol.164.12.6166.

Mitchem, J. B. *et al.* (2013) 'Targeting Tumor-Infiltrating Macrophages Decreases Tumor-Initiating Cells, Relieves Immunosuppression, and Improves Chemotherapeutic Responses', *Cancer Research*. American Association for Cancer Research, 73(3), pp. 1128–1141. doi: 10.1158/0008-5472.CAN-12-2731.

Moran, A. E. *et al.* (2011) 'T cell receptor signal strength in Treg and iNKT cell development demonstrated by a novel fluorescent reporter mouse', *Journal of Experimental Medicine*, 208(6), pp. 1279–1289.

Morishita, A. *et al.* (2018) 'Cell Specific Matrix Metalloproteinase-1 Regulates Lung Metastasis Synergistically with Smoke Exposure', *Journal of cancer research forecast*. NIH Public Access, 1(2). Available at: https://www.ncbi.nlm.nih.gov/pmc/articles/PMC6380525/ (Accessed: 9 October 2019).

Mossadegh-Keller, N. *et al.* (2013) 'M-CSF instructs myeloid lineage fate in single haematopoietic stem cells', *Nature*, 497(7448), pp. 239–243. doi: 10.1038/nature12026.

Mouchemore, K. A. *et al.* (2013) 'Specific inhibition of PI3K p110δ inhibits CSF-1-induced macrophage spreading and invasive capacity.', *The FEBS journal*. NIH Public Access, 280(21), pp. 5228–36. doi: 10.1111/febs.12316.

Movahedi, Kiavash *et al.* (2010) 'Different Tumor Microenvironments Contain Functionally Distinct Subsets of Macrophages Derived from Ly6C(high) Monocytes', *Cancer Research*. American Association for Cancer Research, 70(14), pp. 5728–5739. doi: 10.1158/0008-5472.CAN-09-4672.

Movahedi, K. *et al.* (2010) 'Different Tumor Microenvironments Contain Functionally Distinct Subsets of Macrophages Derived from Ly6C(high) Monocytes', *Cancer Research*. American Association for Cancer Research, 70(14), pp. 5728–5739. doi: 10.1158/0008-5472.CAN-09-4672.

Mucenski, M. L. *et al.* (1991) 'A functional c-myb gene is required for normal murine fetal hepatic hematopoiesis', *Cell*. Cell Press, 65(4), pp. 677–689. doi: 10.1016/0092-8674(91)90099-K.

Müller, A. *et al.* (2001) 'Involvement of chemokine receptors in breast cancer metastasis', *Nature 2001 410:6824*. Nature Publishing Group, 410(6824), pp. 50–56. doi: 10.1038/35065016.

Müller, S. *et al.* (2017) 'Single-cell profiling of human gliomas reveals macrophage ontogeny as a basis for regional differences in macrophage activation in the tumor microenvironment', *Genome Biology*, 18. doi: 10.1186/s13059-017-1362-4.

Mun, S. H., Park, P. S. U. and Park-Min, K. H. (2020) 'The M-CSF receptor in osteoclasts and beyond', *Experimental & Molecular Medicine 2020 52:8*. Nature Publishing Group, 52(8), pp. 1239–1254. doi: 10.1038/s12276-020-0484-z.

Munn, D. H. *et al.* (2005) 'GCN2 kinase in T cells mediates proliferative arrest and anergy induction in

response to indoleamine 2,3-dioxygenase', *Immunity*. Cell Press, 22(5), pp. 633–642. doi: 10.1016/j.immuni.2005.03.013.

Murdoch, C. (2004) 'Mechanisms regulating the recruitment of macrophages into hypoxic areas of tumors and other ischemic tissues', *Blood*, 104(8), pp. 2224–2234. doi: 10.1182/blood-2004-03-1109.

Murray, P. J. *et al.* (2014) 'Macrophage Activation and Polarization: Nomenclature and Experimental Guidelines', *Immunity*. Elsevier, 41(1), pp. 14–20. doi: 10.1016/J.IMMUNI.2014.06.008.

de Nadaï, P. *et al.* (2006) 'Involvement of CCL18 in allergic asthma.', *The Journal of Immunology*. The American Association of Immunologists, 177(3), pp. 2025.1-2025. doi: 10.4049/jimmunol.177.3.2025.

Nadella, V. *et al.* (2015) 'Transglutaminase 2 interacts with syndecan-4 and CD44 at the surface of human macrophages to promote removal of apoptotic cells', *Biochimica et Biophysica Acta - Molecular Cell Research*. Elsevier, 1853(1), pp. 201–212. doi: 10.1016/j.bbamcr.2014.09.020.

Nahrendorf, M. and Swirski, F. K. (2016) 'Abandoning M1/M2 for a Network Model of Macrophage Function', *Circulation research*. NIH Public Access, 119(3), p. 414. doi: 10.1161/CIRCRESAHA.116.309194.

Naito, M. *et al.* (1991) 'Abnormal differentiation of tissue macrophage populations in "osteopetrosis" (op) mice defective in the production of macrophage colony-stimulating factor.', *The American Journal of Pathology*. American Society for Investigative Pathology, 139(3), p. 657. Available at: /pmc/articles/PMC1886220/?report=abstract (Accessed: 22 January 2022).

Nakamichi, Y., Udagawa, N. and Takahashi, N. (2013) 'IL-34 and CSF-1: Similarities and differences', *Journal of Bone and Mineral Metabolism*. Springer Japan, 31(5), pp. 486–495. doi: 10.1007/S00774-013-0476-3/FIGURES/4.

Nakamura, K. *et al.* (2004) ' TGF-β1 Plays an Important Role in the Mechanism of CD4 + CD25 + Regulatory T Cell Activity in Both Humans and Mice ', *The Journal of Immunology*. The American Association of Immunologists, 172(2), pp. 834–842. doi: 10.4049/jimmunol.172.2.834.

Nayak, A. *et al.* (2012) 'Complement and non-complement activating functions of C1q: A prototypical innate immune molecule', *Innate Immunity*, 18(2), pp. 350–363. Available at: https://journals.sagepub.com/doi/full/10.1177/1753425910396252.

Negorev, D. *et al.* (2018) 'Human neutrophils can mimic myeloid-derived suppressor cells (PMN-MDSC) and suppress microbead or lectin-induced T cell proliferation through artefactual mechanisms', *Scientific Reports*, 8(1), p. 3135. doi: 10.1038/s41598-018-21450-6.

Newsholme, P., Gordon, S. and Newsholme, E. A. (1987) 'Rates of utilization and fates of glucose, glutamine, pyruvate, fatty acids and ketone bodies by mouse macrophages', *Biochemical Journal*, 242(3), pp. 631–636. doi: 10.1042/bj2420631.

Nixon, N. A. *et al.* (2018) 'Current landscape of immunotherapy in the treatment of solid tumours, with future opportunities and challenges', *Current Oncology*. Multimed Inc., 25(5), pp. e373–e384. doi: 10.3747/co.25.3840.

Noman, M. Z. *et al.* (2014) 'PD-L1 is a novel direct target of HIF-1α, and its blockade under hypoxia enhanced: MDSC-mediated T cell activation', *Journal of Experimental Medicine*. Rockefeller University Press, 211(5), pp. 781–790. doi: 10.1084/jem.20131916.

Norton, K. A., Popel, A. S. and Pandey, N. B. (2015) 'Heterogeneity of chemokine cell-surface receptor expression in triple-negative breast cancer', *American Journal of Cancer Research*. e-Century Publishing Corporation, 5(4), p. 1295. Available at: /pmc/articles/PMC4473311/ (Accessed: 30 January 2022).

Nouri-Aria, K. T. *et al.* (2004) 'Grass Pollen Immunotherapy Induces Mucosal and Peripheral IL-10

Responses and Blocking IgG Activity', *The Journal of Immunology*. The American Association of Immunologists, 172(5), pp. 3252–3259. doi: 10.4049/jimmunol.172.5.3252.

Odaka, C. *et al.* (2003) 'Murine Macrophages Produce Secretory Leukocyte Protease Inhibitor During Clearance of Apoptotic Cells: Implications for Resolution of the Inflammatory Response', *The Journal of Immunology*. The American Association of Immunologists, 171(3), pp. 1507–1514. doi: 10.4049/jimmunol.171.3.1507.

Oderup, C. *et al.* (2006) 'Cytotoxic T lymphocyte antigen-4-dependent down-modulation of costimulatory molecules on dendritic cells in CD4+ CD25+ regulatory T-cell-mediated suppression', *Immunology*. John Wiley & Sons, Ltd, 118(2), pp. 240–249. doi: 10.1111/j.1365-2567.2006.02362.x.

Okada, H. *et al.* (1998) 'AML1(−/−) embryos do not express certain hematopoiesis-related gene transcripts including those of the PU.1 gene', *Oncogene*, 17(18), pp. 2287–2293. doi: 10.1038/sj.onc.1202151.

Okkenhaug, K. *et al.* (2002) 'Impaired B and T cell antigen receptor signaling in p110δ PI 3-kinase mutant mice', *Science*, 297(5583), pp. 1031–1034. doi: 10.1126/SCIENCE.1073560.

Onda, M., Kobayashi, K. and Pastan, I. (2019) 'Depletion of regulatory T cells in tumors with an anti-CD25 immunotoxin induces CD8 T cell-mediated systemic antitumor immunity', *Proceedings of the National Academy of Sciences of the United States of America*. National Academy of Sciences, 116(10), pp. 4575–4582. doi: 10.1073/pnas.1820388116.

Onodera, T. *et al.* (2015) 'Adipose tissue macrophages induce PPARγ-high FOXP3+ regulatory T cells', *Scientific Reports*. Nature Publishing Group, 5(1), pp. 1–12. doi: 10.1038/srep16801.

Opperman, K. S. *et al.* (2019) 'Clodronate-Liposome Mediated Macrophage Depletion Abrogates Multiple Myeloma Tumor Establishment In Vivo', *Neoplasia (United States)*. Neoplasia Press, Inc., 21(8), pp. 777–787. doi: 10.1016/j.neo.2019.05.006.

Opzoomer, J. W. *et al.* (2021) 'Macrophages orchestrate the expansion of a pro-angiogenic perivascular niche during cancer progression', *bioRxiv*. Cold Spring Harbor Laboratory, p. 2020.10.30.361907. doi: 10.1101/2020.10.30.361907.

Orecchioni, M. *et al.* (2019) 'Macrophage polarization: Different gene signatures in M1(Lps+) vs. Classically and M2(LPS-) vs. Alternatively activated macrophages', *Frontiers in Immunology*. Frontiers Media S.A., p. 1084. doi: 10.3389/fimmu.2019.01084.

Ossovskaya, V. *et al.* (2011) 'Exploring Molecular Pathways of Triple-Negative Breast Cancer', *Genes and Cancer*. Impact Journals, LLC, 2(9), pp. 870–879. doi: 10.1177/1947601911432496.

Ouyang, Q. *et al.* (2016) 'The membrane complement regulatory protein CD59 promotes tumor growth and predicts poor prognosis in breast cancer', *International Journal of Oncology*. Spandidos Publications, 48(5), pp. 2015–2024. doi: 10.3892/IJO.2016.3408.

Van Overmeire, E. *et al.* (2016) 'M-CSF and GM-CSF receptor signaling differentially regulate monocyte maturation and macrophage polarization in the tumor microenvironment', *Cancer Research*. American Association for Cancer Research Inc., 76(1), pp. 35–42. doi: 10.1158/0008-5472.CAN-15-0869.

Paget, S. (1889) 'THE DISTRIBUTION OF SECONDARY GROWTHS IN CANCER OF THE BREAST.', *The Lancet*, 133(3421), pp. 571–573. doi: 10.1016/S0140-6736(00)49915-0.

Palumbo, J. S. and Degen, J. L. (2007) 'Mechanisms linking tumor cell-associated procoagulant function to tumor metastasis', *Thrombosis Research*. Elsevier, 120(SUPPL. 2), pp. S22–S28. doi: 10.1016/S0049-3848(07)70127-5.

Pandiyan, P. *et al.* (2007) 'CD4+CD25+Foxp3+ regulatory T cells induce cytokine deprivation-mediated apoptosis of effector CD4+ T cells', *Nature Immunology*. Nature Publishing Group, 8(12), pp. 1353–1362. doi: 10.1038/ni1536.

Pappenheimer, A. M. *et al.* (1982) 'Diphtheria Toxin and Related Proteins: Effect of Route of Injection on Toxicity and the Determination of Cytotoxicity for Various Cultured Cells | The Journal of Infectious Diseases | Oxford Academic', *The Journal of Infectious Diseases*, 145(1), pp. 94–102. Available at: https://academic.oup.com/jid/article-abstract/145/1/94/944588 (Accessed: 1 April 2020).

Patton, D. T. *et al.* (2006) ' Cutting Edge: The Phosphoinositide 3-Kinase p110δ Is Critical for the Function of CD4 + CD25 + Foxp3 + Regulatory T Cells ', *The Journal of Immunology*. The American Association of Immunologists, 177(10), pp. 6598–6602. doi: 10.4049/jimmunol.177.10.6598.

Pedroza-Gonzalez, A. *et al.* (2015) 'Tumor-infiltrating plasmacytoid dendritic cells promote immunosuppression by Tr1 cells in human liver tumors', *Oncoimmunology*. Taylor & Francis, 4(6). doi: 10.1080/2162402X.2015.1008355.

Pei, B. X. *et al.* (2014) 'Interstitial tumor-associated macrophages combined with tumor-derived colony-stimulating factor-1 and interleukin-6, a novel prognostic biomarker in non-small cell lung cancer', *Journal of Thoracic and Cardiovascular Surgery*. Mosby Inc., 148(4), pp. 1208-1216.e2. doi: 10.1016/j.jtcvs.2014.05.003.

Peng, H. *et al.* (2017) 'Reprogramming Tumor-Associated Macrophages to Reverse EGFRT790M Resistance by Dual-Targeting Codelivery of Gefitinib/Vorinostat', *Nano Letters*. American Chemical Society, 17(12), pp. 7684–7690. doi: 10.1021/acs.nanolett.7b03756.

Perdiguero, E. G. and Geissmann, F. (2015) 'The development and maintenance of resident macrophages', *Nature Immunology*, 17(1), pp. 2–8. doi: 10.1038/ni.3341.

Perrotta, C. *et al.* (2018) 'Nitric oxide generated by tumor-associated macrophages is responsible for cancer resistance to cisplatin and correlated with syntaxin 4 and acid sphingomyelinase inhibition', *Frontiers in Immunology*. Frontiers Media S.A., 9(MAY). doi: 10.3389/fimmu.2018.01186.

Piaggio, F. *et al.* (2016) 'A novel liposomal Clodronate depletes tumor-associated macrophages in primary and metastatic melanoma: Anti-angiogenic and anti-tumor effects', *Journal of Controlled Release*. Elsevier B.V., 223, pp. 165–177. doi: 10.1016/j.jconrel.2015.12.037.

Pierson, W. *et al.* (2013) 'Antiapoptotic Mcl-1 is critical for the survival and niche-filling capacity of Foxp3+ regulatory T cells', *Nature Immunology*. NIH Public Access, 14(9), pp. 959–965. doi: 10.1038/ni.2649.

Pivarcsi, A. *et al.* (2004) 'CC Chemokine Ligand 18, An Atopic Dermatitis-Associated and Dendritic Cell-Derived Chemokine, Is Regulated by Staphylococcal Products and Allergen Exposure', *The Journal of Immunology*. The American Association of Immunologists, 173(9), pp. 5810–5817. doi: 10.4049/jimmunol.173.9.5810.

Pixley, F. J. and Stanley, E. R. (2004) 'CSF-1 regulation of the wandering macrophage: complexity in action.', *Trends in cell biology*. Elsevier, 14(11), pp. 628–38. doi: 10.1016/j.tcb.2004.09.016.

Plitas, G. *et al.* (2016) 'Regulatory T Cells Exhibit Distinct Features in Human Breast Cancer', *Immunity*. Cell Press, 45(5), pp. 1122–1134. doi: 10.1016/j.immuni.2016.10.032.

Plow, E. F. *et al.* (2016) 'Of Kindlins and Cancer', *Discoveries*. Applied Systems, srl, 4(2), p. e59. doi: 10.15190/d.2016.6.

Poczobutt, J. M. *et al.* (2016) 'Expression Profiling of Macrophages Reveals Multiple Populations with Distinct Biological Roles in an Immunocompetent Orthotopic Model of Lung Cancer', *The Journal of Immunology*, 196(6), pp. 2847–2859. doi: 10.4049/jimmunol.1502364.

Polfliet, M. M. J. *et al.* (2001) 'A method for the selective depletion of perivascular and meningeal macrophages in the central nervous system', *Journal of Neuroimmunology*. Elsevier, 116(2), pp. 188–195. doi: 10.1016/S0165-5728(01)00282-X.

Priceman, S. J. *et al.* (2010) 'Targeting distinct tumor-infiltrating myeloid cells by inhibiting CSF-1

receptor: Combating tumor evasion of antiangiogenic therapy', *Blood*. The American Society of Hematology, 115(7), pp. 1461–1471. doi: 10.1182/blood-2009-08-237412.

Priece, L. K. H. *et al.* (1992) 'The predominant form of secreted colony stimulating factor-1 is a proteoglycan. | Enhanced Reader', *The Journal of biological chemistry*, 267(4), pp. 2190–2199.

Qian, B. *et al.* (2009a) 'A distinct macrophage population mediates metastatic breast cancer cell extravasation, establishment and growth', *PLoS ONE*, 4(8). doi: 10.1371/journal.pone.0006562.

Qian, B. *et al.* (2009b) 'A distinct macrophage population mediates metastatic breast cancer cell extravasation, establishment and growth', *PLoS ONE*. Public Library of Science, 4(8). doi: 10.1371/journal.pone.0006562.

Qiu, S.-Q. *et al.* (2018) 'Tumor-associated macrophages in breast cancer: Innocent bystander or important player?', *Cancer Treatment Reviews*. W.B. Saunders, 70, pp. 178–189. doi: 10.1016/J.CTRV.2018.08.010.

Rao, A. *et al.* (2021) 'Exploring tissue architecture using spatial transcriptomics', *Nature*. NIH Public Access, 596(7871), p. 211. doi: 10.1038/S41586-021-03634-9.

Rider, E. D., Ikegami, M. and Jobe, A. H. (1992) 'Localization of alveolar surfactant clearance in rabbit lung cells', *https://doi.org/10.1152/ajplung.1992.263.2.L201*. American Physiological Society Bethesda, MD . doi: 10.1152/AJPLUNG.1992.263.2.L201.

Ridnour, L. A. *et al.* (2008) 'Molecular mechanisms for discrete nitric oxide levels in cancer', *Nitric Oxide - Biology and Chemistry*. Academic Press, pp. 73–76. doi: 10.1016/j.niox.2008.04.006.

Rios, E. J. and Kalesnikoff, J. (2015) 'FcεRI expression and dynamics on mast cells', *Methods in molecular biology (Clifton, N.J.)*. Methods Mol Biol, 1220, pp. 239–255. doi: 10.1007/978-1-4939-1568-2_15.

Rodriguez de la Fuente, L. *et al.* (2021) 'Tumor dissociation of highly viable cell suspensions for single-cell omic analyses in mouse models of breast cancer', *STAR Protocols*. Elsevier BV, 2(4), p. 100841. doi: 10.1016/J.XPRO.2021.100841.

Rodriguez, P. C. *et al.* (2002) 'Regulation of T cell receptor CD3ζ chain expression by L-arginine', *Journal of Biological Chemistry*. American Society for Biochemistry and Molecular Biology, 277(24), pp. 21123–21129. doi: 10.1074/jbc.M110675200.

Rolfe, B. E. *et al.* (2021) 'T Cell Responses + Neutrophil and CD4 to Melanoma Tumorigenesis by Inhibiting The Complement C3a Receptor Contributes'. doi: 10.4049/jimmunol.1600210.

Romero-Moreno, R. *et al.* (2019) 'The CXCL5/CXCR2 axis is sufficient to promote breast cancer colonization during bone metastasis', *Nature Communications 2019 10:1*. Nature Publishing Group, 10(1), pp. 1–14. doi: 10.1038/s41467-019-12108-6.

Van Rooijen, N. *et al.* (1990) 'Depletion and repopulation of macrophages in spleen and liver of rat after intravenous treatment with liposome-encapsulated dichloromethylene diphosphonate', *Cell and Tissue Research*. Springer-Verlag, 260(2), pp. 215–222. doi: 10.1007/BF00318625.

Rooijen, N. Van and Sanders, A. (1994) 'Liposome mediated depletion of macrophages: mechanism of action, preparation of liposomes and applications', *Journal of Immunological Methods*, 174(1–2), pp. 83–93. doi: 10.1016/0022-1759(94)90012-4.

Van Rooijen, N., Sanders, A. and Van Den Berg, T. K. (1996) 'Apoptosis of macrophages induced by liposome-mediated intracellular delivery of clodronate and propamidine', *Journal of Immunological Methods*. Elsevier B.V., 193(1), pp. 93–99. doi: 10.1016/0022-1759(96)00056-7.

Rostam, H. M. *et al.* (2017) 'Image based Machine Learning for identification of macrophage subsets', *Scientific Reports*. Nature Publishing Group, 7(1). doi: 10.1038/s41598-017-03780-z.

Röszer, T. (2018) 'Understanding the Biology of Self-Renewing Macrophages', *Cells*. Multidisciplinary

Digital Publishing Institute (MDPI), 7(8). doi: 10.3390/CELLS7080103.

Roumenina, L. T. *et al.* (2019) 'Tumor Cells Hijack Macrophage-Produced Complement C1q to Promote Tumor Growth', *Cancer Immunology Research2*, 7(7), pp. 1091–1105. Available at: https://doi.org/10.1158/2326-6066.CIR-18-0891.

Roussel, M. F. (1997) 'Regulation of cell cycle entry and G1 progression by CSF-1', *Molecular Reproduction and Development*. John Wiley & Sons, Ltd, 46(1), pp. 11–18. doi: 10.1002/(SICI)1098-2795(199701)46:1<11::AID-MRD3>3.0.CO;2-U.

Ruffell, B. *et al.* (2014) 'Macrophage IL-10 Blocks CD8+ T Cell-Dependent Responses to Chemotherapy by Suppressing IL-12 Expression in Intratumoral Dendritic Cells', *Cancer Cell*. Cell Press, 26(5), pp. 623–637. doi: 10.1016/j.ccell.2014.09.006.

Ryan, G. R. *et al.* (2001) 'Rescue of the colony-stimulating factor 1 (CSF-1)–nullizygous mouse (Csf1 op /Csf1 op) phenotype with a CSF-1 transgene and identification of sites of local CSF-1 synthesis', *Blood*, 98, pp. 74–84. Available at: http://www.bloodjournal.org/content/98/1/74.short?sso-checked=true.

Sadhu, C. *et al.* (2003) 'Essential Role of Phosphoinositide 3-Kinase δ in Neutrophil Directional Movement', *The Journal of Immunology*. American Association of Immunologists, 170(5), pp. 2647–2654. doi: 10.4049/JIMMUNOL.170.5.2647.

Sakaguchi, S. *et al.* (1995) 'Immunologic self-tolerance maintained by activated T cells expressing IL-2 receptor alpha-chains (CD25). Breakdown of a single mechanism of self-tolerance causes various autoimmune diseases.', *Journal of immunology (Baltimore, Md. : 1950)*. American Association of Immunologists, 155(3), pp. 1151–64. Available at: http://www.ncbi.nlm.nih.gov/pubmed/7636184 (Accessed: 2 March 2020).

Sakaguchi, S. *et al.* (2001) 'Immunologic tolerance maintained by CD25+ CD4+ regulatory T cells: their common role in controlling autoimmunity, tumor immunity, and transplantation tolerance', *Immunological Reviews*. John Wiley & Sons, Ltd, 182(1), pp. 18–32. doi: 10.1034/j.1600-065X.2001.1820102.x.

Sami, E. *et al.* (2020) 'The immunosuppressive microenvironment in BRCA1-IRIS-overexpressing TNBC tumors is induced by bidirectional interaction with tumor-associated macrophages', *Cancer Research*. American Association for Cancer Research Inc., 80(5), pp. 1102–1117. doi: 10.1158/0008-5472.CAN-19-2374.

Santoni, M. *et al.* (2018) 'Triple negative breast cancer: Key role of Tumor-Associated Macrophages in regulating the activity of anti-PD-1/PD-L1 agents', *Biochimica et Biophysica Acta - Reviews on Cancer*. Elsevier B.V., pp. 78–84. doi: 10.1016/j.bbcan.2017.10.007.

Sasada, T. *et al.* (2003) 'CD4+CD25+ regulatory T cells in patients with gastrointestinal malignancies: Possible involvement of regulatory T cells in disease progression', *Cancer*, 98(5), pp. 1089–1099. doi: 10.1002/cncr.11618.

Sato, E. *et al.* (2005) 'Intraepithelial CD8+ tumor-infiltrating lymphocytes and a high CD8+/regulatory T cell ratio are associated with favorable prognosis in ovarian cancer', *Proceedings of the National Academy of Sciences of the United States of America*, 102(51), pp. 18538–18543. doi: 10.1073/pnas.0509182102.

Savagner, P. (2015) 'Epithelial–Mesenchymal Transitions: From Cell Plasticity to Concept Elasticity', *Current Topics in Developmental Biology*. Academic Press, 112, pp. 273–300. doi: 10.1016/BS.CTDB.2014.11.021.

Schmidt, A. *et al.* (2016) 'Human macrophages induce CD4 + Foxp3 + regulatory T cells via binding and re-release of TGF-β', *Immunology and Cell Biology*. Nature Publishing Group, 94(8), pp. 747–762. doi: 10.1038/icb.2016.34.

Schulz, D. *et al.* (2019) 'In-Depth Characterization of Monocyte-Derived Macrophages using a Mass

Cytometry-Based Phagocytosis Assay', *Scientific Reports 2019 9:1*. Nature Publishing Group, 9(1), pp. 1–12. doi: 10.1038/s41598-018-38127-9.

Sconocchia, G. *et al.* (2011) 'Tumor infiltration by FcγRIII (CD16)+ myeloid cells is associated with improved survival in patients with colorectal carcinoma.', *International journal of cancer*. NIH Public Access, 128(11), pp. 2663–72. doi: 10.1002/ijc.25609.

Scott, E. *et al.* (1994) 'Requirement of transcription factor PU.1 in the development of multiple hematopoietic lineages', *Science*, 265(5178), pp. 1573–1577. doi: 10.1126/science.8079170.

Scurr, M. *et al.* (2014) 'Highly prevalent colorectal cancer-infiltrating LAP+ Foxp3− T cells exhibit more potent immunosuppressive activity than Foxp3+ regulatory T cells', *Mucosal Immunology*. Nature Publishing Group, 7(2), p. 428. doi: 10.1038/MI.2013.62.

Segal, B. M., Glass, D. D. and Shevach, E. M. (2002) 'Cutting Edge: IL-10-producing CD4+ T cells mediate tumor rejection', *Journal of immunology (Baltimore, Md. : 1950)*. J Immunol, 168(1), pp. 1–4. doi: 10.4049/JIMMUNOL.168.1.1.

Setoguchi, R. *et al.* (2005) 'Homeostatic maintenance of natural Foxp3+ CD25+ CD4+ regulatory T cells by interleukin (IL)-2 and induction of autoimmune disease by IL-2 neutralization', *Journal of Experimental Medicine*. The Rockefeller University Press, 201(5), pp. 723–735. doi: 10.1084/jem.20041982.

Shalek, A. K. *et al.* (2014) 'Single-cell RNA-seq reveals dynamic paracrine control of cellular variation', *Nature*, 510(7505), pp. 363–369. doi: 10.1038/nature13437.

Shankaran, V. *et al.* (2001) 'IFNγ and lymphocytes prevent primary tumour development and shape tumour immunogenicity', *Nature*. Nature Publishing Group, 410(6832), pp. 1107–1111. doi: 10.1038/35074122.

Sharif, O. *et al.* (2019) 'Macrophage rewiring by nutrient associated PI3K dependent pathways', *Frontiers in Immunology*. Frontiers Media S.A. doi: 10.3389/fimmu.2019.02002.

Shaw, T. N. *et al.* (2018) 'Tissue-resident macrophages in the intestine are long lived and defined by Tim-4 and CD4 expression.', *The Journal of experimental medicine*. The Rockefeller University Press, 215(6), pp. 1507–1518. doi: 10.1084/jem.20180019.

Shen, M. *et al.* (2014) 'Tumor-Associated Neutrophils as a New Prognostic Factor in Cancer: A Systematic Review and Meta-Analysis', *PLOS ONE*. Public Library of Science, 9(6), p. e98259. doi: 10.1371/JOURNAL.PONE.0098259.

Shiao, S. L. *et al.* (2015) 'TH2-polarized CD4+ T Cells and macrophages limit efficacy of radiotherapy', *Cancer Immunology Research*. American Association for Cancer Research Inc., 3(5), pp. 518–525. doi: 10.1158/2326-6066.CIR-14-0232.

Shih, F. F. *et al.* (2004) 'Massive Thymic Deletion Results in Systemic Autoimmunity through Elimination of CD4+ CD25+ T Regulatory Cells', *Journal of Experimental Medicine*. The Rockefeller University Press, 199(3), pp. 323–335. doi: 10.1084/jem.20031137.

Shimizu-Hirota, R. *et al.* (2012) 'MT1-MMP regulates the PI3Kδ·Mi-2/NuRD-dependent control of macrophage immune function', *Genes & Development*. Cold Spring Harbor Laboratory Press, 26(4), pp. 395–413. doi: 10.1101/GAD.178749.111.

Shimizu, J., Yamazaki, S. and Sakaguchi, S. (1999) 'Induction of Tumor Immunity by Removing CD25+CD4+ T Cells: A Common Basis Between Tumor Immunity and Autoimmunity', *The Journal of Immunology*, 163(10).

Shree, T. *et al.* (2011) 'Macrophages and cathepsin proteases blunt chemotherapeutic response in breast cancer', *Genes and Development*, 25(23), pp. 2465–2479. doi: 10.1101/gad.180331.111.

Shu, C. *et al.* (2020) 'C3a-C3aR signaling promotes breast cancer lung metastasis via modulating carcinoma associated fibroblasts', *Journal of Experimental & Clinical Cancer Research : CR*. BioMed

Central, 39(1). doi: 10.1186/S13046-019-1515-2.

Shweiki, D. *et al.* (1992) 'Vascular endothelial growth factor induced by hypoxia may mediate hypoxia-initiated angiogenesis', *Nature*. Nature Publishing Group, 359(6398), pp. 843–845. doi: 10.1038/359843a0.

Sica, A. *et al.* (2000) 'Autocrine Production of IL-10 Mediates Defective IL-12 Production and NF-κB Activation in Tumor-Associated Macrophages', *The Journal of Immunology*. The American Association of Immunologists, 164(2), pp. 762–767. doi: 10.4049/jimmunol.164.2.762.

Sica, G. L. *et al.* (2003) 'B7-H4, a Molecule of the B7 Family, Negatively Regulates T Cell Immunity', *Immunity*. Cell Press, 18(6), pp. 849–861. doi: 10.1016/S1074-7613(03)00152-3.

Simon, S. and Labarriere, N. (2017) 'PD-1 expression on tumor-specific T cells: Friend or foe for immunotherapy?', *OncoImmunology*. Taylor and Francis Inc., 7(1). doi: 10.1080/2162402X.2017.1364828.

De Simone, M. *et al.* (2016) 'Transcriptional Landscape of Human Tissue Lymphocytes Unveils Uniqueness of Tumor-Infiltrating T Regulatory Cells', *Immunity*. Cell Press, 45(5), pp. 1135–1147. doi: 10.1016/j.immuni.2016.10.021.

Slyper, M. *et al.* (2020) 'A single-cell and single-nucleus RNA-Seq toolbox for fresh and frozen human tumors', *Nature Medicine 2020 26:5*. Nature Publishing Group, 26(5), pp. 792–802. doi: 10.1038/s41591-020-0844-1.

Smith, A. M. *et al.* (2013) 'M-CSF increases proliferation and phagocytosis while modulating receptor and transcription factor expression in adult human microglia', *Journal of Neuroinflammation*. BioMed Central, 10(1), pp. 1–15. doi: 10.1186/1742-2094-10-85.

Sojka, D. K., Huang, Y. and Fowell, D. J. (2008) 'Mechanisms of regulatory T-cell suppression – a diverse arsenal for a moving target', *Immunology*, 124(1), pp. 12–23. Available at: https://onlinelibrary.wiley.com/doi/abs/10.1111/j.1365-2567.2008.02813.x.

Sossey-Alaoui, K. *et al.* (2017) 'Kindlin-2 regulates the growth of breast cancer tumors by activating CSF-1–mediated macrophage infiltration', *Cancer Research*. American Association for Cancer Research Inc., 77(18), pp. 5129–5141. doi: 10.1158/0008-5472.CAN-16-2337.

Stagg, A. J. *et al.* (2001) 'Isolation of Mouse Spleen Dendritic Cells', *Dendritic Cell Protocols*, 64(5), pp. 9–22. doi: 10.1385/1-59259-150-7:9.

Stamenkovic, I. (2003) 'Extracellular matrix remodelling: the role of matrix metalloproteinases', *The Journal of Pathology*. John Wiley & Sons, Ltd, 200(4), pp. 448–464. doi: 10.1002/path.1400.

Stanley, E. R. *et al.* (1983) 'CSF-1?A mononuclear phagocyte lineage-specific hemopoietic growth factor', *Journal of Cellular Biochemistry*. John Wiley & Sons, Ltd, 21(2), pp. 151–159. doi: 10.1002/jcb.240210206.

Stanley, E. R., Chen, D. M. and Lin, H. S. (1978) 'Induction of macrophage production and proliferation by a purified colony stimulating factor', *Nature*. Nature Publishing Group, pp. 168–170. doi: 10.1038/274168a0.

Stanley, E. R. and Chitu, V. (2014) 'CSF-1 Receptor Signaling in Myeloid Cells', *Perspectives in Biology*, 6.

Starr, T. K., Jameson, S. C. and Hogquist, K. A. (2003) 'Positive and Negative Selection of T Cells', *Annual Review of Immunology*, 21, pp. 139–176.

Stathopoulou, C. *et al.* (2018) 'PD-1 Inhibitory Receptor Downregulates Asparaginyl Endopeptidase and Maintains Foxp3 Transcription Factor Stability in Induced Regulatory T Cells', *Immunity*. Cell Press, 49(2), pp. 247-263.e7. doi: 10.1016/j.immuni.2018.05.006.

Steeg, P. S. (2006) 'Tumor metastasis: mechanistic insights and clinical challenges', *Nature Medicine*.

Nature Publishing Group, 12(8), pp. 895–904. doi: 10.1038/nm1469.

Stein, M. *et al.* (1992) 'Interleukin 4 potently enhances murine macrophage mannose receptor activity: a marker of alternative immunologic macrophage activation.', *The Journal of experimental medicine*. The Rockefeller University Press, 176(1), pp. 287–92. doi: 10.1084/jem.176.1.287.

Strachan, D. C. *et al.* (2013) 'CSF1R inhibition delays cervical and mammary tumor growth in murine models by attenuating the turnover of tumor-associated macrophages and enhancing infiltration by CD8+ T cells', *Oncoimmunology*. Taylor & Francis, 2(12). doi: 10.4161/ONCI.26968.

Strack, E. *et al.* (2020) 'Identification of tumor-associated macrophage subsets that are associated with breast cancer prognosis', *Clinical and Translational Medicine*. John Wiley & Sons, Ltd, 10(8), p. e239. doi: 10.1002/CTM2.239.

Strutz, F. *et al.* (2002) 'Role of basic fibroblast growth factor-2 in epithelial-mesenchymal transformation', *Kidney International*. Elsevier, 61(5), pp. 1714–1728. doi: 10.1046/J.1523-1755.2002.00333.X.

Su, S. *et al.* (2018) 'Immune Checkpoint Inhibition Overcomes ADCP-Induced Immunosuppression by Macrophages', *Cell*. Cell Press, 175(2), pp. 442-457.e23. doi: 10.1016/j.cell.2018.09.007.

Suárez-Fueyo, A. *et al.* (2014) 'Inhibition of PI3Kδ Reduces Kidney Infiltration by Macrophages and Ameliorates Systemic Lupus in the Mouse', *The Journal of Immunology*. The American Association of Immunologists, 193(2), pp. 544–554. doi: 10.4049/jimmunol.1400350.

Sugimura, K. *et al.* (2015) 'High infiltration of tumor-associated macrophages is associated with a poor response to chemotherapy and poor prognosis of patients undergoing neoadjuvant chemotherapy for esophageal cancer', *Journal of Surgical Oncology*. John Wiley and Sons Inc., 111(6), pp. 752–759. doi: 10.1002/jso.23881.

Sun, W. *et al.* (2017) 'A positive-feedback loop between tumour infiltrating activated Treg cells and type 2-skewed macrophages is essential for progression of laryngeal squamous cell carcinoma', *British Journal of Cancer*. Nature Publishing Group, 117(11), pp. 1631–1643. doi: 10.1038/bjc.2017.329.

Sweet, M. J. *et al.* (2002) 'Colony-stimulating factor-1 suppresses responses to CpG DNA and expression of toll-like receptor 9 but enhances responses to lipopolysaccharide in murine macrophages.', *Journal of immunology (Baltimore, Md. : 1950)*, 168(1), pp. 392–9. Available at: http://www.ncbi.nlm.nih.gov/pubmed/11751985 (Accessed: 27 March 2019).

Swiecki, M. *et al.* (2014) 'Plasmacytoid Dendritic Cells of SiglecH Encompasses More Than Control Diphtheria Toxin Receptor under the Cell Depletion in Mice That Express', *J Immunol References*, 192, pp. 4409–4416. doi: 10.4049/jimmunol.1303135.

Swierczak, A. *et al.* (2014) 'The promotion of breast cancer metastasis caused by inhibition of CSF-1R/CSF-1 signaling is blocked by targeting the G-CSF receptor', *Cancer Immunology Research*. American Association for Cancer Research Inc., 2(8), pp. 765–776. doi: 10.1158/2326-6066.CIR-13-0190.

Szymczak-Workman, A. L., Workman, C. J. and Vignali, D. A. A. (2009) 'Cutting Edge: Regulatory T Cells Do Not Require Stimulation through Their TCR to Suppress', *The Journal of Immunology*. American Association of Immunologists, 182(9), pp. 5188–5192. doi: 10.4049/JIMMUNOL.0803123.

Taams, L. S. *et al.* (2005) 'Modulation of monocyte/macrophage function by human CD4+CD25+ regulatory T cells', *Human Immunology*. Elsevier Inc., 66(3), pp. 222–230. doi: 10.1016/j.humimm.2004.12.006.

Taheri, F. *et al.* (2001) 'L-Arginine regulates the expression of the T-cell receptor zeta chain (CD3zeta) in Jurkat cells.', *Clinical cancer research : an official journal of the American Association for Cancer Research*. American Association for Cancer Research, 7(3 Suppl), pp. 958s-965s. Available at: http://www.ncbi.nlm.nih.gov/pubmed/11300497 (Accessed: 26 March 2020).

Takada, K. *et al.* (2018) 'Use of the tumor-infiltrating CD8 to FOXP3 lymphocyte ratio in predicting treatment responses to combination therapy with pertuzumab, trastuzumab, and docetaxel for advanced HER2-positive breast cancer', *Journal of Translational Medicine*. BioMed Central Ltd., 16(1), p. 86. doi: 10.1186/s12967-018-1460-4.

Takahashi, T. *et al.* (2000) 'Immunologic self-tolerance maintained by CD25+CD4+ regulatory T cells constitutively expressing cytotoxic T lymphocyte-associated antigen 4', *Journal of Experimental Medicine*. The Rockefeller University Press, 192(2), pp. 303–309. doi: 10.1084/jem.192.2.303.

Takanaski, S. *et al.* (1994) 'Interleukin 10 inhibits lipopolysaccharide-induced survival and cytokine production by human peripheral blood eosinophils', *Journal of Experimental Medicine*. The Rockefeller University Press, 180(2), pp. 711–715. doi: 10.1084/jem.180.2.711.

Takase, K. and Saito, T. (1995) 'T cell activation', in *Ryumachi*. NIH Public Access, pp. 853–861. doi: 10.1146/annurev.immunol.021908.132706.

Takeda, A., Sasaki, N. and Miyasaka, M. (2017) 'The molecular cues regulating immune cell trafficking.', *Proceedings of the Japan Academy. Series B, Physical and biological sciences*. The Japan Academy, 93(4), pp. 183–195. doi: 10.2183/pjab.93.012.

Taylor, P. R. *et al.* (2005) 'MACROPHAGE RECEPTORS AND IMMUNE RECOGNITION', *Annual Review of Immunology*. Annual Reviews, 23(1), pp. 901–944. doi: 10.1146/annurev.immunol.23.021704.115816.

Teng, M. W. L. *et al.* (2010) 'Conditional regulatory T-cell depletion releases adaptive immunity preventing carcinogenesis and suppressing established tumor growth', *Cancer Research*. American Association for Cancer Research, 70(20), pp. 7800–7809. doi: 10.1158/0008-5472.CAN-10-1681.

Terabe, M. *et al.* (2003) 'Transforming Growth Factor-β Production and Myeloid Cells Are an Effector Mechanism through Which CD1d-restricted T Cells Block Cytotoxic T Lymphocyte-mediated Tumor Immunosurveillance: Abrogation Prevents Tumor Recurrence', *Journal of Experimental Medicine*. The Rockefeller University Press, 198(11), pp. 1741–1752. doi: 10.1084/jem.20022227.

Teresa Pinto, A. *et al.* (2016) 'Ionizing radiation modulates human macrophages towards a pro-inflammatory phenotype preserving their pro-invasive and pro-angiogenic capacities', *Scientific Reports*. Nature Publishing Group, 6. doi: 10.1038/srep18765.

Terness, P. *et al.* (2002) 'Inhibition of allogeneic T cell proliferation by indoleamine 2,3-dioxygenase-expressing dendritic cells: Mediation of suppression by tryptophan metabolites', *Journal of Experimental Medicine*. The Rockefeller University Press, 196(4), pp. 447–457. doi: 10.1084/jem.20020052.

Teschendorff, A. E. *et al.* (2007) 'An immune response gene expression module identifies a good prognosis subtype in estrogen receptor negative breast cancer', *Genome Biology*. BioMed Central, 8(8), p. R157. doi: 10.1186/gb-2007-8-8-r157.

Theisen, D. J. *et al.* (2019) 'Batf3-Dependent Genes Control Tumor Rejection Induced by Dendritic Cells Independently of Cross-Presentation', *Cancer Immunology Research*. American Association for Cancer Research, 7(1), pp. 29–39. doi: 10.1158/2326-6066.CIR-18-0138.

Thepen, T., Van Rooijen, N. and Kraal, G. (1989) 'Alveolar macrophage elimination in vivo is associated with an increase in pulmonary immune response in mice', *Journal of Experimental Medicine*. The Rockefeller University Press, 170(2), pp. 499–509. doi: 10.1084/jem.170.2.499.

Thiery, J. P. *et al.* (2009) 'Epithelial-Mesenchymal Transitions in Development and Disease', *Cell*. Cell Press, 139(5), pp. 871–890. doi: 10.1016/J.CELL.2009.11.007.

Thomas, M. S. *et al.* (2008) 'The p110γ isoform of phosphatidylinositol 3-kinase regulates migration of effector CD4 T lymphocytes into peripheral inflammatory sites', *Journal of Leukocyte Biology*. Wiley-Blackwell, 84(3), pp. 814–823. doi: 10.1189/jlb.0807561.

Thornton, A. M. and Shevach, E. M. (1998) 'CD4+CD25+ immunoregulatory T cells suppress polyclonal T cell activation in vitro by inhibiting interleukin 2 production', *Journal of Experimental Medicine*. The Rockefeller University Press, 188(2), pp. 287–296. doi: 10.1084/jem.188.2.287.

Tian, T. *et al.* (2015) 'Increased circulating CD14(+)HLA-DR-/low myeloid-derived suppressor cells are associated with poor prognosis in patients with small-cell lung cancer', *Cancer Biomarkers*. IOS Press, 15(4), pp. 425–432. doi: 10.3233/CBM-150473.

Timaner, M. *et al.* (2015) 'Dequalinium blocks macrophage-induced metastasis following local radiation', *Oncotarget*. Impact Journals LLC, 6(29), pp. 27537–27554. doi: 10.18632/oncotarget.4826.

Travis, E. L. (1980) 'The sequence of histological changes in mouse lungs after single doses of X-rays', *International Journal of Radiation Oncology, Biology, Physics*, 6(3), pp. 345–347. doi: 10.1016/0360-3016(80)90145-5.

Tripathi, C. *et al.* (2014) 'Macrophages are recruited to hypoxic tumor areas and acquire a pro-angiogenic M2-polarized phenotype via hypoxic cancer cell derived cytokines Oncostatin M and Eotaxin.', *Oncotarget*. Impact Journals, LLC, 5(14), pp. 5350–68. doi: 10.18632/oncotarget.2110.

Tsan, M.-F. and Gao, B. (2005) 'Effect of Depleting Tumor-Associated Macrophages on Breast Cancer Growth and Response to Chemotherapy'. Available at: https://apps.dtic.mil/sti/citations/ADA454757 (Accessed: 26 January 2022).

Tseng, D. *et al.* (2013) 'Anti-CD47 antibody-mediated phagocytosis of cancer by macrophages primes an effective antitumor T-cell response', *Proceedings of the National Academy of Sciences of the United States of America*. National Academy of Sciences, 110(27), pp. 11103–11108. doi: 10.1073/pnas.1305569110.

Tsujimoto, Y. (1998) 'Role of Bcl-2 family proteins in apoptosis: Apoptosomes or mitochondria?', *Genes to Cells*, pp. 697–707. doi: 10.1046/j.1365-2443.1998.00223.x.

Tushinski, R. J. *et al.* (1982) 'Survival of mononuclear phagocytes depends on a lineage-specific growth factor that the differentiated cells selectively destroy', *Cell*, 28(1), pp. 71–81. doi: 10.1016/0092-8674(82)90376-2.

Tushinski, R. J. and Stanley, E. R. (1985) 'The regulation of mononuclear phagocyte entry into S phase by the colony stimulating factor CSF-1', *Journal of Cellular Physiology*. John Wiley & Sons, Ltd, 122(2), pp. 221–228. doi: 10.1002/jcp.1041220210.

Tymoszuk, P. *et al.* (2014) 'In situ proliferation contributes to accumulation of tumor-associated macrophages in spontaneous mammary tumors', *European Journal of Immunology*. Wiley-Blackwell, 44(8), pp. 2247–2262. doi: 10.1002/eji.201344304.

Ueno, T. *et al.* (2000) 'Significance of Macrophage Chemoattractant Protein-1 in Macrophage Recruitment, Angiogenesis, and Survival in Human Breast Cancer', *Clinical Cancer Research*, 6(8).

Uhlig, H. H. *et al.* (2006) ' Characterization of Foxp3 + CD4 + CD25 + and IL-10-Secreting CD4 + CD25 + T Cells during Cure of Colitis ', *The Journal of Immunology*. The American Association of Immunologists, 177(9), pp. 5852–5860. doi: 10.4049/jimmunol.177.9.5852.

Usman, M. W. *et al.* (2018) 'Macrophages confer resistance to PI3K inhibitor GDC-0941 in breast cancer through the activation of NF-κB signaling', *Cell Death & Disease 2018 9:8*. Nature Publishing Group, 9(8), pp. 1–12. doi: 10.1038/s41419-018-0849-6.

Usuda, H. *et al.* (1994) 'Ultrastructure of macrophages and dendritic cells in osteopetrosis (op) mutant mice lacking macrophage colony-stimulating factor (M-CSF/CSF-1) activity', *J.SUBMICROSC.CYTOL.PATHOL.*, 26(1), pp. 111–119.

Valković, T. *et al.* (2002) 'Correlation between vascular endothelial growth factor, angiogenesis, and tumor-associated macrophages in invasive ductal breast carcinoma', *Virchows Archiv*. Springer-

Verlag, 440(6), pp. 583–588. doi: 10.1007/s004280100458.

Vanhaesebroeck, B. *et al.* (2010) 'The emerging mechanisms of isoform-specific PI3K signalling', *Nature Reviews Molecular Cell Biology*. Nature Publishing Group, pp. 329–341. doi: 10.1038/nrm2882.

Vicari, A. P., Caux, C. and Trinchieri, G. (2002) 'Tumour escape from immune surveillance through dendritic cell inactivation', *Seminars in Cancer Biology*. Academic Press, 12(1), pp. 33–42. doi: 10.1006/SCBI.2001.0400.

Villarreal, D. O. *et al.* (2018) 'Targeting CCR8 induces protective antitumor immunity and enhances vaccine-induced responses in colon cancer', *Cancer Research*. American Association for Cancer Research Inc., 78(18), pp. 5340–5348. doi: 10.1158/0008-5472.CAN-18-1119.

Vinay, D. S. and Kwon, B. S. (2010) 'CD11c+CD8+ T cells: Two-faced adaptive immune regulators', *Cellular Immunology*, pp. 18–22. doi: 10.1016/j.cellimm.2010.05.010.

Viola, A. *et al.* (2019) 'The metabolic signature of macrophage responses', *Frontiers in Immunology*. Frontiers Media S.A. doi: 10.3389/fimmu.2019.01462.

de Visser, K. E., Eichten, A. and Coussens, L. M. (2006) 'Paradoxical roles of the immune system during cancer development', *Nature Reviews Cancer*. Nature Publishing Group, 6(1), pp. 24–37. doi: 10.1038/nrc1782.

Vitale, D. (2001) *Interpreting mRNA electropherograms Application*.

Volodko, N. *et al.* (1998) 'Tumour-associated macrophages in breast cancer and their prognostic correlations', *The Breast*. Churchill Livingstone, 7(2), pp. 99–105. doi: 10.1016/S0960-9776(98)90065-0.

Voskoboinik, I., Whisstock, J. C. and Trapani, J. A. (2015) 'Perforin and granzymes: Function, dysfunction and human pathology', *Nature Reviews Immunology*. Nature Publishing Group, pp. 388–400. doi: 10.1038/nri3839.

Voss, J. J. L. P. *et al.* (2017) 'Modulation of macrophage antitumor potential by apoptotic lymphoma cells', *Cell Death and Differentiation*. Nature Publishing Group, 24(6), pp. 971–983. doi: 10.1038/cdd.2016.132.

Wagenblast, E. *et al.* (2015) 'A model of breast cancer heterogeneity reveals vascular mimicry as a driver of metastasis', *Nature*. Nature Publishing Group, 520(7547), pp. 358–362. doi: 10.1038/nature14403.

Wagner, J. *et al.* (2019) 'A Single-Cell Atlas of the Tumor and Immune Ecosystem of Human Breast Cancer', *Cell*. Cell Press, 177(5), pp. 1330-1345.e18. doi: 10.1016/j.cell.2019.03.005.

Waldhauer, I. and Steinle, A. (2008) 'NK cells and cancer immunosurveillance', *Oncogene*. Nature Publishing Group, 27(45), pp. 5932–5943. doi: 10.1038/onc.2008.267.

Wang, G. L. *et al.* (1995) 'Hypoxia-inducible factor 1 is a basic-helix-loop-helix-PAS heterodimer regulated by cellular O2 tension.', *Proceedings of the National Academy of Sciences of the United States of America*. National Academy of Sciences, 92(12), pp. 5510–4. doi: 10.1073/pnas.92.12.5510.

Wang, J. *et al.* (2007) 'Transient expression of FOXP3 in human activated nonregulatory CD4+ T cells', *European Journal of Immunology*. John Wiley & Sons, Ltd, 37(1), pp. 129–138. doi: 10.1002/eji.200636435.

Wang, Jian-sheng *et al.* (2016) 'High tumor-associated macrophages infiltration is associated with poor prognosis and may contribute to the phenomenon of epithelial–mesenchymal transition in gastric cancer', *OncoTargets and Therapy*, Volume 9, pp. 3975–3983. doi: 10.2147/OTT.S103112.

Wang, Junhua *et al.* (2016) 'Repeated Long-Term DT Application in the DEREG Mouse Induces a Neutralizing Anti-DT Antibody Response', *Journal of Immunology Research*. Hindawi Limited, 2016.

doi: 10.1155/2016/1450398.

Wang, K., Wei, G. and Liu, D. (2012) 'CD19: a biomarker for B cell development, lymphoma diagnosis and therapy', *Experimental Hematology & Oncology*. BioMed Central, 1(1), p. 36. doi: 10.1186/2162-3619-1-36.

Wang, Y. -Q., Berezovska, O. and Fedoroff, S. (1999) 'Expression of colony stimulating factor-1 receptor (CSF-1R) by CNS neurons in mice', *Journal of Neuroscience Research*. John Wiley & Sons, Ltd, 57(5), pp. 616–632. doi: 10.1002/(SICI)1097-4547(19990901)57:5<616::AID-JNR4>3.0.CO;2-E.

Wang, Y. J. *et al.* (2019) 'Comparative analysis of commercially available single-cell RNA sequencing platforms for their performance in complex human tissues', *bioRxiv*. Cold Spring Harbor Laboratory, p. 541433. doi: 10.1101/541433.

Watkins, S. K. *et al.* (2012) 'Isolation of immune cells from primary tumors.', *Journal of visualized experiments : JoVE*. MyJoVE Corporation, (64), p. e3952. doi: 10.3791/3952.

Weber, M. R. *et al.* (2016) 'Activated tumor cell integrin αvβ3 cooperates with platelets to promote extravasation and metastasis from the blood stream', *Thrombosis Research*. Elsevier Ltd, 140(Suppl 1), pp. S27–S36. doi: 10.1016/S0049-3848(16)30095-0.

Wei, S. *et al.* (2010) 'Functional overlap but differential expression of CSF-1 and IL-34 in their CSF-1 receptor-mediated regulation of myeloid cells', *Journal of Leukocyte Biology*. The Society for Leukocyte Biology, 88(3), p. 495. doi: 10.1189/JLB.1209822.

Wei, S., Kryczek, I. and Zou, W. (2006) 'Regulatory T-cell compartmentalization and trafficking', *Blood*. The American Society of Hematology, pp. 426–431. doi: 10.1182/blood-2006-01-0177.

Whetton, A. D. and Dexter, T. M. (1989) 'Myeloid haemopoietic growth factors', *BBA - Reviews on Cancer*, pp. 111–132. doi: 10.1016/0304-419X(89)90038-3.

Wiktor-Jedrzejczak, W. *et al.* (1990) 'Total absence of colony-stimulating factor 1 in the macrophage-deficient osteopetrotic (op/op) mouse.', *Proceedings of the National Academy of Sciences of the United States of America*. National Academy of Sciences, 87(12), pp. 4828–32. Available at: http://www.ncbi.nlm.nih.gov/pubmed/2191302 (Accessed: 27 March 2019).

Wilson, W. H. (2013) 'Treatment strategies for aggressive lymphomas: what works?', *Hematology / the Education Program of the American Society of Hematology. American Society of Hematology. Education Program*. American Society of Hematology, pp. 584–590. doi: 10.1182/asheducation-2013.1.584.

Worthington Biochemical Online Tissue Dissociation Guide (2011) *Worthington Biochemical Online Tissue Dissociation Guide*. Available at: http://www.worthington-biochem.com/tissuedissociation/citations.html (Accessed: 15 January 2019).

Wu, C. *et al.* (2018) 'Spleen mediates a distinct hematopoietic progenitor response supporting tumor-promoting myelopoiesis', *The Journal of clinical investigation*, 128(8), pp. 3425–3438.

Wyatt Shields, C. *et al.* (2020) 'Cellular backpacks for macrophage immunotherapy', *Science Advances*. American Association for the Advancement of Science, 6(18), p. eaaz6579. doi: 10.1126/sciadv.aaz6579.

Wyckoff, J. *et al.* (2004) 'A Paracrine Loop between Tumor Cells and Macrophages Is Required for Tumor Cell Migration in Mammary Tumors', *Cancer Research*, 64(19), pp. 7022–7029. doi: 10.1158/0008-5472.CAN-04-1449.

Xu, J. *et al.* (2013) 'CSF1R signaling blockade stanches tumor-infiltrating myeloid cells and improves the efficacy of radiotherapy in prostate cancer', *Cancer Research*. American Association for Cancer Research, 73(9), pp. 2782–2794. doi: 10.1158/0008-5472.CAN-12-3981.

Xu, N. *et al.* (2012) 'Akt: A Double-Edged Sword in Cell Proliferation and Genome Stability', *journal of oncology*. Available at: https://www.ncbi.nlm.nih.gov/pmc/articles/PMC3317191/ (Accessed: 30

March 2020).

Xuan, Q. J. *et al.* (2014) 'Tumor-associated macrophages are correlated with tamoxifen resistance in the postmenopausal breast cancer patients', *Pathology and Oncology Research*. Kluwer Academic Publishers, 20(3), pp. 619–624. doi: 10.1007/s12253-013-9740-z.

Yamaguchi, H. and Condeelis, J. (2007) 'Regulation of the actin cytoskeleton in cancer cell migration and invasion', *Biochimica et Biophysica Acta - Molecular Cell Research*. NIH Public Access, pp. 642–652. doi: 10.1016/j.bbamcr.2006.07.001.

Yan, H. H. *et al.* (2010) 'Gr-1+CD11b+ myeloid cells tip the balance of immune protection to tumor promotion in the premetastatic lung', *Cancer Research*. NIH Public Access, 70(15), pp. 6139–6149. doi: 10.1158/0008-5472.CAN-10-0706.

Yang, C. *et al.* (2015) 'Increased drug resistance in breast cancer by tumor-associated macrophages through IL-10/STAT3/bcl-2 signaling pathway', *Medical Oncology*. Humana Press Inc., 32(2), pp. 1–8. doi: 10.1007/s12032-014-0352-6.

Yang, J. *et al.* (2004) 'Twist, a Master Regulator of Morphogenesis, Plays an Essential Role in Tumor Metastasis', *Cell*. Cell Press, 117(7), pp. 927–939. doi: 10.1016/J.CELL.2004.06.006.

Yang, L. *et al.* (2020) 'Disease progression model of 4T1 metastatic breast cancer', *Journal of Pharmacokinetics and Pharmacodynamics*. Springer, 47(1), pp. 105–116. doi: 10.1007/S10928-020-09673-5/FIGURES/5.

Yángüez, E. *et al.* (2013) 'ISG15 Regulates Peritoneal Macrophages Functionality against Viral Infection', *PLoS Pathogens*. Edited by P. Feng, 9(10), p. e1003632. doi: 10.1371/journal.ppat.1003632.

Yao, Y., Xu, X. H. and Jin, L. (2019) 'Macrophage Polarization in Physiological and Pathological Pregnancy', *Frontiers in Immunology*. Frontiers Media SA, 10(MAR), p. 792. doi: 10.3389/FIMMU.2019.00792.

Ye, X. *et al.* (2012) 'Tumor-Associated Microglia/Macrophages Enhance the Invasion of Glioma Stem-like Cells via TGF-β1 Signaling Pathway', *The Journal of Immunology*. The American Association of Immunologists, 189(1), pp. 444–453. doi: 10.4049/jimmunol.1103248.

Yin, Y. *et al.* (2017) 'The immune-microenvironment confers chemoresistance of colorectal cancer through macrophage-derived IL6', *Clinical Cancer Research*. American Association for Cancer Research Inc., 23(23), pp. 7375–7387. doi: 10.1158/1078-0432.CCR-17-1283.

Yona, S. *et al.* (2013) 'Fate mapping reveals origins and dynamics of monocytes and tissue macrophages under homeostasis.', *Immunity*. NIH Public Access, 38(1), pp. 79–91. doi: 10.1016/j.immuni.2012.12.001.

Yoshimura, T. *et al.* (2016) 'Induction of monocyte chemoattractant proteins in macrophages via the production of granulocyte/macrophage colony-stimulating factor by breast cancer cells', *Frontiers in Immunology*. Frontiers Media S.A., 7(JAN). doi: 10.3389/fimmu.2016.00002.

Yoshimura, T. *et al.* (2019) 'Cancer cell-derived granulocyte-macrophage colony-stimulating factor is dispensable for the progression of 4T1 murine breast cancer', *International Journal of Molecular Sciences*. MDPI AG, 20(24). doi: 10.3390/ijms20246342.

Youn, J.-I. *et al.* (2008) 'Subsets of Myeloid-Derived Suppressor Cells in Tumor-Bearing Mice', *The Journal of Immunology*. American Association of Immunologists, 181(8), pp. 5791–5802. doi: 10.4049/JIMMUNOL.181.8.5791.

Yuan, J. *et al.* (2019) 'High expression of CD47 in triple negative breast cancer is associated with epithelial-mesenchymal transition and poor prognosis', *Oncology Letters*. Spandidos Publications, 18(3), pp. 3249–3255. doi: 10.3892/ol.2019.10618.

Zeisberger, S. M. *et al.* (2006) 'Clodronate-liposome-mediated depletion of tumour-associated

macrophages: A new and highly effective antiangiogenic therapy approach', *British Journal of Cancer*. Nature Publishing Group, 95(3), pp. 272–281. doi: 10.1038/sj.bjc.6603240.

Zelnak, A. B. and O'Regan, R. M. (2015) 'Optimizing endocrine therapy for breast cancer', *JNCCN Journal of the National Comprehensive Cancer Network*. Harborside Press, pp. e56–e64. doi: 10.6004/jnccn.2015.0125.

Zhang, Q. wen *et al.* (2012) 'Prognostic Significance of Tumor-Associated Macrophages in Solid Tumor: A Meta-Analysis of the Literature', *PLoS ONE*. PLoS One, 7(12). doi: 10.1371/journal.pone.0050946.

Zhang, Y. *et al.* (2013) 'High-Infiltration of Tumor-Associated Macrophages Predicts Unfavorable Clinical Outcome for Node-Negative Breast Cancer', *PLoS ONE*. Edited by J. Q. Cheng. Public Library of Science, 8(9), p. e76147. doi: 10.1371/journal.pone.0076147.

Zhang, Y. *et al.* (2017) 'Tumacrophage: Macrophages transformed into tumor stem-like cells by virulent genetic material from tumor cells', *Oncotarget*. Impact Journals LLC, 8(47), pp. 82326–82343. doi: 10.18632/oncotarget.19320.

Zhang, Y. *et al.* (2018) 'Establishment of a murine breast tumor model by subcutaneous or orthotopic implantation', *Oncology Letters*. Spandidos Publications, 15(5), p. 6233. doi: 10.3892/OL.2018.8113.

Zhang, Y. *et al.* (2020) 'Regulatory T-cell Depletion Alters the Tumor Microenvironment and Accelerates Pancreatic Carcinogenesis', *Cancer discovery*. NLM (Medline), 10(3), pp. 422–439. doi: 10.1158/2159-8290.CD-19-0958.

Zheng, P.-P., Kros, J. M. and Li, J. (2018) 'Approved CAR T cell therapies: ice bucket challenges on glaring safety risks and long-term impacts', *Drug Discovery Today*. Elsevier Current Trends, 23(6), pp. 1175–1182. doi: 10.1016/J.DRUDIS.2018.02.012.

Zheng, X. *et al.* (2015) 'Epithelial-to-mesenchymal transition is dispensable for metastasis but induces chemoresistance in pancreatic cancer.', *Nature*. NIH Public Access, 527(7579), pp. 525–530. doi: 10.1038/nature16064.

Zhu, Y. *et al.* (2017) 'Tissue-Resident Macrophages in Pancreatic Ductal Adenocarcinoma Originate from Embryonic Hematopoiesis and Promote Tumor Progression.', *Immunity*. NIH Public Access, 47(2), pp. 323-338.e6. doi: 10.1016/j.immuni.2017.07.014.

Zitvogel, L. *et al.* (2008) 'Immunological aspects of cancer chemotherapy', *Nature Reviews Immunology*. Nature Publishing Group, pp. 59–73. doi: 10.1038/nri2216.

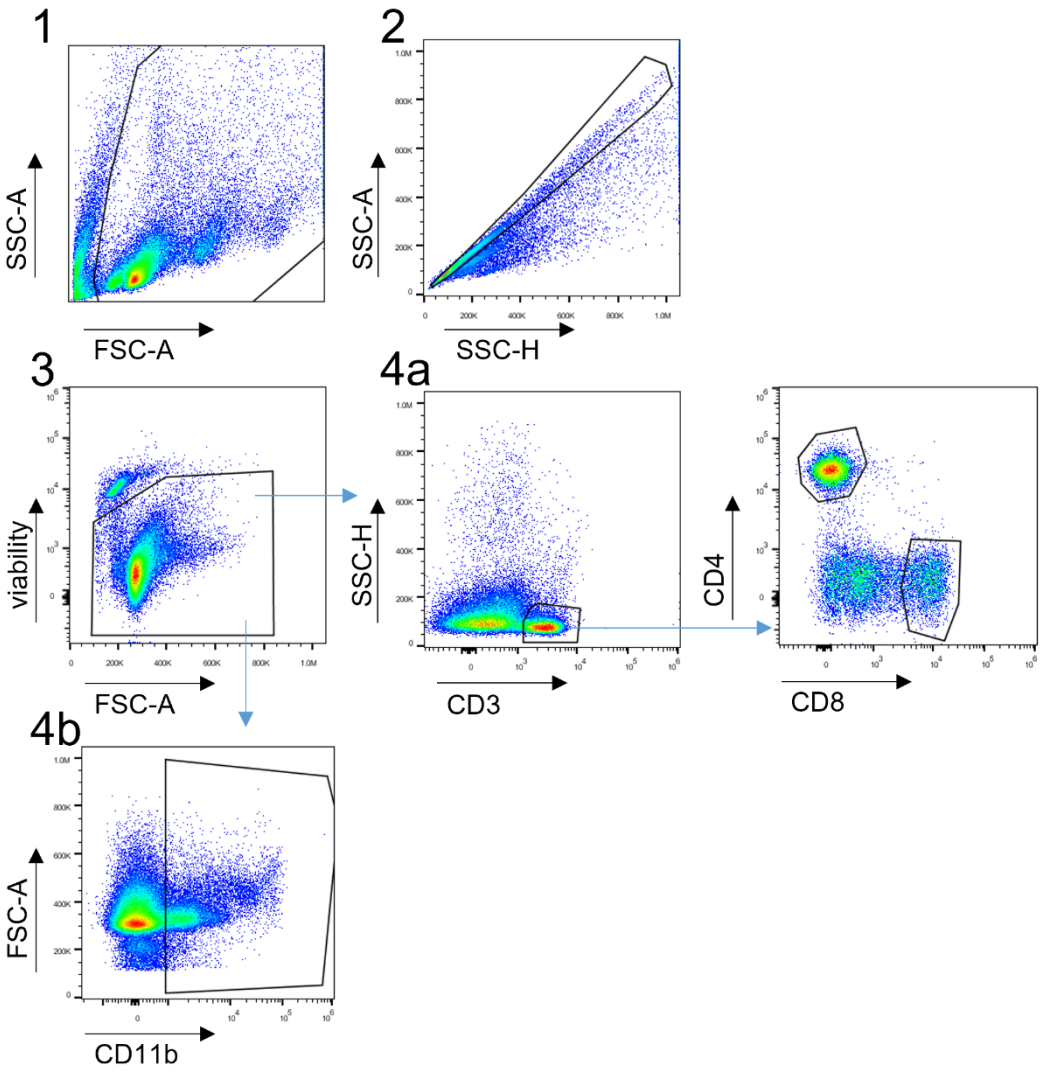

Supplementary Figure S1: Gating strategy to identify CD11b$^+$ cells and T cells via flow cytometry

Cells extracted from mouse spleens were gated to remove debris (1) and doublets (2). Cells were then selected based on low expression of a viability dye (3) before being gated on the expression of CD3, CD4 and CD8 (4a) or CD11b (4b).

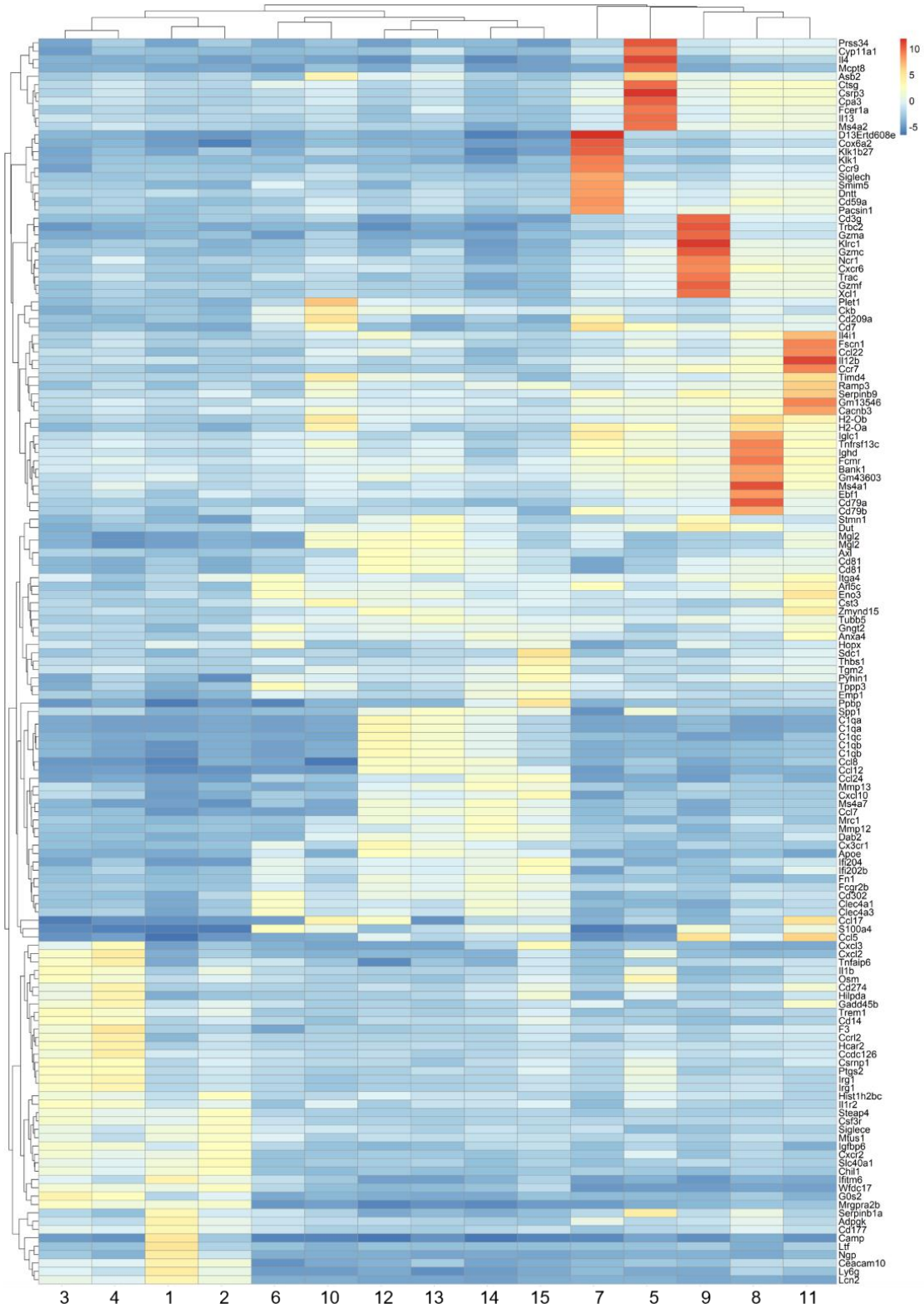

Supplementary Figure S2: log2 fold changes in significant genes determining clusters

Heatmap of log2 fold changes of top 10 genes significantly upregulated in clusters identified by Cell Ranger t-SNE clustering (numbers 1-15 correspond to populations);

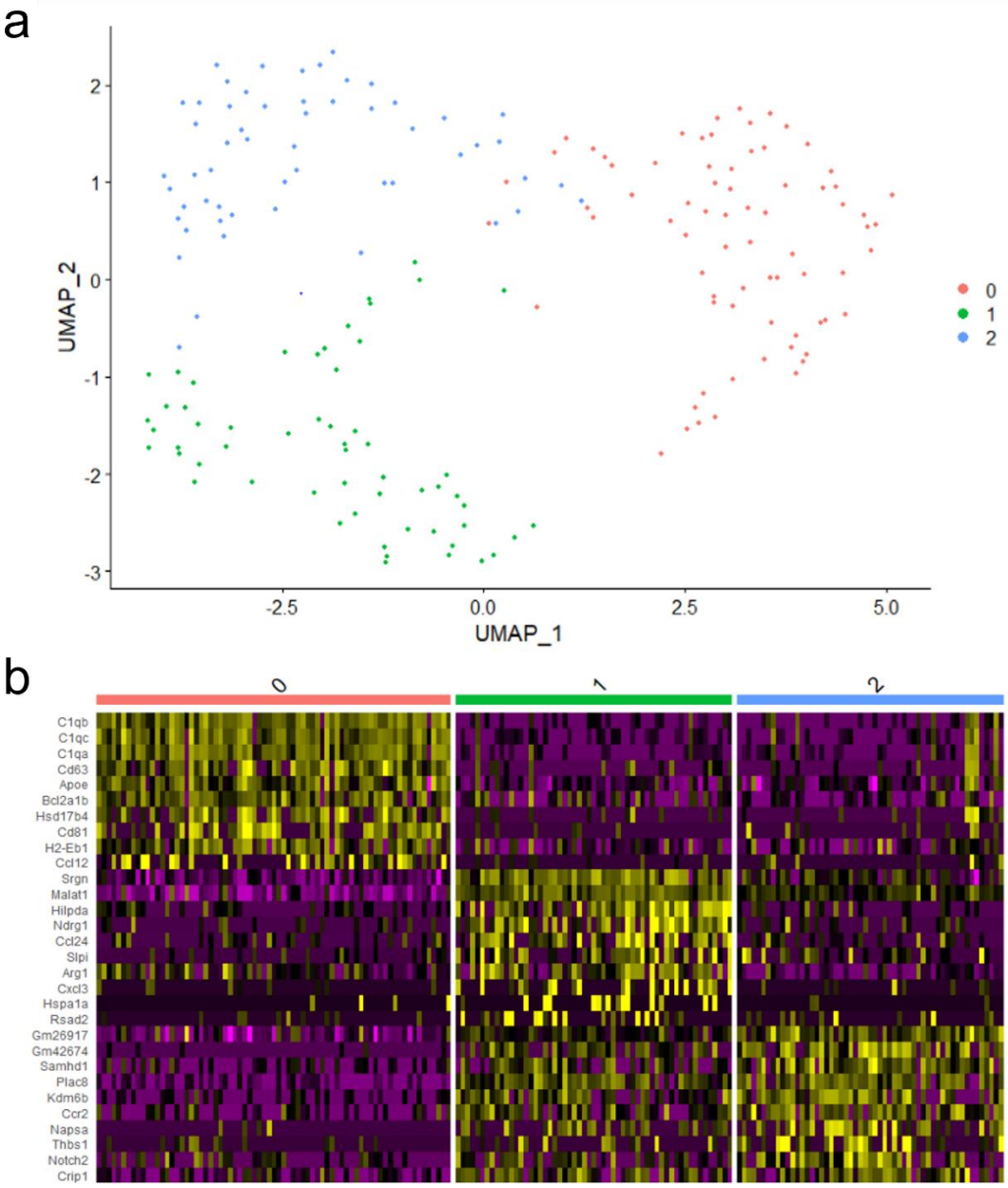

Supplementary figure S3: UMAP clustering of macrophage cell IDs

Cell IDs corresponding to macrophage populations as clustered by Cell Ranger were extracted and UMAP clustering was performed.

a) UMAP cluster and b) heatmap of top 10 markers expressed by different UMAP clusters: Dims = 1:10, k.param=20, prune.SNN=1/15, data resolution = 0.5;

Cluster 0 corresponds to Cell Ranger cluster 12/13, cluster 1 corresponds to Cell Ranger cluster 15, cluster 2 corresponds to Cell Ranger cluster 14.

N = 511 cells

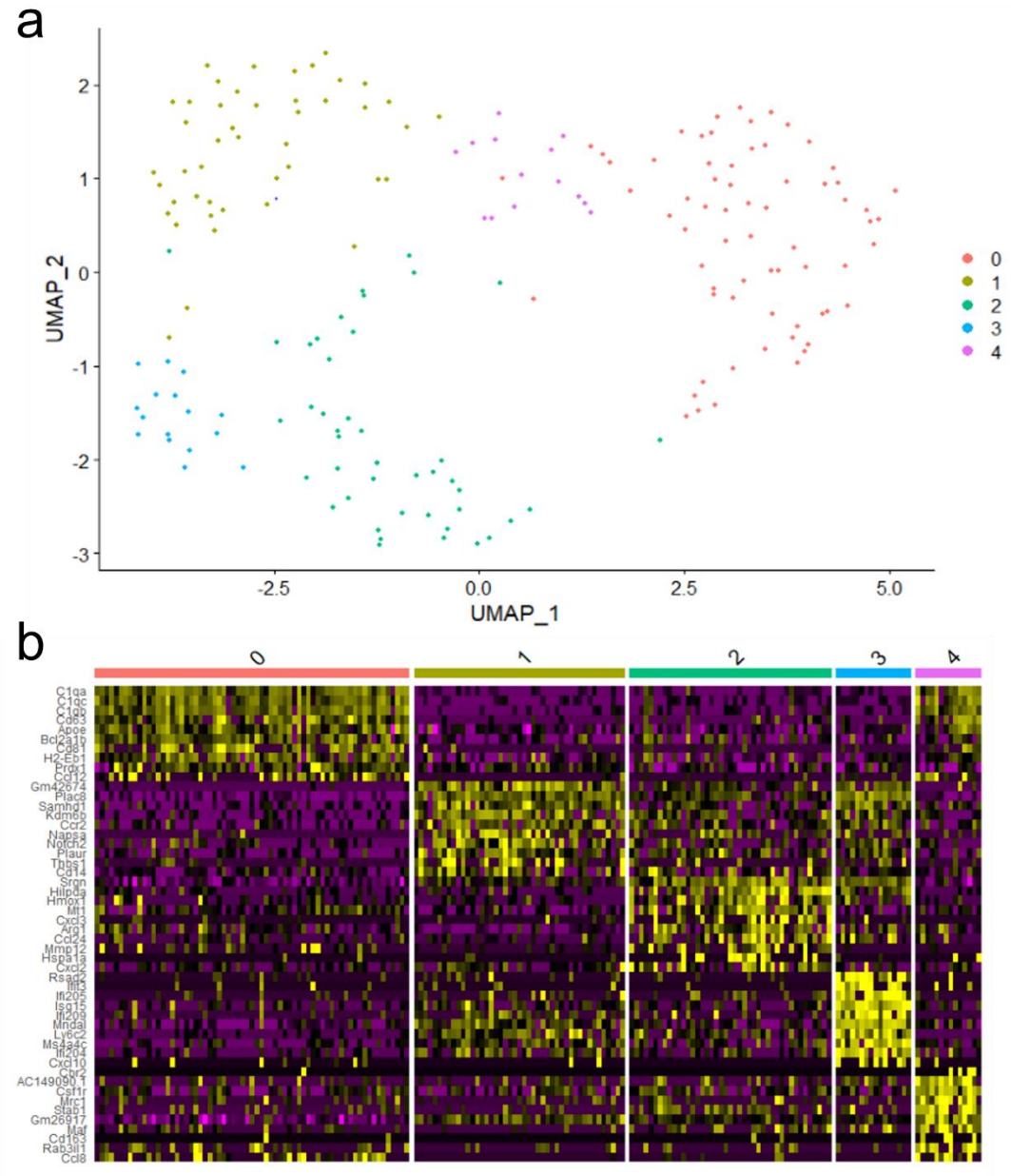

Supplementary figure S4: UMAP clustering of macrophage cell IDs

Cell IDs corresponding to macrophage populations as clustered by Cell Ranger were extracted and UMAP clustering was performed.

a) UMAP cluster and b) heatmap of top 10 markers expressed by different UMAP clusters: Dims = 1:10, k.param=20, prune.SNN=1/15, data resolution = 1;

Cluster 0 corresponds to Cell Ranger cluster 13, cluster 1 corresponds to Cell Ranger cluster 14, clusters 2 and 3 correspond to Cell Ranger cluster 15, cluster 4 corresponds to Cell Ranger cluster 12.

N = 511 cells

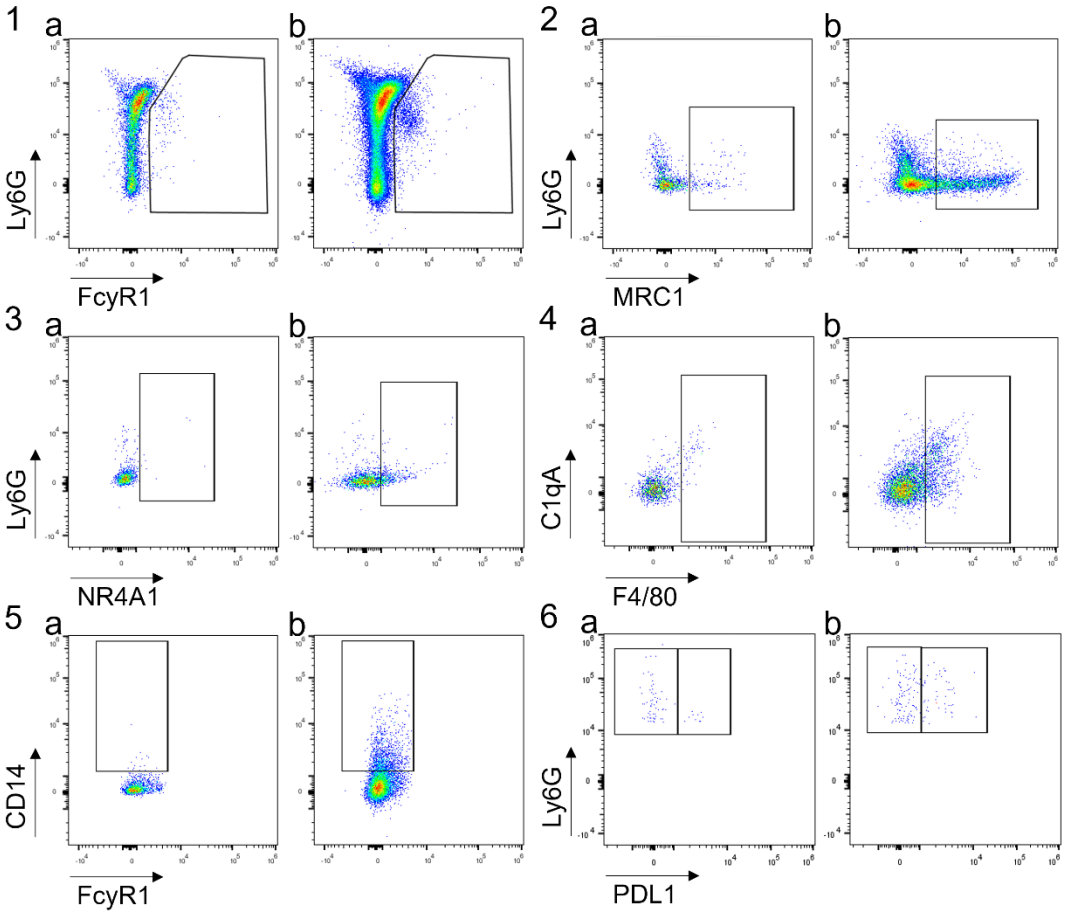

Supplementary figure S5: Fluorescence minus one (FMO) controls for cell population defining antibodies

Cells extracted from 4T1 tumours 3 weeks after tumour cell injection were gated to remove debris, doublets, dead cells and tumour cells as described before. FMO controls (a) or full stains (b) for FcyR1 (1), MRC1 (2), NR4A1 (3), C1qA (4), CD14 (5) and PDL1 (6).

Cells were pre-gated to be $FcyR1^{+}$ (2, 3), $FcyR1^{+}$ $Ly6C^{-}$ (4), $FcyR1^{-}$ Ly6c- (5), $FcyR1^{-}$ $Ly6C^{-}$ $CD14^{+}$ (6). FACS plots are representative of typical 4T1 tumours harvested 21 days after tumour cell injection.

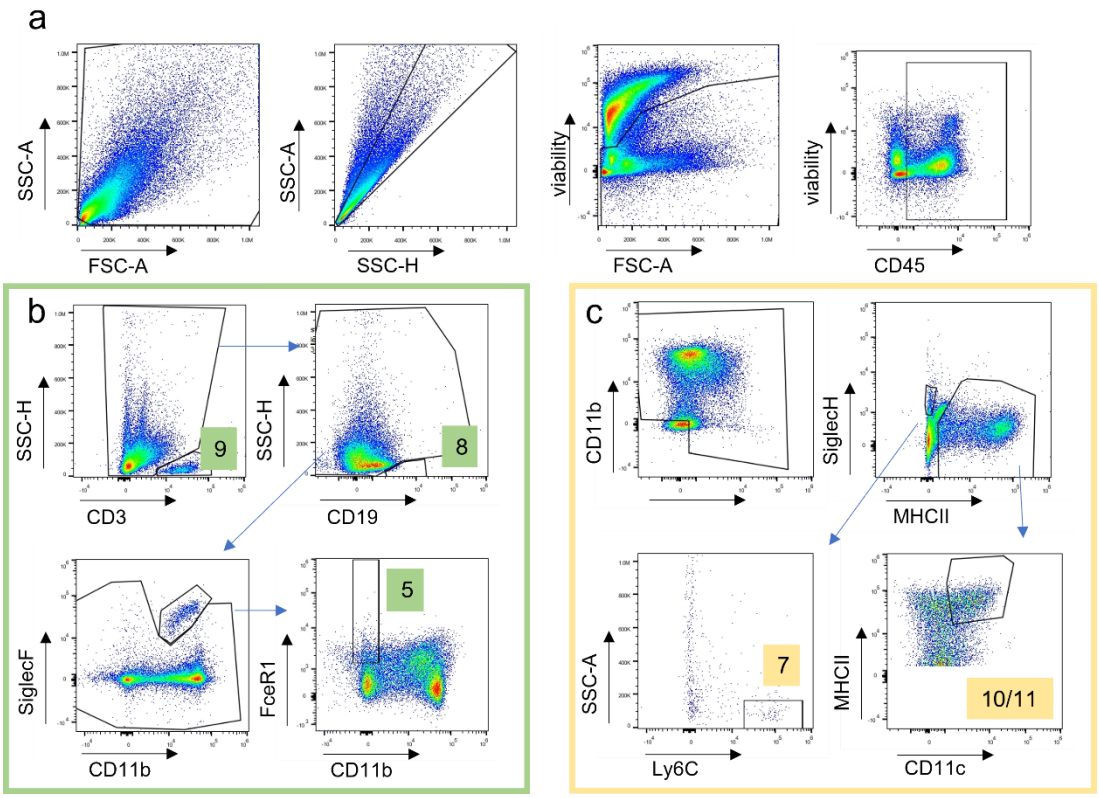

Supplementary figure S6: Gating strategy to identify "rest" populations via flow cytometry

a) Cells extracted from 4T1 tumours 3 weeks after tumour cell injection were gated to remove debris and doublets. Cells were then selected based on low expression of a viability dye, before being gated on the expression of CD45 and further gated according to strategy b or c.

b) Gating strategy for lymphocytes and mast cells: T cells (9) were selected based on expression of CD3. From the CD3 negative population B cells (8) were gated based on low side scatter height and expression of CD19. From the CD19 negative population eosinophils were removed based on expression of SiglecF and CD11b, remaining cells were gated on FceR1 to capture mast cells (5).

c) The CD11b/CD11c negative portion of cells was removed. Remaining cells were gated based on expression of SiglecH and Ly6C as well as low side scatter area (plasmacytoid DCs, 7) and CD11c/MHCII (DCs, 10/11).

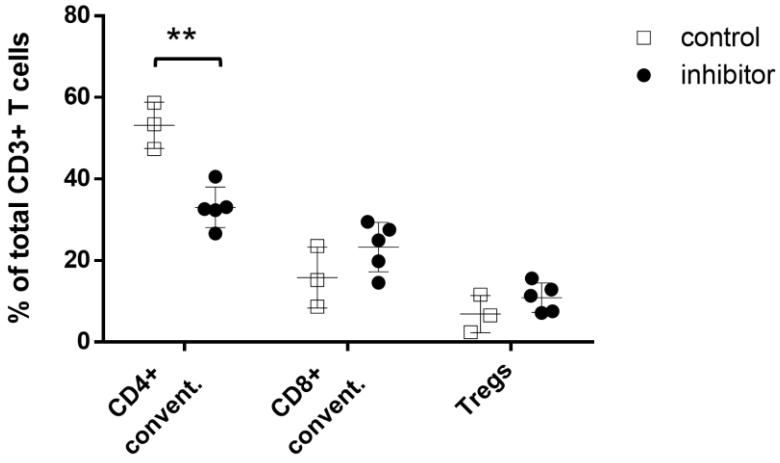

Supplementary Figure S7 : GW2580 reduces CD4$^+$ conventional T cells

Mice were treated with GW2580 or PBS (control) via oral gavage . Graphs show CD4+ and CD8+ conventional T cells and Tregs as % of total CD3+ cells recovered.

Data were analysed by two-way RM ANOVA with Sidak's multiple comparisons test: treatment: $F(1, 6) = 7.775$, $p = 0.0316$; cell types: $F(2, 12) = 57.67$, $p < 0.0001$; interaction: $F(2, 12) = 10.61$, $p = 0.0022$

**, $P \leq 0.01$; *, $P \leq 0.05$

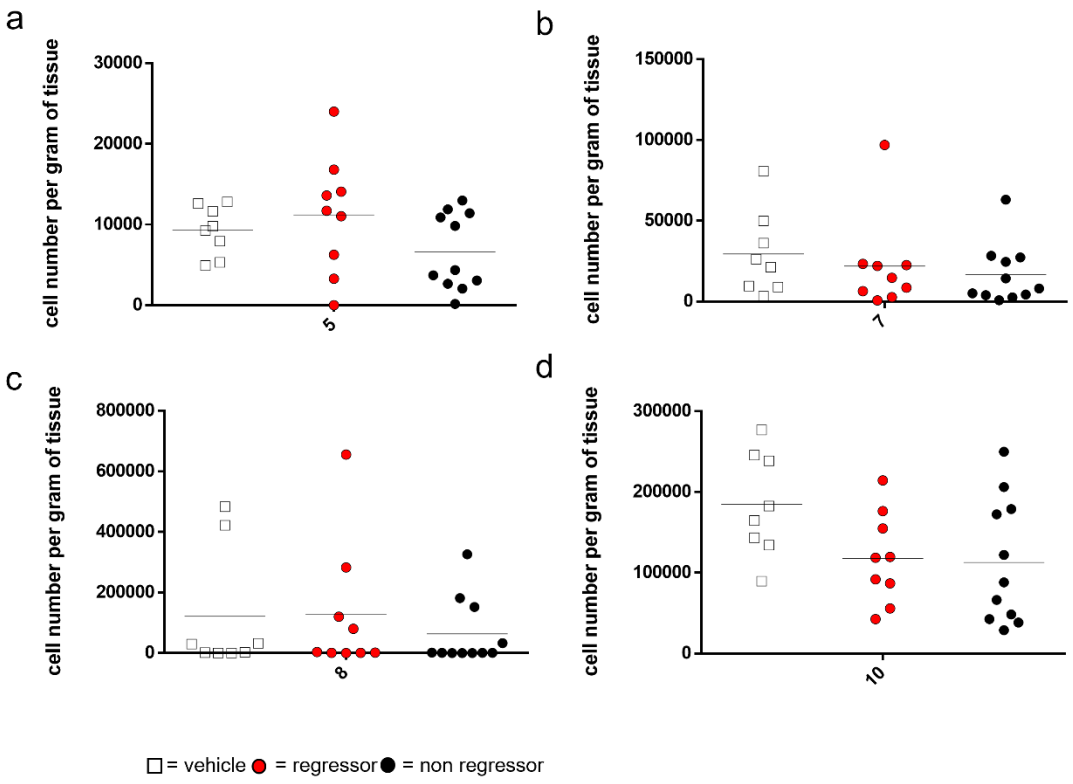

Supplementary figure S8: PI-3065 treatment does not significantly impact most tumour infiltrating immune cell populations

Mice bearing 4T1 tumours were treated with PI-3065 or vehicle as previously described. Tumours were harvested on day 19 after 4T1 inoculation. Graphs showing numbers of a) mast cells (5), b) plasmacytoid DCs (7), c) B cells (8) and d) DCs (10) per gram of tumour tissue. N = 8 for vehicles, 19 for treatment (9 regressors, 10 non regressors);

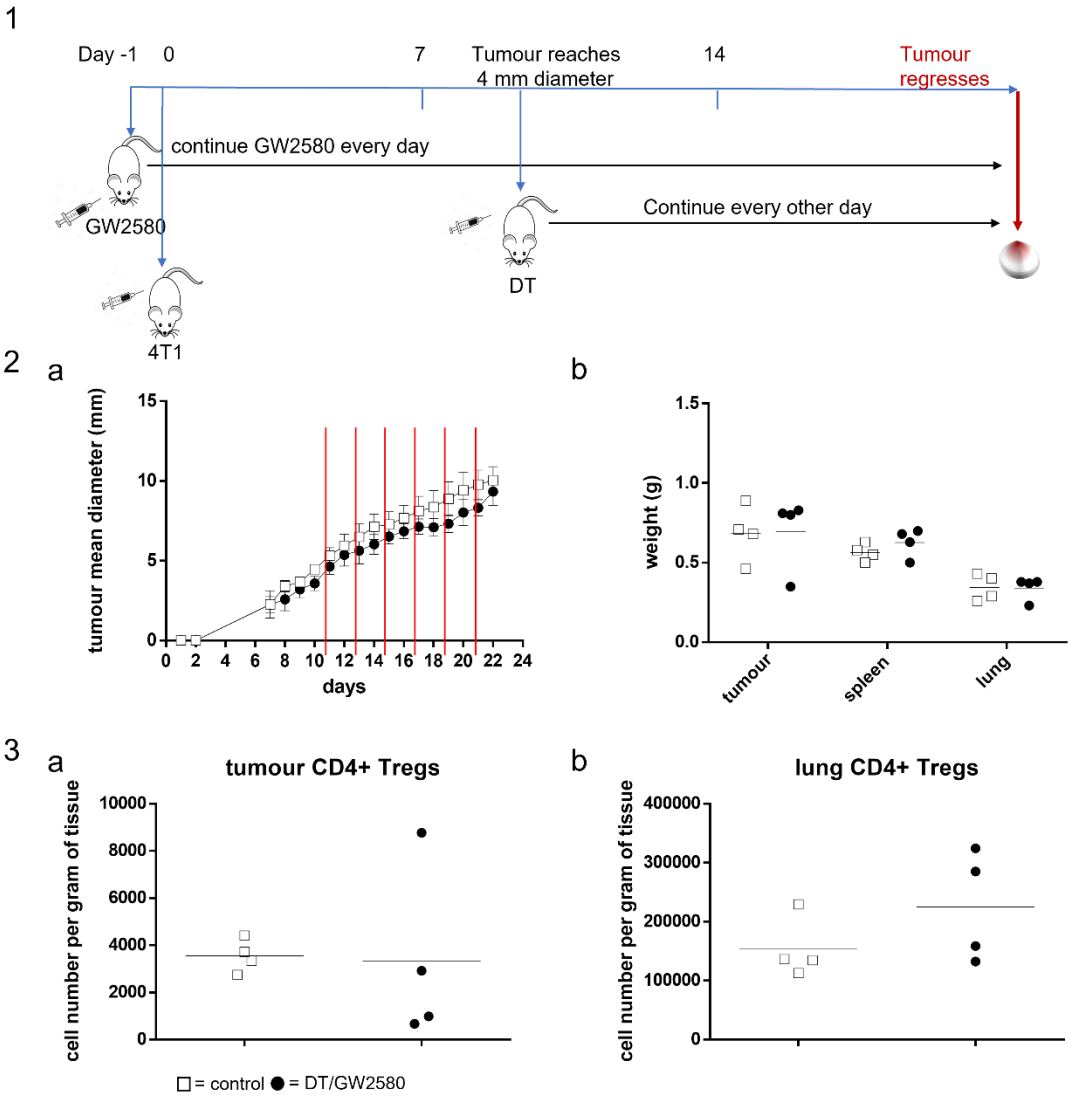

Supplementary Figure S9: Combination of GW2580 and DT treatment only initially slows tumour growth at earlier timepoint

1) Mice were treated with GW2580 or PBS (control) via oral gavage one day before injection of 4T1 cells. GW2580 treatment was continued once per day. Once tumours reached an average of 4 mm in diameter treatment with DT was commenced and injections were continued every other day. Tumours were harvested once a humane endpoint was reached or at 28 days after 4T1 inoculation.

2) Growth curve (a) and organ weights (b) of DEREG and DEREG$^-$ mice bearing 4T1 tumours treated with DT and GW2580 (DT/GW2580, black circle) or vehicle (control, white square). Tumours were harvested on day 21 after 4T1 inoculation. Red lines illustrate DT treatment.

3) Numbers of CD4$^+$ Tregs in tumours (a) and lungs (b) of DT/GW2580 treated DEREG or control DEREG$^-$ mice

Whole experiment: N = 4 for controls, 4 for treatment